MULTIDIMENSIONAL MULTIRATE FILTERS AND FILTER BANKS: THEORY, DESIGN, AND IMPLEMENTATION

Thesis by

Tsuhan Chen

In Partial Fulfillment of the Requirements
for the Degree of
Doctor of Philosophy

California Institute of Technology
Pasadena, California
1993

(Submitted May 10, 1993)

Acknowledgement

First of all, I would like to thank Professor P. P. Vaidyanathan. It is my greatest fortune to have him as my advisor. I appreciate so much his insightful inspiration and constant encouragement. Not only is he the best advisor, he is also the best friend. The friendship between us is what has been keeping me going for these years, and it will keep me going for the rest of my life. Without him, my graduate study would not have been meaningful. If there is ever a reason that I should want to stay being a student at Caltech, it is because of him. In him, I see a devoted educator and top-grade researcher, a role model which I found very difficult to follow. This is no way that I can thank him enough. I can only try to keep up with him (maybe one hundredth of his level) in my career, hoping that he will not regret once having a student like me.

I also want to thank Professors Yaser S. Abu-Mostafa, Joel N. Franklin, Robert J. McEliece, Edward C. Posner, and Dr. Marvin K. Simon. I appreciate their interest in and comments on my work, and their time serving in my examination committees. I am also extremely fortunate to be in classes taught by them and other professors at Caltech. I admire their excellent teaching and I know I will benefit from them when I become a professor myself in the future.

I would also like to thank Dr. Laif Swanson and Dr. Fabrizio Pollara at the Jet Propulsion Laboratory, for the opportunities of learning from their knowledge and working under their guidance.

I also wish to thank my colleagues and friends, Dr. Truong Nguyen, Dr. David Koilpillai, Dr. Vinay Sathe, Dr. Ian Galton, Dr. Tsz-Mei Ko, Dr. Petros Mouchtaris, Dr. Michael Mandell, Dr. Anand Soman, Igor Djoković, Ming-Chieh Lee, See-May Phoong, and Lin-Yuen Pei. I am grateful to them for the fruitful discussions and helpful criticism. I thank them and other friends of mine at Caltech, for those enjoyable moments which they have been so generous to share with me. Their presence adds a lot of pleasure to my life at Caltech.

Finally and most of all, I am grateful to my wife, Shufen. As a husband who is engaged in work most of the time, I thank her for supporting me for so many years. I thank her for sharing with me good times and bad times. In fact, with her by my side, I do not recall I have ever had any bad times. However, I owe her so much for those times she has had to spend alone because of my involvement in work. If there is anything that I can offer her, it would be my deepest love for her.

Abstract

Multidimensional (MD) multirate systems, which find applications in the coding and compression of image and video data, and in high definition television (HDTV) systems, have recently attracted much attention. Central to these systems is the idea of sampling lattices. The basic building blocks in an MD multirate system are the decimation matrix $\mathbf{M}$, the expansion matrix $\mathbf{L}$, and MD digital filters. When $\mathbf{M}$ and $\mathbf{L}$ are diagonal, most of the one-dimensional (1D) multirate results can be extended automatically, using separable approaches (i.e., separate operations in each dimension). Separable approaches are commonly used in practice due to their low complexity in implementation. However, nonseparable operations, with respect to nondiagonal decimation and expansion matrices, often provide more flexibility and better performance. Several applications, such as the conversion between progressive and interlaced video signals, actually require the use of nonseparable operations. For the nonseparable case, extensions of 1D results to the MD case are nontrivial. In this thesis, we will introduce some developments in these extensions. The three main results are: the design of nonseparable MD filters and filter banks derived from 1D filters, the commutativity of MD decimators and expanders and its applications to the efficient polyphase implementation of MD rational decimation systems, and the vector space framework for unifying MD filter bank and wavelet theory. In particular, properties of integer matrices like matrix fraction descriptions, coprimeness, the Bezout identity, etc., of which the polynomial versions are known in system theory, are used for the first time in the area of multirate signal processing.

Table of Contents

1. Introduction **1**

1.1. Nonseparable versus Separable Operations 2

1.2. Scope and Outline 7

2. Fundamentals of Multidimensional Multirate Systems **12**

2.1. Notations 12

2.2. Basic Building Blocks of Multidimensional Multirate Systems 13

2.3. Basic Concepts of MD Multirate Signal Processing 15

2.4. Multidimensional Filter Banks 17

2.5. Summary of Notations and Abbreviations 19

3. Multidimensional Filters and Filter Banks Derived from One-Dimensional Filters **22**

3.1. Introduction 22

3.2. The Impulse Response of An Ideal Lowpass Filter 24

3.3. Design Procedure 27

3.4. Efficient Implementation 33

3.5. Applications 35

3.6. Multidimensional Uniform DFT QMF Banks 36

3.7. Modification of the Design Procedure 48

3.8. Conclusions 51

4. The Role of Integer Matrices in Multidimensional Multirate Systems **52**

4.1. Introduction 52

4.2. Gcrd, Gcld, Lcrm, and Lclm 57

4.3. *Polyphase Implementation of Rational Sampling Rate Alteration* 62

4.4. *Multidimensional Delay-Chain Systems* 67

4.5. *Periodicity Matrices of Decimated Signals* 70

4.6. *Emerging Results from Other Authors* 73

4.7. *Concluding Remarks* 74

4.8. *Appendix* 74

5. Vector Space Framework for Unification of One-Dimensional and Multidimensional Filter Bank Theory 76

5.1. *Introduction* 76

5.2. *Analysis/Synthesis Scheme in the Vector Space Framework* 79

5.3. *Applications to Filter Banks* 85

5.4. *Filter Banks and Transmultiplexers* 90

5.5. *Linear Independence of Synthesis Vectors* 91

5.6. *Multidimensional Subband Convolution Theorem* 96

5.7. *The Wavelet Transform* 106

5.8. *Remarks and Conclusions* 108

5.9. *Appendices* 110

Bibliography 113

Alphabetical Listing by Authors 113

Selected References by Topic 120

List of Figures

Fig. 1.1-1. Various splitting of 2D signals: (a) and (b) are associated with separable operations, (c) is nonseparable, and (d) is separable four-band splitting. 3

Fig. 1.1-2. Nonseparable subband coding of the 'Lena' image: (a) frequency splitting, (b) the reconstructed image at 0.2021 bit/pixel. 4

Fig. 1.1-3. Separable subband coding of the 'Lena' image: (a) frequency splitting, (b) the reconstructed image at 0.2021 bit/pixel. 5

Fig. 1.1-4. Sampling lattices in the time-spatial domain for: (a) progressive signals, and (b) interlaced signals. 6

Fig. 1.2-1. Typical passband of decimation/interpolation filters. 7

Fig. 1.2-2. Interchange of a 1D decimator and a 1D expander. 8

Fig. 1.2-3. 1D rational decimation system. 9

Fig. 1.2-4. A 1D perfect reconstruction system. 9

Fig. 1.2-5. 1D delay-chain system. 9

Fig. 2.2-1. 1D (a) decimation system and (b) interpolation system. 14

Fig. 2.2-2. MD (a) decimation system and (b) interpolation system. 15

Fig. 2.3-1. Noble identities. 16

Fig. 2.3-2. Polyphase Identity. 17

Fig. 2.4-1. MD filter bank. 18

Fig. 3.2-1. Frequency response of an ideal lowpass filter. 25

Fig. 3.3-1. Frequency response of filters in Design Example 3.1: (a) $P_F(\omega)$, (b) $H_F^{(s)}(\omega)$, (c) $H_F(\omega)$. 30

Fig. 3.3-2. The filter $G_F(\omega)$ in Design Example 3.2: (a) desired passband, (b) frequency response. 31

Fig. 3.4-1. Efficient implementation of an MD filter. 34

Fig. 3.5-1. The generating vectors of a 2D parallelepiped. 36

Fig. 3.5-2. Filters which can be obtained by using the proposed method. 37

Fig. 3.6-1. MD uniform DFT QMF bank. 38

Fig. 3.6-2. Frequency response of filters in Design Example 3.3: (a) $P_{F,0}(\omega)$, (b) $H_{F,\mathbf{m}_0}(\omega)$, (c) $T_F(\omega)$. 44

Fig. 3.6-3. Passband supports of analysis filters in Design Example 3.4. 45

Fig. 3.6-4. Frequency response of filters in Design Example 3.4: (a) $P_{F,0}(\omega)$, (b) $H_{F,\mathbf{m}_0}(\omega)$, (c) $T_F(\omega)$. 46

Fig. 3.6-5. 1D IIR QMF bank with no AMD. 47

Fig. 3.6-6. Polyphase implementation of an MD IIR QMF bank. 47

Fig. 3.6-7. MD IIR QMF bank with PR property (Design Example 3.6). 48

Fig. 3.6-8. Frequency response of filters in Design Example 3.5: (a) $P_{F,0}(\omega)$, (b) $H_{F,\mathbf{m}_0}(\omega)$, (c) $T_F(\omega)$. 49

Fig. 3.6-9. Group delays of Design Example 3.5: (a) $\tau_0(\omega)$, (b) $\tau_1(\omega)$. 50

Fig. 4.1-1. 1D rational decimation system. 54

Fig. 4.1-2. Two types of polyphase implementations of a 1D rational decimation system. .. 54

Fig. 4.1-3. Successive redrawing of polyphase implementations of a 1D rational decimation system. 55

Fig. 4.1-4. 1D delay-chain system. 56

Fig. 4.3-1. MD rational decimation system. 62

Fig. 4.3-2. Two types of polyphase implementations of an MD rational decimation system. 63

Fig. 4.3-3. Successive redrawing of polyphase implementations of an MD rational decimation system. 64

Fig. 4.3-4. Interchange of an MD decimator and an MD expander. 65

Fig. 4.4-1. MD delay-chain system. 68

Fig. 4.4-2. MD delay-chain system redrawn. 69

Fig. 4.5-1. Decimation of MD signals. 72

Fig. 4.6-1. Relaxed commutativity. 73

Fig. 5.1-1. 1D uniformly decimated filter bank. 77

Fig. 5.1-2. MD nonuniform rational filter bank. 78

Fig. 5.4-1. MD transmultiplexer. 90

Fig. 5.5-1. MD uniform maximally decimated filter bank. 92

Fig. 5.5-2. MD uniform synthesis filter bank. 93

Fig. 5.5-3. One branch of an MD uniformly decimated filter bank converted from a nonuniform filter bank. 96

Fig. 5.6-1. MD PR rational filter bank, (a) with input $x(\mathbf{n})$, and (b) with input $g(\mathbf{n})$. 97

Fig. 5.6-2. MD PR uniform filter bank, (a) with input $x(\mathbf{n})$, and (b) with input $g(\mathbf{n})$. 98

Fig. 5.6-3. MD PR rational filter bank, with interchanged analysis and synthesis filters, and with input $y(\mathbf{n})$. 100

Fig. 5.6-4. MD subband convolution of $x(\mathbf{n})$ and $y(\mathbf{n})$. 101

Fig. 5.6-5. Obtaining the $\mathbf{L}$-fold decimated version of $x(\mathbf{n}) * y(\mathbf{n})$. 103

Fig. 5.7-1. Filter bank implementation of a DWT/IDWT system with input $x(t)$. The signal $x_{\mathrm{DWT}}(k, n)$ in this figure indicates a continuous-time impulse train. 108

Fig. 5.7-2. DWT subband convolution of $x(t)$ and $y(t)$. 109

1

Introduction

For the one-dimensional (1D) case, multirate techniques allow the sampling rate in a system to vary from point to point. The basic building blocks are decimators and expanders (also referred to as downsamplers and upsamplers, respectively) [Crochiere and Rabiner, 1983], [Vetterli, 1987], [Vaidyanathan, 1990a]. A typical application of 1D multirate systems is the subband coding of speech [Crochiere et al., 1976],[Jayant and Noll, 1984] and music [Veldhuis et al., 1989]. For a recent review of 1D multirate signal processing, see [Vaidyanathan, 1990a].

Recently, these multirate ideas have been extended to two and higher dimensional systems by a number of authors. Multidimensional (MD) multirate systems find applications in the coding and compression of image and video data [Vetterli, 1984], [Woods and O'Neil, 1986], [Gharavi and Tabatabai, 1988], [Smith and Eddins, 1990], [Woods, 1991], [Bamberger and Smith, 1992], in sampling format conversions between various video standards [Mersereau and Speake, 1983], [Dubois, 1985], high-definition television (HDTV) systems [Vetterli, Kovačević, and Le Gall, 1990], [Rao and Yip, 1990], [Kunt, 1992], and so on. Central to these systems is the idea of lattices [Cassels, 1959], [Newman, 1972] which is closely related to the concepts of MD generalized sampling [Petersen and Middleton, 1962], decimation, and expansion.

An excellent review of MD multirate systems including key notations and concepts is given in [Viscito and Allebach, 1991]. Chapter 2 of this thesis also provides a summary of these. The key building blocks in MD multirate systems are the decimation matrix $\mathbf{M}$ and the expansion matrix $\mathbf{L}$. With D denoting the number of dimensions, these are $D \times D$ nonsingular integer matrices. When these matrices are diagonal, most of the 1D results can be extended automatically by performing operations in each dimension *separately.* However, for the nondiagonal case, these extensions are nontrivial and require more complicated notations and matrix operations. Some of these extensions, e.g., polyphase decomposition and maximally decimated perfect reconstruction (PR) systems, have already been successfully made by some authors [Vetterli, 1984], [Ansari and Lau, 1987], [Ansari and Lee, 1988], [Viscito and Allebach, 1988], [Liu and Vaidyanathan, 1988], [Karlsson and Vetterli, 1990], [Vaidyanathan, 1990b], [Viscito and Allebach, 1991]. However, there still exist several 1D results in multirate processing, for which the MD extensions are even more difficult. These nonseparable extensions are the major results of this thesis.

1.1. NONSEPARABLE VERSUS SEPARABLE OPERATIONS

In practice, separable operations are mostly used because of their low implementation complexity. However, nonseparable operations with respect to nondiagonal decimation/expansion matrices are also very important from both theoretical and practical points of view. Nonseparable operations, which include separable operations as a special case, offer more flexibility and better performance, and are required in some applications.

As an example, consider the subband coding scheme, where we want to separate a signal into a number of subbands, with each subband corresponding to signal components in a certain frequency band. These subband signals are then decimated and quantized. Consider the case where we want to separate a two-dimensional image into two parts, the 'low' frequency band and the 'high' frequency band. Suppose only separable operations (separable filtering) are allowed. We can split the signal into two bands with respect to either the horizontal frequency ω_0 or the vertical frequency ω_1, as shown in Fig. 1.1-1(a) and Fig. 1.1-1(b).

However, if nonseparable operations (nonseparable filters) are used, we can split the image as in Fig. 1.1-1(c), where the center square represents the low frequency band and the rest represents the high frequency band. We see that the low frequency band in Fig. 1.1-1(c) is more desirable for this purpose, while those in Fig. 1.1-1(a) and Fig. 1.1-1(b) are elongated either in ω_0 or ω_1. This shows the flexibility offered by nonseparable operations. To get more 'regular' subband supports (i.e., supports which are unchanged when ω_0 and ω_1 are interchanged) when only separable filtering is allowed, we need to use the four-band splitting shown in Fig. 1.1-1(d).

For some applications, e.g., multiresolution signal decomposition [Mallat, 1989], the frequency splitting is performed repeatedly on the low frequency band, such that at each step the 'resolution' of the resulting low band signal is decreased by some factor. For example, if we start from Fig. 1.1-1(c) (nonseparable) and repeatedly split the low band signal using the same splitting, we get the frequency spitting in Fig. 1.1-2(a).

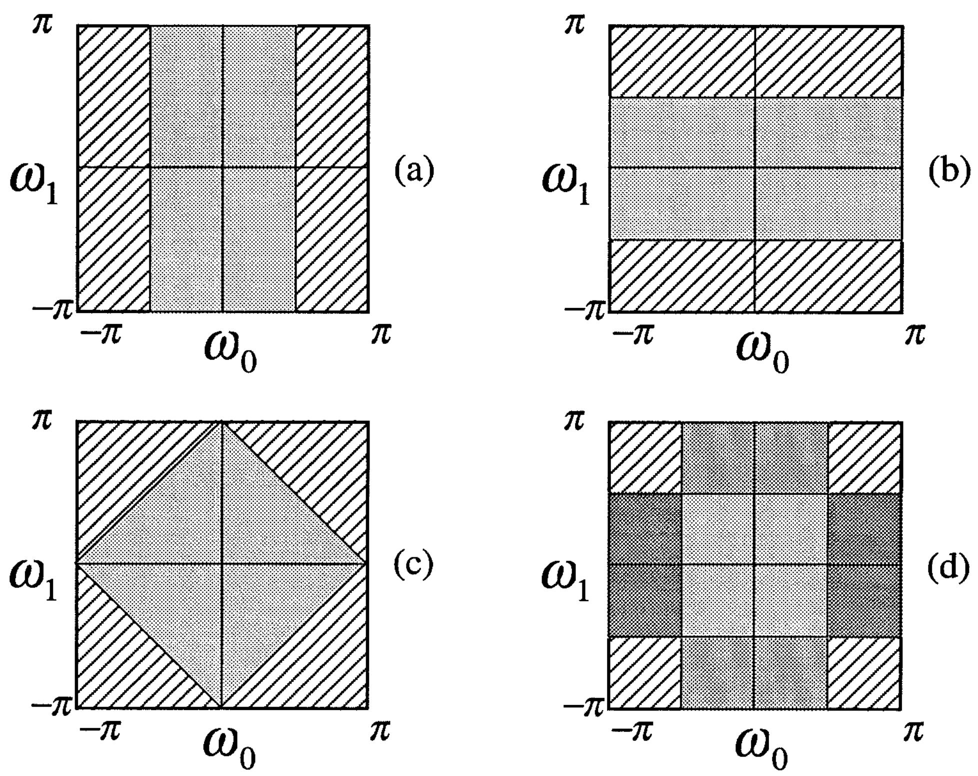

Figure 1.1-1 Various splitting of 2D signals: (a) and (b) are associated with separable operations, (c) is nonseparable, and (d) is separable four-band splitting.

On the other hand, if we start from Fig. 1.1-1(a) and (b) (separable), we get the frequency spitting in Fig. 1.1-3(a). Although both nonseparable and separable approaches provide a resolution reduction factor of one half at each step, we see that Fig. 1.1-3(a) is less desirable because the subband supports are not as regular as those in Fig. 1.1-2(a). Of course, we can start from the separable four-band splitting in Fig. 1.1-1(d) to get more regular subband supports, but in this case the resolution reduction factor at each step is one quarter, instead of one half.

Nonseparable operations give better performance, too. Consider the application of subband coding again. With nonseparable operations, we can split an image in the frequency domain into nine subband signals (Fig. 1.1-2(a)). Since these subband signals are bandlimited, they can be decimated (see Section 9 for more details) to keep the total number of samples unchanged. We then quantize these decimated signals according to their energy. (In practice, perceptual properties of the human visual system are also taken into account.) For example, since the energy of most real-world images tends to concentrate in the low frequency region, we usually assign a larger number of bits

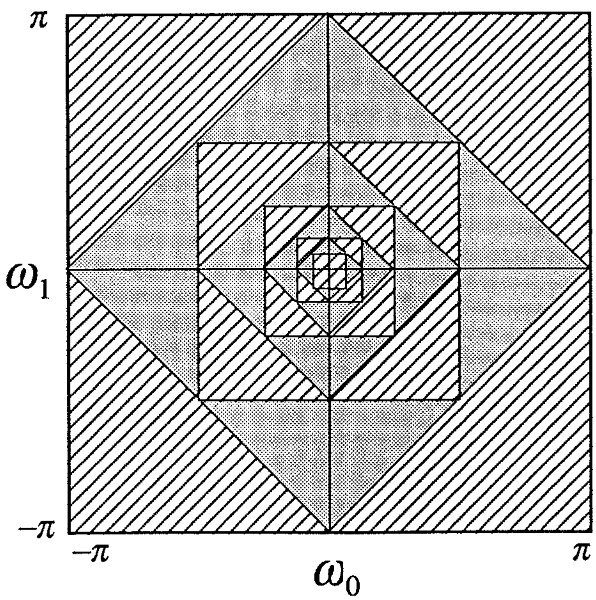

(a)

(b)

Figure 1.1-2 Nonseparable subband coding of the 'Lena' image: (a) frequency splitting, (b) the reconstructed image at 0.2021 bit/pixel.

to a lower frequency band. By doing these, we reduce the data rate of images. These signals are then recombined to reconstruct the original image. Fig. 1.1-2(b) shows the reconstructed image of

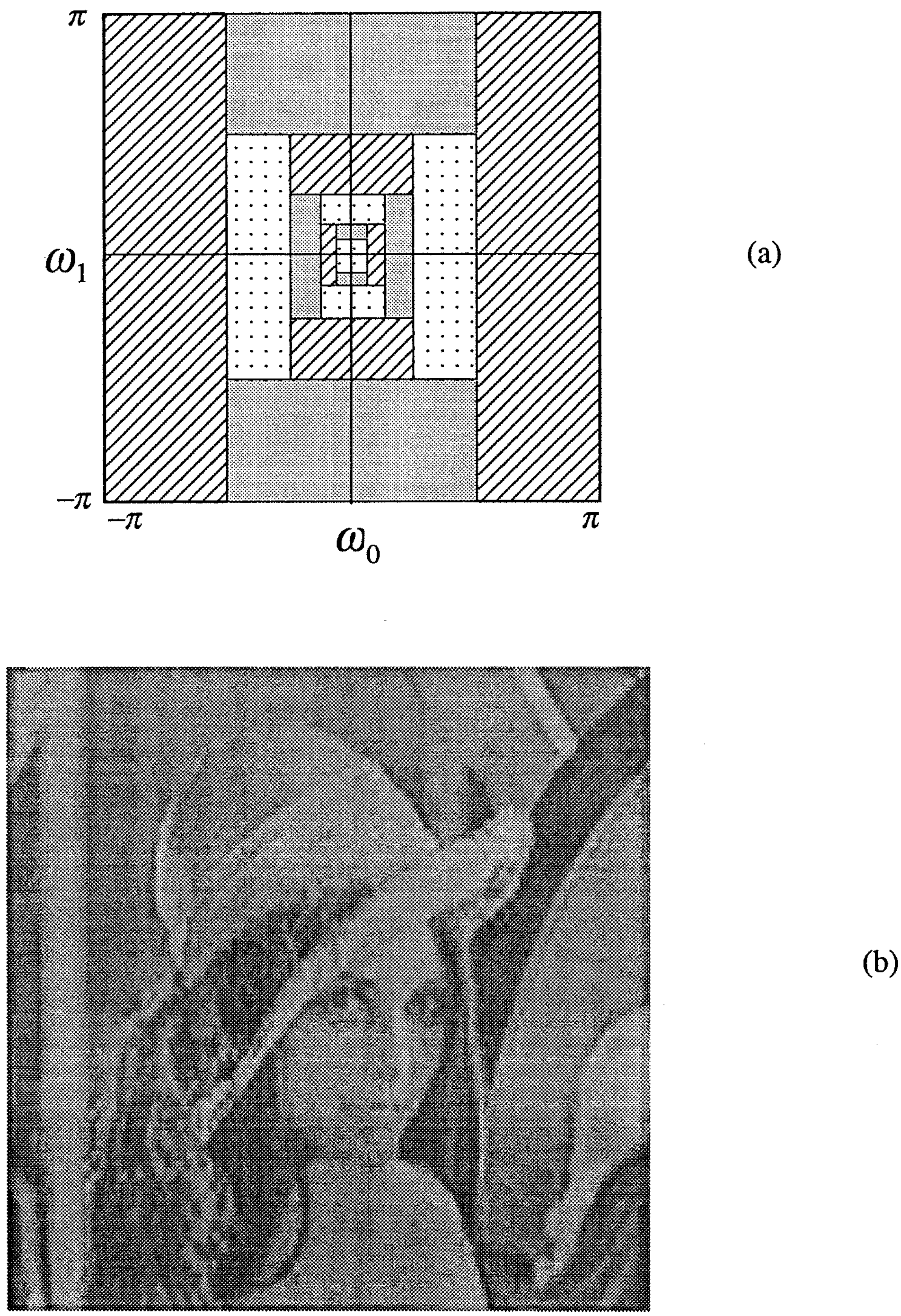

Figure 1.1-3 Separable subband coding of the 'Lena' image: (a) frequency splitting, (b) the reconstructed image at 0.2021 bit/pixel.

'Lena' which has been quantized to 0.2021 bit per pixel. On the other hand, by using only separable

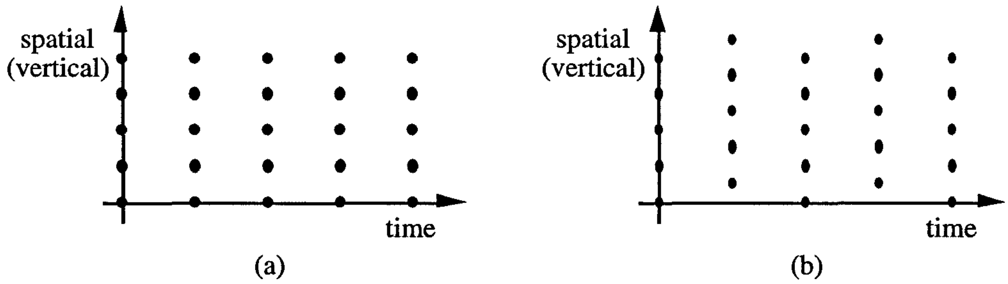

Figure 1.1-4 Sampling lattices in the time-spatial domain for: (a) progressive signals, and (b) interlaced signals.

filtering, we can obtain the splitting as in Fig. 1.1-3(a). For this case, the reconstructed image of 'Lena' (quantized with the same bit rate, 0.2021 bit/pixel) is shown in Fig. 1.1-3(b). We can see the better performance obtained by using nonseparable operations in this example.

Remark: The purpose of the above example is only to compare the performance of separable operations and nonseparable operations. By using more complicated coding schemes on the subband signals, e.g., vector quantization, adaptive bit allocation, etc., coded images with higher quality and lower bit rate can be obtained [Rao and Yip, 1990], [Woods, 1991], [Malvar, 1992]. However, those are not the main points of this example.

For some applications, nonseparable operations are required. The conversion between progressive and interlaced video signals is one example [Dubois, 1985], [Vetterli, Kovačević, and Le Gall, 1990]. Progressive signals are obtained by sampling video signals on a rectangular lattice in the time-spatial(vertical) domain, as shown in Fig. 1.1-4(a). On the other hand, interlaced signals are obtained by sampling on a nonseparable lattice shown in Fig. 1.1-4(b), which is also called the quincunx lattice. The conversion between these two kinds of signals can be achieved by expansion, filtering, and decimation. All of these require nonseparable operations. Another example is directional subband coding, where nondiagonal decimators and nonseparable filters are used to extract image components in different directions [Bamberger, 1990], [Bamberger and Smith, 1992].

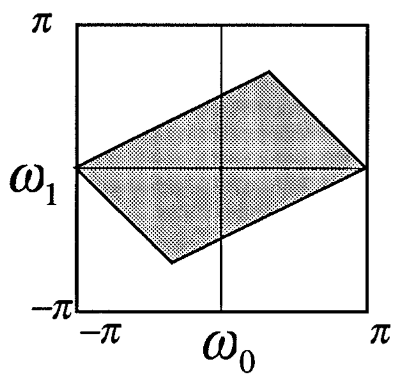

Figure 1.2-1 Typical passband of decimation/interpolation filters.

1.2. SCOPE AND OUTLINE

In Chapter 2, we first introduce the notations used in the thesis and some fundamentals of MD multirate systems. We then present the three main results of the thesis in the following chapters. These results are summarized below.

MD Filters and Filter Banks Derived From 1D Filters (Chapter 3)

In MD multirate signal processing, filters with parallelepiped-shaped passband supports are required to avoid aliasing which may be caused by decimation, and to eliminate image components due to expansion (see Section 2.2). With **M** denoting the decimation/expansion matrix, these filters typically have passband in the region

$$\boldsymbol{\omega} = \pi \mathbf{M}^{-T}\mathbf{x} \quad \mathbf{x} \in [-1, 1)^D. \tag{1.2.1}$$

In the MD frequency domain, such region forms a parallelepiped. In the 2D case, this region becomes a parallelogram defined by

$$-\pi \leq M_{00}\omega_0 + M_{10}\omega_1 < \pi, \ -\pi \leq M_{01}\omega_0 + M_{11}\omega_1 < \pi, \tag{1.2.2}$$

where M_{ij}'s are the elements of the 2×2 matrix **M** (as in [Ansari and Lau, 1987], [Ansari and Lee, 1988], [Bamberger, 1990], [Bamberger and Smith, 1992]). Fig. 1.2-1 shows this region for the case

$$\mathbf{M} = \begin{bmatrix} 1 & -1 \\ 1 & 2 \end{bmatrix}. \tag{1.2.3}$$

Clearly, when **M** is not diagonal, these filters are not separable.

Both the design and implementation of nonseparable filters are more complex than those of separable filters [Dudgeon and Mersereau, 1984]. In fact, the complexity grows *exponentially* with

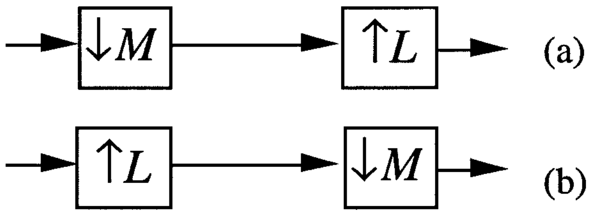

Figure 1.2-2 Interchange of a 1D decimator and a 1D expander.

the number of dimensions D. Some authors have proposed efficient techniques for the design of some 2D special filters, e.g., fan filters, diamond-shaped filters, and directional filters, by starting from 1D prototype filters [Ansari and Lau, 1987], [Ansari, 1987], [Ansari and Lee, 1988], [Renfors, 1989], [Bamberger, 1990], [Bamberger and Smith, 1992]. In Chapter 2, we will describe a general method which works for an arbitrary number of dimensions and arbitrary $\mathbf{M}$ [Chen and Vaidyanathan, 1991], [Chen and Vaidyanathan, 1993d]. With this method, every filter having a parallelepiped-shaped passband support can be obtained by first designing an appropriate 1D prototype filter and then performing a simple transformation. Not only filters, MD filter banks can be designed, too. Hence, with this method, the design as well as implementation complexity only grows *linearly* with the number of dimensions.

Integer Matrices and MD Multirate Systems (Chapter 4)

The greatest common divisor (gcd), least common multiple (lcm), and coprimeness of integers are well-known and appear in the contexts of 1D multirate systems very often. Here are some examples:

1. An M-fold decimator and an L-fold expander can be interchanged (i.e., the system in Fig. 1.2-2(a) is equivalent to the system in Fig. 1.2-2(b)) if and only if M and L are relatively prime (coprime) [Vaidyanathan, 1990a].
2. Rational decimation systems, as shown in Fig. 1.2-3, play a very important role in audio systems. This scheme permits us to alter the sampling rate of a sequence by a rational number M/L. The filter $H(z)$ is used to suppress image components generated by the L-fold expander and eliminate aliasing due to the M-fold decimator. Note that the implementation in Fig. 1.2-3 has the disadvantage that the filter $H(z)$ has to operate at a higher rate, i.e., L times the input rate. It turns out that we can improve the efficiency by using the technique introduced in [Hsiao, 1987]. We shall refer to this technique as the rational polyphase implementation (RPI). The RPI technique works if and only if M and L are coprime.

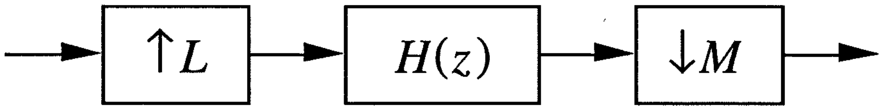

Figure 1.2-3 1D rational decimation system.

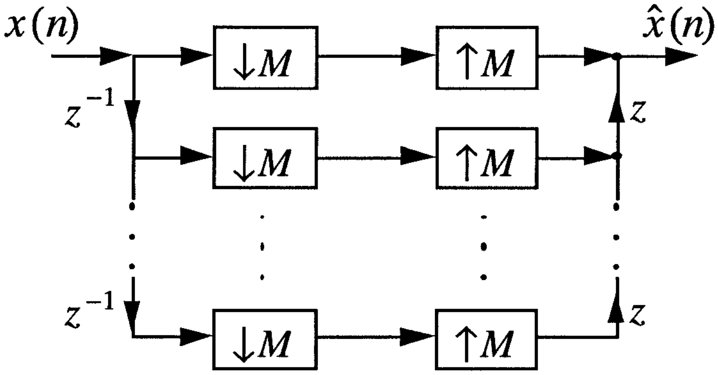

Figure 1.2-4 A 1D perfect reconstruction system.

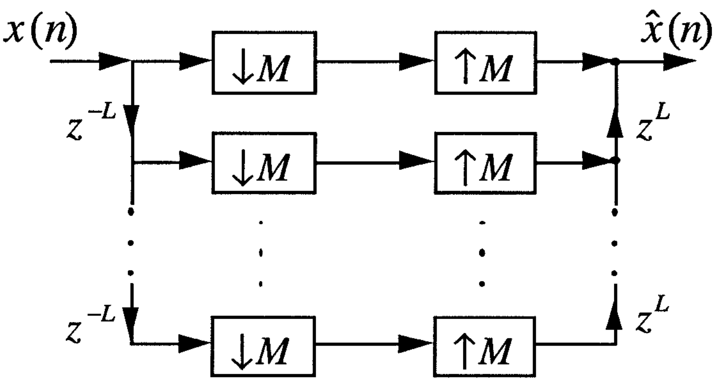

Figure 1.2-5 1D delay-chain system.

3. It is easily verified that the system in Fig. 1.2-4 is a PR system, i.e., $\widehat{x}(n) = x(n)$. This system is fundamental to many 1D maximally decimated PR filter banks [Vaidyanathan, 1990a]. We can generalize this by replacing every z with z^L and obtain the so-called delay-chain system in Fig. 1.2-5. This system is a PR system if and only if L and M are coprime [Nguyen and Vaidyanathan, 1988, Lemma A.2]. The case where $L \neq 1$ is required in some applications where pairs of analysis filters are constrained by symmetry conditions [Nguyen and Vaidyanathan, 1988].

4. When a periodic signal $x(n)$ with period L is decimated by a factor of M to obtain $y(n) = x(Mn)$, the period of $y(n)$ is $L/\gcd(M, L) = \text{lcm}(M, L)/M$. Also, when a *cyclo-wide-sense-stationary* (CWSS) random sequence $x(n)$ with period L is decimated by M, the resulting sequence is still CWSS, and has period $L/\gcd(M, L) = \text{lcm}(M, L)/M$ [Sathe and Vaidyanathan, 1993].

In Chapter 4, we shall extend all these ideas to the MD case. To do so, we need the concepts of gcd, lcm, and coprimeness for *matrices.* For polynomial matrices, the greatest common left/right divisors (gcld/gcrd), right/left coprimeness, matrix fraction descriptions, the Smith-form, the Smith-McMillan form, and so on, are well-known in the system theory area [Gantmacher, 1977], [Kailath, 1980], [Vidyasagar, 1985]. In fact, these properties can be also applied to the integer matrix case. In Chapter 4, we will introduce the concepts of least common right multiples (lcrm) and least common left multiples (lclm), and several properties of them. By using all these tools, we can extend the above-mentioned four issues to the MD case. The following results, which appeared in [Chen and Vaidyanathan, 1992a], [Chen and Vaidyanathan, 1992b], [Chen and Vaidyanathan, 1993a], can be obtained:

1. An $\mathbf{M}$-fold decimator and an $\mathbf{L}$-fold expander are interchangeable if and only if $\mathbf{M}$ and $\mathbf{L}$ commute (i.e., $\mathbf{ML} = \mathbf{LM}$) and are coprime. In general, we have to distinguish right coprimeness and left coprimeness for the matrix case. However, we will show that when $\mathbf{ML} = \mathbf{LM}$, right coprimeness and left coprimeness are equivalent. This interchangeability problem was first addressed in [Kovačević and Vetterli, 1991b] for upper triangular $\mathbf{M}$ and $\mathbf{L}$ in the 2D case.

2. An MD decimation system with rational decimation ratio (in this case, a matrix) $\mathbf{H} = \mathbf{L}^{-1}\mathbf{M}$ finds applications in the conversion of images or video data between different sampling standards. MD rational decimation systems can be implemented efficiently by using the so-called MD RPI technique whenever $\mathbf{M}$ and $\mathbf{L}$ are left coprime (Section 4.3).

3. An MD delay-chain system (which is an extension of Fig. 1.2-5, to be defined later) is a PR system if $\mathbf{LM}$ is an lcrm of of $\mathbf{M}$ and $\mathbf{L}$. However, the necessary condition for this is still an open problem. One potential application of MD delay-chain systems is to design MD filter banks where the analysis and synthesis filters have a certain symmetry. The research on this is under progress.

4. When an MD periodic signal $x(\mathbf{n})$ with periodicity matrix $\mathbf{L}$ is decimated by a factor of $\mathbf{M}$, the periodicity matrix of the resulting sequence is $\mathbf{M}^{-1}\,\text{lcrm}(\mathbf{M}, \mathbf{L})$, where lcrm(M,L) denotes an lcrm of $\mathbf{M}$ and $\mathbf{L}$. A similar result holds for the random signal case.

The Vector Space Framework and Filter Bank Theory (Chapter 5)

A number of results in filter bank theory can be viewed using vector space notations. This simplifies the proofs of many important results. In Chapter 5, we will introduce the framework of vector space, and then use this framework to derive some known and some new filter bank results as well. For example, the relation among the Hermitian image property, orthonormality, and the perfect reconstruction (PR) property is well-known for the case of one-dimensional (1D) analysis/synthesis filter banks [Vaidyanathan, 1987b]. We can prove the same result in a more general vector space setting. We will show that even the most general filter banks, namely, *multidimensional nonuniform filter banks* with *rational* decimation matrices, become a special case of this vector space framework. Therefore, many results in 1D filter bank theory are hence extended to the multidimensional case. Some examples are: the equivalence of biorthonormality and the PR property, the interchangeability of analysis and synthesis filters, the connection between analysis/synthesis filter banks and synthesis/analysis transmultiplexers, etc. We can also obtain the subband convolution scheme by starting from the generalized Parseval's relation in vector space notations. Furthermore, several theoretical results of wavelet transform can also be derived using this framework, including the wavelet convolution theorem.

2

Fundamentals of Multidimensional Multirate Systems

An excellent review of multidimensional (MD) multirate systems including key notations and concepts is given in [Viscito and Allebach, 1991]. Some of the notations we use in this thesis are slightly modified versions of those in [Viscito and Allebach, 1991], and suit our discussions better. Other basic concepts of MD multirate signal processing can be found in [Dudgeon and Mersereau, 1984], [Vetterli, 1984], [Dubois, 1985], [Karlsson and Vetterli, 1990], [Vaidyanathan, 1990b], [Vaidyanathan, 1993a, Chapter 12]. In this chapter, we will present some fundamentals of MD signal processing which are crucial for our discussions in the following chapters.

2.1. NOTATIONS

Through out the thesis, we use lowercase boldfaced letters to denote vectors (mostly column vectors, unless specified otherwise), and capital boldfaced letters to denote matrices. The symbol $\mathbf{I}_k$ denotes the $k \times k$ identity matrix (with subscript often omitted). The notations $\mathbf{A}^T$, $\mathbf{A}^{-1}$, $\mathbf{A}^{-T}$, and $\mathbf{A}^*$ denote the transpose, the inverse, and the inverse transpose, and the conjugate of the matrix $\mathbf{A}$, respectively. The row and column indices typically begin from zero. With D denoting the number of dimensions, $\mathbf{n} = [n_0 \quad n_1 \quad \cdots \quad n_{D-1}]^T$ is the 'time'-domain index of MD discrete signals. For example, $x(\mathbf{n})$ in the two-dimensional (2D) case represents an image. Note that all n_i's are integers. The symbol $\mathcal{N}$ denotes the set of all $D \times 1$ integer vectors. Therefore, we have $\mathbf{n} \in \mathcal{N}$. The real vector $\boldsymbol{\omega} = [\omega_0 \quad \omega_1 \quad \cdots \quad \omega_{D-1}]^T$ is the frequency-domain variable of MD signals. For example, $X_F(\boldsymbol{\omega})$ represents the Fourier transform of $x(\mathbf{n})$ and is defined as

$$X_F(\boldsymbol{\omega}) = \sum_{\mathbf{n} \in \mathcal{N}} x(\mathbf{n})\, e^{-j\boldsymbol{\omega}^T \mathbf{n}} \tag{2.1.1}$$

if the summation converges. By definition, the Fourier transform of an MD signal has periodicity matrix $2\pi\mathbf{I}$ (see Section 2.3). The inverse Fourier transform is given by

$$x(\mathbf{n}) = \frac{1}{(2\pi)^D} \int_{\boldsymbol{\omega}\in[-\pi,\pi)^D} X_F(\boldsymbol{\omega})\, e^{j\boldsymbol{\omega}^T\mathbf{n}}\, d\boldsymbol{\omega} \tag{2.1.2}$$

where $[a,b)^D$ denotes the set of $D \times 1$ real vectors $\mathbf{x}$ with components x_i in the range $a \leq x_i < b$. We say $x(\mathbf{n})$ and $X_F(\boldsymbol{\omega})$ form a Fourier transform pair, and denote this as

$$x(\mathbf{n}) \longleftrightarrow X_F(\boldsymbol{\omega}). \tag{2.1.3}$$

For the one-dimensional (1D) case, i.e., $D = 1$, $X_F(\omega)$ is also written as $X(e^{j\omega})$ which shows the periodicity of 2π explicitly.

The complex vector $\mathbf{z} = [\,z_0 \quad z_1 \quad \cdots \quad z_{D-1}\,]^T$ is the variable of the $\mathbf{z}$-transform of MD signals. For example, the $\mathbf{z}$-transform of $x(\mathbf{n})$, where it converges, is given by

$$X(\mathbf{z}) = \sum_{\mathbf{n}\in\mathcal{N}} x(\mathbf{n})\, \mathbf{z}^{-\mathbf{n}}. \tag{2.1.4}$$

Note that a vector raised to a vector power, as in $\mathbf{z}^{-\mathbf{n}}$ above, gives a scalar defined as

$$\mathbf{z}^{\mathbf{n}} \triangleq z_0^{n_0} z_1^{n_1} \cdots z_{D-1}^{n_{D-1}}. \tag{2.1.5}$$

We say $x(\mathbf{n})$ and $X(\mathbf{z})$ form a $\mathbf{z}$-transform pair, which is denoted as

$$x(\mathbf{n}) \longleftrightarrow X(\mathbf{z}). \tag{2.1.6}$$

Note also the subscript F is used to distinguish the Fourier transform from the $\mathbf{z}$-transform. It is clear that $X_F(\boldsymbol{\omega})$ can be obtained by evaluating $X(\mathbf{z})$ at $z_i = e^{j\omega_i}$ for $i = 0, \ldots, D-1$, if it exists.

2.2. BASIC BUILDING BLOCKS OF MULTIDIMENSIONAL MULTIRATE SYSTEMS

Decimation

The $\mathbf{M}$-fold decimated version of $x(\mathbf{n})$ is defined as $y(\mathbf{n}) = x(\mathbf{Mn})$, where $\mathbf{M}$ is a nonsingular integer matrix called the decimation matrix. In the frequency domain, the relation is

$$Y_F(\boldsymbol{\omega}) = \frac{1}{J(\mathbf{M})} \sum_{\mathbf{k}\in\mathcal{N}(\mathbf{M}^T)} X_F\big(\mathbf{M}^{-T}(\boldsymbol{\omega} - 2\pi\mathbf{k})\big) \tag{2.2.1}$$

where $\mathcal{N}(\mathbf{M}^T)$ is the set of all integer vectors of the form $\mathbf{M}^T\mathbf{x}$, $\mathbf{x} \in [0,1)^D$. Also, $J(\mathbf{M})$ denotes the absolute determinant of $\mathbf{M}$, i.e., $|\det \mathbf{M}|$. This is equal to the number of elements in $\mathcal{N}(\mathbf{M})$ and the number of elements in $\mathcal{N}(\mathbf{M}^T)$. The $\mathbf{z}$-domain relation of decimation requires more involved notations [Viscito and Allebach, 1991]. Fortunately, for the theoretic derivations of MD multirate results, the frequency-domain relation shown above is usually enough.

Expansion

For a nonsingular integer matrix $\mathbf{L}$, the $\mathbf{L}$-fold expanded version of $x(\mathbf{n})$ is defined as

$$y(\mathbf{n}) = \begin{cases} x(\mathbf{L}^{-1}\mathbf{n}) & \mathbf{n} \in LAT(\mathbf{L}) \\ 0 & \text{otherwise.} \end{cases} \tag{2.2.2}$$

In the above equation, $LAT(\mathbf{L})$ (the *lattice* generated by $\mathbf{L}$ [Cassels, 1959], [Newman, 1972], [Dubois, 1985]) denotes the set of all vectors of the form $\mathbf{Lm}$, $\mathbf{m} \in \mathcal{N}$. Clearly, the condition $\mathbf{n} \in LAT(\mathbf{L})$ above is equivalent to $\mathbf{L}^{-1}\mathbf{n} \in \mathcal{N}$. The matrix $\mathbf{L}$ is called the expansion matrix. The corresponding frequency-domain relation of expansion is

$$Y_F(\boldsymbol{\omega}) = X_F(\mathbf{L}^T\boldsymbol{\omega}). \tag{2.2.3}$$

In the $\mathbf{z}$ domain, the relation becomes

$$Y(\mathbf{z}) = X(\mathbf{z}^{\mathbf{L}}). \tag{2.2.4}$$

The notation of a vector raised to a matrix power, as in $\mathbf{z}^{\mathbf{L}}$ above, is a $D \times 1$ vector defined as

$$\mathbf{z}^{\mathbf{P}} \triangleq [\mathbf{z}^{\mathbf{p}_0} \quad \mathbf{z}^{\mathbf{p}_1} \quad \ldots \mathbf{z}^{\mathbf{p}_{D-1}}]^T \tag{2.2.5}$$

where $\mathbf{p}_i$ is the ith column of $\mathbf{P}$.

Decimation Filters and Interpolation Filters

For the 1D case, the input to a decimator is usually pre-filtered by a so-called 'decimation filter' to avoid aliasing. On the other hand, the expander is usually followed by an 'interpolation filter' to suppress the image components due to the expander. These are shown in Fig. 2.2-1. For M-fold decimation/expansion, the decimation/interpolation filter typically has passband in the range $\omega \in [-\pi/M, \pi/M)$ [Vaidyanathan, 1990a].

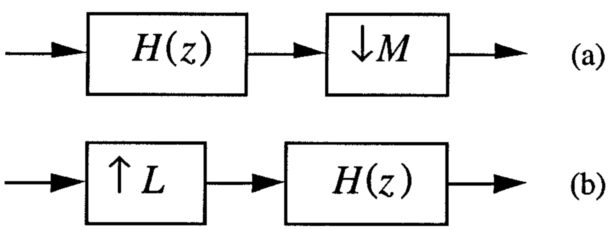

Figure 2.2-1 1D (a) decimation system and (b) interpolation system.

For MD decimation and expansion also, such filters are necessary, as indicated in Fig. 2.2-2. Given the decimation/expansion matrix $\mathbf{M}$, these filters typically have parallelepiped-shaped passband support in the region

$$\boldsymbol{\omega} = \pi\mathbf{M}^{-T}\mathbf{x} + 2\pi\mathbf{k}, \qquad \mathbf{x} \in [-1,1)^D,\ \mathbf{k} \in \mathcal{N}. \tag{2.2.6}$$

Note that some other choices of passband regions are possible [Bamberger, 1990], [Chen and Vaidyanathan, 1993c]. We see that the region specified in (2.2.6) is symmetric with respect to the origin. We can use an abbreviated notation to indicate the above region. Let $SPD(\mathbf{V})$ (Symmetric ParallelepipeD of $\mathbf{V}$) denote the set of all real vectors of the form $\mathbf{Vx}$, where $\mathbf{x} \in [-1,1)^D$. We can rewrite (2.2.6) as

$$\boldsymbol{\omega} \in SPD(\pi\mathbf{M}^{-T}) + 2\pi\mathbf{k}, \qquad \mathbf{k} \in \mathcal{N}. \tag{2.2.7}$$

Recall that Fig. 1.2-1 shows the typical passband $SPD(\pi\mathbf{M}^{-T})$ for the $\mathbf{M}$ given in (1.2.3).

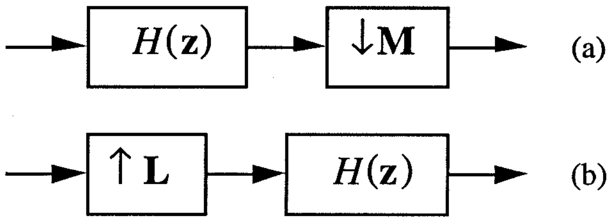

Figure 2.2-2 MD (a) decimation system and (b) interpolation system.

Remark: The term $2\pi\mathbf{k}$ in either (2.2.6) or (2.2.7) shows that $SPD(\pi\mathbf{M}^{-T})$ is repeated every 2π in each dimension. We often say that the passband support of the filter is given by $SPD(\pi\mathbf{M}^{-T})$, and take the periodicity for granted, i.e., do not show the term $2\pi\mathbf{k}$ explicitly.

2.3. BASIC CONCEPTS OF MD MULTIRATE SIGNAL PROCESSING

Division Theorem for Integer Vectors

Every integer vector $\mathbf{n}$ can be expressed as $\mathbf{n} = \mathbf{k} + \mathbf{M}\mathbf{n}_0$, for some $\mathbf{k} \in \mathcal{N}(\mathbf{M})$, and $\mathbf{n}_0 \in \mathcal{N}$. Moreover, $\mathbf{k}$ and $\mathbf{n}_0$ are unique for a given $\mathbf{n}$. We denote this relation as $\mathbf{k} = \mathbf{n} \bmod \mathbf{M}$, or $\mathbf{k} = ((\mathbf{n}))_{\mathbf{M}}$, and say $\mathbf{k}$ is the "remainder" of the division.

Multidimensional Polyphase Decomposition

The polyphase components of $x(\mathbf{n})$ with respect to a given $\mathbf{M}$ are defined as

$$\begin{aligned} &e_{\mathbf{k}}(\mathbf{n}) = x(\mathbf{Mn} + \mathbf{k}), \qquad \text{(Type 1)} \\ \text{or}\quad &r_{\mathbf{k}}(\mathbf{n}) = x(\mathbf{Mn} - \mathbf{k}), \qquad \text{(Type 2)} \end{aligned} \tag{2.3.1}$$

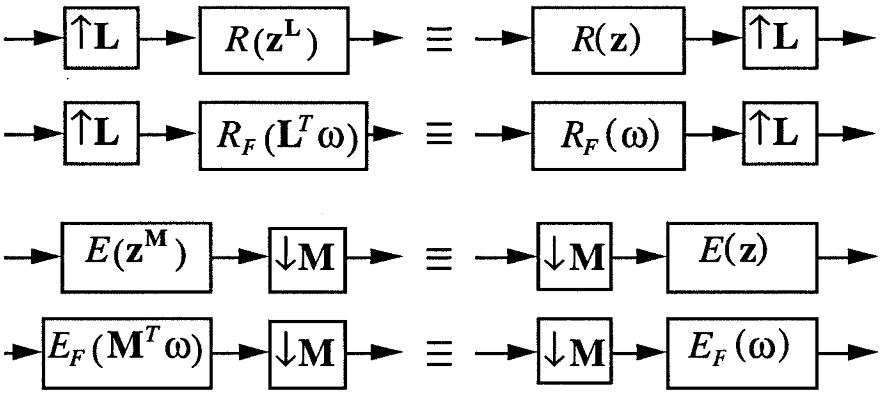

Figure 2.3-1 Noble identities.

where $\mathbf{k} \in \mathcal{N}(\mathbf{M})$. So $\mathbf{k}$ can take on $J(\mathbf{M})$ different values. These are ordered as $\mathbf{k}_0, \mathbf{k}_1, \ldots, \mathbf{k}_{J(\mathbf{M})-1}$. Usually, $\mathbf{k}_0$ is taken to be the zero vector $\mathbf{0}$. In the frequency domain, the polyphase decomposition of $X_F(\omega)$ can be expressed as

$$\begin{aligned} X_F(\omega) &= \sum_{\mathbf{k}\in\mathcal{N}(\mathbf{M})} e^{-j\omega^T\mathbf{k}} E_{F,\mathbf{k}}(\mathbf{M}^T\omega), \qquad \text{(Type 1)} \\ \text{or} \quad X_F(\omega) &= \sum_{\mathbf{k}\in\mathcal{N}(\mathbf{M})} e^{j\omega^T\mathbf{k}} R_{F,\mathbf{k}}(\mathbf{M}^T\omega). \qquad \text{(Type 2)} \end{aligned} \tag{2.3.2}$$

In the $\mathbf{z}$ domain, these become

$$\begin{aligned} X(\mathbf{z}) &= \sum_{\mathbf{k}\in\mathcal{N}(\mathbf{M})} \mathbf{z}^{-\mathbf{k}} E_{\mathbf{k}}(\mathbf{z}^{\mathbf{M}}), \qquad \text{(Type 1)} \\ \text{or} \quad X(\mathbf{z}) &= \sum_{\mathbf{k}\in\mathcal{N}(\mathbf{M})} \mathbf{z}^{\mathbf{k}} R_{\mathbf{k}}(\mathbf{z}^{\mathbf{M}}). \qquad \text{(Type 2)} \end{aligned} \tag{2.3.3}$$

Note that $\mathbf{z}^{\mathbf{k}}$ (or $e^{j\omega^T\mathbf{k}}$) is an 'advance' operator, which advances an MD signal by a vector amount $\mathbf{k}$. Similarly, $\mathbf{z}^{-\mathbf{k}}$ (or $e^{-j\omega^T\mathbf{k}}$) is a 'delay' operator which shifts (delays) an MD signal by $\mathbf{k}$.

Noble Identities

These are rules which permit us to move decimators and expanders across transfer functions. For example, a filter followed by a $\mathbf{L}$-fold expander is equivalent to the expander followed by the $\mathbf{L}$-fold expanded version of the same filter. Also, a $\mathbf{M}$-fold decimator followed by a filter is equivalent to the $\mathbf{M}$-fold expanded version of the same filter followed by the decimator. Fig. 2.3-1 shows these rules.

The Polyphase Identity

We can easily verify the polyphase identity shown in Fig. 2.3-2, where $E_0(\mathbf{z})$ is the $\mathbf{0}$th polyphase

Figure 2.3-2 Polyphase Identity.

component of $H(\mathbf{z})$. In other words, $E_0(\mathbf{z})$ is the $\mathbf{z}$-transform of the $\mathbf{M}$-fold decimated version of $h(\mathbf{n})$.

Periodicity and Cyclo-Wide-Sense-Stationarity

An MD function $f(\mathbf{x})$ is said to be periodic with periodicity matrix $\mathbf{P}$ if $f(\mathbf{x}+\mathbf{Pk}) = f(\mathbf{x})$, $\forall \mathbf{k} \in \mathcal{N}$. An MD random signal $x(\mathbf{n})$ is said to be *cyclo-wide-sense-stationary* with periodicity matrix $\mathbf{L}$ (denoted as $(\text{CWSS})_{\mathbf{L}}$) if both $E[x(\mathbf{n})]$ (the statistical mean) and $R_{xx}(\mathbf{n},\mathbf{m}) \triangleq E[x(\mathbf{n})x^*(\mathbf{n}-\mathbf{m})]$ (the autocorrelation function) are periodic in $\mathbf{n}$ with periodicity matrix $\mathbf{L}$.

Zero-Phase Filters

A filter having purely real frequency response is called a zero-phase filter. The time domain requirement for zero-phase filters is $f(\mathbf{n}) = f^*(-\mathbf{n})$ [Dudgeon and Mersereau, 1984, Page 113]. Zero-phase filters introduce no phase distortion, and this is important in many image processing applications.

Nyquist (Mth Band) Property

A Nyquist filter has impulse response $f(\mathbf{n})$ satisfying $f(\mathbf{Mn}) = 0$, for all $\mathbf{n} \neq \mathbf{0}$, where $\mathbf{M}$ is some integer matrix. Such filters are also called $\mathbf{M}$th band filters. When used as interpolation filters, these filters have the advantage that the values of existing samples can be preserved, i.e., there is no intersample interference.

2.4. MULTIDIMENSIONAL FILTER BANKS

An MD analysis/synthesis filter bank with decimation/expansion matrix $\mathbf{M}$ is shown in Fig. 2.4-1(a). When the number of channels is equal to $J(\mathbf{M})$, this is called a maximally decimated filter bank. In general, this system is a linear time-varying (LTV) system. We want to choose analysis filters $H_i(\mathbf{z})$ and synthesis filters $F_i(\mathbf{z})$ properly such that this system satisfies the following properties:

1. Passband supports of analysis filters partition the whole frequency range $[-\pi,\pi)^D$ and each analysis filter has good stopband response (large stopband attenuation).

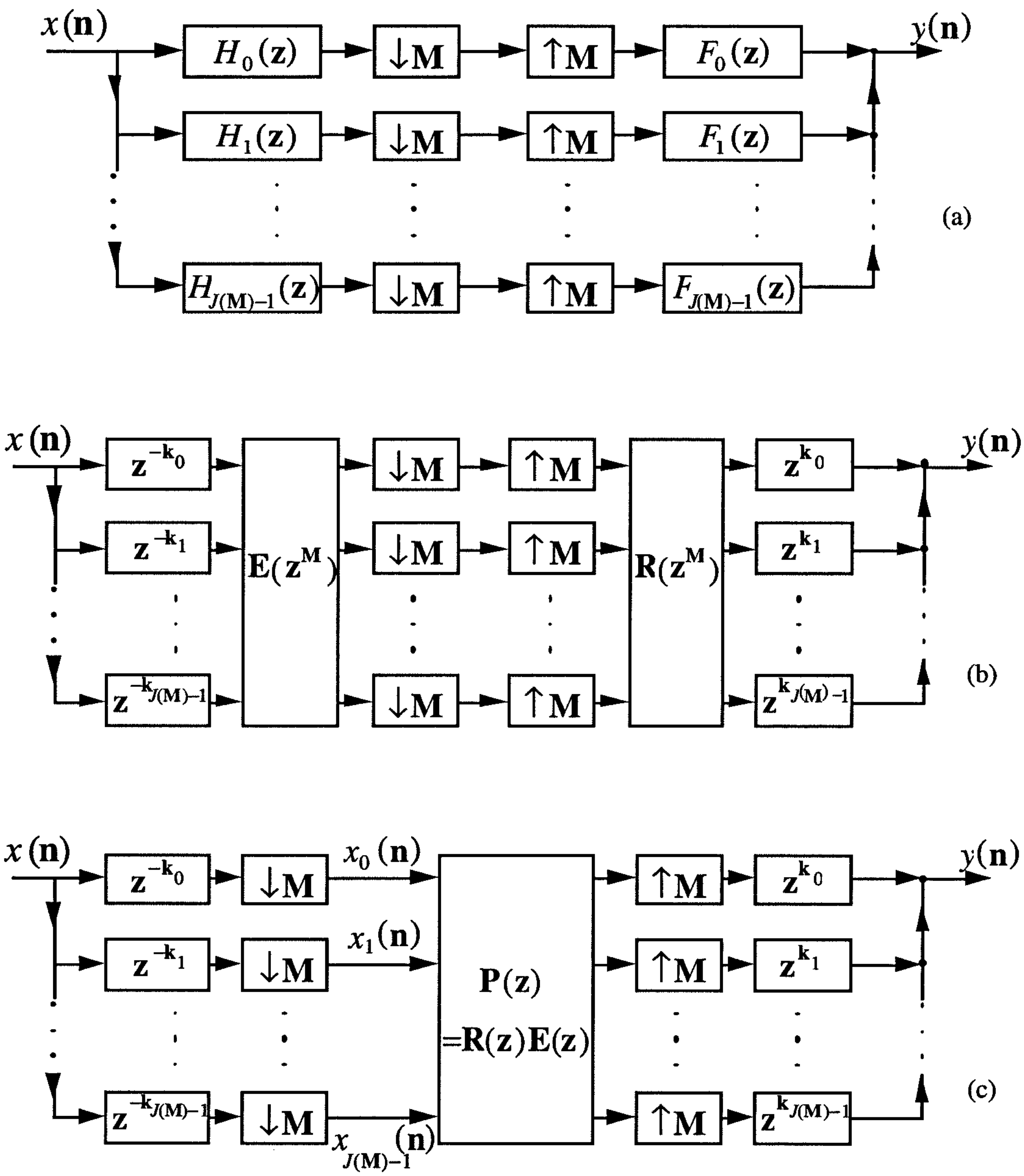

Figure 2.4-1 MD filter bank.

2. There is no alias distortion (ALD). That is, the system is linear time-invariant (LTI), so $Y(\mathbf{z}) = T(\mathbf{z})X(\mathbf{z})$. We call $T(\mathbf{z})$ the overall transfer function of this system.

3. There is no amplitude distortion (AMD). That is, given the system is indeed LTI, we want the overall transfer function $T(\mathbf{z})$ to be allpass, i.e., $|T_F(\omega)| = 1$ for all ω. When this can not be satisfied, we want at least the system to have *small* AMD, i.e., $|T_F(\omega)| \approx 1$.

4. There is no phase distortion (PHD). That is, given the system is indeed LTI, we want the overall transfer function $T(\mathbf{z})$ to have zero phase.

When a system satisfies Conditions 2,3 and 4, the transfer function $T(\mathbf{z})$ must be unity so $y(\mathbf{n}) = x(\mathbf{n})$ and we say this system achieves perfect reconstruction (PR).

Using the polyphase decomposition, we can represent each analysis filter and synthesis filter in the form

$$H_l(\mathbf{z}) = \sum_{\mathbf{k}_i \in \mathcal{N}(\mathbf{M})} \mathbf{z}^{-\mathbf{k}_i} E_{l,i}(\mathbf{z}^{\mathbf{M}}) \qquad l = 0, \ldots, J(\mathbf{M}) - 1 \tag{2.4.1}$$

and

$$F_l(\mathbf{z}) = \sum_{\mathbf{k}_i \in \mathcal{N}(\mathbf{M})} \mathbf{z}^{\mathbf{k}_i} R_{i,l}(\mathbf{z}^{\mathbf{M}}) \qquad l = 0, \ldots, J(\mathbf{M}) - 1. \tag{2.4.2}$$

Note that the vectors in $\mathcal{N}(\mathbf{M})$ are ordered as $\mathbf{k}_0, \mathbf{k}_1, \ldots, \mathbf{k}_{J(\mathbf{M})-1}$ and $\mathbf{k}_0$ is usually chosen to be the zero vector $\mathbf{0}$. Then, we can redraw this system as in Fig. 2.4-1(b). The $J(\mathbf{M}) \times J(\mathbf{M})$ matrices $\mathbf{E}(\mathbf{z})$ and $\mathbf{R}(\mathbf{z})$ with elements $E_{l,i}(\mathbf{z})$ and $R_{i,l}(\mathbf{z})$ are called the polyphase matrices for the analysis bank and the synthesis bank, respectively.

MD Noble identities allow us to move the decimators and expanders across $\mathbf{E}(\mathbf{z}^{\mathbf{M}})$ and $\mathbf{R}(\mathbf{z}^{\mathbf{M}})$, respectively, and obtain Fig. 2.4-1(c), where $\mathbf{P}(\mathbf{z}) = \mathbf{R}(\mathbf{z})\mathbf{E}(\mathbf{z})$. It can be verified that when $\mathbf{P}(\mathbf{z}) = \mathbf{I}$, the filter bank achieves PR. When the decimation/expansion matrix $\mathbf{M}$ is diagonal, it has been shown that the filter bank system is alias-free if and only if the corresponding $\mathbf{P}(\mathbf{z})$ is *multidimensional pseudocirculant* [Liu and Vaidyanathan, 1988]. For the nondiagonal case, conditions for freedom from aliasing have been given in [Viscito and Allebach, 1988], [Karlsson and Vetterli, 1990], [Viscito and Allebach, 1991] in terms of eigenvectors and eigenvalues of $\mathbf{P}(\mathbf{z})$. The most general necessary and sufficient conditions on $\mathbf{P}(\mathbf{z})$ such that the system is free from aliasing, and such that the system achieves PR, can be found in [Chen and Vaidyanathan, 1993b].

2.5. SUMMARY OF NOTATIONS AND ABBREVIATIONS

All the notations and abbreviations used in this thesis are summarized here for quick reference:

Notations

D: number of dimensions.

$\mathcal{N}$: set of all $D \times 1$ integer vectors.

$[a, b)^D$: set of $D \times 1$ real vectors $\mathbf{x}$ with components x_i in the range $a \leq x_i < b$.

$\mathbf{n} = [n_0 \quad n_1 \quad \cdots \quad n_{D-1}]^T$: 'time'-domain index of MD discrete signals. Note that $\mathbf{n} \in \mathcal{N}$.

$\boldsymbol{\omega} = [\,\omega_0 \quad \omega_1 \quad \cdots \quad \omega_{D-1}\,]^T$: frequency-domain variable of the Fourier transform of MD discrete signals.

$x(\mathbf{n}) \longleftrightarrow X_F(\boldsymbol{\omega})$: Fourier transform pair.

$\mathbf{z} = [\,z_0 \quad z_1 \quad \cdots \quad z_{D-1}\,]^T$: variable of the $\mathbf{z}$-transform of MD signals.

$x(\mathbf{n}) \longleftrightarrow X(\mathbf{z})$: $\mathbf{z}$-transform pair.

$\mathbf{z}^{\mathbf{P}} \triangleq [\,\mathbf{z}^{\mathbf{p}_0} \quad \mathbf{z}^{\mathbf{p}_1} \quad \cdots \mathbf{z}^{\mathbf{p}_{D-1}}\,]^T$, where $\mathbf{p}_i$ is the i-th column of $\mathbf{P}$.

$\mathcal{N}(\mathbf{M})$: set of all integer vectors of the form $\mathbf{M}\mathbf{x}$, $\mathbf{x} \in [0,1)^D$.

$J(\mathbf{M})$: number of elements in $\mathcal{N}(\mathbf{M})$, which is equal to $|\det \mathbf{M}|$ (the absolute determinant of $\mathbf{M}$).

$LAT(\mathbf{V})$ (LATtice of $\mathbf{V}$): set of all vectors of the form $\mathbf{V}\mathbf{n}$, for $\mathbf{n} \in \mathcal{N}$. This set is called the lattice generated by the matrix $\mathbf{V}$. In general, $\mathbf{V}$ is a $D \times D$ nonsingular real matrix.

$SPD(\mathbf{V})$ (Symmetric ParallelepipeD generated by $\mathbf{V}$): set of all real vectors of the form $\mathbf{V}\mathbf{x}$, where $\mathbf{x} \in [-1,1)^D$. This set forms a parallelepiped-shaped region, which is symmetric with respect to the origin, in the D-dimensional space.

$FPD(\mathbf{V})$ (Fundamental ParallelepipeD generated by $\mathbf{V}$): set of all real vectors of the form $\mathbf{V}\mathbf{x}$, $\mathbf{x} \in [0,1)^D$.

$\mathcal{N}(\mathbf{M})$: set of all integer vectors of the form $\mathbf{M}\,\mathbf{x}$, $\mathbf{x} \in [0,1)^D$. In general, $\mathbf{M}$ is a $D \times D$ nonsingular integer matrix.

$J(\mathbf{M})$: absolute determinant of $\mathbf{M}$, i.e., $|\det \mathbf{M}|$. This is also equal to the number of elements in $\mathcal{N}(\mathbf{M})$.

$\widehat{\mathbf{M}}$: a matrix defined as $J(\mathbf{M}) \cdot \mathbf{M}^{-1}$. Note that $\widehat{\mathbf{M}} = \pm$[adjugate of $\mathbf{M}$], so $\widehat{\mathbf{M}}$ is also an integer matrix.

Abbreviation

1D: one-dimensional.

2D: two-dimensional.

BIBO stability: bounded-input-bounded-output stability.

$(\mathrm{CWSS})_{\mathbf{L}}$: cyclo-wide-sense-stationary with periodicity matrix $\mathbf{L}$.

DFT: discrete Fourier transform.

LTI: linear time-invariant.

MD: multidimensional.

MFD: matrix fraction description.

PR: perfect reconstruction.

QMF banks: quadrature mirror filter banks.

RPI: rational polyphase implementation.

3

Multidimensional Filters and Filter Banks Derived from One-Dimensional Filters

3.1. INTRODUCTION

In this chapter, we present a method by which every multidimensional (MD) filter with an arbitrary parallelepiped-shaped passband support can be designed and implemented efficiently. We show that all such filters can be designed starting from an appropriate one-dimensional prototype filter and performing a simple transformation. With D denoting the number of dimensions, we hence reduce the complexity of design as well as implementation of the MD filter from $\mathcal{O}(N^D)$ to $\mathcal{O}(N)$. Furthermore, by using the polyphase technique, we can obtain an implementation with complexity of only $2N$ in the two-dimensional special case. With our method, the Nyquist constraint and zero-phase requirement can be satisfied easily. In the IIR case, stability of the designed filters is also easily achieved. Even though the designed filters are in general non-separable, these filters have *separable polyphase components.* One special application of this method is in MD multirate signal processing, where filters with parallelepiped-shaped passbands are used in decimation, interpolation and filter banks. Some generalizations and other applications of this approach, including MD uniform DFT quadrature mirror filter banks which achieve perfect reconstruction, are studied. Several design examples are also given.

In the field of MD multirate signal processing, MD filters with parallelepiped-shaped passbands are used commonly, especially as decimation filters and interpolation filters (see Section 2.2). For various reasons [Dudgeon and Mersereau, 1984], both the design and implementation of such filters are more complex than in the one-dimensional (1D) case. In the two-dimensional (2D) case, some authors have proposed efficient techniques to design diamond filters, fan filters, and directional filters, by starting from a 1D prototype [Lau and Ansari, 1986], [Ansari and Lau, 1987], [Ansari, 1987], [Ansari and Lee, 1988], [Bamberger, 1990], [Bamberger and Smith, 1992]. While these methods are very valuable (both for design and implementation) as shown in these references, they do not place in evidence a technique for generalization to arbitrary dimensions and arbitrary parallelepiped-shaped passbands. We will present a method which works for arbitrary dimensions and arbitrary parallelepiped-shaped passbands.

For example, given the decimation/expansion matrix $\mathbf{M}$, we first design a 1D lowpass prototype filter $p(n)$ with passband cutoff frequency at $\pi/|\det \mathbf{M}|$, i.e., $\pi/J(\mathbf{M})$. We then define the impulse response $h(\mathbf{n})$ of the MD filter as follows:

Step 1. First define the MD separable filter $h^{(s)}(\mathbf{n}) \triangleq p(n_0)p(n_1)\cdots p(n_{D-1})$.

Step 2. Then define $h(\mathbf{n}) = c_0 h^{(s)}(\widehat{\mathbf{M}}\mathbf{n})$, where $\widehat{\mathbf{M}} \triangleq J(\mathbf{M}) \cdot \mathbf{M}^{-1} = \pm$[adjugate of $\mathbf{M}$] and c_0 is some scale factor.

We will prove in this chapter that the resulting filter $h(\mathbf{n})$, with frequency response $H_F(\boldsymbol{\omega})$, is a lowpass filter having the passband support in

$$\boldsymbol{\omega} = \pi \mathbf{M}^{-T}\mathbf{x}, \qquad \text{with } \mathbf{x} \in [-1, 1)^D \tag{3.1.1}$$

as is the case in many of the 2D designs of [Lau and Ansari, 1986], [Ansari and Lau, 1987], [Ansari, 1987], [Ansari and Lee, 1988], [Bamberger, 1990], [Bamberger and Smith, 1992]. Even though $h(\mathbf{n})$ is in general not separable, its polyphase components with respect to $\mathbf{M}$ are indeed separable, as shown later.

Using the notation of $SPD(\cdot)$, (3.1.1) can be written as $\boldsymbol{\omega} \in SPD(\pi\mathbf{M}^{-T})$. Note that this region is not an arbitrary parallelepiped, but governed by the integer matrix $\mathbf{M}$. To represent an arbitrary parallelepiped, we need to use $\pi\mathbf{H}^{-T}\mathbf{x}$, where $\mathbf{x} \in [-1, 1)^D$ and $\mathbf{H}$ is a nonsingular matrix with *rational* elements. (The irrational case can be approximated by a rational matrix $\mathbf{H}$.) In Sections 3.2 and 3.3, we will state in details the general procedure for designing filters with such arbitrary parallelepiped-shaped passband supports.

The above design rule and its proof are the same for any parallelepiped-shaped passbands, and for any number of dimensions. In this respect our method differs from, and generalizes, earlier ones. Note that the 1D prototype filter depends only on $J(\mathbf{M})$. As done in [Ansari and Lau, 1987] and [Bamberger and Smith, 1992], we also provide bounds on the passband and stopband ripples of the resulting MD filter in terms of the ripples of the 1D prototype. We will also exploit the above relation between 1D and MD filters to obtain efficient polyphase implementations (Section 3.4).

With our method, the Nyquist constraint and zero-phase requirement can be satisfied easily. Also, the designed filters all have separable polyphase components. In the IIR case, the stability of the resulting filters is also guaranteed. In addition to filters with parallelepiped-shaped passbands, many other filters can be designed by minor combinations of these filters (Section 3.5). Because our method results in a close relation between the polyphase components of the 1D prototype and those of the resulting MD filter, the design and implementation of MD uniform DFT quadrature mirror filter (QMF) banks can be simplified (Section 3.6). Many useful MD DFT QMF banks, including those that achieve perfect reconstruction (PR), are presented, together with several design examples. We will also make some comments about how to deal with the case when the passband support is very small (Section 3.7).

3.2. THE IMPULSE RESPONSE OF AN IDEAL LOWPASS FILTER

In this section we give the key equation which can be considered to be the theoretical foundation for the rest of the chapter. Let $\mathbf{M}$ be a $D \times D$ nonsingular integer matrix. To prevent aliasing due to the $\mathbf{M}$-fold decimation (or eliminate images in the $\mathbf{M}$-fold expansion), a decimation (or interpolation) filter $H_F(\boldsymbol{\omega})$ is necessary. Typically, this filter has a parallelepiped-shaped passband support in

$$\boldsymbol{\omega} = \pi \mathbf{M}^{-T}\mathbf{x} + 2\pi\mathbf{k}, \qquad \mathbf{x} \in [-1,1)^D,\ \mathbf{k} \in \mathcal{N}. \tag{3.2.1}$$

Let $H_F(\boldsymbol{\omega})$ denote the frequency response of an ideal lowpass decimation/interpolation filter for the $\mathbf{M}$-fold decimator/expander. In other words,

$$H_F(\boldsymbol{\omega}) = \begin{cases} 1 & \text{if } \boldsymbol{\omega} \in SPD(\pi\mathbf{M}^{-T}) \\ 0 & \text{otherwise.} \end{cases} \tag{3.2.2}$$

Let $h(\mathbf{n})$ denote the impulse response of $H_F(\boldsymbol{\omega})$. We now obtain an expression for $h(\mathbf{n})$. This expression will reveal a fundamental relation to 1D lowpass filters, and enable us to design $H_F(\boldsymbol{\omega})$ starting from a 1D prototype. Using the inverse Fourier transform, we obtain

$$\begin{aligned} h(\mathbf{n}) &= \frac{1}{(2\pi)^D} \int_{\boldsymbol{\omega} \in SPD(\pi\mathbf{M}^{-T})} e^{j\boldsymbol{\omega}^T\mathbf{n}} d\boldsymbol{\omega} \\ &= \frac{1}{2^D J(\mathbf{M})} \int_{\mathbf{x} \in [-1,1)^D} e^{j\pi\mathbf{x}^T\mathbf{M}^{-1}\mathbf{n}} d\mathbf{x} \qquad (\boldsymbol{\omega} = \pi\mathbf{M}^{-T}\mathbf{x}) \\ &= \frac{1}{2^D J(\mathbf{M})} \int_{\mathbf{x} \in [-1,1)^D} e^{j\pi\mathbf{x}^T\mathbf{m}} d\mathbf{x} \qquad (\mathbf{m} = \mathbf{M}^{-1}\mathbf{n}) \\ &= \frac{1}{2^D J(\mathbf{M})} \prod_{i=0}^{D-1} \int_{x_i=-1}^{1} e^{j\pi m_i x_i} dx_i \end{aligned} \tag{3.2.3}$$

where m_i are the components of the $D \times 1$ vector

$$\mathbf{m} = \mathbf{M}^{-1}\mathbf{n} = \frac{\widehat{\mathbf{M}}\mathbf{n}}{J(\mathbf{M})} \tag{3.2.4}$$

with $\widehat{\mathbf{M}} \triangleq J(\mathbf{M}) \cdot \mathbf{M}^{-1} = \pm$[adjugate of $\mathbf{M}$]. Evidently, $\widehat{\mathbf{M}}$ is also an integer matrix. Note, however, that $\mathbf{m}$ is a real (not an integer) vector. From the above we obtain

$$h(\mathbf{n}) = \frac{1}{J(\mathbf{M})} \prod_{i=0}^{D-1} \frac{\sin(\pi m_i)}{\pi m_i}. \tag{3.2.5}$$

Relationship to 1D Filters

Consider a 1D ideal filter with frequency response $P_F(\omega)$ as shown in Fig. 3.2-1. Computing its inverse Fourier transform, we obtain the impulse response

$$p(n) = \frac{\sin(\frac{\pi n}{J(\mathbf{M})})}{\pi n}. \tag{3.2.6}$$

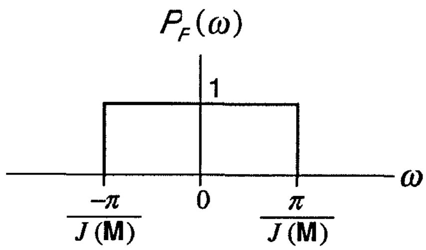

Figure 3.2-1 Frequency response of an ideal lowpass filter.

Starting from this prototype filter $P_F(\omega)$, suppose we define the D-dimensional filter

$$H_F^{(s)}(\omega) = P_F(\omega_0)P_F(\omega_1)\dots P_F(\omega_{D-1}). \tag{3.2.7}$$

This is a separable lowpass filter, with passband support in $SPD(\pi\mathbf{I}/J(\mathbf{M}))$. This implies that its impulse response is

$$\begin{aligned} h^{(s)}(\mathbf{n}) &= p(n_0)p(n_1)\dots p(n_{D-1}) \\ &= \prod_{i=0}^{D-1} \frac{\sin(\frac{\pi n_i}{J(\mathbf{M})})}{\pi n_i}. \end{aligned} \tag{3.2.8}$$

Now consider the quantity $h^{(s)}(\widehat{\mathbf{M}}\mathbf{n})$, which is the $\widehat{\mathbf{M}}$-fold decimated version of $h^{(s)}(\mathbf{n})$. Since $\widehat{\mathbf{M}}\mathbf{n} = J(\mathbf{M})\mathbf{M}^{-1}\mathbf{n} = J(\mathbf{M})\mathbf{m}$, we get

$$h^{(s)}(\widehat{\mathbf{M}}\mathbf{n}) = h^{(s)}(J(\mathbf{M})\mathbf{m}) = \prod_{i=0}^{D-1} \frac{\sin(\pi m_i)}{\pi J(\mathbf{M}) m_i} = \frac{1}{J(\mathbf{M})^D} \prod_{i=0}^{D-1} \frac{\sin(\pi m_i)}{\pi m_i}. \tag{3.2.9}$$

Comparing (3.2.9) with (3.2.5), we obtain the following very simple relation between $h(\mathbf{n})$ and $h^{(s)}(\widehat{\mathbf{M}}\mathbf{n})$:

$$h(\mathbf{n}) = c_0 h^{(s)}(\widehat{\mathbf{M}}\mathbf{n}), \tag{3.2.10}$$

where $c_0 = [J(\mathbf{M})]^{D-1} = J(\widehat{\mathbf{M}})$. In other words, $h(\mathbf{n})$ is obtained simply by $\widehat{\mathbf{M}}$-fold decimation of the D-dimensional separable sequence $h^{(s)}(\mathbf{n})$, followed by scaling with c_0!

Rational case

We will generalize this result to ideal filters with the passband support in $SPD(\pi\mathbf{H}^{-T})$, where $\mathbf{H}$ is a $D \times D$ nonsingular matrix with *rational* elements. Because any irrational matrix can be approximated by rational matrices, this covers any parallelepiped-shaped passband support.

Consider an ideal lowpass filter which has the passband region in $SPD(\pi\mathbf{H}^{-T})$, i.e.,

$$G_F(\boldsymbol{\omega}) = \begin{cases} 1 & \text{if } \boldsymbol{\omega} \in SPD(\pi\mathbf{H}^{-T}) \\ 0 & \text{otherwise.} \end{cases} \tag{3.2.11}$$

Similarly as in (3.2.3)–(3.2.5), we can obtain the inverse Fourier transform of $G_F(\boldsymbol{\omega})$

$$g(\mathbf{n}) = \frac{1}{J(\mathbf{H})} \prod_{i=0}^{D-1} \frac{\sin(\pi q_i)}{\pi q_i} \tag{3.2.12}$$

where $\mathbf{q} = [q_0 \ \cdots \ q_{D-1}]^T = \mathbf{H}^{-1}\mathbf{n}$. Meanwhile, by using the so-called *matrix fraction description* (MFD), any nonsingular rational matrix can be expressed in its left MFD as $\mathbf{H} = \mathbf{L}^{-1}\mathbf{M}$, where $\mathbf{L}$ and $\mathbf{M}$ are some nonsingular integer matrices [Kailath, 1980], [Vidyasagar, 1985]. See also Section 4.2 for more details on the MFD. Let us consider $h(\mathbf{L}\mathbf{n})$, the $\mathbf{L}$-fold decimated version of $h(\mathbf{n})$ in (3.2.5). We get

$$h(\mathbf{L}\mathbf{n}) = \frac{1}{J(\mathbf{M})} \prod_{i=0}^{D-1} \frac{\sin(\pi q_i)}{\pi q_i}, \qquad \text{where } \mathbf{q} = \mathbf{M}^{-1}\mathbf{L}\mathbf{n} = \mathbf{H}^{-1}\mathbf{n}. \tag{3.2.13}$$

Comparing (3.2.12) and (3.2.13), we obtain the following relation between $h(\mathbf{n})$ and $g(\mathbf{n})$:

$$g(\mathbf{n}) = c_1 h(\mathbf{L}\mathbf{n}), \tag{3.2.14}$$

where $c_1 = J(\mathbf{M})/J(\mathbf{H}) = J(\mathbf{L})$. In other words, $g(\mathbf{n})$ is obtained simply by $\mathbf{L}$-fold decimation of $h(\mathbf{n})$, followed by scaling with c_1.

3.3. DESIGN PROCEDURE

Motivated by the conclusion in Section 3.2, we can design an MD filter with the passband support $SPD(\pi \mathbf{H}^{-T})$ as follows:

Step 1. Find a left MFD of $\mathbf{H}$, say $\mathbf{H} = \mathbf{L}^{-1}\mathbf{M}$.

Step 2. Design a 1D lowpass prototype filter $p(n)$, which can have either finite impulse response (FIR) or infinite impulse response (IIR), with passband region $\big[-\pi/J(\mathbf{M}),\ \pi/J(\mathbf{M})\big)$.

Step 3. Construct the separable MD filter $h^{(s)}(\mathbf{n})$ from $p(n)$ as

$$h^{(s)}(\mathbf{n}) = p(n_0)p(n_1)\cdots p(n_{D-1}). \tag{3.3.1}$$

Step 4. Define $h(\mathbf{n}) \triangleq c_0 h^{(s)}(\widehat{\mathbf{M}}\mathbf{n})$, where $c_0 = J(\widehat{\mathbf{M}})$.

Step 5. Define $g(\mathbf{n}) \triangleq c_1 h(\mathbf{L}\mathbf{n})$, where $c_1 = J(\mathbf{L})$.

Note that Step 4 and Step 5 can be combined as one step: $g(\mathbf{n}) \triangleq c h^{(s)}(\widehat{\mathbf{ML}}\mathbf{n})$, where $c = c_0 c_1 = J(\widehat{\mathbf{ML}})$. Also, when $\mathbf{H}$ is itself an integer matrix (so $\mathbf{L}$ can be chosen as an identity matrix), we can omit Step 5 and simply use the resulting filter $H_F(\boldsymbol{\omega})$ of Step 4.

Remarks on the Choice of M and L

1. Since we decimate $h(\mathbf{n})$ by a factor of $\mathbf{L}$ to obtain $g(\mathbf{n})$, there is a 'design overhead factor' of $J(\mathbf{L})$. To reduce such overhead, we need to find a left MFD of $\mathbf{H}$ where $\mathbf{L}$ has the smallest absolute determinant. For this purpose, it turns out that we should choose the so-called *irreducible* left MFD of $\mathbf{H}$, which is a left MFD where $\mathbf{M}$ and $\mathbf{L}$ are left coprime [Kailath, 1980], [Vidyasagar, 1985].

2. Instead of choosing an irreducible MFD, we can choose an MFD where $\mathbf{M}$ is diagonal. This is always possible because $\mathbf{H}^{-1} = \mathbf{M}^{-1}\mathbf{L}$ and we can simply let m_{ii} (the diagonal elements of $\mathbf{M}$) be the least common multiple of denominators in the ith row of $\mathbf{H}^{-1}$. The advantage of diagonal $\mathbf{M}$ is that the design of $h(\mathbf{n})$ becomes trivial since it can be done separately in each dimension. However, we pay the expense that the overhead factor $J(\mathbf{L})$ may be higher than the one in an irreducible MFD. Therefore, whether diagonal $\mathbf{M}$ or irreducible MFD should be used depends on the matrix $\mathbf{H}$.

Analysis of Ripple Sizes

Because $H_F^{(s)}(\omega)$ is not ideal, decimation operations in Step 4 and Step 5 cause some aliasing, both in the passband and the stopband. We now proceed to analyze these ripple sizes, and obtain bounds in the same way as done in [Ansari, 1987] and [Bamberger and Smith, 1992]. Suppose the prototype filter $P_F(\omega)$ has passband ripple δ_1 and stopband ripple δ_2. Then, it is clear that the frequency response of $H_F^{(s)}(\omega)$ will satisfy

$$\begin{aligned} (1-\delta_1)^D \le |H_F^{(s)}(\omega)| \le (1+\delta_1)^D \qquad & \text{in the passband,} \\ 0 \le |H_F^{(s)}(\omega)| \le (1+\delta_1)^{D-1}\delta_2 \qquad & \text{in the stopband.} \end{aligned} \tag{3.3.2}$$

When $\delta_1,\ \delta_2 \ll 1$, we have

$$\begin{aligned} (1 \pm \delta_1)^D &\approx 1 \pm D\delta_1, \\ \text{and} \quad (1+\delta_1)^{D-1}\delta_2 &\approx \delta_2. \end{aligned} \tag{3.3.3}$$

Therefore, the passband and stopband ripples of $H_F^{(s)}(\omega)$ are approximately $D\delta_1$ and δ_2, respectively. Since $h(\mathbf{n}) = J(\widehat{\mathbf{M}})\, h^{(s)}(\widehat{\mathbf{M}}\mathbf{n})$, we obtain

$$H_F(\omega) = \sum_{\mathbf{k}\in\mathcal{N}(\widehat{\mathbf{M}}^T)} H_F^{(s)}\big(\widehat{\mathbf{M}}^{-T}(\omega - 2\pi\mathbf{k})\big). \tag{3.3.4}$$

We can see that $H_F(\omega)$ is the sum of the 'stretched' version $H_F^{(s)}\big(\widehat{\mathbf{M}}^{-T}\omega\big)$ and $J(\widehat{\mathbf{M}})-1$ 'shifted' versions of it. Therefore, the passband ripple of $H_F(\omega)$ is at most the sum of one passband ripple and $J(\widehat{\mathbf{M}})-1$ stopband ripples of $H_F^{(s)}(\omega)$, and the stopband ripple of $H_F(\omega)$ is at most the sum of $J(\widehat{\mathbf{M}})$ stopband ripples of $H_F^{(s)}(\omega)$. Hence, the peak passband and stopband ripples of the resulting filter $H_F(\omega)$ should be upper bounded by

$$\delta_{1,h} = \big(J(\widehat{\mathbf{M}})-1\big)\,\delta_2 + D\delta_1, \qquad \text{and} \qquad \delta_{2,h} = J(\widehat{\mathbf{M}})\,\delta_2. \tag{3.3.5}$$

Similarly, we can obtain that the resulting passband and stopband ripple sizes of $g(\mathbf{n})$ are upper bounded by

$$\widetilde{\delta}_1 = \big(J(\mathbf{L})-1\big)\,\delta_{2,h} + \delta_{1,h} \qquad \text{and} \qquad \widetilde{\delta}_2 = J(\mathbf{L})\,\delta_{2,h}. \tag{3.3.6}$$

Note that the resulting ripples generally will be less than these upper bounds. To design $G_F(\omega)$, we simply choose δ_1 and δ_2 small enough so that the resulting $G_F(\omega)$ satisfies the specifications.

Remark: Similar bounds of ripple sizes for the case of 2D diamond filters and directional filters can be found in [Ansari, 1987] and [Bamberger and Smith, 1992].

Comparison with previous results. The technique of transforming a 2D filter with separable rectangular passband into some particular shapes by a change of variables has been mentioned in

[Lau and Ansari, 1986], [Ansari and Lau, 1987], [Ansari, 1987], [Ansari and Lee, 1988], [Bamberger, 1990], [Bamberger and Smith, 1992]. However, our method presents the required prototype filter and the required transform (namely, decimation by $\widehat{\mathbf{ML}}$) for any number of dimensions and any parallelepiped-shaped passband supports.

Design Example 3.1: We choose

$$\mathbf{H} = \begin{bmatrix} 1 & -1 \\ 1 & 2 \end{bmatrix}. \tag{3.3.7}$$

The desired passband support is same as in Fig. 1.2-1. Because $\mathbf{H}$ is itself an integer matrix, Step 5 can be omitted and $H_F(\boldsymbol{\omega})$ will be the desired filter. We use linear programming [Rabiner and Gold, 1975, Section 3.19] to design the prototype filter $P_F(\omega)$, a zero-phase Nyquist FIR filter with length $N = 59$, passband ripple $\delta_1 = 0.01994$, and stopband ripple $\delta_2 = 0.00888$ (i.e., stopband attenuation $A_s = -41.03\text{dB}$), shown in Fig. 3.3-1(a). Following the steps described previously, we obtain $H_F^{(s)}(\boldsymbol{\omega})$ and $H_F(\boldsymbol{\omega})$, as shown in Fig. 3.3-1(b) and Fig. 3.3-1(c). The resulting $H_F(\boldsymbol{\omega})$ has passband ripple $\delta_1' = 0.03931$ and stopband ripple $\delta_2' = 0.01778$ (-35.00dB), which are indeed smaller than the estimated values ($\delta_{1,h} = 0.05765$, $\delta_{2,h} = 0.02664$).

Design Example 3.2: Suppose we want to design a filter $g(\mathbf{n})$ which has passband in the shaded region of Fig. 3.3-2(a). This region can be expressed as $SPD(\pi\mathbf{H}^{-T})$, where

$$\mathbf{H} = \begin{bmatrix} 3/5 & -6/5 \\ 6/5 & 3/5 \end{bmatrix} = \underbrace{\begin{bmatrix} 1 & 2 \\ -2 & 1 \end{bmatrix}^{-1}}_{\mathbf{L}^{-1}} \underbrace{\begin{bmatrix} 3 & 0 \\ 0 & 3 \end{bmatrix}}_{\mathbf{M}}. \tag{3.3.8}$$

(The computation of irreducible MFDs can be found in [Kailath, 1980], [Vidyasagar, 1985], [Chen and Vaidyanathan, 1993a].) For this case, the matrix $\mathbf{M}$ turns out to be diagonal and we can utilize the filter $h^{(s)}(\mathbf{n})$ in Design Example 3.1. This filter is decimated by $\mathbf{L}$ and scaled by $J(\mathbf{L})$ to obtain $g(\mathbf{n})$. The resulting frequency response $G_F(\boldsymbol{\omega})$, which has passband ripple size $\delta_1' = 0.02719$ and stopband ripple size $\delta_2' = 0.03038$ (-30.35dB), is shown in Fig. 3.3-2(b).

Separability of the Polyphase Components

When used in multirate applications, e.g., decimation filters, interpolation filters, and filter banks, filters are usually implemented in polyphase components [Vaidyanathan, 1990b], [Viscito and Allebach, 1991]. In these applications, the implementation of a filter is efficient (with complexity $\mathcal{O}(N)$) as long as its polyphase components are separable, even though the filter itself may be nonseparable. We now show that the proposed design procedure results in filters with separable polyphase components. This fact also helps us in designing uniform DFT filter banks, which will be explained later.

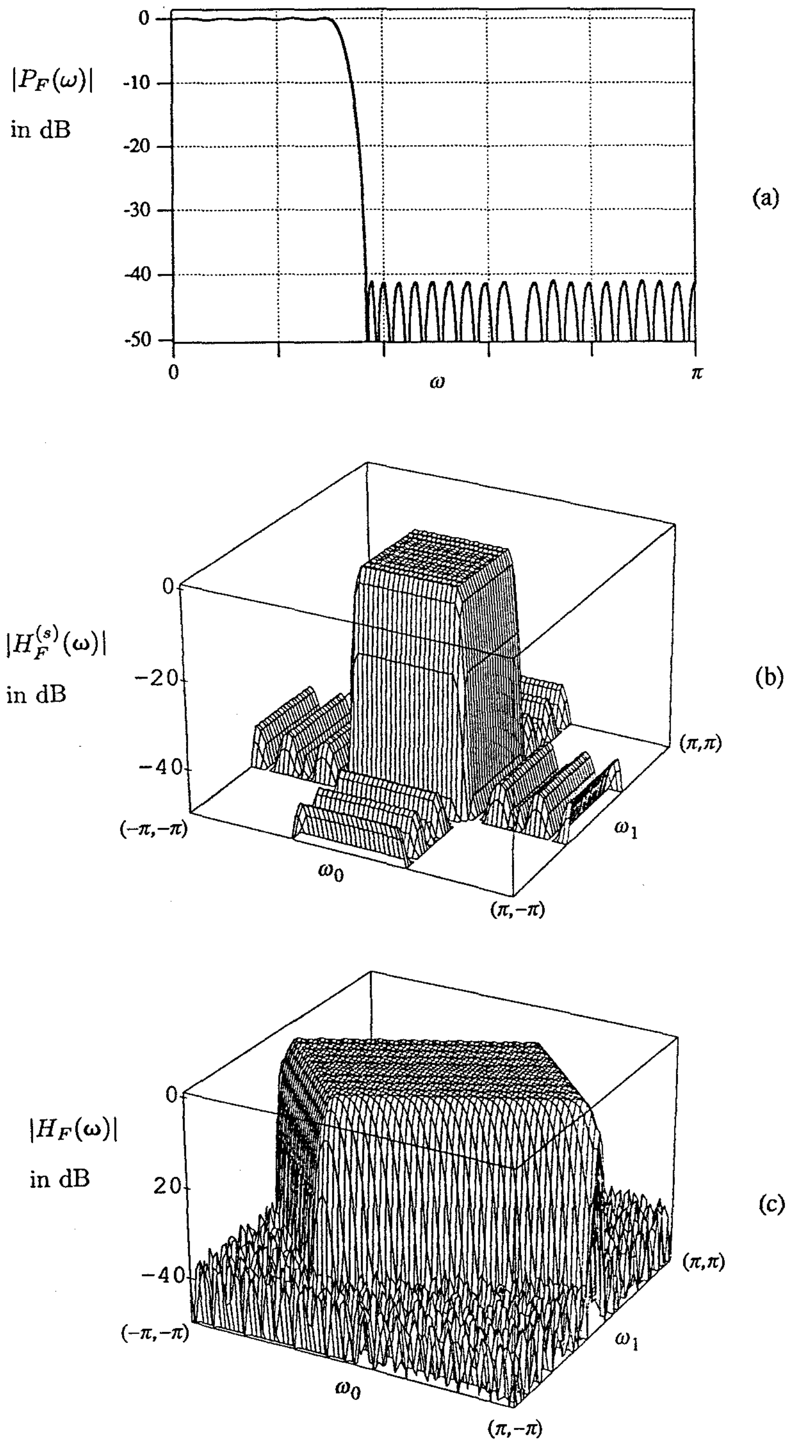

Figure 3.3-1 Frequency response of filters in Design Example 3.1: (a) $P_F(\omega)$, (b) $H_F^{(s)}(\omega)$, (c) $H_F(\omega)$.

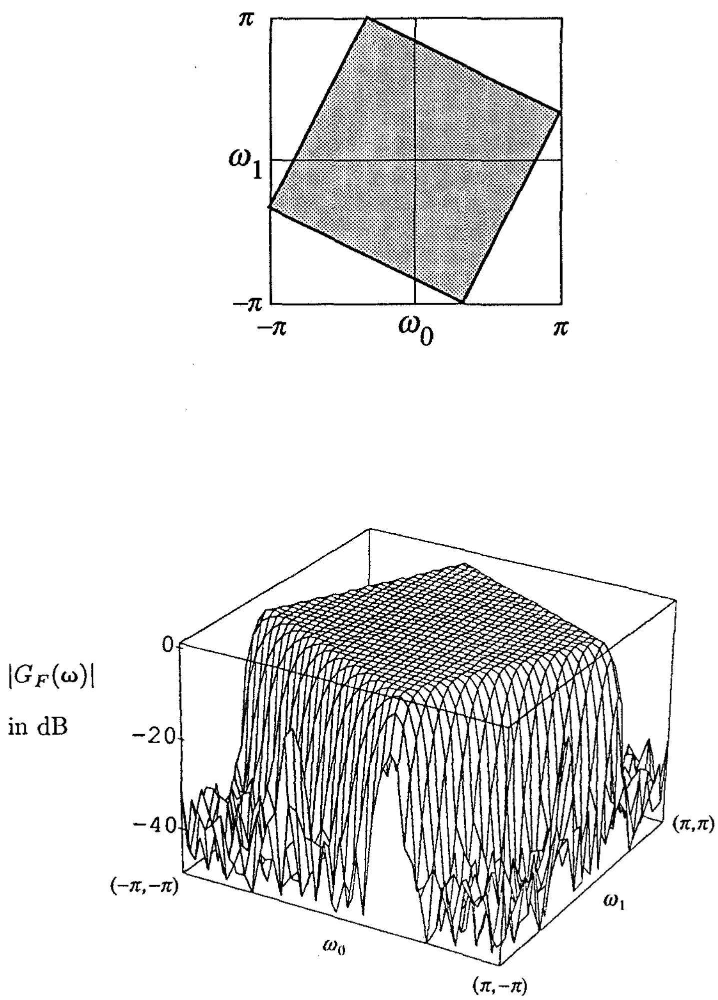

(a)

(b)

Figure 3.3-2 The filter $G_F(\omega)$ in Design Example 3.2: (a) desired passband, (b) frequency response.

Remark: A method of designing 2D diamond-shaped filters having two separable polyphase components was proposed in [Ansari and Lau, 1987]. From this point of view, our method is indeed a generalization of the results therein.

Since the polyphase decomposition is defined only with respect to integer matrices, we only have to discuss the filter $h(\mathbf{n})$ obtained by using Steps 2, 3, and 4 with respect to the integer matrix $\mathbf{M}$. We now prove that all these polyphase components are separable. In fact, we can show these polyphase components can be separated into polyphase components of the 1D filter $P_F(\omega)$. Consider

$e_{\mathbf{k}}(\mathbf{n})$, the **k**th polyphase component of of $h(\mathbf{n})$. We have

$$\begin{aligned} e_{\mathbf{k}}(\mathbf{n}) &= h(\mathbf{Mn}+\mathbf{k}) \\ &= c_0 h^{(s)}(\widehat{\mathbf{M}}\mathbf{Mn}+\widehat{\mathbf{M}}\mathbf{k}) \\ &= c_0 h^{(s)}(J(\mathbf{M})\mathbf{n}+\widehat{\mathbf{M}}\mathbf{k}). \end{aligned} \tag{3.3.9}$$

Let $\mathbf{l}=[l_0 \quad l_1 \quad \cdots \quad l_{D-1}]^T=\widehat{\mathbf{M}}\mathbf{k}$, then

$$e_{\mathbf{k}}(\mathbf{n}) = c_0 p(J(\mathbf{M})n_0+l_0)p(J(\mathbf{M})n_1+l_1)\cdots p(J(\mathbf{M})n_{D-1}+l_{D-1}). \tag{3.3.10}$$

Therefore, $e_{\mathbf{k}}(\mathbf{n})$'s are separable. Since $\mathbf{k} \in \mathcal{N}(\mathbf{M})$, it can be verified that $\mathbf{l} \in \mathcal{N}(J(\mathbf{M})\mathbf{I})$, so $0 \le l_i \le J(\mathbf{M})-1$. We thus conclude that $e_{\mathbf{k}}(\mathbf{n})$'s can be separated into Type 1 polyphase components of $p(n)$.

Preservation of the Zero-Phase Property

Our filter design method *preserves* the zero-phase property, i.e., if the 1D filter has zero phase, the resulting MD filter $G_F(\boldsymbol{\omega})$ also has zero phase. To show this, suppose the 1D prototype $p(n)$ has zero phase, i.e., $p(n)=p^*(-n)$. From (3.3.1), we know $h^{(s)}(\mathbf{n})=h^{(s)*}(-\mathbf{n})$. Then, $g(\mathbf{n}) = c\,h^{(s)}(\widehat{\mathbf{M}}\mathbf{Ln}) = c\,h^{(s)*}(-\widehat{\mathbf{M}}\mathbf{Ln}) = g^*(-\mathbf{n})$, so that $g(\mathbf{n})$ also has zero phase.

Preservation of the Stability

If we begin with a stable IIR prototype filter $p(n)$, the resulting $g(\mathbf{n})$ is also guaranteed to be stable. This is justified as follows. By the definition of bounded-input-bounded-output (BIBO) stability, $p(n)$ is stable if and only if $\sum_n |p(n)|$ is finite. Since

$$\begin{aligned} \sum_{\mathbf{n}} |g(\mathbf{n})| &= c\sum_{\mathbf{n}}\left|h^{(s)}(\widehat{\mathbf{M}}\mathbf{Ln})\right| \le c\sum_{\mathbf{n}}\left|h^{(s)}(\mathbf{n})\right| \\ &= c\sum_{n_0}|p(n_0)|\sum_{n_1}|p(n_1)|\cdots\sum_{n_{D-1}}|p(n_{D-1})| \\ &= c\Big(\sum_{n}|p(n)|\Big)^D, \end{aligned} \tag{3.3.11}$$

$\sum_{\mathbf{n}}|g(\mathbf{n})|$ is also finite. Therefore, $g(\mathbf{n})$ is also stable.

Preservation of the Nyquist (Mth Band) Property

With our method, the Nyquist property is also preserved. More precisely, let $p(n)$ be Nyquist, i.e., $p(J(\mathbf{M})\,n)=0$, for $n\neq 0$. From (3.3.1), we therefore have $h^{(s)}(J(\mathbf{M})\,\mathbf{n})=0$, for $\mathbf{n}\neq\mathbf{0}$. Then, $h(\mathbf{M}\,\mathbf{n}) = c_0h^{(s)}(\widehat{\mathbf{M}}\,\mathbf{M}\,\mathbf{n}) = c_0h^{(s)}(J(\mathbf{M})\,\mathbf{n}) = 0$, for $\mathbf{n}\neq\mathbf{0}$, so $h(\mathbf{n})$ is also Nyquist (**M**th band). Furthermore, if we generalize the Nyquist property for the rational case to be: $f(\mathbf{Hn})=0$ whenever

$\mathbf{Hn}$ is a nonzero integer vector (Hth band property), it can be verified that the resulting $g(\mathbf{n})$ has Nyquist property as well.

Causality of Designed Filters

Suppose we start from a 1D causal filter $p(n)$. The separable MD filter $h^{(s)}(\mathbf{n})$ obtained in (3.3.1) is obviously causal (i.e., $h^{(s)}(\mathbf{n})$ is nonzero only when all n_i's are nonnegative). When $h^{(s)}(\mathbf{n})$ is decimated by $\widehat{\mathbf{ML}}$, the resulting $g(\mathbf{n})$ may or may not be causal, depending on $\widehat{\mathbf{ML}}$. It can be shown that $g(\mathbf{n})$ is still causal if and only if all the elements in $(\widehat{\mathbf{ML}})^{-1}$ are nonnegative, which is equivalent to the condition that all the elements in $\mathbf{H}$ be nonnegative.

Even though $g(\mathbf{n})$ may not remain causal for some choices of $\mathbf{H}$, this is not a significant problem because we do not implement $g(\mathbf{n})$ directly. As shown later in the following section, $h^{(s)}(\mathbf{n})$, which is causal and stable as long as $p(n)$ is causal stable, is the filter to be implemented.

3.4. EFFICIENT IMPLEMENTATION

Because of the separability of $H_F^{(s)}(\boldsymbol{\omega})$, the proposed method is efficient not only in the design, but also in the implementation. We shall present a polyphase implementation in which the complexity (number of arithmetic operations per filter output sample) grows linearly with the filter length N, i.e., $\mathcal{O}(N)$, instead of $\mathcal{O}(N^D)$.

We shall take the 2D case for our example. Suppose $p(n)$ in Step 2 has N coefficients. Therefore, $h^{(s)}(\mathbf{n})$ has N^2 coefficients and $g(\mathbf{n})$ has approximately $N^2/J(\widehat{\mathbf{ML}})$ coefficients. Hence, to implement $g(\mathbf{n})$ directly requires approximately $N^2/J(\widehat{\mathbf{ML}})$ "arithmetic operations per computed output pixel" (OPP's). Instead of direct implementation, we shall derive an efficient implementation as follows:

Using the polyphase identity in Fig. 2.3-2, we can schematically represent $G_F(\boldsymbol{\omega})$ in terms of $H_F^{(s)}(\boldsymbol{\omega})$ as in Fig. 3.4-1(a), since $g(\mathbf{n})$ is the $\widehat{\mathbf{ML}}$-fold decimated version of $ch^{(s)}(\mathbf{n})$. Because $H_F^{(s)}(\boldsymbol{\omega})$ is separable, i.e.,

$$H_F^{(s)}(\boldsymbol{\omega}) = \underbrace{P_F(\omega_0)}_{G_{F,0}(\boldsymbol{\omega})} \cdot \underbrace{P_F(\omega_1)}_{G_{F,1}(\boldsymbol{\omega})}, \tag{3.4.1}$$

we obtain the implementation in Fig. 3.4-1(b). We see this implementation requires only $J(\widehat{\mathbf{ML}})\cdot 2N$ OPP's, where the factor $J(\widehat{\mathbf{ML}})$ is due to the $\widehat{\mathbf{ML}}$-fold expander. Hence we have reduced the complexity from $\mathcal{O}(N^2)$ to $\mathcal{O}(N)$. Note that this holds for the FIR case as well as the IIR case.

Due to the $\widehat{\mathbf{ML}}$-fold expander, the input to $G_{F,0}(\boldsymbol{\omega})$ has several zero-valued samples. Due to the $\widehat{\mathbf{ML}}$-fold decimator, a large portion of the output of $G_{F,1}(\boldsymbol{\omega})$ is dropped. For the FIR case, we

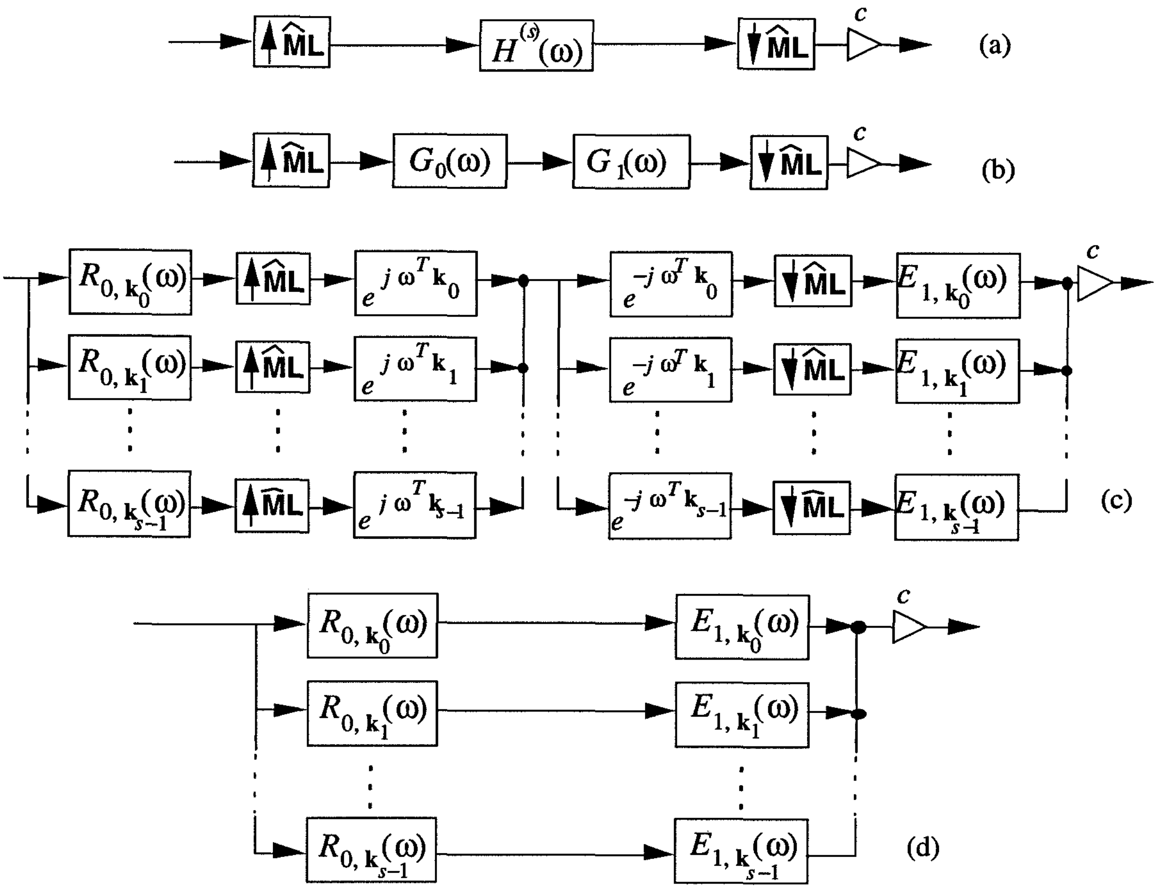

Figure 3.4-1 Efficient implementation of an MD filter.

can avoid this inefficiency by using polyphase decompositions. We decompose $G_{F,0}(\omega)$ and $G_{F,1}(\omega)$ into polyphase components with respect to $\widehat{\mathbf{ML}}$, so

$$\begin{aligned} G_{F,0}(\omega) &= \sum_{\mathbf{k}_j \in \mathcal{N}(\widehat{\mathbf{ML}})} e^{j\omega^T\mathbf{k}_j} R_{F,0,\mathbf{k}_j}((\widehat{\mathbf{ML}})^T\omega), \qquad \text{(Type 2)} \\ \text{and}\quad G_{F,1}(\omega) &= \sum_{\mathbf{k}_j \in \mathcal{N}(\widehat{\mathbf{ML}})} e^{-j\omega^T\mathbf{k}_j} E_{F,1,\mathbf{k}_j}((\widehat{\mathbf{ML}})^T\omega). \qquad \text{(Type 1)} \end{aligned} \tag{3.4.2}$$

Then, we can use Noble identities (Fig. 2.3-1) to move the decimators and expanders, and obtain the more efficient implementation in Fig. 3.4-1(c), where $s = J(\widehat{\mathbf{ML}})$. Now, consider the transfer function, $D_{F,i,j}(\omega)$, from the output of $R_{F,0,\mathbf{k}_i}(\omega)$ to the input of $E_{F,1,\mathbf{k}_j}(\omega)$, where $\mathbf{k}_i, \mathbf{k}_j \in \mathcal{N}(\widehat{\mathbf{ML}})$. Using the polyphase identity again, we know

$$D_{F,i,j}(\omega) = \widehat{\mathbf{ML}}\text{-fold decimated version of } e^{j\omega^T(\mathbf{k}_i - \mathbf{k}_j)}. \tag{3.4.3}$$

Then, it can be easily shown that

$$D_{F,i,j}(\omega) = \begin{cases} 1, & \mathbf{k}_i = \mathbf{k}_j \\ 0, & \text{otherwise.} \end{cases} \tag{3.4.4}$$

Therefore, Fig. 3.4-1(c) is equivalent to Fig. 3.4-1(d), where the number of required OPP's is reduced to only $2N$.

Remarks:

1. These discussions hold for FIR as well as IIR cases. For the IIR case, although polyphase technique still works, the implementation we obtain in Fig. 3.4-1(d) may require more OPP's than Fig. 3.4-1(b).
2. Recall that in Design Example 3.1, the number of OPP's required for the efficient implementation of Fig. 3.4-1(d) is only $2N = 118$, while direct implementation would require approximately $N^2/J(\widehat{\mathbf{M}}) = 59^2/3 \approx 1160$ OPP's.
3. It is easy to extend the above discussion to the case of more than two dimensions. For the D-dimensional case, direct implementation of $G_F(\omega)$ requires $N^D/J(\widehat{\mathbf{ML}})$ OPP's. Instead, we can implement it as in Fig. 3.4-1(a). Now, $H_F^{(s)}(\omega) = \prod_{i=0}^{D-1} G_{F,i}(\omega)$, where $G_{F,i}(\omega) = P_F(\omega_i)$. We can apply polyphase technique on $G_{F,0}(\omega)$ and $G_{F,D-1}(\omega)$, which then requires only $2N$ OPP's. Since implementing all the other $G_{F,1}(\omega), \ldots, G_{F,D-2}(\omega)$ still requires $(D-2)J(\widehat{\mathbf{ML}})\,N$ OPP's, the total number of OPP's required is $2N + (D-2)J(\widehat{\mathbf{ML}})\,N$. The complexity is still in $\mathcal{O}(N)$.

3.5. APPLICATIONS

Given the integer matrix $\mathbf{M}$, we have shown how to design the decimation filter and interpolation filter with respect to $\mathbf{M}$. On the other hand, in practical filter design (other than decimation filters and interpolation filters), we are sometimes given the specifications of the passband (the shape of the parallelepiped) instead of $\mathbf{M}$. Therefore, we need a systematic way to find the corresponding $\mathbf{H}$, so that we can design the filter. To do this, we notice that every parallelepiped-shaped passband can be expressed as

$$SPD(\mathbf{P}) + 2\pi\mathbf{m}, \qquad \mathbf{m} \in \mathcal{N} \tag{3.5.1}$$

where the columns of $\mathbf{P}$ can be called the generating vectors. Fig. 3.5-1 shows the generating vectors, $\mathbf{p}_0$ and $\mathbf{p}_1$, for a 2D parallelepiped. Comparing (3.5.1) with $SPD(\pi\mathbf{H}^{-T})$, we know that if we let

$$\mathbf{H} = \pi\mathbf{P}^{-T} \tag{3.5.2}$$

and follow the design procedure in Section 3.3, the resulting filter will have the desired passband as in (3.5.1).

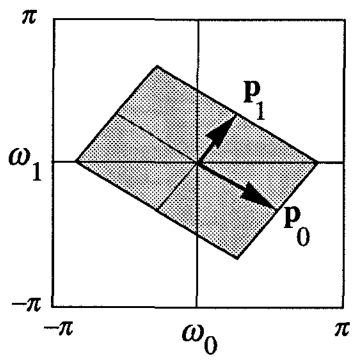

Figure 3.5-1 The generating vectors of a 2D parallelepiped.

Once we design a filter with some parallelepiped-shaped passband, many other filters can be designed in a straightforward way. Fig. 3.5-2 shows some 2D examples of these filters. First, if we choose $p(n)$ in Step 2 to be a bandpass filter, we can get $H_F(\omega)$ as in Fig. 3.5-2(a). Second, we know that the modulation in the time domain leads to a shift in the frequency domain, as in the following relation:

$$h(\mathbf{n})\, e^{j\mathbf{b}^T\mathbf{n}} \quad \longleftrightarrow \quad H_F(\omega - \mathbf{b}). \tag{3.5.3}$$

Therefore, every filter with a parallelepiped-shaped passband which is not centered at the origin can be obtained simply by modulating a filter with the passband centered at the origin. For example, filters in Fig. 3.5-2(b), including the fan filter, can be designed using the proposed approach followed by a proper modulation. Finally, since the sum (or difference) of zero-phase filters is still a zero-phase filter with the passband being the sum (or difference) of the passbands of these filters, all the filters in Fig. 3.5-2(c), including hexagonal filters, can be obtained easily.

3.6. MULTIDIMENSIONAL UNIFORM DFT QMF BANKS

The proposed design procedure also applies to the design of MD uniform DFT QMF banks. We shall show that all the properties which can be achieved in 1D uniform DFT QMF banks [Swaminathan and Vaidyanathan, 1986], [Vaidyanathan, 1987c], can be extended into MD using this approach.

Let J denote $J(\mathbf{M})$ for simplicity. A J-channel maximally-decimated QMF bank is shown in Fig. 3.6-1(a). In general, this system is a linear time-varying (LTV) system. We want to choose analysis filters $H_{F,\mathbf{m}_i}(\omega)$'s and synthesis filters $F_{F,\mathbf{m}_i}(\omega)$'s properly such that this system has the properties mentioned in Section 2.4. A special QMF bank is the so-called uniform DFT QMF bank,

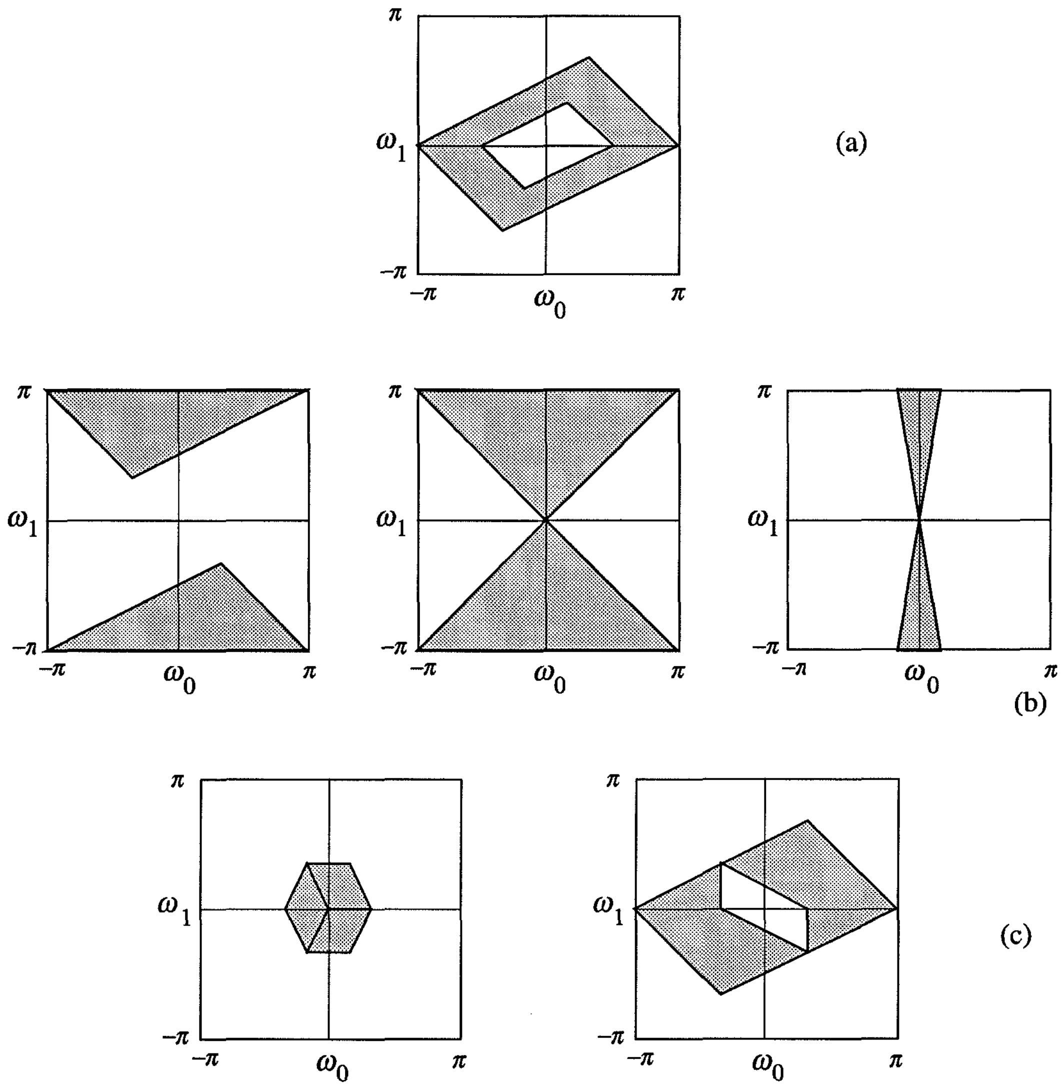

Figure 3.5-2 Filters which can be obtained by using the proposed method.

where the analysis filters and the synthesis filters are related as

$$\begin{aligned} H_{F,\mathbf{m}_i}(\omega) &= H_{F,\mathbf{m}_0}(\omega - 2\pi\mathbf{M}^{-T}\mathbf{m}_i), \\ F_{F,\mathbf{m}_i}(\omega) &= F_{F,\mathbf{m}_0}(\omega - 2\pi\mathbf{M}^{-T}\mathbf{m}_i), \end{aligned} \tag{3.6.1}$$

with $\mathbf{m}_i \in \mathcal{N}(\mathbf{M}^T)$. Because filters in all other channels are completely determined by the filters in the 0th channel, $H_{F,\mathbf{m}_0}(\omega)$ and $F_{F,\mathbf{m}_0}(\omega)$ are called the prototype analysis filter and synthesis filter, respectively. If we let $H_{F,\mathbf{m}_0}(\omega)$ have passband support in $SPD(\pi\mathbf{M}^{-T})$, then it can be shown that the passband supports of analysis filters cover the whole frequency range $[-\pi,\pi)^D$. It can be verified that this system can be redrawn as Fig. 3.6-1(b), where the $E_{F,\mathbf{k}_j}(\omega)$'s are the Type 1 polyphase components of the prototype analysis filter $H_{F,\mathbf{m}_0}(\omega)$ with respect to $\mathbf{M}$, and the $R_{F,\mathbf{k}_j}(\omega)$'s are the

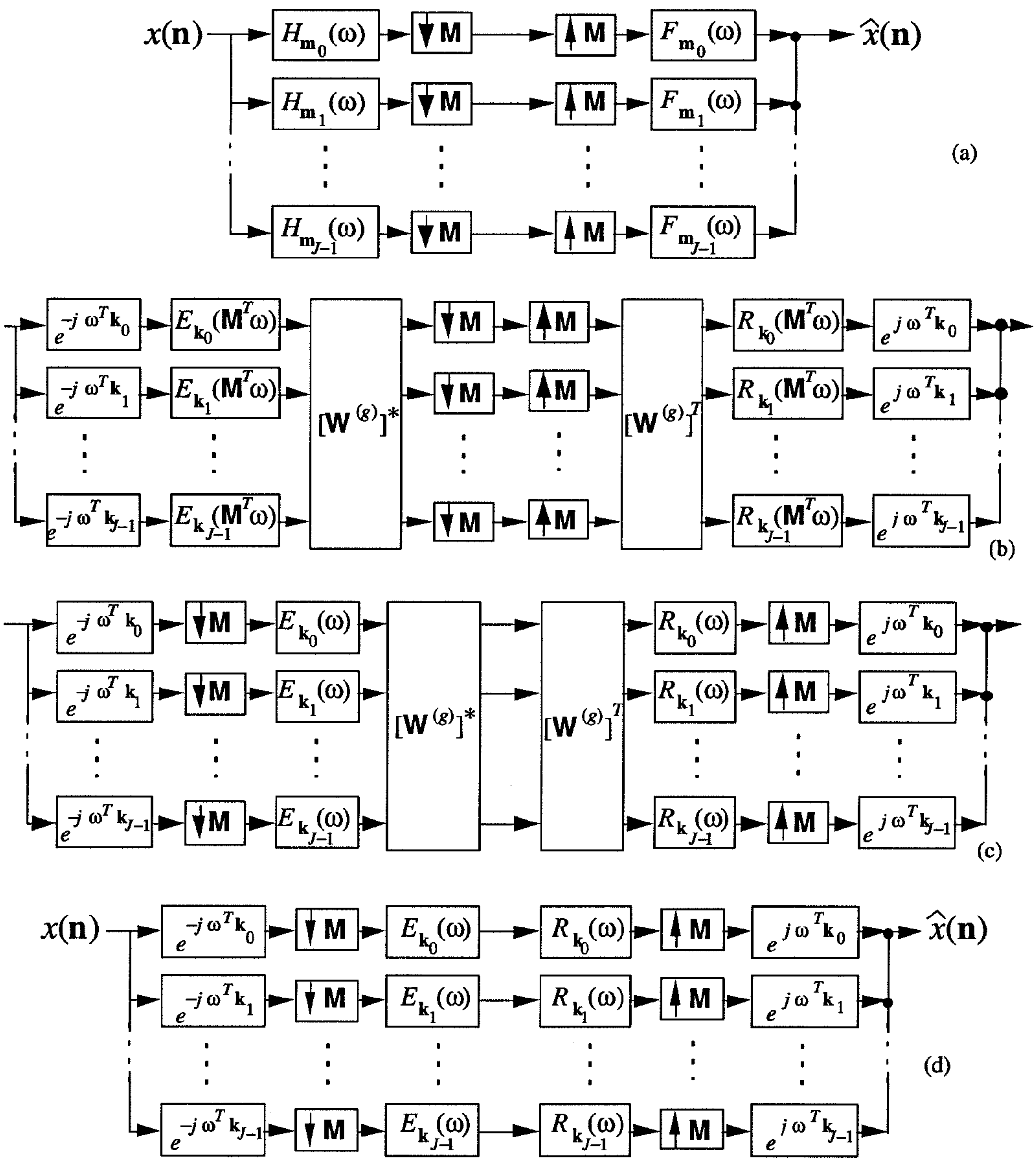

Figure 3.6-1 MD uniform DFT QMF bank.

Type 2 polyphase components of the prototype synthesis filter $F_{F,\mathbf{m}_0}(\boldsymbol{\omega})$. Also, the $J \times J$ matrix, $\mathbf{W}^{(g)}$, is called the generalized DFT matrix [Dudgeon and Mersereau, 1984], [Vaidyanathan, 1990b], with its (i,j)th element defined as

$$[\mathbf{W}^{(g)}]_{i,j} = e^{-j2\pi \mathbf{m}_i^T \mathbf{M}^{-1} \mathbf{k}_j} \qquad \mathbf{m}_i \in \mathcal{N}(\mathbf{M}^T),\ \mathbf{k}_j \in \mathcal{N}(\mathbf{M}). \tag{3.6.2}$$

Using Noble identities to move the decimators and expanders, we get the equivalent system in Fig. 3.6-1(c). It can be shown that $\mathbf{W}^{(g)}$ is unitary, with $[\mathbf{W}^{(g)}]^T[\mathbf{W}^{(g)}]^* = J\mathbf{I}$. Therefore, Fig. 3.6-1(c) can be redrawn as Fig. 3.6-1(d) (with the scale J omitted).

There are many ways of choosing $E_{F,\mathbf{k}_j}(\omega)$'s and $R_{F,\mathbf{k}_j}(\omega)$'s, depending on properties we want the system to have. For example,

1. We can choose $E_{F,\mathbf{k}_j}(\omega)$'s and $R_{F,\mathbf{k}_j}(\omega)$'s such that

$$R_{F,\mathbf{k}_j}(\omega)E_{F,\mathbf{k}_j}(\omega) = R_{F,\mathbf{k}_0}(\omega)E_{F,\mathbf{k}_0}(\omega) \qquad \text{for } j = 0, \ldots, J-1. \tag{3.6.3}$$

In other words, $R_{F,\mathbf{k}_j}(\omega)E_{F,\mathbf{k}_j}(\omega)$ is independent with j. Then, we get a system that is free from aliasing. For this case, the overall transfer function is

$$T_F(\omega) = R_{F,\mathbf{k}_0}(\mathbf{M}^T\omega)E_{F,\mathbf{k}_0}(\mathbf{M}^T\omega). \tag{3.6.4}$$

This can be seen by using Noble identities to move all $E_{F,\mathbf{k}_j}(\omega)$'s and $R_{F,\mathbf{k}_j}(\omega)$'s to the right across **M**-fold expanders and realizing that the rest part is an identity system. In fact, (3.6.3) is necessary and sufficient for the system to be alias-free (see [Chen and Vaidyanathan, 1993b] for details).

2. If we choose $R_{F,\mathbf{k}_j}(\omega) = 1/E_{F,\mathbf{k}_j}(\omega)$, we get a PR system. However, this choice may result in unstable synthesis filters, just as in the 1D case [Vaidyanathan, 1987c].

3. If we choose

$$R_{F,\mathbf{k}_j}(\omega) = \prod_{\substack{\mathbf{k}_i \in \mathcal{N}(\mathbf{M}) \\ i \neq j}} E_{F,\mathbf{k}_i}(\omega), \tag{3.6.5}$$

we obtain a system which is free from aliasing and has overall transfer function

$$T_F(\omega) = \prod_{\mathbf{k}_j \in \mathcal{N}(\mathbf{M})} E_{F,\mathbf{k}_j}(\mathbf{M}^T\omega). \tag{3.6.6}$$

3a. If analysis filters are all FIR, then synthesis filters will also be FIR, hence there is no stability problem. However, for the FIR case, if we want a PR system where $T_F(\omega)$ equals unity, then all $E_{F,\mathbf{k}_j}(\omega)$'s must be pure delays and hence each analysis filter has only J nonzero coefficients. For nontrivial filters with more then J nonzero coefficients, we can only make $T_F(\omega)$ zero-phase (no PHD) and optimize coefficients of $E_{F,\mathbf{k}_j}(\omega)$'s (coefficients of $H_{F,\mathbf{m}_0}(\omega)$) such that $|T_F(\omega)| \approx 1$ (small AMD). The counterpart of this in the 1D case was presented in [Swaminathan and Vaidyanathan, 1986].

3b. We can choose $E_{F,\mathbf{k}_j}(\omega)$'s to be stable IIR allpass functions ($|E_{F,\mathbf{k}_j}(\omega)| = 1$ for all ω). Then, all the analysis filters and synthesis filters as well are stable. From (3.6.6), we know $|T_F(\omega)| = 1$ hence AMD is completely eliminated. In this case, $T_F(\omega)$ is a stable IIR transfer function so PHD can not be avoided. In applications where phase information is important (e.g., in 2D image processing), an allpass filter can be cascaded with this system to equalize its phase response. The 1D counterpart of this can be found in [Vaidyanathan, 1987c], [Vaidyanathan, 1987a].

4. We can choose $E_{F,\mathbf{k}_j}(\boldsymbol{\omega})$'s to be stable IIR allpass functions (same as in Case 3b above) and let

$$R_{F,\mathbf{k}_j}(\boldsymbol{\omega}) = E^*_{F,\mathbf{k}_j}(\boldsymbol{\omega}). \tag{3.6.7}$$

Now, in each channel of Fig. 3.6-1(d), we have $R_{F,\mathbf{k}_j}(\boldsymbol{\omega})E_{F,\mathbf{k}_j}(\boldsymbol{\omega}) = E^*_{F,\mathbf{k}_j}(\boldsymbol{\omega})E_{F,\mathbf{k}_j}(\boldsymbol{\omega}) = |E_{F,\mathbf{k}_j}(\boldsymbol{\omega})|^2 = 1$. So, $T_F(\boldsymbol{\omega}) = 1$ and we get a PR system. Note that (3.6.7) implies $r_{\mathbf{k}_j}(\mathbf{n}) = e^*_{\mathbf{k}_j}(-\mathbf{n})$ so $r_{\mathbf{k}_j}(\mathbf{n})$ is also stable. However, if $e_{\mathbf{k}_j}(\mathbf{n})$ are chosen to be causal, $r_{\mathbf{k}_j}(\mathbf{n})$ becomes anticausal. This problem of anticausal synthesis filters can be solved by running the filters *backwards* [Ansari and Lau, 1987], [Ramstad, 1988], [Mitra et al., 1992], [Chen and Vaidyanathan, 1992d].

Although the above theoretical derivation may seem to be easy, direct optimization of filter coefficients is often unreasonably difficult due to the large number of parameters to be optimized, especially when D is large. Furthermore, the large number of OPP's required in direct implementation is also a problem. Our approach overcomes these two difficulties. We now show that starting from an appropriate 1D uniform DFT QMF bank, we can derive an MD uniform DFT QMF bank with $H_{F,\mathbf{m}_0}(\boldsymbol{\omega})$ having support $SPD(\pi\mathbf{M}^{-T})$.

Design Procedure

Step 1. Design the prototype analysis/synthesis filters, $P_{F,0}(\omega)$ and $Q_{F,0}(\omega)$, of a 1D J-channel uniform DFT QMF bank. Let $P_{F,0}(\omega)$ have passband support in $[-\pi/J, \pi/J)$.

Step 2. Construct the separable MD filters $H^{(s)}_{F,\mathbf{k}_0}(\boldsymbol{\omega})$ and $F^{(s)}_{F,\mathbf{k}_0}(\boldsymbol{\omega})$ as

$$\begin{aligned} H^{(s)}_{F,\mathbf{k}_0}(\boldsymbol{\omega}) &= P_{F,0}(\omega_0)P_{F,0}(\omega_1)\cdots P_{F,0}(\omega_{D-1}), \\ F^{(s)}_{F,\mathbf{k}_0}(\boldsymbol{\omega}) &= Q_{F,0}(\omega_0)Q_{F,0}(\omega_1)\cdots Q_{F,0}(\omega_{D-1}). \end{aligned} \tag{3.6.8}$$

Step 3. Define $h_{\mathbf{m}_0}(\mathbf{n}) \triangleq h^{(s)}_{\mathbf{k}_0}(\widehat{\mathbf{M}}\mathbf{n})$ and $f_{\mathbf{m}_0}(\mathbf{n}) \triangleq f^{(s)}_{\mathbf{k}_0}(\widehat{\mathbf{M}}\mathbf{n})$. That is, decimate $h^{(s)}_{\mathbf{k}_0}(\mathbf{n})$ and $f^{(s)}_{\mathbf{k}_0}(\mathbf{n})$ by $\widehat{\mathbf{M}}$. As explained previously, the resulting $H_{F,\mathbf{m}_0}(\boldsymbol{\omega})$ has support in $SPD(\pi\mathbf{M}^{-T})$.

After $H_{F,\mathbf{m}_0}(\boldsymbol{\omega})$ and $F_{F,\mathbf{m}_0}(\boldsymbol{\omega})$ are obtained, we may implement the MD QMF bank as in Fig. 3.6-1(c). It has been shown in Section 3.3 that all the $E_{F,\mathbf{k}_j}(\boldsymbol{\omega})$'s and $R_{F,\mathbf{k}_j}(\boldsymbol{\omega})$'s are separable, even though $H_{F,\mathbf{m}_0}(\boldsymbol{\omega})$ and $F_{F,\mathbf{m}_0}(\boldsymbol{\omega})$ are not separable. Therefore, this indeed gives a very efficient implementation.

Since filters in an MD DFT filter bank are all determined by one prototype filter, it is not counter-intuitive that we can apply our method in Section 3.3 to the prototype filter of a 1D DFT filter bank and obtain the MD prototype filter. However, the following claim is non-trivial:

Claim: The $H_{F,\mathbf{m}_0}(\boldsymbol{\omega})$ and $F_{F,\mathbf{m}_0}(\boldsymbol{\omega})$ obtained are the desired prototype filters for a J-channel MD uniform DFT QMF bank. This filter bank will have all the properties that the original 1D J-channel uniform DFT QMF bank has. For example, if the 1D DFT filter bank system is PR, the resulting MD DFT filter bank system is also PR. Similarly, the design method preserves other properties like: no ALD, no or small AMD, and no PHD.

Justification

Consider the J-channel 1D uniform DFT QMF bank which we start from. Let $B_{F,k}(\omega)$'s denote Type 1 polyphase components of the prototype analysis filter $P_{F,0}(\omega)$, and $S_{F,k}(\omega)$'s denote Type 2 polyphase components of the prototype synthesis filter $Q_{F,0}(\omega)$. Suppose this is a system without aliasing, i.e.,

$$S_{F,k}(\omega)B_{F,k}(\omega) = S_{F,0}(\omega)B_{F,0}(\omega) \qquad \text{for } k = 0, \ldots, J-1. \tag{3.6.9}$$

It has been proved in Section 3.3 that polyphase components of the resulting MD filters are related with those of 1D filters as:

$$E_{F,\mathbf{k}_j}(\boldsymbol{\omega}) = B_{F,l_0}(\omega_0) \cdots B_{F,l_{D-1}}(\omega_{D-1}), \tag{3.6.10}$$

and

$$R_{F,\mathbf{k}_j}(\boldsymbol{\omega}) = S_{F,l_0}(\omega_0) \cdots S_{F,l_{D-1}}(\omega_{D-1}), \tag{3.6.11}$$

where $[l_0 \quad l_1 \quad \cdots \quad l_{D-1}]^T = \mathbf{l} = \widehat{\mathbf{M}}\mathbf{k}_j$. Considering $R_{F,\mathbf{k}_j}(\boldsymbol{\omega})E_{F,\mathbf{k}_j}(\boldsymbol{\omega})$, we obtain

$$R_{F,\mathbf{k}_j}(\boldsymbol{\omega})E_{F,\mathbf{k}_j}(\boldsymbol{\omega}) = \prod_{i=0}^{D-1} S_{F,l_i}(\omega_i)B_{F,l_i}(\omega_i) = \prod_{i=0}^{D-1} S_{F,0}(\omega_i)B_{F,0}(\omega_i). \tag{3.6.12}$$

Since $R_{F,\mathbf{k}_j}(\boldsymbol{\omega})E_{F,\mathbf{k}_j}(\boldsymbol{\omega})$ is independent with j, the resulting MD QMF bank is also free from aliasing with overall transfer function

$$T_F(\boldsymbol{\omega}) = R_{F,\mathbf{k}_0}(\mathbf{M}^T\boldsymbol{\omega})E_{F,\mathbf{k}_0}(\mathbf{M}^T\boldsymbol{\omega}). \tag{3.6.13}$$

Given that both the 1D and MD DFT QMF banks are alias-free, let us take a closer look at these transfer functions. Define $\mathbf{e}_i$ to be a $D \times 1$ vector with zero elements except that the ith element is unity. Then, (3.6.12) can be written as

$$R_{F,\mathbf{k}_j}(\boldsymbol{\omega})E_{F,\mathbf{k}_j}(\boldsymbol{\omega}) = \prod_{i=0}^{D-1} S_{F,0}(\mathbf{e}_i^T\boldsymbol{\omega})B_{F,0}(\mathbf{e}_i^T\boldsymbol{\omega}), \tag{3.6.14}$$

and (3.6.13) becomes

$$T_F(\omega) = \prod_{i=0}^{D-1} S_{F,0}(\mathbf{e}_i^T \mathbf{M}^T \omega) B_{F,0}(\mathbf{e}_i^T \mathbf{M}^T \omega). \tag{3.6.15}$$

Let $V_F(\omega)$ denote the overall transfer function of the 1D QMF bank. Under the alias-free condition, we know $V_F(\omega) = B_{F,0}(J\omega) S_{F,0}(J\omega)$. Define $T_F^{(s)}(\omega)$ as

$$T_F^{(s)}(\omega) \triangleq \prod_{i=0}^{D-1} V_F(\omega_i). \tag{3.6.16}$$

Since $J\omega_i = J\mathbf{e}_i^T \omega = \mathbf{e}_i^T \mathbf{M}^T \widehat{\mathbf{M}}^T \omega$, (3.6.16) can be written as

$$T_F^{(s)}(\omega) = \prod_{i=0}^{D-1} S_{F,0}(J\omega_i) B_{F,0}(J\omega_i) = \prod_{i=0}^{D-1} S_{F,0}(\mathbf{e}_i^T \mathbf{M}^T \widehat{\mathbf{M}}^T \omega) B_{F,0}(\mathbf{e}_i^T \mathbf{M}^T \widehat{\mathbf{M}}^T \omega). \tag{3.6.17}$$

Comparing (3.6.15) and (3.6.17), we see that

$$T_F^{(s)}(\omega) = T_F(\widehat{\mathbf{M}}^T \omega), \tag{3.6.18}$$

i.e., $T_F^{(s)}(\omega)$ is exactly the $\widehat{\mathbf{M}}$-fold expanded version of $T_F(\omega)$. Note that (3.6.18) can be written as

$$T_F(\omega) = T_F^{(s)}(\widehat{\mathbf{M}}^{-T} \omega). \tag{3.6.19}$$

Also note that $T_F(\omega)$ is the $\widehat{\mathbf{M}}$-fold decimated version of $T_F^{(s)}(\omega)$ so that the transfer function of the designed MD QMF bank can be obtained by $\widehat{\mathbf{M}}$-fold decimating the product of the 1D overall transfer function $V_F(\omega)$ in each dimension.

Now, it is easy to show that other properties about AMD, PHD, PR are preserved.

1. Given there is no ALD, we need to discuss properties about AMD.

   1a. For the FIR case, we can optimize filter coefficients in the 1D filter bank such that $|V_F(\omega)| \approx 1\ \forall \omega$. From (3.6.16) and (3.6.19), we see that $|T_F(\omega)| \approx 1\ \forall \omega$, too. That is, AMD remains small. More specifically, if $V_F(\omega)$ has ripple size δ, the resulting ripple sizes of both $T_F^{(s)}(\omega)$ and $T_F(\omega)$ are at most $D\delta$.

   1b. For the IIR case, we can start from 1D prototype filters with allpass polyphase components and make $V_F(\omega)$ to be allpass (no AMD). From (3.6.16) and (3.6.19), we can see that $T_F(\omega)$ is still an allpass function. Therefore, there is no AMD in the resulting MD filter bank.

2. Given there is no ALD, suppose the 1D overall transfer function $V_F(\omega)$ has zero phase, i.e., $V_F(\omega)$ is real for all ω. From (3.6.16) and (3.6.19), we can conclude that $T_F(\omega)$ is real for all ω (zero phase) so there is no PHD.

3. Finally, suppose the original system satisfies PR so that $V_F(\omega) = 1$. From (3.6.16) and (3.6.19), we can easily conclude that $T_F(\boldsymbol{\omega}) = 1$ so PR is preserved.

There are many useful 1D DFT filter banks in literature [Swaminathan and Vaidyanathan, 1986], [Vaidyanathan, 1987c], [Vaidyanathan, 1987a], [Ramstad, 1988]. We can apply our method to each of these and derive many useful MD filter banks. In the following, we present several examples.

MD Filter Bank Derived from Johnston's Filters (Two-Channel Case)

Design Example 3.3: The most commonly used 1D DFT QMF bank is the two-channel FIR case. Johnston designed such filter banks for various specifications and the optimized filter coefficients were tabulated [Johnston, 1980], [Crochiere and Rabiner, 1983]. These systems have no ALD, no PHD, and small AMD. Fig. 3.6-2(a) shows the frequency response of the prototype analysis filter $P_{F,0}(\omega)$ (which is named 32D in Johnston's table). We can apply our method to derive a two-channel MD DFT QMF bank for any decimation matrix $\mathbf{M}$ with $J(\mathbf{M}) = 2$. As an example, we choose

$$\mathbf{M} = \begin{bmatrix} 1 & 1 \\ -1 & 1 \end{bmatrix} \tag{3.6.20}$$

which defines the so-called quincunx lattice. Applying the design procedure, we obtain the 2D prototype analysis filter $H_{F,\mathbf{m}_0}(\boldsymbol{\omega})$, as shown in Fig. 3.6-2(b). According to relations in (3.6.1), the other analysis filter $H_{F,\mathbf{m}_1}(\boldsymbol{\omega})$ is obtained by shifting $H_{F,\mathbf{m}_0}(\boldsymbol{\omega})$, i.e., $H_{F,\mathbf{m}_1}(\omega_0, \omega_1) = H_{F,\mathbf{m}_0}(\omega_0 - \pi, \omega_1 - \pi)$. The overall transfer function $T_F(\boldsymbol{\omega})$, which is zero-phase and has magnitude close to unity, is shown in Fig. 3.6-2(c).

Remark: The idea of using Johnston's results to derive 2D quincunx QMF bank has been proposed in [Vaidyanathan, 1993a]. Our method generalizes this result and is able to derive any two-channel DFT QMF bank for arbitrary $\mathbf{M}$ (with $J(\mathbf{M}) = 2$) and any number of dimensions.

MD FIR Filter Bank (with More than Two Channels)

Design Example 3.4: This is also an FIR example. Let $\mathbf{M}$ be same as in Design Example 3.1, so there are three channels and the passband supports of these three analysis filters can be chosen as in Fig. 3.6-3. We use the coefficients obtained in Example 2 of [Swaminathan and Vaidyanathan, 1986] to form $P_{F,0}(\omega)$, the optimal zero-phase prototype analysis filter of a 3-channel 1D uniform DFT QMF bank. It has length $N = 49$, passband ripple $\delta_1 = 0.001406$, and stopband ripple $\delta_2 = 0.003245$ (-49.78dB), as shown in Fig. 3.6-4(a). For this 1D filter bank, the overall transfer function is close to unity with the ripple size $\delta = 0.004226$. Following the steps described earlier, we obtain $H_{F,\mathbf{m}_0}(\boldsymbol{\omega})$, which is shown in Fig. 3.6-4(b), with passband ripple $\delta_1' = 0.003398$, and

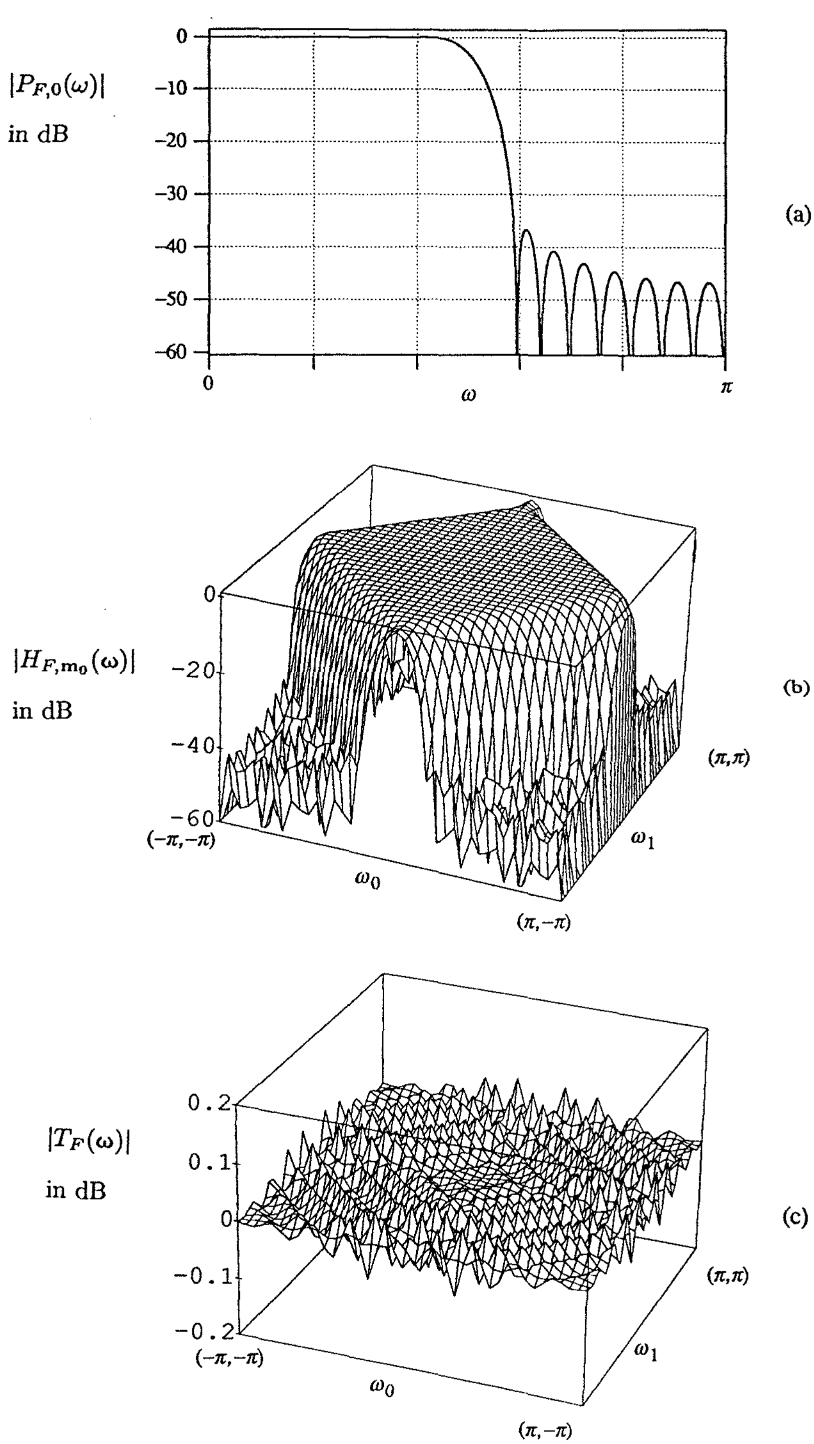

Figure 3.6-2 Frequency response of filters in Design Example 3.3: (a) $P_{F,0}(\omega)$, (b) $H_{F,\mathbf{m}_0}(\omega)$, (c) $T_F(\omega)$.

stopband ripple $\delta_2' = 0.00570$ (-44.88dB). The resulting overall transfer function $T_F(\omega)$ is also shown in Fig. 3.6-4(c), which has ripple size $\delta' = 0.00847$.

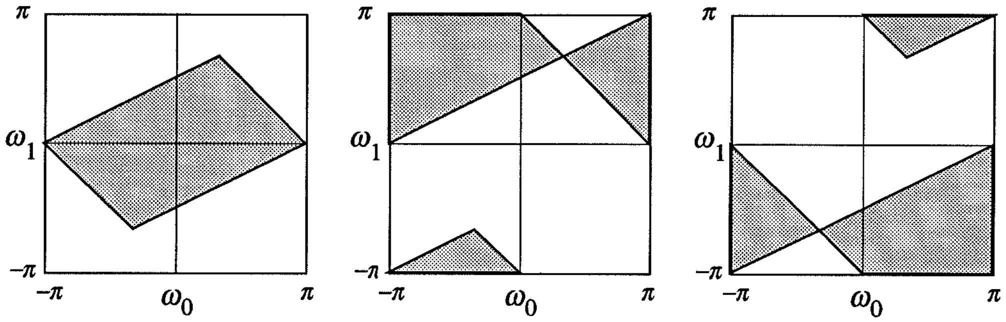

Figure 3.6-3 Passband supports of analysis filters in Design Example 3.4.

MD IIR Allpass-Based Filter Bank

Design Example 3.5: We now present an example with IIR filters. We start from a 1D DFT QMF bank in which the prototype analysis filter $P_{F,0}(\omega)$ has allpass polyphase components. For the 1D two channel case, it has been described how the design of common digital IIR filters can be modified to design IIR filters with two allpass polyphase components and how this can be used in two-channel QMF banks [Vaidyanathan, 1987a]. Such a system gives very efficient implementation of alias-free filter banks with no AMD. For example, by using only one multiplication per input sample in the analysis filter bank, we can obtained analysis filters with more than 37dB stopband attenuation, as illustrated later. For the case of more channels, the design of 1D IIR filters with allpass polyphase components has also been addressed in [Renfors and Saramäki, 1987]. Our method can be applied to derive MD DFT QMF banks from results in both [Vaidyanathan, 1987a] and [Renfors and Saramäki, 1987]. Again, let us consider the quincunx case for simplicity. We start from a 1D fifth order prototype filter $P_0(z)$ with two allpass polyphase components. More specifically, let $P_0(z) = E_0(z^2) + z^{-1}E_1(z^2)$ where

$$E_0(z) = 0.5\frac{\alpha_0 + z^{-1}}{1 + \alpha_0 z^{-1}} \qquad \text{and} \qquad E_1(z) = 0.5\frac{\alpha_1 + z^{-1}}{1 + \alpha_1 z^{-1}}. \tag{3.6.21}$$

If we choose the synthesis filters as in Fig. 3.6-5, the overall transfer function of this 1D QMF bank is $2E_0(z^2)E_1(z^2)$. Using the method described in [Vaidyanathan, 1987a], we obtain $\alpha_0 = 0.226634$ and $\alpha_1 = 0.703653$. The frequency response of $P_{F,0}(\omega)$ is shown in Fig. 3.6-8(a). Applying our method, we can obtain the MD prototype analysis filter $H_{\mathbf{m}_0}$ with allpass and separable polyphase components (as proved in Section 3.3)

$$E_{F,\mathbf{k}_0}(\omega) = E_{F,0}(\omega_0)E_{F,0}(\omega_1) \qquad \text{and} \qquad E_{F,\mathbf{k}_1}(\omega) = E_{F,1}(\omega_0)E_{F,1}(\omega_1). \tag{3.6.22}$$

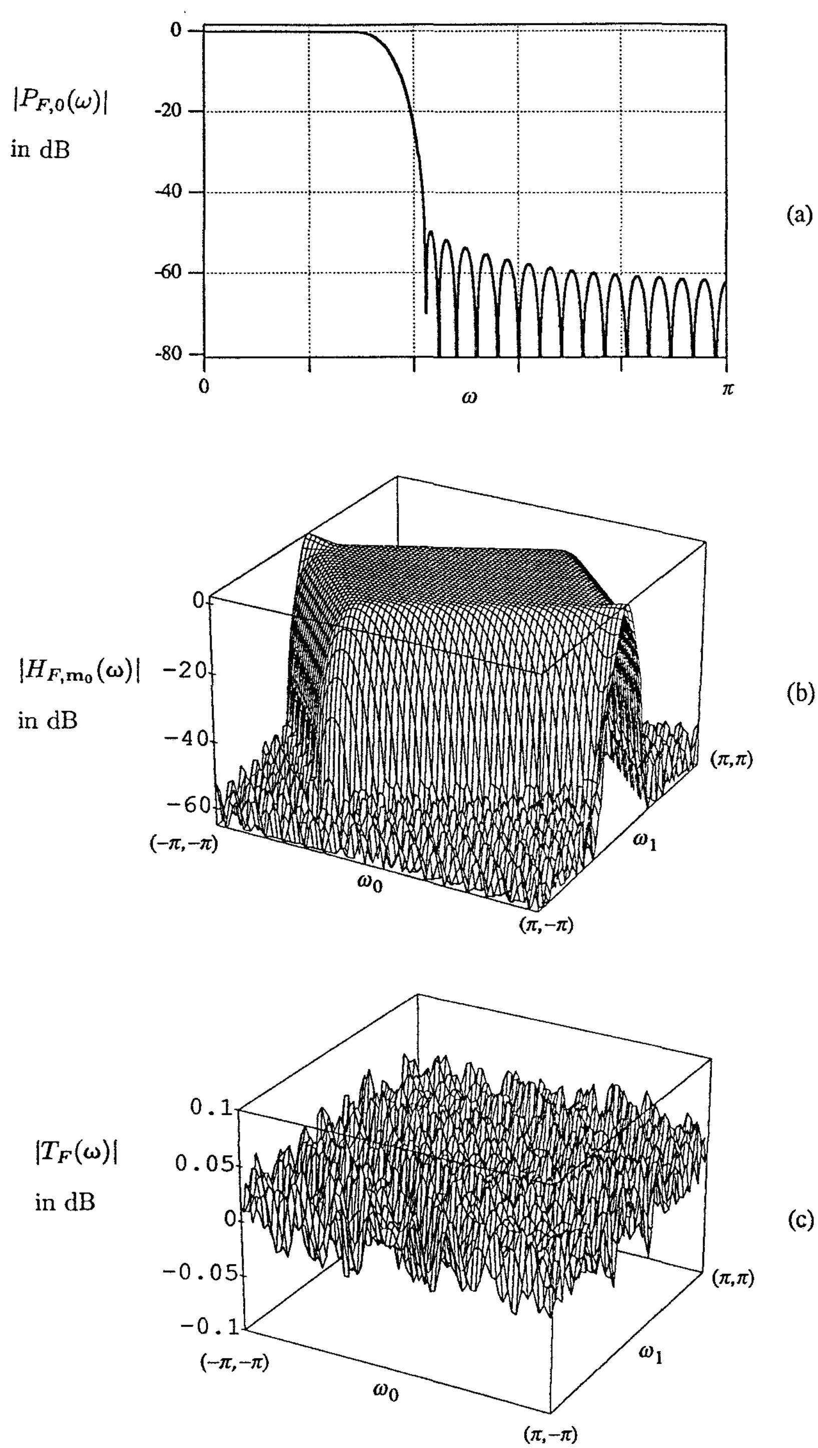

Figure 3.6-4 Frequency response of filters in Design Example 3.4: (a) $P_{F,0}(\omega)$, (b) $H_{F,\mathbf{m}_0}(\omega)$, (c) $T_F(\omega)$.

The frequency response of $H_{F,\mathbf{m}_0}(\omega)$ is shown in Fig. 3.6-8(b). Then, we can choose the polyphase component of synthesis filters as in (3.6.5) and obtain the system in Fig. 3.6-6 which is free from ALD and AMD. This system has the overall transfer function $T_F(\omega) = 2E_{F,\mathbf{k}_0}(\mathbf{M}^T\omega)E_{F,\mathbf{k}_1}(\mathbf{M}^T\omega)$ which is indeed allpass. The phase response of $T_F(\omega)$ is shown in Fig. 3.6-8(c), which is not zero-phase and hence PHD exists. When PHD is not desired, we can cascade the system with an allpass function to equalize the phase response. The overall group delays $\tau_0(\omega)$ and $\tau_1(\omega)$, which are defined as

$$\tau_0(\omega) \triangleq -\frac{\partial}{\partial\omega_0}[\text{phase of } T_F(\omega)] \quad \text{and} \quad \tau_1(\omega) \triangleq -\frac{\partial}{\partial\omega_1}[\text{phase of } T_F(\omega)], \tag{3.6.23}$$

are shown in Fig. 3.6-9(a) and Fig. 3.6-9(b). Note that all 2D filters in this case are separable and only four multipliers are required in analysis filters. Furthermore, since these multipliers operate at half of the input rate, we need only two multiplications per input pixel to obtain analysis filters with more than 35dB stopband attenuation.

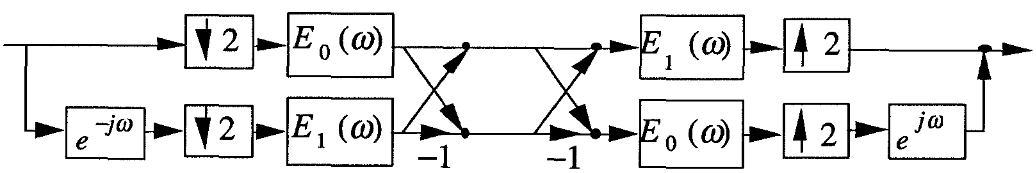

Figure 3.6-5 1D IIR QMF bank with no AMD.

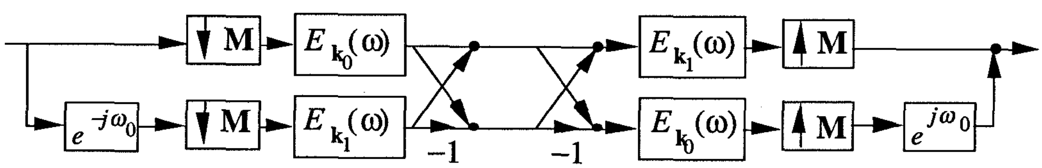

Figure 3.6-6 Polyphase implementation of an MD IIR QMF bank.

Remark: Although we use the 2D quincunx case as the example, the proposed method applies to arbitrary M and arbitrary number of dimensions.

MD IIR Perfect Reconstruction Filter Bank

Design Example 3.6: We can choose analysis filters same as in Design Example 3.5, but we choose synthesis filters according to (3.6.7) instead. Hence, we obtain the system in Fig. 3.6-7 which achieves PR. For the quincunx case, this idea has been presented in [Ansari and Lau, 1987]. Our method generalizes this to arbitrary M and arbitrary number of dimensions. Note that synthesis filters in this case are stable but anticausal. This can be solved by running the filters backwards [Ramstad, 1988] with properly chosen initial conditions [Mitra et al., 1992], [Chen and Vaidyanathan, 1992d]. In summary, since our method results in MD filters with separable polyphase components, all the results in [Ramstad, 1988], [Mitra et al., 1992], and [Chen and Vaidyanathan, 1992d] can be extended to the MD case automatically.

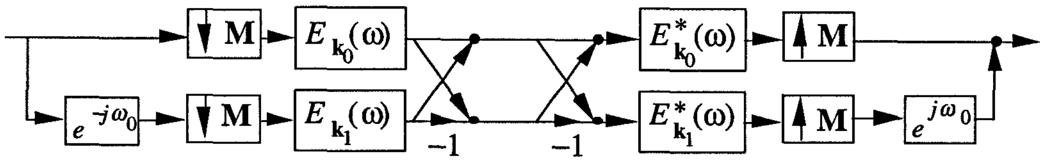

Figure 3.6-7 MD IIR QMF bank with PR property (Design Example 3.6).

3.7. MODIFICATION OF THE DESIGN PROCEDURE

The value of $J(\mathbf{M})$ may be very large in some applications, so the passband of the 1D prototype $P_F(\omega)$ becomes very narrow. In this case, the required filter order is very large. To deal with this problem, one can use interpolated FIR (IFIR) approach [Neuvo, Dong, and Mitra, 1984] to design $P_F(\omega)$. The other way is to exploit the common factors (if not unity) in each row of $\mathbf{M}$, as follows:

Step 1. Decompose $\mathbf{M}$ into $\mathbf{M} = \mathbf{M_p}\mathbf{\Lambda}$, where $\mathbf{\Lambda}$ is a diagonal matrix with diagonal elements $\lambda_i > 0$, and λ_i is the greatest common divisor of the elements in the ith column of $\mathbf{M}$.

Step 2. Design the 1D lowpass filters $p_0(n), \ldots, p_{D-1}(n)$. Each filter $p_i(n)$ should have the passband region $[-\frac{\pi}{J(\mathbf{M_p})\lambda_i}, \frac{\pi}{J(\mathbf{M_p})\lambda_i})$. It is easy to see that all these filters have passband wider than $[-\frac{\pi}{J(\mathbf{M})}, \frac{\pi}{J(\mathbf{M})})$, thus requiring less filter order than in procedures Section 3.3.

Step 3. Construct $h^{(s)}(\mathbf{n})$ as

$$h^{(s)}(\mathbf{n}) = p_0(n_0)p_1(n_1)\cdots p_{D-1}(n_{D-1}) \tag{3.7.1}$$

so,

$$H_F^{(s)}(\boldsymbol{\omega}) = P_{F,0}(\omega_0)P_{F,1}(\omega_1)\cdots P_{F,D-1}(\omega_{D-1}). \tag{3.7.2}$$

Step 4. Define $h(\mathbf{n}) \triangleq c_0 h^{(s)}(\widehat{\mathbf{M}}_\mathbf{p}\,\mathbf{n})$, where $\widehat{\mathbf{M}}_\mathbf{p} \triangleq J(\widehat{\mathbf{M}}_\mathbf{p}) \cdot \widehat{\mathbf{M}}_\mathbf{p}^{-1}$ and $c_0 = J(\widehat{\mathbf{M}}_\mathbf{p})$.

We have to show that $H_F(\boldsymbol{\omega})$ has the desired passband. From (3.7.2), $H_F^{(s)}(\boldsymbol{\omega})$ has passband

$$\frac{\pi}{J(\mathbf{M_p})}\mathbf{\Lambda}^{-1}\mathbf{x} + 2\pi\mathbf{k}', \qquad \mathbf{x} \in [-1,1)^D,\ \mathbf{k}' \in \mathcal{N}. \tag{3.7.3}$$

Therefore, using (2.2.1) with $\mathbf{M}$ replaced by $\widehat{\mathbf{M}}_\mathbf{p}$, we know that $H_F(\boldsymbol{\omega})$ has passband

$$\begin{aligned}
&\widehat{\mathbf{M}}_\mathbf{p}^T\left(\frac{\pi}{J(\mathbf{M_p})}\mathbf{\Lambda}^{-1}\mathbf{x} + 2\pi\mathbf{k}'\right) + 2\pi\mathbf{k} \qquad \mathbf{x} \in [-1,1)^D,\ \mathbf{k}' \in \mathcal{N},\ \mathbf{k} \in \mathcal{N}(\widehat{\mathbf{M}}_\mathbf{p}^T)\\
&= \frac{\pi}{J(\mathbf{M_p})}\widehat{\mathbf{M}}_\mathbf{p}^T\mathbf{\Lambda}^{-1}\mathbf{x} + 2\pi\widehat{\mathbf{M}}_\mathbf{p}^T\mathbf{k}' + 2\pi\mathbf{k}\\
&= \pi\mathbf{M}_\mathbf{p}^{-T}\mathbf{\Lambda}^{-1}\mathbf{x} + 2\pi(\widehat{\mathbf{M}}_\mathbf{p}^T\mathbf{k}' + \mathbf{k})\\
&= \pi\mathbf{M}^{-T}\mathbf{x} + 2\pi\mathbf{m} \qquad \mathbf{x} \in [-1,1)^D,\ \mathbf{m} \in \mathcal{N}.
\end{aligned} \tag{3.7.4}$$

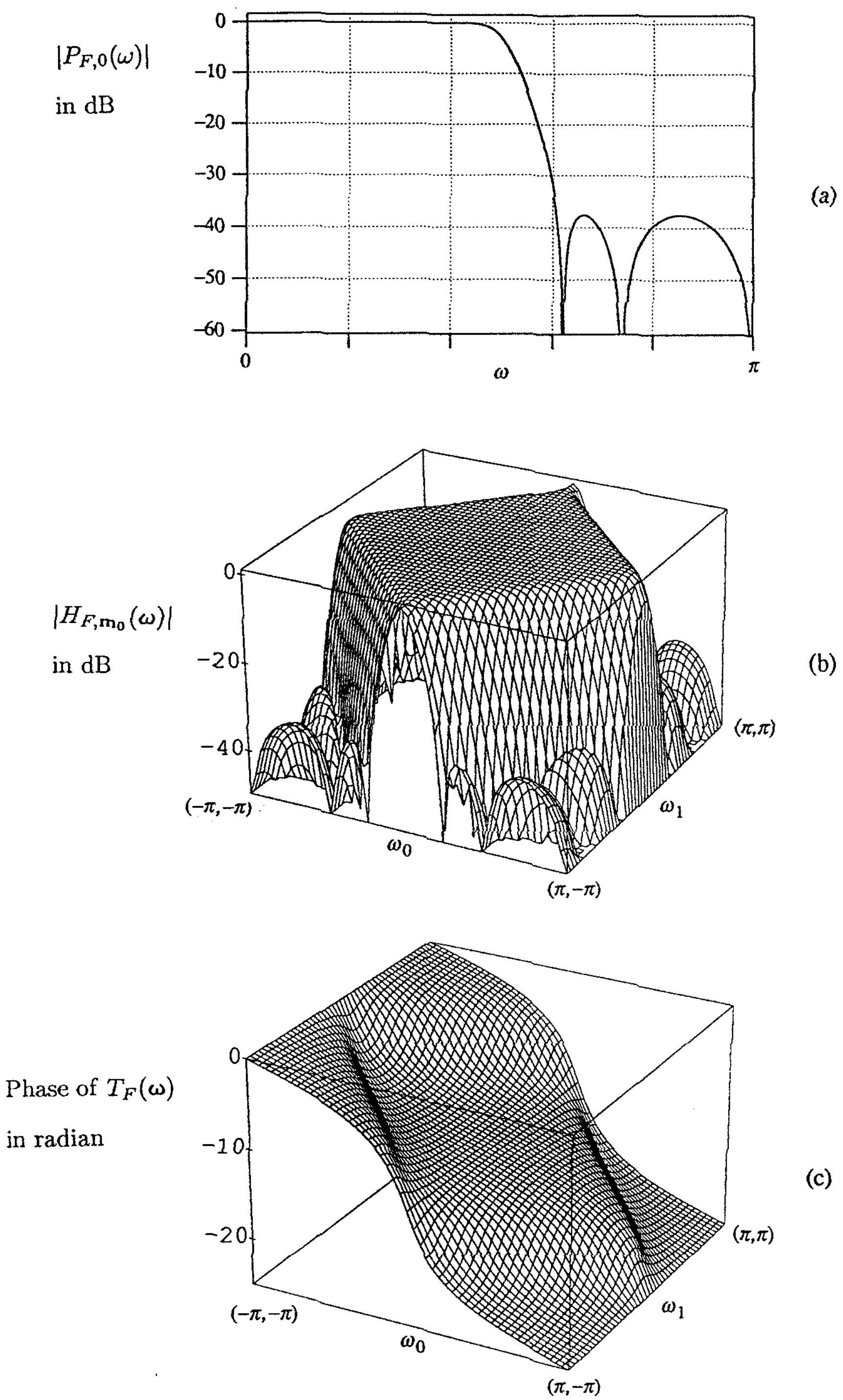

Figure 3.6-8 Frequency response of filters in Design Example 3.5: (a) $P_{F,0}(\omega)$, (b) $H_{F,\mathbf{m}_0}(\omega)$, (c) $T_F(\omega)$.

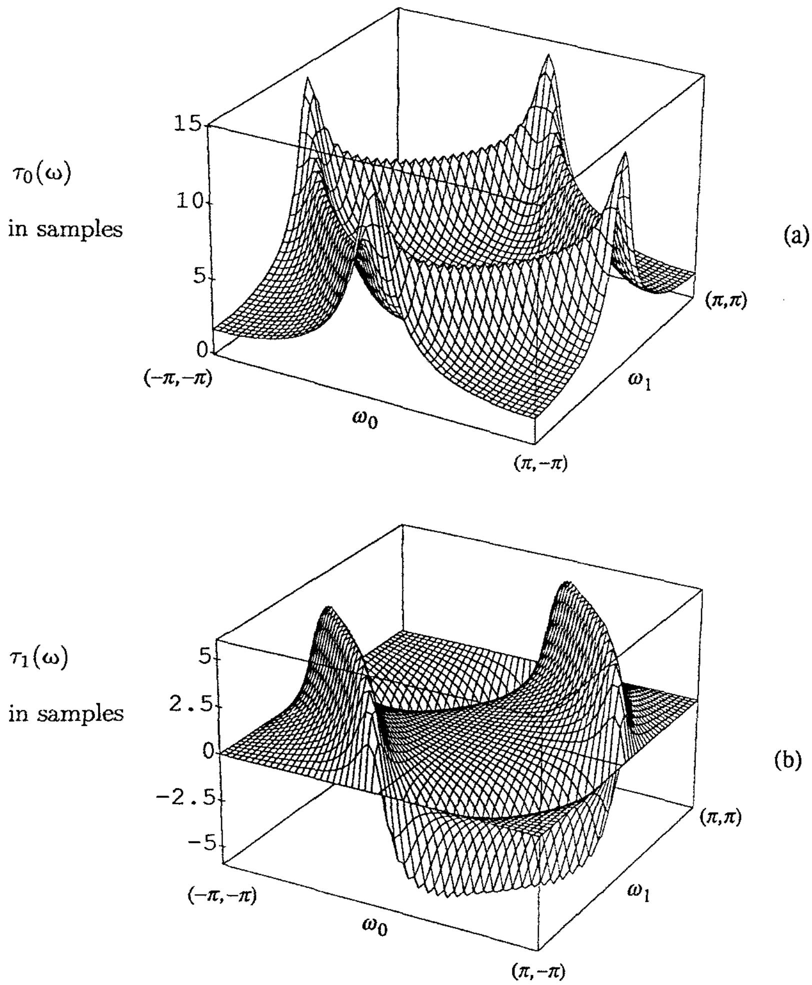

Figure 3.6-9 Group delays of Design Example 3.5: (a) $\tau_0(\omega)$, (b) $\tau_1(\omega)$.

Now, we will show that Nyquist and zero-phase properties are still preserved by the modified method.

Proof: Suppose that all $p_i(n)$'s are Nyquist, i.e., $p_i(J(\mathbf{M_p})\lambda_i n) = 0$ for $n \neq 0$. From (3.7.1), we therefore have $h^{(s)}(J(\mathbf{M_p})\mathbf{\Lambda}\,\mathbf{n}) = 0$, for $\mathbf{n} \neq \mathbf{0}$. So, $h(\mathbf{M}\,\mathbf{n}) = c_0 h^{(s)}(\widehat{\mathbf{M}}_\mathbf{p}\mathbf{M}\mathbf{n}) = c_0 h^{(s)}(J(\mathbf{M_p})\mathbf{M_p}^{-1}\mathbf{M}\mathbf{n}) = c_0 h^{(s)}(J(\mathbf{M_p})\mathbf{\Lambda}\mathbf{n}) = 0$, for $\mathbf{n} \neq \mathbf{0}$. Therefore, $H_F(\omega)$ is also Nyquist (ML1 th band). Next, suppose that all $p_i(n)$'s have zero phase, i.e., $p_i(n) = p_i^*(-n)$, $\forall i$. From (3.7.1), we know $h^{(s)}(\mathbf{n}) = h^{(s)*}(-\mathbf{n})$. Then, $h(\mathbf{n}) = c_0 h^{(s)}(\widehat{\mathbf{M}}_\mathbf{p}\,\mathbf{n}) = c_0 h^{(s)*}(-\widehat{\mathbf{M}}_\mathbf{p}\,\mathbf{n}) = h^*(-\mathbf{n})$, so that $H_F(\omega)$ also has zero-phase. $\triangle\triangle\triangle$

Moreover, for the IIR case, if all the $p_i(n)$'s are stable, it can be easily shown that the resulting $h(\mathbf{n})$ is also stable.

Here, we have to point out that this modified method doesn't apply to every $\mathbf{M}$ with large $J(\mathbf{M})$. For example, the matrix

$$\mathbf{M} = \begin{bmatrix} 10 & -1 \\ -1 & 10 \end{bmatrix} \tag{3.7.5}$$

with $J(\mathbf{M}) = 99$, does not have nonunit common factors among each column. Whenever this happens, we can use IFIR technique instead.

3.8. CONCLUSIONS

In MD multirate signal processing, filters with parallelepiped-shaped passbands governed by the decimation/expansion matrix (an integer matrix) play an important role. In this chapter, we have presented a method of designing such filters by starting with a proper 1D prototype filter and then using a simple transformation. These filters, although nonseparable, have separable polyphase components. Efficient polyphase implementations of these MD filters with complexity only proportional to a 1D filter are also presented. Important properties such as the Nyquist constraint, zero-phase constraint and BIBO stability can be easily achieved by using this method. We have shown several applications of the presented method, including many useful MD uniform DFT QMF banks and corresponding design examples. We have also generalized our method so that filters with an arbitrary parallelepiped-shaped passband (not necessary governed by an integer matrix) can be designed.

4

The Role of Integer Matrices in Multidimensional Multirate Systems

4.1. INTRODUCTION

The basic building blocks in a multidimensional (MD) multirate system are the decimation matrix $\mathbf{M}$ and the expansion matrix $\mathbf{L}$. For the D-dimensional case these are $D \times D$ nonsingular integer matrices. When these matrices are diagonal, most of the one-dimensional (1D) results can be extended automatically (by performing operations in each dimension *separately*). However, for the non-diagonal case, these extensions are non-trivial and require more complicated notations and matrix operations. An example is the development of polyphase representation for rational (rather than integer) sampling rate alterations. In the 1D case, this development relies on the commutativity of decimators and expanders, which is possible whenever M and L are relatively prime (coprime). The conditions for commutativity in the two-dimensional (2D) case have recently been developed successfully in [Kovačević and Vetterli, 1991b]. In the MD case, the results are more involved. In this chapter, we shall address some problems of this nature, including: (i) the commutativity of MD decimators and expanders, and the development of polyphase representation for rational sampling rate alterations, (ii) the perfect-reconstruction properties of MD delay-chain systems, and (iii) the periodicity properties of decimated periodic signals. Some preliminary results have been reported by the authors in [Chen and Vaidyanathan, 1992a], [Chen and Vaidyanathan, 1992b]. Our discussions are based on several key properties of integer matrices, including greatest common divisors and least common multiples, which we first review. These properties are analogous to those of polynomial matrices, some of which have been used in system theoretic work (e.g., matrix fraction descriptions, coprime matrices, Smith-form and so on).

Chapter Outline

Before formulating and solving these problems, in Section 4.2, we introduce some properties of integer matrices.† These are crucial to our discussions because of the role played by the decimation and expansion matrices. Some of these properties are analogous to those of polynomial matrices, which have been well-developed by researchers in system theory, e.g., matrix fraction descriptions, greatest common right/left divisors (gcrd/gcld), coprime matrices, Smith-form and so on [Kailath, 1980], [Vidyasagar, 1985]. We also review the concepts of the least common right multiple (lcrm) and least common left multiple (lclm) of integer matrices [MacDuffee, 1946, p. 35] and develop further properties of these. We shall also present an approach of finding an lcrm/lclm of two integer matrices, which is very useful in practical applications.

All of these will be applied in deriving many of the new multirate results which are summarized next.

Polyphase Structures for Rational Sampling Rate Alterations (Section 4.3)

In 1D, multirate techniques permit us to alter the sampling rate of a sequence by a rational fraction, e.g., to reduce the sampling rate by M/L. Fig. 4.1-1 shows a scheme to achieve this. Note that the filter $H(z)$ is used to suppress image components generated by the L-fold expander and to eliminate aliasing owing to the M-fold decimator as well. In MD, also it is often necessary to interface images (or video data) between systems which use different sampling methods (different sampling lattices) [Mersereau and Speake, 1983], [Dubois, 1985]. The conversion between the European and North American television systems, and the conversion between high definition television (HDTV) signals and conventional television signals [Vetterli, Kovačević, and Le Gall, 1990] are two examples.

For the 1D case, using the polyphase approach, we can implement Fig. 4.1-1 more efficiently as in either Fig. 4.1-2(a) or Fig. 4.1-2(b) (for the case $M = 3$ and $L = 2$). Then, it seems that we cannot improve the efficiency anymore because we cannot use Noble identities [Vaidyanathan, 1990a], [Crochiere and Rabiner, 1983] to move the expanders further to the right (or the decimators further to the left). However, it turns out that we can still do so by using the technique introduced in [Hsiao, 1987]. We shall refer to this technique as the rational polyphase implementation (RPI). Fig. 4.1-3 shows the development of the RPI technique by successively redrawing the rational dec-

† In fact, these properties can be applied to matrices with elements from a so-called "principle ideal domain" (pid) [MacDuffee, 1946], [Forney, 1970], [Newman, 1972], [Vidyasagar, 1985]. The set of integers and the set of polynomials with coefficients belonging to a field are two examples of pid's.

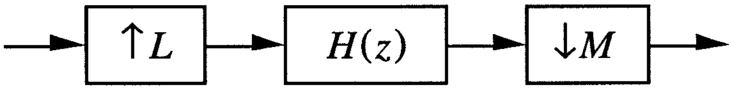

Figure 4.1-1 1D rational decimation system.

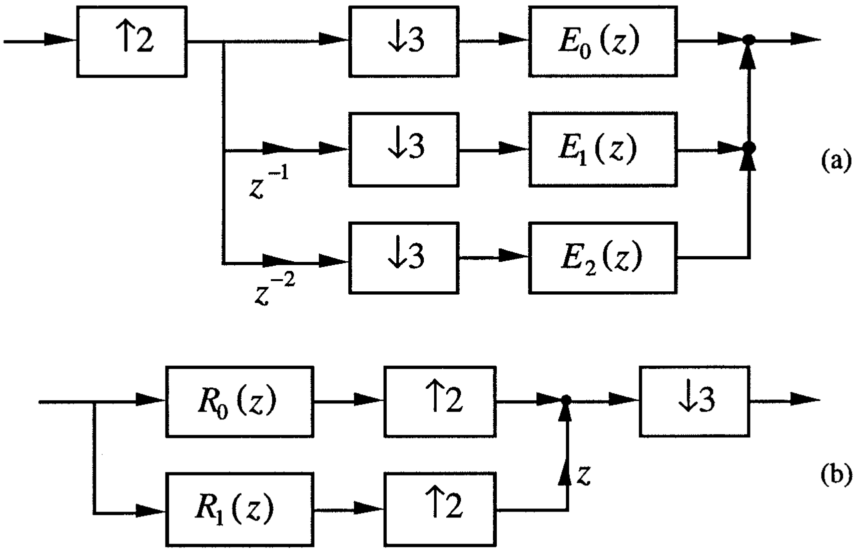

Figure 4.1-2 Two types of polyphase implementations of a 1D rational decimation system.

imation circuit. Starting from Fig. 4.1-2(a), we replace z^{-1} by $z^2 z^{-3}$ and z^{-2} by $z^4 z^{-6}$, so we get Fig. 4.1-3(a). Note that when M and L are relatively prime (coprime), we are able to express every integer k as $Lk_1 + Mk_2$ for some integers k_1 and k_2 (Euclid's theorem). With the help of Noble identities, Fig. 4.1-3(a) can be redrawn as Fig. 4.1-3(b). Next, we can interchange the expanders and decimators when M and L are coprime [Vaidyanathan, 1990a], and obtain Fig. 4.1-3(c). Finally we can perform Type 2 polyphase decomposition on $E_i(z)$'s with respect to L, and get Fig. 4.1-3(d). In summary, Fig. 4.1-3(d) is equivalent to Fig. 4.1-2(a) but now each arithmetic operation is performed at its lowest rate. Note that the RPI technique works if and only if M and L are coprime.

New results of Section 4.3. In Section 4.3, we will extend this polyphase technique for MD systems and show that the necessary and sufficient conditions for its feasibility are: (1) $\mathbf{ML} = \mathbf{LM}$ (i.e., $\mathbf{M}$ and $\mathbf{L}$ commute) and (2) $\mathbf{M}$ and $\mathbf{L}$ are coprime. The coprimeness of matrices will be defined later in Section 4.2. Note that, in general, we have to distinguish left coprimeness and right coprimeness for the matrix case. However, we will show that if $\mathbf{ML} = \mathbf{LM}$, left coprimeness and right coprimeness are equivalent.

We should point out that the conditions for commutativity of an M-fold decimator and an

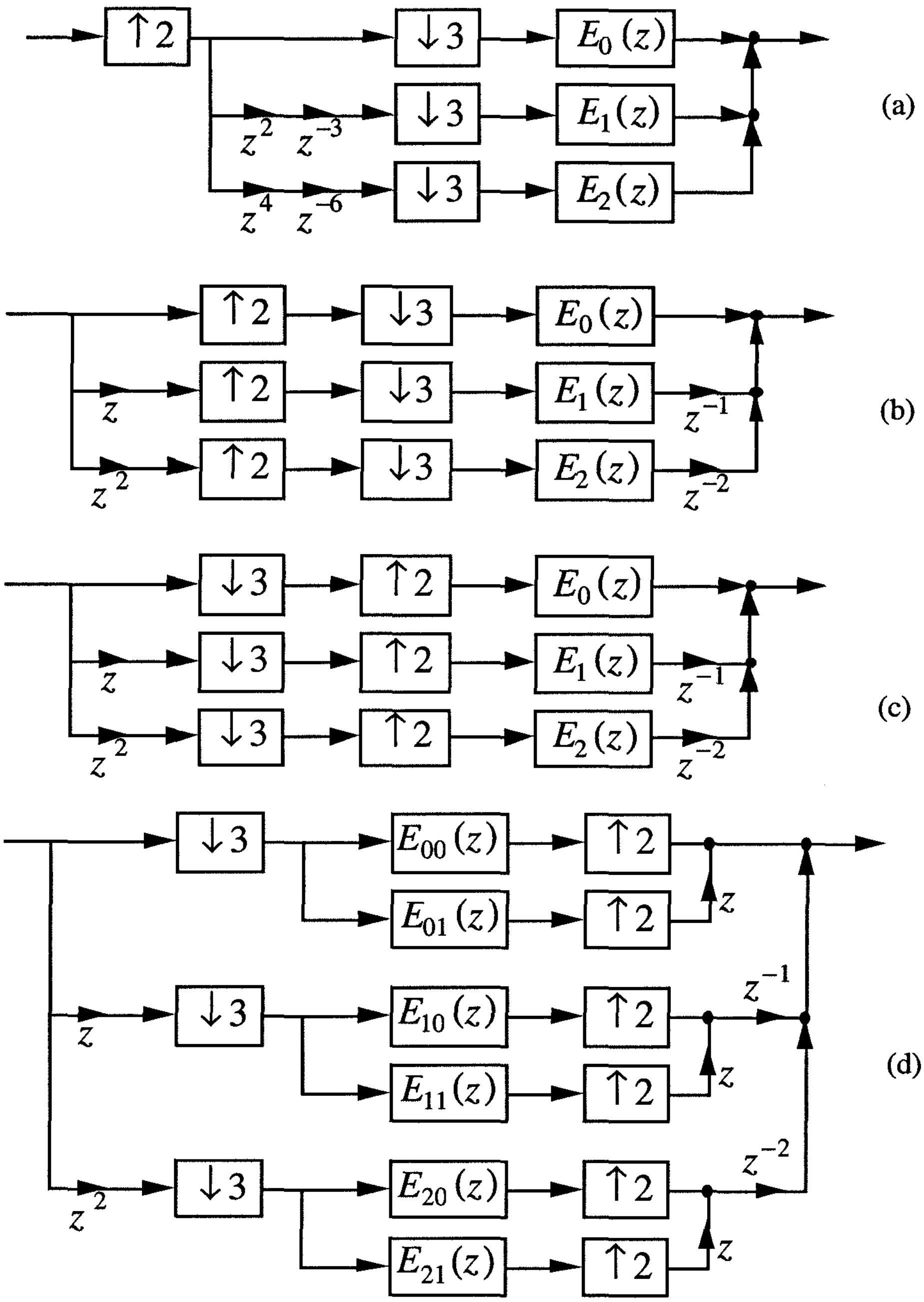

Figure 4.1-3 Successive redrawing of polyphase implementations of a 1D rational decimation system.

L-fold expander has been generalized to the 2D case in [Kovačević and Vetterli, 1991b], where the conditions are given for upper triangular **M** and **L**. In Section 4.3, we will present conditions which hold for any number of dimensions without any assumption on **M** and **L**.

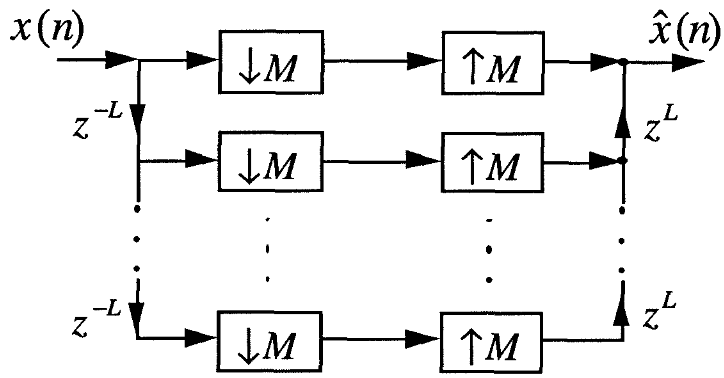

Figure 4.1-4 1D delay-chain system.

Generalized Delay-chain Systems (Section 4.4)

A 1D delay-chain system is shown in Fig. 4.1-4. It has been shown that this is a perfect-reconstruction (PR) system (i.e., $\hat{x}(n) = x(n)$) if and only if L and M are coprime [Nguyen and Vaidyanathan, 1988, Lemma A.2]. This system is fundamental to many 1D maximally decimated PR filter banks [Vaidyanathan, 1990a]. The case where $L = 1$ in Fig. 4.1-4 is most common. The case where $L \neq 1$ is also required in some applications where pairs of analysis filters are constrained by symmetry conditions [Nguyen and Vaidyanathan, 1988]. In Section 4.4, we will consider the MD extension of Fig. 4.1-4 and then discuss the conditions for PR.

Periodicity Matrices of Decimated Signals (Section 4.5)

In the 1D case, if a periodic signal $x(n)$ with period L is decimated by a factor of M to obtain $y(n) = x(Mn)$, then the period of $y(n)$ is easily verified to be $L/\gcd(M, L) = \text{lcm}(M, L)/M$. (If further information about $x(n)$ is available, then smaller periods can be found.) We shall extend this result to the MD case, where an MD signal $x(\mathbf{n})$ with periodicity matrix $\mathbf{L}$ is decimated by the matrix $\mathbf{M}$. We will show that the periodicity matrix of $y(\mathbf{n}) = x(\mathbf{Mn})$ is $\mathbf{M}^{-1}\,\text{lcrm}(\mathbf{M}, \mathbf{L})$, where lcrm(**M**,**L**) denotes an lcrm of **M** and **L**. We will also extend these results for stochastic signals. More specifically, assuming that $x(\mathbf{n})$ is *cyclo-wide-sense-stationary* (CWSS) with periodicity matrix **L**, we will derive the periodicity matrix of cyclo-stationarity of $x(\mathbf{Mn})$.

Emerging Results from Other Authors (Section 4.6)

After we submitted [Chen and Vaidyanathan, 1993a], we came to realize via private communication with a number of authors that several other groups were simultaneously coming up with similar and related results, particularly about the commutativity of decimators and expanders. In Section 4.6, we provide mathematical details on these other contributions.

4.2. GCRD, GCLD, LCRM, AND LCLM

In this section, we introduce some properties about integer matrices. As mentioned before, the counterpart of these properties in polynomial matrix case is well-known and well-developed [Gantmacher, 1977], [Kailath, 1980], [Vidyasagar, 1985]. In the appendix of [Vidyasagar, 1985], many of these properties are also given for matrices with elements in a principle ideal domain (pid), which is an even more general case. We omit proofs which can be found in these references. We will review the concepts of the lcrm and lclm for the matrix case [MacDuffee, 1946] and derive several properties, including their relations with gcrd/gcld. We shall also present a method of finding an lcrm/lclm of two integer matrices. All of these will be applied in deriving many of the new multirate results in the following sections.

Preliminaries

An integer matrix $\mathbf{U}$ is called unimodular if $[\det \mathbf{U}] = \pm 1$, i.e., $J(\mathbf{U}) = 1$. Clearly, for unimodular $\mathbf{U}$, $\mathbf{U}^{-1} = [\text{adjugate of } \mathbf{U}]/[\det \mathbf{U}]$ is also an integer matrix, and is unimodular. If there exists a unimodular integer matrix $\mathbf{V}$ such that $\mathbf{A} = \mathbf{B}\mathbf{V}$, we say $\mathbf{A}$ is a right associate of $\mathbf{B}$, and denote this as $\mathbf{A} \overset{R}{=} \mathbf{B}$ [MacDuffee, 1946], [Vidyasagar, 1985]. Clearly, $\mathbf{A} \overset{R}{=} \mathbf{B}$ if and only if $\mathbf{B} \overset{R}{=} \mathbf{A}$. It can be shown that $LAT(\mathbf{A}) = LAT(\mathbf{B})$ if and only if $\mathbf{A} \overset{R}{=} \mathbf{B}$. Similarly, $\mathbf{A}$ is a left associate of $\mathbf{B}$ (denoted as $A \overset{L}{=} B$) if $\mathbf{A} = \mathbf{U}\mathbf{B}$ for some unimodular integer matrix $\mathbf{U}$.

Gcrd and Gcld [MacDuffee, 1946], [Kailath, 1980], [Vidyasagar, 1985]

Definitions:

1. The integer matrix $\mathbf{R}$ is a right divisor (rd) of $\mathbf{M}$ if $\mathbf{M} = \mathbf{P}\mathbf{R}$ for some integer matrix $\mathbf{P}$.
2. The integer matrix $\mathbf{R}$ is a common right divisor of $\mathbf{M}$ and $\mathbf{L}$ (denoted by crd($\mathbf{M}$,$\mathbf{L}$)) if $\mathbf{M} = \mathbf{P}\mathbf{R}$ and $\mathbf{L} = \mathbf{Q}\mathbf{R}$ for some integer matrices $\mathbf{P}$ and $\mathbf{Q}$.
3. The integer matrix $\mathbf{R}_0$ is a greatest common right divisor of $\mathbf{M}$ and $\mathbf{L}$ (denoted by gcrd($\mathbf{M}$,$\mathbf{L}$)) if

   i) $\mathbf{R}_0$ is a crd($\mathbf{M}$,$\mathbf{L}$).

   ii) If $\mathbf{R}$ is another crd($\mathbf{M}$,$\mathbf{L}$), $\mathbf{R}_0 = \mathbf{S}\mathbf{R}$ for some integer matrix $\mathbf{S}$.
4. Two matrices $\mathbf{M}$ and $\mathbf{L}$ are right coprime if all their crd's are unimodular.

Properties:

1. The gcrd is not unique. In fact, all gcrd's of two given integer matrices are left associate of one another. Hence, we should write "$\mathbf{R}_0 \stackrel{L}{=} \text{gcrd}(\mathbf{M}, \mathbf{L})$" (instead of "$\mathbf{R}_0 = \text{gcrd}(\mathbf{M}, \mathbf{L})$") to express "$\mathbf{R}_0$ is a gcrd of **M** and **L**".
2. Given $\mathbf{M} = \mathbf{PR}$ and $\mathbf{L} = \mathbf{QR}$. Then, **R** is a gcrd(M,L) if and only if **P** and **Q** are right coprime.
3. Let $\mathbf{R}_0$ be a gcrd(M,L). There exist integer matrices **A** and **B** such that $\mathbf{AM}+\mathbf{BL} = \mathbf{R}_0$. This is the extension of the Euclid's theorem.
4. Suppose **M** and **L** are right coprime. There exist integer matrices **A** and **B** such that $\mathbf{AM} + \mathbf{BL} = \mathbf{I}$. This is called the generalized Bezout theorem.

Remarks:

1. The left divisor (ld), common left divisor (cld), greatest common left divisor (gcld) and left coprimeness are defined similarly.
2. The proof of the existence of gcrd/gcld and methods for finding gcrd/gcld can be found in [MacDuffee, 1946], [Kailath, 1980], [Vidyasagar, 1985].

Smith-form and Smith-McMillan Form [Gantmacher, 1977], [Kailath, 1980], [Vidyasagar, 1985]

Smith-form: Any nonsingular integer matrix **M** can always be decomposed as $\mathbf{M} = \mathbf{U\Lambda V}$ where **U** and **V** are unimodular integer matrices and $\mathbf{\Lambda}$ is a diagonal matrix with nonzero integer elements on the diagonal.

Remarks: The Smith-form has been used outside the control-theory literature more than once. For example, the Smith-form for polynomial matrices with coefficients in a *finite field* has been mentioned and applied in convolutional coding theory in [Forney, 1970]. A special Smith-form was used to design MD filter banks in [Viscito and Allebach, 1988]. The Smith-form for *integer matrices* has been used in [Dudgeon and Mersereau, 1984, Problem 2.20] and [Guessoum and Mersereau, 1986] for computing the MD discrete Fourier transform, and was used in the MD *multirate* systems to exploit the decimation/expansion matrices in [Vaidyanathan, 1991a], [Vaidyanathan, 1991b].

Smith-McMillan form: Any nonsingular matrix **H** with rational elements can always be decomposed as $\mathbf{H} = \mathbf{U\Lambda V}$ where **U** and **V** are unimodular integer matrices and $\mathbf{\Lambda}$ is a diagonal matrix with nonzero rational elements on the diagonal.

Right/Left Matrix Fraction Description (MFD)

Any nonsingular matrix $\mathbf{H}$ with rational elements can be expressed as $\mathbf{H} = \mathbf{P}_1\mathbf{Q}_1^{-1}$ (right MFD), or as $\mathbf{H} = \mathbf{Q}_2^{-1}\mathbf{P}_2$ (left MFD), where $\mathbf{P}_i$'s and $\mathbf{Q}_i$'s are nonsingular integer matrices. A right MFD is said to be irreducible if $\mathbf{P}_1$ and $\mathbf{Q}_1$ are right coprime. Similarly, a left MFD is said to be irreducible if $\mathbf{P}_2$ and $\mathbf{Q}_2$ are left coprime [Kailath, 1980], [Vidyasagar, 1985].

It can be shown that if $\mathbf{P}_1\mathbf{Q}_1^{-1}$ and $\mathbf{P'}_1\mathbf{Q'}_1^{-1}$ are both irreducible right MFD's of $\mathbf{H}$, then there exist unimodular $\mathbf{V}$ such that $\mathbf{P}'_1 = \mathbf{P}_1\mathbf{V}$ and $\mathbf{Q}'_1 = \mathbf{Q}_1\mathbf{V}$, i.e., $\mathbf{P}'_1$ and $\mathbf{Q}'_1$ are right associates of $\mathbf{P}_1$ and $\mathbf{Q}_1$ with the same $\mathbf{V}$. Therefore, all the denominator matrices (the $\mathbf{Q}$'s) of the irreducible right MFD's have the same absolute determinant d_1. Similarly, we can show that all the denominator matrices of the irreducible left MFD's have the same absolute determinant d_2. These, in turn, are equal, i.e., $d_1 = d_2$, as explained later.

Computation of irreducible MFD's using the Smith-McMillan form [Vidyasagar, 1985]: For a given rational matrix $\mathbf{H}$, first decompose it into Smith-McMillan form, $\mathbf{H} = \mathbf{U}\mathbf{\Lambda}\mathbf{V}$, where $\mathbf{\Lambda} = \text{diag}[\lambda_0, \ldots, \lambda_{D-1}]$. Then, represent all the rational $\lambda_i = \alpha_i/\beta_i$ in their irreducible forms (α_i and β_i are coprime integers for all i). Let $\mathbf{\Lambda}_\alpha = \text{diag}[\alpha_0, \ldots, \alpha_{D-1}]$ and $\mathbf{\Lambda}_\beta = \text{diag}[\beta_0, \ldots, \beta_{D-1}]$ so that

$$\mathbf{H} = \underbrace{\mathbf{U}\mathbf{\Lambda}_\alpha}_{\mathbf{P}_1}\underbrace{\mathbf{\Lambda}_\beta^{-1}\mathbf{V}}_{\mathbf{Q}_1^{-1}} = \underbrace{\mathbf{U}\mathbf{\Lambda}_\beta^{-1}}_{\mathbf{Q}_2^{-1}}\underbrace{\mathbf{\Lambda}_\alpha\mathbf{V}}_{\mathbf{P}_2}. \tag{4.2.1}$$

It can be shown that $\mathbf{P}_1$ and $\mathbf{Q}_1$ are right coprime and $\mathbf{P}_2$ and $\mathbf{Q}_2$ are left coprime, so $\mathbf{P}_1\mathbf{Q}_1^{-1}$ and $\mathbf{Q}_2^{-1}\mathbf{P}_2$ are irreducible MFD's.

Note that (4.2.1) tells us that there exist *one* irreducible right MFD and *one* irreducible left MFD of which the denominator matrices have the same absolute determinant, since $J(\mathbf{Q}_1) = J(\mathbf{\Lambda}_\beta) = J(\mathbf{Q}_2)$. Summarizing, we have proved the following:

Fact 1. For all irreducible right and left MFD's of a nonsingular rational matrix, the denominator matrices have the same absolute determinant.

Lcrm and Lclm

Definitions:

1. $\mathbf{R}$ is a right multiple (rm) of $\mathbf{M}$ if $\mathbf{R} = \mathbf{MP}$ for some integer matrix $\mathbf{P}$, i.e., if $\mathbf{M}$ is a left divisor of $\mathbf{R}$.

2. $\mathbf{R}$ is a common right multiple of $\mathbf{M}$ and $\mathbf{L}$ (denoted as crm(M,L)) if $\mathbf{R} = \mathbf{MP} = \mathbf{LQ}$ for some integer matrices $\mathbf{P}$ and $\mathbf{Q}$.

3. $\mathbf{R}_0$ is a least common right multiple of $\mathbf{M}$ and $\mathbf{L}$ (denoted as lcrm(M,L)) if

   i) $\mathbf{R}_0$ is a nonsingular crm(M,L).

   ii) If $\mathbf{R}$ is another nonsingular crm(M,L), then $\mathbf{R} = \mathbf{R}_0\mathbf{S}$ for some integer matrix $\mathbf{S}$.

Remark on singularity: Singular crm is of less importance because given any nonsingular crm(M,L), we can always postmultiply it by a singular matrix to get a singular crm(M,L). Also, if either $\mathbf{M}$ or $\mathbf{L}$ is singular, all crm(M,L)'s are singular and it is meaningless to discuss the lcrm(M,L). For these various reasons, by definition we restrict the lcrm to be nonsingular and to be defined only for nonsingular $\mathbf{M}$ and $\mathbf{L}$. This is slightly different from the definition in [MacDuffee, 1946], but more proper for our discussions. This is also consistent with the convention for the 1D case, where we exclude zero as a least common multiple although it is a multiple of any integer.

Note that crm(M,L) and lcrm(M,L) are not unique. According to the above definitions, we can prove the following:

Lemma 4.1.

(a) If $\mathbf{A}$ and $\mathbf{B}$ are both lcrm(M,L), then $\mathbf{A} \stackrel{R}{=} \mathbf{B}$ [MacDuffee, 1946].

(b) Let $\mathbf{B}$ be an lcrm(M,L). Then, $\mathbf{A}$ is also an lcrm(M,L) if and only if $\mathbf{A} \stackrel{R}{=} \mathbf{B}$.

Proofs:

(a) According to the definition of lcrm, we have $\mathbf{A} = \mathbf{BS}$ and $\mathbf{B} = \mathbf{AT}$. Then, $\mathbf{A} = \mathbf{BS} = \mathbf{ATS}$, so $\mathbf{TS} = \mathbf{I}$. This implies both $\mathbf{S}$ and $\mathbf{T}$ are unimodular, i.e., $\mathbf{A} \stackrel{R}{=} \mathbf{B}$.

(b) The 'only if' part follows directly from (a). We proceed to prove the 'if' part. Suppose $\mathbf{A} = \mathbf{BU}$, where $\mathbf{U}$ is unimodular. Clearly, $\mathbf{A}$ is a crm of $\mathbf{M}$ and $\mathbf{L}$. Since $\mathbf{B}$ is an lcrm of $\mathbf{M}$ and $\mathbf{L}$, any crm of $\mathbf{M}$ and $\mathbf{L}$, say $\mathbf{R}$, can be written as $\mathbf{R} = \mathbf{BS}$. So, we have

$$\mathbf{R} = \underbrace{\mathbf{BU}}_{\mathbf{A}}\underbrace{\mathbf{U}^{-1}\mathbf{S}}_{\mathbf{S}'} \tag{4.2.2}$$

where $\mathbf{S}'$ is also an integer matrix. This proves that $\mathbf{A}$ is an lcrm. △△△

Remarks:

1. It can be easily verified that there exists at least one crm(M,L), which is

$$\mathbf{R} = \mathbf{M}\big(\pm[\text{adjugate of } \mathbf{M}]\mathbf{L}\big) = \mathbf{L}\big(J(\mathbf{M})\mathbf{I}\big). \tag{4.2.3}$$

   On the other hand, the existence of a nonsingular lcrm of any two nonsingular matrices is guaranteed by a constructive method which will be described later.

2. From the above properties, it also can be easily verified that an lcrm is a nonsingular crm with the smallest absolute determinant. And, all the lcrm(M,L)'s have the same absolute determinant. In particular, Lemma 4.1 says that the lcrm(M,L) is unique up to postmultiplication by a unimodular matrix. Therefore, for consistency in notation, we should write "$\mathbf{R}_0 \overset{R}{=} \mathrm{lcrm}(\mathbf{M},\mathbf{L})$" (instead of "$\mathbf{R}_0 = \mathrm{lcrm}(\mathbf{M},\mathbf{L})$") to express "$\mathbf{R}_0$ is an lcrm of $\mathbf{M}$ and $\mathbf{L}$".

Next, we can relate lcrm together with gcrd and right coprimeness by the following theorem:

Theorem 4.1. Let $\mathbf{R}$ be a nonsingular crm(M,L), i.e., $\mathbf{R} = \mathbf{MP} = \mathbf{LQ}$. Then, $\mathbf{R}$ is an lcrm(M,L) if and only if $\mathbf{P}$ and $\mathbf{Q}$ are right coprime.

Proof:

1) If $\mathbf{P}$ and $\mathbf{Q}$ are not right coprime, then there exists an $\mathbf{X}$ which is not unimodular such that $\mathbf{P} = \mathbf{P'X}$ and $\mathbf{Q} = \mathbf{Q'X}$. Therefore, we have

$$\mathbf{R} = \underbrace{\mathbf{MP'}}_{\mathbf{R'}}\mathbf{X} = \underbrace{\mathbf{LQ'}}_{\mathbf{R'}}\mathbf{X}. \tag{4.2.4}$$

Clearly, $\mathbf{R} = \mathbf{R'X}$, and $\mathbf{R'}$ is a crm of $\mathbf{M}$ and $\mathbf{L}$. Suppose $\mathbf{R}$ is an lcrm of $\mathbf{M}$ and $\mathbf{L}$, then $\mathbf{R'} = \mathbf{RS}$ according to the definition of lcrm. Then, $\mathbf{R} = \mathbf{R'X} = \mathbf{RSX}$, which implies both $\mathbf{X}$ and $\mathbf{S}$ must be unimodular and leads to contradiction. Hence we conclude that if $\mathbf{P}$ and $\mathbf{Q}$ are not right coprime, $\mathbf{R}$ is not an lcrm of $\mathbf{M}$ and $\mathbf{L}$.

2) Next, suppose $\mathbf{P}$ and $\mathbf{Q}$ are right coprime, we have to prove that $\mathbf{R}$ is an lcrm of $\mathbf{M}$ and $\mathbf{L}$. Let $\mathbf{R'}$ be any other nonsingular crm of $\mathbf{M}$ and $\mathbf{L}$, i.e., $\mathbf{R'} = \mathbf{MP'} = \mathbf{LQ'}$. Clearly, $\mathbf{P'}$ is nonsingular. Because $\mathbf{P}$ and $\mathbf{Q}$ are right coprime, there exist integer matrices $\mathbf{A}$ and $\mathbf{B}$ such that $\mathbf{AP} + \mathbf{BQ} = \mathbf{I}$ (generalized Bezout theorem). Replacing $\mathbf{Q}$ with $\mathbf{Q'P'^{-1}P}$, we can rewrite this as

$$\mathbf{AP'P'^{-1}P} + \mathbf{BQ'P'^{-1}P} = \mathbf{I}. \tag{4.2.5}$$

Postmultiplying both sides by $\mathbf{P^{-1}P'}$, we get

$$\underbrace{\mathbf{AP'} + \mathbf{BQ'}}_{\mathbf{S}} = \mathbf{P^{-1}P'}. \tag{4.2.6}$$

So, $\mathbf{P'} = \mathbf{PS}$ and hence $\mathbf{R'} = \mathbf{RS}$. From the definition of lcrm, $\mathbf{R}$ is indeed an lcrm(M,L). $\triangle\triangle\triangle$

Remark: The left multiple (lm), common left multiple (clm), and least common left multiple (lclm) can be defined similarly. All the properties above can also be derived similarly.

Computation of Lcrm/Lclm Using MFD's

A method of computing an lcrm/lclm of two nonsingular matrices can be found in [MacDuffee, 1946, p. 36]. However, the above-mentioned irreducible MFD's give us an alternative. This also gives a constructive way of proving the existence of a nonsingular lcrm/lclm of two nonsingular matrices.

To compute an lcrm of nonsingular $\mathbf{M}$ and $\mathbf{L}$, we let $\mathbf{H} = \mathbf{M}^{-1}\mathbf{L}$ (which is also nonsingular) and compute one irreducible right MFD of $\mathbf{H}$ as in (4.2.1), so we have $\mathbf{M}^{-1}\mathbf{L} = \mathbf{P}_1\mathbf{Q}_1^{-1}$ where $\mathbf{P}_1$ and $\mathbf{Q}_1$ are right coprime. Therefore, $\mathbf{MP}_1 = \mathbf{LQ}_1$. Denote this as $\mathbf{R}$. Using Theorem 4.1, we can conclude that $\mathbf{R}$ is an lcrm(M,L). Similarly, if we let $\mathbf{H}' = \mathbf{LM}^{-1}$ and compute one irreducible left MFD of it using (4.2.1), then $\mathbf{R}' = \mathbf{P}_2\mathbf{M} = \mathbf{Q}_2\mathbf{L}$ is an lclm(M,L).

4.3. POLYPHASE IMPLEMENTATION OF RATIONAL SAMPLING RATE ALTERATION

A 1D sampling rate alteration system with decimation ratio M/L can be implemented efficiently by using the rational polyphase implementation (RPI) as in Fig. 4.1-3(d). For this technique to work, M and L should be coprime. In this section, we shall extend this technique to the MD case, which finds applications in conversions of images or video data between different sampling standards. An MD decimation system with rational decimation ratio (in this case, a matrix) $\mathbf{H} = \mathbf{L}^{-1}\mathbf{M}$ is shown in Fig. 4.3-1. As an example, if we choose

$$\mathbf{L} = \begin{bmatrix} 2 & 0 \\ 0 & 1 \end{bmatrix} \quad \text{and} \quad \mathbf{M} = \begin{bmatrix} 1 & 1 \\ 1 & -1 \end{bmatrix},$$

we can convert rectangularly sampled images to hexagonally sampled ones, as shown in [Mersereau and Speake, 1983, Fig. 6]. As in 1D case, the MD filter $H(\mathbf{z})$ in Fig. 4.3-1 is used to suppress image components generated by the $\mathbf{L}$-fold expander and eliminate aliasing owing to the $\mathbf{M}$-fold decimator.

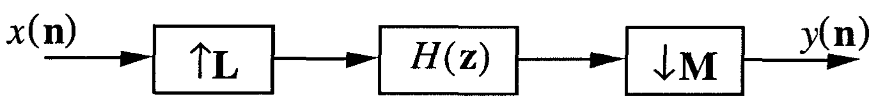

Figure 4.3-1 MD rational decimation system.

We can use the MD polyphase decomposition to implement this system more efficiently as in either Fig. 4.3-2(a) or Fig. 4.3-2(b). The numbers of branches in Fig. 4.3-2(a) and Fig. 4.3-2(b) are $J(\mathbf{M})$ and $J(\mathbf{L})$, respectively. For simplicity, figures only show the case where $J(\mathbf{M}) = 3$ and

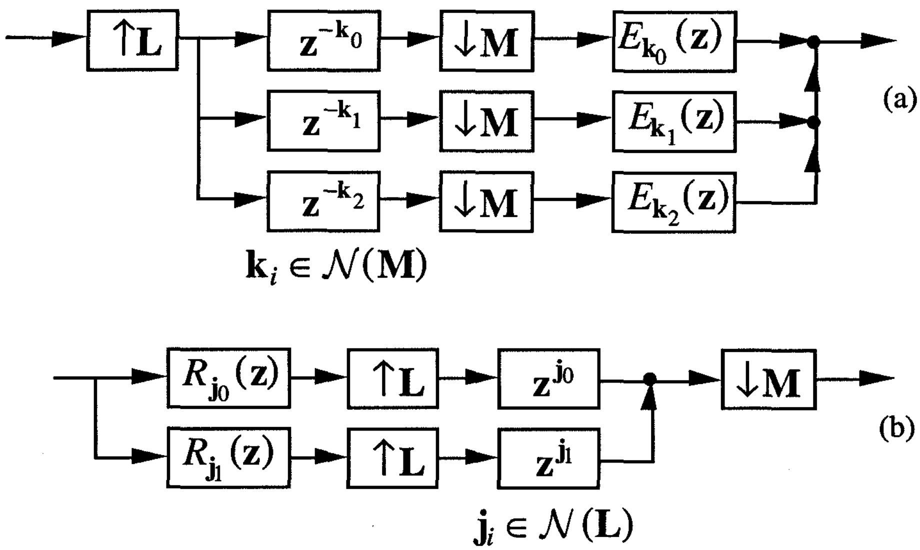

Figure 4.3-2 Two types of polyphase implementations of an MD rational decimation system.

$J(\mathbf{L}) = 2$. We can use the RPI technique to improve the efficiency even further. Fig. 4.3-3 shows this by successively redrawing the circuit of Fig. 4.3-2(a).

Starting from Fig. 4.3-2(a), suppose it is possible to replace every $\mathbf{k}_i$ in $\mathcal{N}(\mathbf{M})$ with $\mathbf{M}\mathbf{k}_{i1} + \mathbf{L}\mathbf{k}_{i2}$, where $\mathbf{k}_{i1}$ and $\mathbf{k}_{i2}$ are some integer vectors. Hence we get Fig. 4.3-3(a). With the help of Noble identities, Fig. 4.3-3(a) can be redrawn as Fig. 4.3-3(b). Next, suppose we can interchange the expanders and decimators to obtain Fig. 4.3-3(c). We can then perform Type 2 polyphase decomposition on $E_{\mathbf{k}_i}(\mathbf{z})$'s with respect to $\mathbf{L}$, and get Fig. 4.3-3(d). In summary, Fig. 4.3-3(d) is equivalent to Fig. 4.3-2(a) but each arithmetic operation is now performed at its lowest rate. Note that the filters $E_{\mathbf{kj}}(\mathbf{z})$ in Fig. 4.3-3(d) are the ML-fold polyphase components (up to a certain delay) of $H(\mathbf{z})$.

To summarize, we can see that the following two issues should be considered for the above technique to work:

(1) Every $\mathbf{k}_i$ in $\mathcal{N}(\mathbf{M})$ should be expressible in the form of $\mathbf{k}_i = \mathbf{M}\mathbf{k}_{i1} + \mathbf{L}\mathbf{k}_{i2}$, where $\mathbf{k}_{i1}$ and $\mathbf{k}_{i2}$ are some integer vectors.

(2) The decimators and the expanders should be interchangeable.

We shall devote the rest of this section to the proof of the following amazingly simple and clear statement:

Theorem 4.2. The above two issues are satisfied if and only if

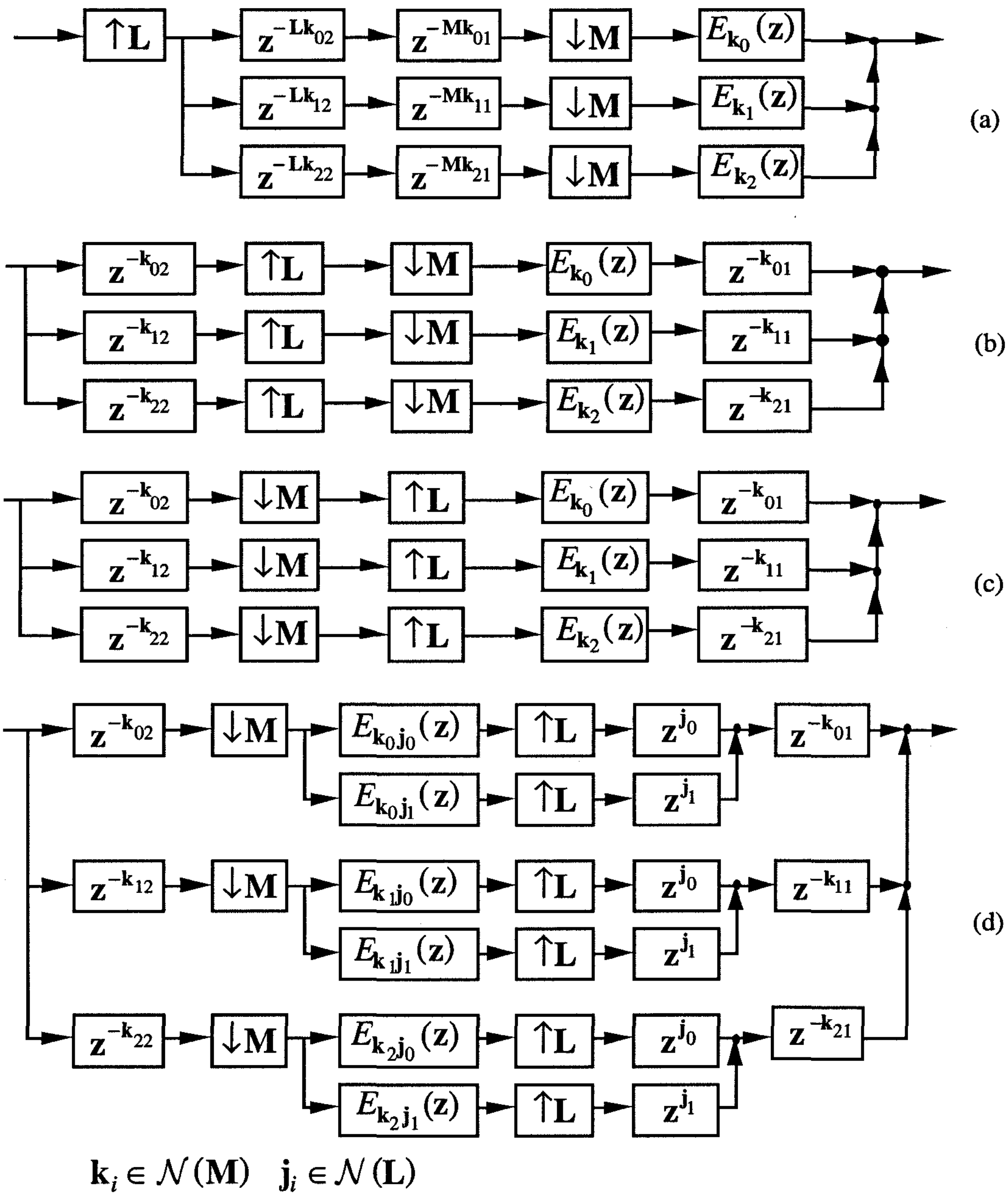

Figure 4.3-3 Successive redrawing of polyphase implementations of an MD rational decimation system.

1. $\mathbf{ML} = \mathbf{LM}$, i.e., $\mathbf{M}$ and $\mathbf{L}$ commute.
2. $\mathbf{M}$ and $\mathbf{L}$ are coprime. (As we will show, left coprimeness is equivalent to right coprimeness when $\mathbf{ML} = \mathbf{LM}$.)

We first deal with the interchangeability of decimators and expanders and prove the following theorem:

Theorem 4.3. The **L**-fold expander and the **M**-fold decimator can be interchanged if and only if

1. $\mathbf{ML} = \mathbf{LM}$.
2. **ML** is an lcrm(M,L), i.e., $\mathbf{ML} \overset{R}{=} \text{lcrm}(\mathbf{M}, \mathbf{L})$. (Given $\mathbf{ML} = \mathbf{LM}$, this condition can be shown to be equivalent to the coprimeness of **M** and **L**. See Theorem 4.4.)

Comments:

1. These two conditions can be easily tested. While the test for '$\mathbf{ML} = \mathbf{LM}$' is straightforward, the test for coprimeness (i.e., the computation of a gcrd/gcld) is also easy and can be found in [MacDuffee, 1946], [Kailath, 1980], [Vidyasagar, 1985].
2. In the 1D case, Condition 1 is automatic, and Condition 2 is equivalent to coprimeness.

Proof: Consider $y_1(\mathbf{n})$ and $y_2(\mathbf{n})$ in Fig. 4.3-4. From the definitions of **M**-fold decimation and **L**-fold expansion, we have

$$y_1(\mathbf{n}) = \begin{cases} x(\mathbf{ML}^{-1}\mathbf{n}) & \mathbf{n} \in LAT(\mathbf{L}) \\ 0 & \text{otherwise}, \end{cases} \tag{4.3.1}$$

and

$$y_2(\mathbf{n}) = \begin{cases} x(\mathbf{L}^{-1}\mathbf{Mn}) & \mathbf{Mn} \in LAT(\mathbf{L}) \\ 0 & \text{otherwise}. \end{cases} \tag{4.3.2}$$

For $y_1(\mathbf{n})$ to be identical to $y_2(\mathbf{n})$, we should in particular have $x(\mathbf{ML}^{-1}\mathbf{n}) = x(\mathbf{L}^{-1}\mathbf{Mn})$ for $\mathbf{n} \in LAT(\mathbf{L})$. Because $x(\mathbf{n})$ is arbitrary, we should have

$$\mathbf{ML}^{-1}\mathbf{n} = \mathbf{L}^{-1}\mathbf{Mn} \qquad \forall \mathbf{n} \in LAT(\mathbf{L}). \tag{4.3.3}$$

Since **L** is not singular, $LAT(\mathbf{L})$ contains D linearly independent vectors. So, the above implies $\mathbf{ML}^{-1} = \mathbf{L}^{-1}\mathbf{M}$, or, $\mathbf{LM} = \mathbf{ML}$.

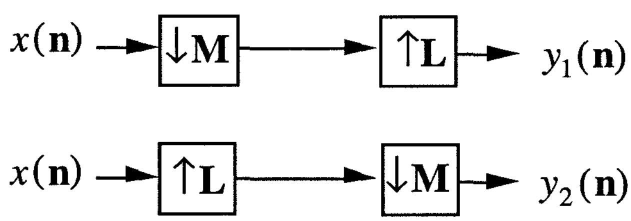

Figure 4.3-4 Interchange of an MD decimator and an MD expander.

In order for $y_1(\mathbf{n}) = y_2(\mathbf{n})$, we also need

$$\mathbf{n} \in LAT(\mathbf{L}) \quad \text{if and only if} \quad \mathbf{Mn} \in LAT(\mathbf{L}). \tag{4.3.4}$$

Since $\mathbf{Mn}$ is also in $LAT(\mathbf{M})$, we know $\mathbf{Mn} \in LAT(\mathbf{L})$ if and only if $\mathbf{Mn} \in LAT(\mathbf{L}) \cap LAT(\mathbf{M})$. It is shown in the Appendix that $LAT(\mathbf{L}) \cap LAT(\mathbf{M}) = LAT(\text{lcrm}(\mathbf{M}, \mathbf{L}))$. Let $\mathbf{MP}$ be an lcrm$(\mathbf{M}, \mathbf{L})$. Then, the right-hand side of (4.3.4) is equivalent to $\mathbf{Mn} \in LAT(\mathbf{MP})$, which is true if and only if $\mathbf{n} \in LAT(\mathbf{P})$. Comparing this with the left-hand side of (4.3.4), we know that for (4.3.4) to be true, $\mathbf{L}$ and $\mathbf{P}$ should generate the same lattice, i.e., $\mathbf{L} \overset{R}{=} \mathbf{P}$. Then, $\mathbf{ML} \overset{R}{=} \mathbf{MP}$ and hence $\mathbf{ML}$ should be an lcrm$(\mathbf{M}, \mathbf{L})$. △△△

Remark: The interchangeability problem was also addressed in [Kovačević and Vetterli, 1991b] for the 2D case for upper triangular $\mathbf{M}$ and $\mathbf{L}$. However, the conditions we proved above work for any $\mathbf{M}$, $\mathbf{L}$ and any number of dimensions. In fact, the result in [Kovačević and Vetterli, 1991b] is a special case of the results presented here.

It turns out that when $\mathbf{ML} = \mathbf{LM}$, the lcrm/lclm and gcrd/gcld (or right/left coprimeness) have very strong relations, as stated in the following theorem:

Theorem 4.4. When $\mathbf{ML} = \mathbf{LM}$, the following four statements are equivalent:

1. $\mathbf{ML}$ is an lcrm$(\mathbf{M}, \mathbf{L})$.
2. $\mathbf{M}$ and $\mathbf{L}$ are right coprime.
3. $\mathbf{M}$ and $\mathbf{L}$ are left coprime.
4. $\mathbf{ML}$ is an lclm$(\mathbf{M}, \mathbf{L})$.

For the 1D case, this theorem simply says "lcm$(M, L) = ML$ if and only if M and L are coprime," a well-known fact!

Proof: Let $\mathbf{R} = \mathbf{ML} = \mathbf{LM}$. Using Theorem 4.1, we know that $\mathbf{R}$ is an lcrm$(\mathbf{M}, \mathbf{L})$ if and only if $\mathbf{L}$ and $\mathbf{M}$ are right coprime. That is, Statement 1 and Statement 2 imply each other. Similarly, we can show that Statement 3 and Statement 4 imply each other.

Next, consider Statement 2 and Statement 3. Let $\mathbf{H} = \mathbf{ML}^{-1} = \mathbf{L}^{-1}\mathbf{M}$. If $\mathbf{M}$ and $\mathbf{L}$ are right coprime, $\mathbf{ML}^{-1}$ is an irreducible right MFD of $\mathbf{H}$. Suppose $\mathbf{M}$ and $\mathbf{L}$ are not left coprime. Let $\mathbf{X}$ (nonunimodular) be a gcld of $\mathbf{M}$ and $\mathbf{L}$, i.e., $\mathbf{M} = \mathbf{XM}'$, $\mathbf{L} = \mathbf{XL}'$ where $\mathbf{M}'$ and $\mathbf{L}'$ are left coprime. Then, $\mathbf{H} = \mathbf{L}'^{-1}\mathbf{M}'$ is a irreducible left MFD. We then have $J(\mathbf{L}') < J(\mathbf{L})$, which violates Fact 1 (Section 4.2). Hence, we conclude that Statement 2 implies Statement 3. Similarly, we can prove that Statement 3 implies Statement 2 and this completes the proof. △△△

Next, we shall consider the feasibility of expressing every $\mathbf{k}_i$ in $\mathcal{N}(\mathbf{M})$ in the form of $\mathbf{k}_i = \mathbf{Mk}_{i1} + \mathbf{Lk}_{i2}$.

Lemma 4.2. If $\mathbf{M}$ and $\mathbf{L}$ are left coprime, then any integer vector $\mathbf{k}$ can be expressed as $\mathbf{k} =$

$\mathbf{M}\mathbf{k}_1 + \mathbf{L}\mathbf{k}_2$ for some $\mathbf{k}_1$ and $\mathbf{k}_2 \in \mathcal{N}$.

Proof: If $\mathbf{M}$ and $\mathbf{L}$ are left coprime, there exist $\mathbf{P}$ and $\mathbf{Q}$ such that $\mathbf{MP} + \mathbf{LQ} = \mathbf{I}$ (generalized Bezout theorem). Then, for any $\mathbf{k} \in \mathcal{N}$,

$$\mathbf{M}\underbrace{\mathbf{Pk}}_{\mathbf{k}_1} + \mathbf{L}\underbrace{\mathbf{Qk}}_{\mathbf{k}_2} = \mathbf{k}. \tag{4.3.5}$$

△△△

Combining Theorems 4.3, 4.4, and Lemma 4.2, we thus complete the proof of Theorem 4.2. We conclude this section with the following result, which is intuitively appealing:

Lemma 4.3. Suppose $\mathbf{ML} = \mathbf{LM}$. Then, any $\mathrm{lcrm}(\mathbf{M}, \mathbf{L})$ and any $\mathrm{gcrd}(\mathbf{M}, \mathbf{L})$ can be related as $\mathrm{lcrm}(\mathbf{M}, \mathbf{L}) \cdot \mathbf{U} \cdot \mathrm{gcrd}(\mathbf{M}, \mathbf{L}) = \mathbf{ML}$ for some unimodular $\mathbf{U}$.

Remark: For the 1D case, this nicely reduces to $\mathrm{lcm}(M, L)\,\mathrm{gcd}(M, L) = ML$. This lemma also holds for the lclm and gcld case, i.e., $\mathrm{gcld}(\mathbf{M}, \mathbf{L}) \cdot \mathbf{U} \cdot \mathrm{lclm}(\mathbf{M}, \mathbf{L}) = \mathbf{ML}$ for some unimodular $\mathbf{U}$.

Proof: Let $\mathbf{Y} = \mathbf{MP} = \mathbf{LQ}$ be an $\mathrm{lcrm}(\mathbf{M}, \mathbf{L})$, so $\mathbf{P}$ and $\mathbf{Q}$ are right coprime (Theorem 4.1). Since $\mathbf{ML} = \mathbf{LM}$ is a crm(M,L), by the definition of lcrm, $\mathbf{ML} = \mathbf{LM} = \mathbf{MPX} = \mathbf{LQX}$ for some integer matrix $\mathbf{X}$. We then have $\mathbf{L} = \mathbf{PX}$ and $\mathbf{M} = \mathbf{QX}$. Because $\mathbf{P}$ and $\mathbf{Q}$ are right coprime, $\mathbf{X}$ is a gcrd(M,L). Clearly, $\mathbf{YX} = \mathbf{ML}$. We know any $\mathrm{lcrm}(\mathbf{M}, \mathbf{L})$ is a right associate of $\mathbf{Y}$ and any $\mathrm{gcrd}(\mathbf{M}, \mathbf{L})$ is a left associate of $\mathbf{X}$. So, we have $\mathrm{lcrm}(\mathbf{M}, \mathbf{L}) \cdot \mathbf{U} \cdot \mathrm{gcrd}(\mathbf{M}, \mathbf{L}) = \mathbf{ML}$ for some unimodular $\mathbf{U}$.

△△△

4.4. MULTIDIMENSIONAL DELAY-CHAIN SYSTEMS

A 1D delay-chain system as shown in Fig. 4.1-4 is a perfect reconstruction (PR) system, i.e., $\widehat{x}(n) = x(n)$, if and only if M and L are coprime. This is shown in [Nguyen and Vaidyanathan, 1988], and applications of this PR system in the design of filter bank systems can also be found therein. We shall now extend this concept to the MD case. One potential application of MD delay-chain systems is to design MD filter banks where the analysis and synthesis filters have a certain symmetry. The research about such symmetry is still in progress.

A MD delay-chain system is shown in Fig. 4.4-1. (The case of $\mathbf{L} = \mathbf{I}$ is most commonly used and is a trivial PR filter bank.) We can see that this is a very special case of MD maximally decimated filter bank [Vaidyanathan, 1990b], [Viscito and Allebach, 1991] with $J(\mathbf{M})$ channels, where the analysis and synthesis filters are only shift-operators (sometimes called 'delays') defined as:

$$H_{\mathbf{k}}(\mathbf{z}) = \mathbf{z}^{-\mathbf{L}\mathbf{k}} \quad \text{and} \quad F_{\mathbf{k}}(\mathbf{z}) = \mathbf{z}^{\mathbf{L}\mathbf{k}} \quad \text{for} \quad \mathbf{k} \in \mathcal{N}(\mathbf{M}). \tag{4.4.1}$$

As before, we assume **M** and **L** are nonsingular to avoid degeneracy. Clearly, Fig. 4.4-1 is an extension of the 1D delay-chain system.

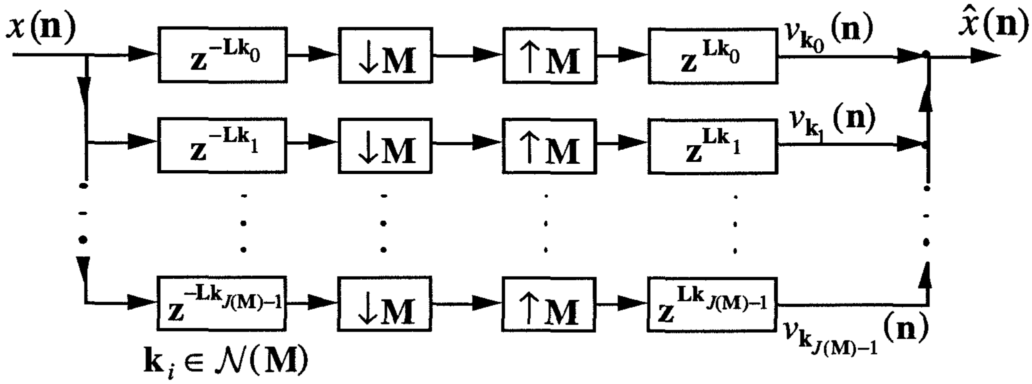

Figure 4.4-1 MD delay-chain system.

Using the definitions of decimation and expansion, we can write the signal $v_{\mathbf{k}}(\mathbf{n})$ in Fig. 4.4-1 for every $\mathbf{k} \in \mathcal{N}(\mathbf{M})$ as follows:

$$v_{\mathbf{k}}(\mathbf{n}) = \begin{cases} x(\mathbf{n}) & \mathbf{n} + \mathbf{Lk} \in LAT(\mathbf{M}), \\ 0 & \text{otherwise.} \end{cases} \tag{4.4.2}$$

Define $\mathcal{L}_{\mathbf{k}} \triangleq \{\mathbf{n} | \mathbf{n} + \mathbf{Lk} \in LAT(\mathbf{M})\}$. Clearly, $\mathcal{L}_{\mathbf{k}}$ is obtained by shifting $LAT(\mathbf{M})$ by $-\mathbf{Lk}$. We can then redraw Fig. 4.4-1 as in Fig. 4.4-2. From Fig. 4.4-2, we can see that $\hat{x}(\mathbf{n}) = x(\mathbf{n})\ \forall \mathbf{n}$ if and only if

$$\bigcup_{\mathbf{k} \in \mathcal{N}(\mathbf{M})} \mathcal{L}_{\mathbf{k}} = \mathcal{N}, \quad \text{and} \quad \bigcap_{\mathbf{k} \in \mathcal{N}(\mathbf{M})} \mathcal{L}_{\mathbf{k}} = \text{empty set.} \tag{4.4.3}$$

It can be verified that the above condition is true if and only if

$$\mathcal{S} \triangleq \{((\mathbf{Lk}))_{\mathbf{M}} \,|\, \mathbf{k} \in \mathcal{N}(\mathbf{M})\} = \mathcal{N}(\mathbf{M}). \tag{4.4.4}$$

From the definition of the modulo notation for integer vectors, all the elements in $\mathcal{S}$ are also in $\mathcal{N}(\mathbf{M})$. Therefore, (4.4.4) is true if and only if all $((\mathbf{Lk}))_{\mathbf{M}}$'s (for $\mathbf{k} \in \mathcal{N}(\mathbf{M})$) are distinct. We now present the following sufficient condition for PR:

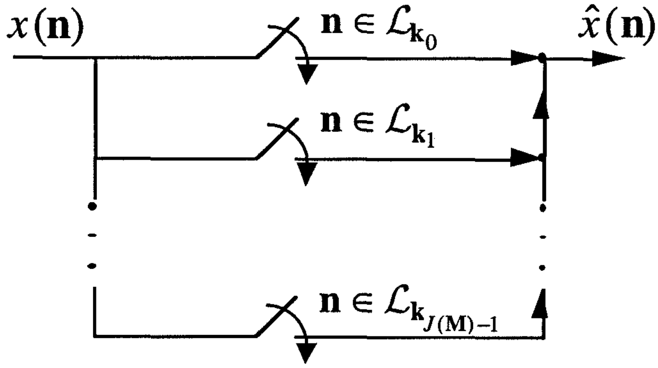

Figure 4.4-2 MD delay-chain system redrawn.

Theorem 4.5. If $\mathbf{LM} \stackrel{R}{=} \mathrm{lcrm}(\mathbf{L}, \mathbf{M})$, the MD delay-chain is PR.

Proof: Suppose $\mathbf{LM} \stackrel{R}{=} \mathrm{lcrm}(\mathbf{L}, \mathbf{M})$, but the MD delay-chain is not PR, i.e., there exist two different $\mathbf{k}_1, \mathbf{k}_2 \in \mathcal{N}(\mathbf{M})$ such that $((\mathbf{Lk}_1))_{\mathbf{M}} = ((\mathbf{Lk}_2))_{\mathbf{M}}$. So, $\mathbf{L}(\mathbf{k}_1 - \mathbf{k}_2) = \mathbf{Mn}$ for some $\mathbf{n} \in \mathcal{N}$. Let $\mathbf{k} = \mathbf{k}_1 - \mathbf{k}_2$. Since $LAT(\mathbf{LM}) = LAT(\mathrm{lcrm}(\mathbf{L}, \mathbf{M})) = LAT(\mathbf{L}) \cap LAT(\mathbf{M})$ (from the Appendix), the above implies $\mathbf{Lk} = \mathbf{Mn} = \mathbf{LMn}'$ for some $\mathbf{n}' \in \mathcal{N}$. So, $\mathbf{k} = \mathbf{Mn}'$. Because $\mathbf{k}_1, \mathbf{k}_2 \in \mathcal{N}(\mathbf{M})$, we can let $\mathbf{k}_i = \mathbf{My}_i$, $i = 1, 2$, where $\mathbf{y}_i \in [0, 1)^D$. So, $\mathbf{k} = \mathbf{My}$, where $\mathbf{y} = \mathbf{y}_1 - \mathbf{y}_2 \in (-1, 1)^D$. Together with $\mathbf{k} = \mathbf{Mn}'$, we thus conclude that $\mathbf{y} = \mathbf{n}' = \mathbf{k} = \mathbf{0}$ ($\mathbf{0}$ stands for the zero vector), so $\mathbf{k}_1 = \mathbf{k}_2$, which leads to contradiction. △△△

However, $\mathbf{LM} \stackrel{R}{=} \mathrm{lcrm}(\mathbf{L}, \mathbf{M})$ is not a necessary condition. An example is:

$$\mathbf{M} = \begin{bmatrix} 1 & -1 \\ 1 & 2 \end{bmatrix} \quad \text{and} \quad \mathbf{L} = \begin{bmatrix} 1 & 0 \\ 0 & 2 \end{bmatrix}. \tag{4.4.5}$$

It is easily checked that the above choice satisfies $\{((\mathbf{Lk}))_{\mathbf{M}} \,|\, \mathbf{k} \in \mathcal{N}(\mathbf{M})\} = \mathcal{N}(\mathbf{M})$ (so the system is PR), but

$$\mathbf{LM} = \begin{bmatrix} 1 & -1 \\ 2 & 4 \end{bmatrix} \tag{4.4.6}$$

is not even a rm of $\mathbf{M}$, since $\mathbf{M}^{-1}\mathbf{LM}$ is not an integer matrix. Furthermore, we can get PR even with some singular $\mathbf{L}$'s. For example, when

$$\mathbf{M} = \begin{bmatrix} 1 & -1 \\ 1 & 2 \end{bmatrix} \quad \text{and} \quad \mathbf{L} = \begin{bmatrix} 0 & 0 \\ 0 & 2 \end{bmatrix}, \tag{4.4.7}$$

we still have

$$\mathcal{S} = \left\{ \begin{bmatrix} 0 \\ 0 \end{bmatrix}, \begin{bmatrix} 0 \\ 1 \end{bmatrix}, \begin{bmatrix} 0 \\ 2 \end{bmatrix} \right\} = \mathcal{N}(\mathbf{M}). \tag{4.4.8}$$

However, if we assume $\mathbf{ML} = \mathbf{LM}$, we can show the following:

Theorem 4.6. If $\mathbf{ML} = \mathbf{LM}$, then the condition $\mathbf{LM} \stackrel{R}{=} \mathrm{lcrm}(\mathbf{L}, \mathbf{M})$ becomes necessary and sufficient for Fig. 4.4-1 to be a PR system.

Proof: Clearly, the sufficiency follows from Theorem 4.5. If $\mathbf{LM}$ is not an lcrm$(\mathbf{L},\mathbf{M})$ (hence $\mathbf{L}$ and $\mathbf{M}$ are not right coprime by Theorem 4.4), we will show that the delay-chain system is not PR. Suppose $\mathbf{MP} = \mathbf{LQ}$ is a lcrm$(\mathbf{L},\mathbf{M})$. Using Lemma 4.3, we know there exists a nonunimodular gcrd$(\mathbf{L},\mathbf{M})$, say $\mathbf{X}$, such that $\mathbf{MPX} = \mathbf{LQX} = \mathbf{ML} = \mathbf{LM}$. Since $\mathbf{X}$ is not unimodular, there exist a nonzero $\mathbf{k} \in \mathcal{N}(\mathbf{X})$. Let $\mathbf{k}' = \mathbf{Qk}$, which is also nonzero. Clearly, $\mathbf{k}' \in \mathcal{N}(\mathbf{QX}) = \mathcal{N}(\mathbf{M})$. Now, we have a nonzero $\mathbf{k}' \in \mathcal{N}(\mathbf{M})$ such that $((\mathbf{Lk}'))_{\mathbf{M}} = ((\mathbf{LQk}))_{\mathbf{M}} = ((\mathbf{MPk}))_{\mathbf{M}} = \mathbf{0}$. We conclude that the elements in $\mathcal{S}$ are not distinct because $((\mathbf{L0}))_{\mathbf{M}}$ is also zero. Hence, the delay-chain is not a PR system. △△△

The condition $\mathbf{ML} = \mathbf{LM}$ is obviously not a necessary assumption in applications. The problem of finding the necessary and sufficient conditions for PR delay-chain systems without assuming $\mathbf{ML} = \mathbf{LM}$ is still open.

4.5. PERIODICITY MATRICES OF DECIMATED SIGNALS

It is well-known that in 1D, a signal with period P is also periodic with period PS where S is any nonzero integer. In MD, a similar fact is true: Let $x(\mathbf{n})$ have periodicity matrix $\mathbf{P}$. If $\mathbf{Q} = \mathbf{PS}$, i.e., $\mathbf{Q}$ is a rm of $\mathbf{P}$, $\mathbf{Q}$ is also a periodicity matrix of $x(\mathbf{n})$ [Dudgeon and Mersereau, 1984, p. 12]. This is easily verified using the definition of periodicity matrices. Since the periodicity matrix of an MD signal is not unique, we are usually interested in those with the smallest absolute determinant. (We exclude the case of singular periodicity matrices.)

We shall consider the following question: when an MD signal $x(\mathbf{n})$ with periodicity matrix $\mathbf{L}$ is decimated by $\mathbf{M}$, is the output $y(\mathbf{n}) = x(\mathbf{Mn})$ periodic? If yes, what is the periodicity matrix? In other words, given $x(\mathbf{n}+\mathbf{Lk}) = x(\mathbf{n})$, $\forall \mathbf{k} \in \mathcal{N}$, we want to find $\mathbf{P}$ such that $y(\mathbf{n}+\mathbf{Pk}) = y(\mathbf{n})$, $\forall \mathbf{k} \in \mathcal{N}$. Since $y(\mathbf{n}+\mathbf{Pk}) = x(\mathbf{Mn}+\mathbf{MPk})$, we can see that $y(\mathbf{n}+\mathbf{Pk}) = y(\mathbf{n})$ if $\mathbf{MPk} = \mathbf{Lq}$ for some $\mathbf{q} \in \mathcal{N}$. Therefore, $\mathbf{P}$ is a periodicity matrix of $y(\mathbf{n})$ if

$$\forall \mathbf{k} \in \mathcal{N},\ \exists\, \mathbf{q} \in \mathcal{N},\ \text{such that } \mathbf{MPk} = \mathbf{Lq}. \tag{4.5.1}$$

Let $\mathbf{k} = \mathbf{e}_0, \ldots, \mathbf{e}_{D-1}$ successively, where $\mathbf{e}_i$'s are columns of the identity matrix $\mathbf{I}$, and collect all the corresponding $\mathbf{q}_0, \ldots, \mathbf{q}_{D-1}$ to form the matrix $\mathbf{Q}$. We see that (4.5.1) is equivalent to

$$\mathbf{MP} = \mathbf{LQ} \quad \text{for some integer matrix } \mathbf{Q}. \tag{4.5.2}$$

This equation clearly says that $\mathbf{MP} = \mathbf{LQ}$ is a crm(M,L). Thus, $\mathbf{P}$ is a periodicity matrix of $y(\mathbf{n})$ if $\mathbf{P} = \mathbf{M}^{-1}\text{crm}(\mathbf{M},\mathbf{L})$. Clearly, $\mathbf{P}$ is not unique. Moreover, using the notation of lcrm, we can conclude that the nonsingular $\mathbf{P}$ which satisfies (4.5.2) with the smallest absolute determinant is $\mathbf{P} = \mathbf{M}^{-1}\text{lcrm}(\mathbf{M}, \mathbf{L})$. Note that (4.5.2) is a *sufficient* condition for $\mathbf{P}$ to be a periodicity matrix of $y(\mathbf{n})$. If further knowledge about $x(\mathbf{n})$ is available, a periodicity matrix with even smaller absolute determinant can be found.

Case of Wide-Sense-Stationary Input

The result for the statistical case is similar. We shall first define wide-sense-stationary (WSS) and cyclo-wide-sense-stationary (CWSS) for the MD statistical process (random signal) as follows:

Definition: Let $R_{xx}(\mathbf{n}, \mathbf{m}) = E[x(\mathbf{n})x^*(\mathbf{n} - \mathbf{m})]$ denote the autocorrelation function of an MD process. The process is said to be WSS if

1. $E[x(\mathbf{n})]$ is a constant.

2. $R_{xx}(\mathbf{n}, \mathbf{m})$ is only a function of $\mathbf{m}$.

Definition: The process $x(\mathbf{n})$ is said to be CWSS with periodicity matrix $\mathbf{L}$ (denoted as $(\text{CWSS})_{\mathbf{L}}$) if

1. $E[x(\mathbf{n})] = E[x(\mathbf{n} + \mathbf{L}\mathbf{k})]$, $\forall \mathbf{k} \in \mathcal{N}$, i.e., $E[x(\mathbf{n})]$ is periodic with periodicity matrix $\mathbf{L}$.

2. $R_{xx}(\mathbf{n}, \mathbf{m}) = R_{xx}(\mathbf{n} + \mathbf{L}\mathbf{k}, \mathbf{m})$, $\forall \mathbf{k}, \mathbf{m} \in \mathcal{N}$, i.e., $R_{xx}(\mathbf{n}, \mathbf{m})$ is periodic with respect to $\mathbf{n}$ with periodicity matrix $\mathbf{L}$.

It is clear from above definitions that if $x(\mathbf{n})$ is $(\text{CWSS})_{\mathbf{L}}$ with unimodular $\mathbf{L}$, $x(\mathbf{n})$ is in fact wide-sense-stationary (WSS). Now, given that $x(\mathbf{n})$ is $(\text{CWSS})_{\mathbf{L}}$, let $y(\mathbf{n}) = x(\mathbf{M}\mathbf{n})$. What can we say about the cyclo-stationarity of $y(\mathbf{n})$? We know $E[y(\mathbf{n})] = E[x(\mathbf{M}\mathbf{n})]$ and $R_{yy}(\mathbf{n}, \mathbf{m}) = E[y(\mathbf{n})y^*(\mathbf{n} - \mathbf{m})] = E[x(\mathbf{M}\mathbf{n})x^*(\mathbf{M}\mathbf{n} - \mathbf{M}\mathbf{m})] = R_{xx}(\mathbf{M}\mathbf{n}, \mathbf{M}\mathbf{m})$. That is, $E[y(\mathbf{n})]$ can be obtained by $\mathbf{M}$-fold decimating $E[x(\mathbf{n})]$, and $R_{yy}(\mathbf{n}, \mathbf{m})$ can be obtained by $\mathbf{M}$-fold decimating $R_{xx}(\mathbf{n}, \mathbf{m})$ with respect to both $\mathbf{n}$ and $\mathbf{m}$. Using the result we obtained for the deterministic case, we can conclude that $E[y(\mathbf{n})]$ has periodicity matrix $\mathbf{P} = \mathbf{M}^{-1}\text{lcrm}(\mathbf{M}, \mathbf{L})$, and $R_{yy}(\mathbf{n}, \mathbf{m})$ also has the same periodicity matrix with respect to $\mathbf{n}$. (Note that the decimation with respect to the second argument $\mathbf{m}$ is not significant here.) Therefore, by the definition of CWSS, we know $y(\mathbf{n})$ is $(\text{CWSS})_{\mathbf{P}}$, with $\mathbf{P} = \mathbf{M}^{-1}\text{lcrm}(\mathbf{M}, \mathbf{L})$.

The above results are summarized in Fig. 4.5-1. Note that in 1D, these simply reduce to $P = \text{lcm}(M, L)/M = L/\gcd(M, L)$ [Sathe and Vaidyanathan, 1993].

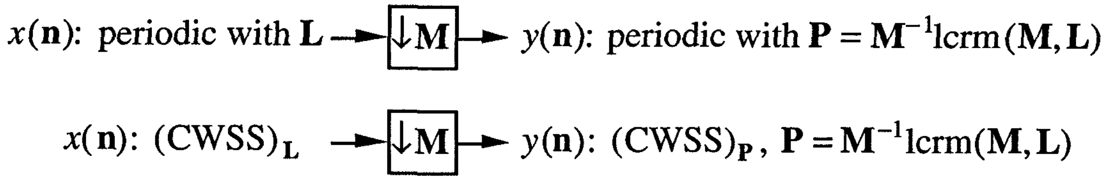

Figure 4.5-1 Decimation of MD signals.

Comments on Fundamental Periodicity Matrices

As mentioned earlier, the periodicity matrix of an MD signal is not unique and we usually are interested in those with the smallest absolute determinant. For this reason, one defines the *fundamental* periodicity matrix as follows:

Definition: $\mathbf{P}_0$ is a fundamental periodicity matrix of $x(\mathbf{n})$ if

i) $\mathbf{P}_0$ is a periodicity matrix of $x(\mathbf{n})$.

ii) Any other periodicity matrix of $x(\mathbf{n})$, say $\mathbf{P}$, can be written as $\mathbf{P} = \mathbf{P}_0\mathbf{S}$ for some integer matrix $\mathbf{S}$. That is, $\mathbf{P}_0$ is a left divisor of all the periodicity matrices of $x(\mathbf{n})$.

It is clear from the above definition that a fundamental periodicity matrix of an MD signal is a periodicity matrix with the smallest absolute determinant (with singular periodicity matrices excluded), and is unique up to postmultiplication by a unimodular matrix. The existence of a fundamental periodicity matrix is assured by the following lemma:

Lemma 4.4. If $\mathbf{P}$ and $\mathbf{P}'$ are both periodicity matrices of $x(\mathbf{n})$, then $\mathrm{gcld}(\mathbf{P},\mathbf{P}')$ is also a periodicity matrix.

Proof: Let $\mathbf{R}$ denote a $\mathrm{gcld}(\mathbf{P},\mathbf{P}')$. There exist integer matrices $\mathbf{A}$ and $\mathbf{B}$ such that $\mathbf{PA}+\mathbf{P}'\mathbf{B}=\mathbf{R}$ (extension of the Euclid's theorem). We then have

$$x(\mathbf{n}+\mathbf{Rk}) = x(\mathbf{n}+\mathbf{P}\underbrace{\mathbf{Ak}}_{\mathbf{k}'}+\mathbf{P}'\underbrace{\mathbf{Bk}}_{\mathbf{k}''}) = x(\mathbf{n}) \qquad \forall \mathbf{k}\in\mathcal{N}. \tag{4.5.3}$$

So, $\mathbf{R}$ is also a periodicity matrix of $x(\mathbf{n})$. △△△

From the above Lemma, we can conclude that, for a given MD signal, a gcld of all the periodicity matrices is indeed a fundamental periodicity matrix. Since a gcld exists, the existence of a fundamental periodicity matrix is also guaranteed.

4.6. EMERGING RESULTS FROM OTHER AUTHORS

After we had submitted [Chen and Vaidyanathan, 1993a] for review in August 1991, we came to realize that the commutativity of MD decimators and expanders was also being considered by several other research groups. This commutativity problem has simultaneously been solved by different groups to different degree.

Evans, McClellan, and Bamberger found the necessary and sufficient conditions of the commutativity to be: (i) $\mathbf{ML} = \mathbf{LM}$ and (ii) lcrm$\mathbf{ML} = \mathbf{MLV}$ where $\mathbf{V}$ is a unimodular matrix [Evans, McClellan, and Bamberger, 1992]. Also, through electronic mail correspondences, we realized that Jon A. Sjogren (AFOSR) has also found similar conditions: (i) $\mathbf{ML} = \mathbf{LM}$ and (ii) the absolute determinant of the generating matrix of the intersection lattice $LAT(\mathbf{M}) \cap LAT(\mathbf{L})$ equals $J(\mathbf{M})J(\mathbf{L})$.

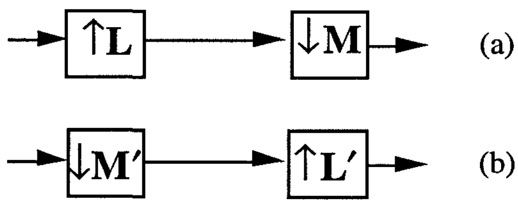

Figure 4.6-1 Relaxed commutativity.

A similar, but more relaxed, commutativity has also been considered. This is shown in Fig. 4.6-1. Gopinath and Burrus found that when $\mathbf{M}$ and $\mathbf{L}$ are left coprime, there exist $\mathbf{M}'$ and $\mathbf{L}'$, which are right coprime, such that the system in Fig. 4.6-1(a) is equivalent to the one in Fig. 4.6-1(b) [Gopinath and Burrus, 1992]. Also, Kalker found that if $\mathbf{M}$ and $\mathbf{L}$ are such that the absolute determinant of the generating matrix of the intersection lattice $LAT(\mathbf{M}) \cap LAT(\mathbf{L})$ equals $J(\mathbf{M})J(\mathbf{L})$, then there exist $\mathbf{M}'$ and $\mathbf{L}'$ such that Fig. 4.6-1(a) and Fig. 4.6-1(b) are equivalent [Kalker, 1992]. Inspired by this relaxed commutativity, we came up with the following lemma related to MFD's:

Lemma 4.5. Given matrices $\mathbf{M}$ and $\mathbf{L}$, we can always find $\mathbf{M}'$ and $\mathbf{L}'$ such that Fig. 4.6-1(a) and Fig. 4.6-1(b) are equivalent by computing an irreducible right MFD of $\mathbf{L}^{-1}\mathbf{M}$, i.e., $\mathbf{L}^{-1}\mathbf{M} = \mathbf{M}'\mathbf{L}'^{-1}$ and $\mathbf{M}'$ and $\mathbf{L}'$ are right coprime. Conversely, given matrices $\mathbf{M}'$ and $\mathbf{L}'$ which are right coprime, we can always find $\mathbf{M}$ and $\mathbf{L}$ such that Fig. 4.6-1(a) and Fig. 4.6-1(b) are equivalent by computing a left MFD of $\mathbf{M}'\mathbf{L}'^{-1}$, i.e., $\mathbf{M}'\mathbf{L}'^{-1} = \mathbf{L}^{-1}\mathbf{M}$.

Proof: By modifying the proof of Theorem 4.3, we can obtain the conditions for Fig. 4.6-1(a) and Fig. 4.6-1(b) to be equivalent: (i) $\mathbf{ML}' = \mathbf{LM}'$ and (ii) $\mathbf{ML}'$ (or $\mathbf{LM}'$) is an lcrm(M,L). Combined with Theorem 4.1, these conditions are equivalent to: (i) $\mathbf{ML}' = \mathbf{LM}'$ and (ii) $\mathbf{M}'$ and $\mathbf{L}'$ are right coprime. Then, the above lemma follows. △△△

Remark: It turns out that we can use this relaxed commutativity in the RPI technique. Then, whenever $\mathbf{M}$ and $\mathbf{L}$ are left coprime, the RPI technique works.

It can be verified that all the above mentioned results are consistent with our results. Comparison of all these results leads to the conclusion that our conditions for commutativity ($\mathbf{ML} = \mathbf{LM}$ and $\mathbf{M}$ and $\mathbf{L}$ are coprime) are very explicit and easy to test.

4.7. CONCLUDING REMARKS

In this chapter, we have formulated and solved various theoretical issues in multidimensional (MD) multirate signal processing, including: the MD polyphase implementation technique for rational sampling rate alterations, the perfect reconstruction properties for the MD delay-chain systems, and the periodicity matrices of decimated MD signals (both deterministic and statistical). We have shown that all these can be solved with the help of the concepts of gcrd, gcld, lcrm and lclm and other related properties for integer matrices. Although we are only interested in integer matrices, all the properties used here also apply to a more general kind of matrices, viz., matrices with elements in a principle ideal domain.

4.8. APPENDIX

In this appendix, we will prove that $LAT(\mathbf{L}) \cap LAT(\mathbf{M}) = LAT(\text{lcrm}(\mathbf{M}, \mathbf{L}))$. A similar statement can be found in [MacDuffee, 1946, p. 38, Theorem 24.2] (although the *lcm* was mistaken to be *gcd*, which might be due to a typographical error in [MacDuffee, 1946]). Since the proof of this statement was omitted in [MacDuffee, 1946], we will now provide a formal proof.

The fact that the intersection of two lattices is also a lattice (which was called the *greatest common submodul* in [MacDuffee, 1946] and the *least common sublattice* in [Dubois, 1985]) is itself a non-trivial issue. To show this, we need the following theorem [Cassels, 1959], [Newman, 1972]:

Theorem 4.A1. A set $\mathcal{V}$ of vectors in the D-dimensional space is a lattice if and only if it satisfies all the following three conditions:

1. If $\mathbf{a} \in \mathcal{V}$ and $\mathbf{b} \in \mathcal{V}$, then $\mathbf{a} \pm \mathbf{b} \in \mathcal{V}$.
2. $\mathcal{V}$ contains D linearly independent vectors.
3. There exists a positive number η such that the zero vector is the only vector in $\mathcal{V}$ with norm less than η.

We use this theorem to show that $\mathcal{V} = LAT(\mathbf{L}) \cap LAT(\mathbf{M})$ is indeed a lattice. Clearly, $\mathcal{V}$ satisfies Condition 1. To show that it satisfies Condition 2, we consider any nonsingular crm of $\mathbf{M}$

and $\mathbf{L}$ (for example, $J(\mathbf{M})\mathbf{L}$), say $\mathbf{K}$. It is easily verified that all the column vectors in $\mathbf{K}$ are in $\mathcal{V}$ and independent. It is also clear that $\mathcal{V}$ satisfies Condition 3 for any $0 < \eta < 1$, since all vectors in $\mathcal{V}$ have integer elements.

We will also need the following lemma (a similar statement can be found in [MacDuffee, 1946, p. 38, Theorem 24.1]):

Lemma 4.A1. $LAT(\mathbf{X}) \subset LAT(\mathbf{Y})$, i.e., $LAT(\mathbf{X})$ is a sublattice of $LAT(\mathbf{Y})$ if and only if $\mathbf{X} = \mathbf{YP}$ for some integer matrix $\mathbf{P}$, i.e., $\mathbf{X}$ is a rm of $\mathbf{Y}$.

Proof:

(1) If $LAT(\mathbf{X}) \subset LAT(\mathbf{Y})$, we have

$$\forall \mathbf{k} \in \mathcal{N},\ \exists \mathbf{p} \in \mathcal{N},\ \text{such that } \mathbf{Xk} = \mathbf{Yp}. \tag{4.8.1}$$

Let $\mathbf{k} = \mathbf{e}_0, \ldots, \mathbf{e}_{D-1}$ ($\mathbf{e}_i$'s same as in Section 4.5) and collect all the corresponding $\mathbf{p}_0, \ldots, \mathbf{p}_{D-1}$ to form the matrix $\mathbf{P}$, we get $\mathbf{X} = \mathbf{YP}$.

(2) Suppose $\mathbf{X} = \mathbf{YP}$. Then, $\mathbf{x} \in LAT(\mathbf{X}) \Rightarrow \mathbf{x} = \mathbf{Xn}$ for some integer $\mathbf{n} \Rightarrow \mathbf{x} = \mathbf{YPn}$. Since $\mathbf{Pn}$ is also an integer vector, $\mathbf{x} \in LAT(\mathbf{Y})$. Hence, we proved $LAT(\mathbf{X}) \subset LAT(\mathbf{Y})$. △△△

We proceed to prove that $LAT(\mathbf{L}) \cap LAT(\mathbf{M}) = LAT(\text{lcrm}(\mathbf{M}, \mathbf{L}))$. Let $LAT(\mathbf{L}) \cap LAT(\mathbf{M}) = LAT(\mathbf{X})$. Because $LAT(\mathbf{X}) \subset LAT(\mathbf{M})$, $\mathbf{X} = \mathbf{MP}$ for some integer matrix $\mathbf{P}$. Similarly, $\mathbf{X} = \mathbf{LQ}$ for some integer matrix $\mathbf{Q}$. So, $\mathbf{X}$ is a crm(**M**,**L**) and hence a rm of $\text{lcrm}(\mathbf{M}, \mathbf{L})$. Using Lemma 4.A1, we can conclude that $LAT(\mathbf{X}) \subset LAT(\text{lcrm}(\mathbf{M}, \mathbf{L}))$. On the other hand, let $\mathbf{MP} = \mathbf{LQ}$ be an crm(**M**,**L**). Using Lemma 4.A1, we know $LAT(\mathbf{MP}) \subset LAT(\mathbf{M})$ and $LAT(\mathbf{LQ}) \subset LAT(\mathbf{L})$. So, we have $LAT(\text{crm}(\mathbf{M}, \mathbf{L})) \subset LAT(\mathbf{M}) \cap LAT(\mathbf{L})$. Hence, in particular, $LAT(\text{lcrm}(\mathbf{M}, \mathbf{L})) \subset LAT(\mathbf{M}) \cap LAT(\mathbf{L}) = LAT(\mathbf{X})$. Therefore, $LAT(\text{lcrm}(\mathbf{M}, \mathbf{L})) = LAT(\mathbf{X}) = LAT(\mathbf{L}) \cap LAT(\mathbf{M})$.

5

Vector Space Framework for Unification of One-Dimensional and Multidimensional Filter Bank Theory

5.1. INTRODUCTION

Recently, maximally decimated analysis/synthesis filter banks have attracted much attention in the area of signal processing. Analysis/synthesis filter banks find applications in subband coding, data compression, transmultiplexing, data encryption, etc. A number of results in filter bank theory can be viewed using vector space notations. This simplifies the proofs of many important results. In this chapter, we will first introduce the framework of vector space, and then use this framework to derive some known and some new filter bank results as well. For example, the relation among the Hermitian image property, orthonormality, and the perfect reconstruction (PR) property is well-known for the case of one-dimensional (1D) analysis/synthesis filter banks [Vaidyanathan, 1987b]. We can prove the same result in a more general vector space setting. We will show that even the most general filter banks, namely, *multidimensional nonuniform filter banks* with *rational* decimation matrices, become a special case of this vector space framework. Therefore, many results in 1D filter bank theory are hence extended to the multidimensional case, with some algebraic manipulations of integer matrices. Some examples are: the equivalence of biorthonormality and the PR property, the interchangeability of analysis and synthesis filters, the connection between analysis/synthesis filter banks and synthesis/analysis transmultiplexers, etc. We also obtain the *subband convolution scheme* by starting from the generalized Parseval's relation in vector space notations. Furthermore, several theoretical results of wavelet transform can also be derived using this framework. In particular, we will derive the so-called *wavelet convolution theorem*.

For example, Fig. 5.1-1 shows the simplest maximally decimated filter bank, a one-dimensional (1D) uniformly decimated filter bank. The input signal $x(n)$ is split into M subbands by analysis filters $H_k(z)$ and then decimated by M (so that the total number of samples is unchanged) to produce the subband signals $x_k(n)$. These subband signals are then processed, e.g., quantized, coded, etc., depending on applications. At the synthesis end, these signals are interpolated by M-fold expanders and synthesis filters $F_k(z)$ and then summed up to give the reconstructed signal $\widehat{x}(n)$. A common requirement in most applications is that, $\widehat{x}(n)$ should be as 'close' to $x(n)$ as possible. More specifically, without the intermediate processing on subband signals $x_k(n)$, we want $\widehat{x}(n) = x(n)$. If this is true, we say that this filter bank achieves the perfect reconstruction (PR) property.

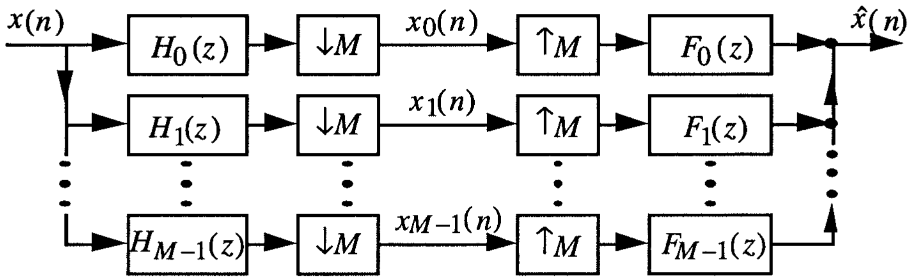

Figure 5.1-1 1D uniformly decimated filter bank.

The theory and design of 1D M-channel uniform filter banks have been successfully addressed in [Vetterli, 1986a], [Smith and Barnwell, 1987], and [Vaidyanathan, 1987b]. The extension to *nonuniformly* decimated filter banks, in which the decimation ratios in each channel are different, has been addressed in [Hoang and Vaidyanathan, 1989], [Nayebi, Barnwell, and Smith, 1991], and [Kovačević and Vetterli, 1991a]. The extension to the multidimensional (MD) nonuniform case was discussed in [Gopinath and Burrus, 1992]. Fig. 5.1-2 shows the most general analysis/synthesis filter bank, namely, an MD nonuniform filter bank with rational decimation ratios (in this case, decimation *matrices*). While $\mathbf{P}_k$ and $\mathbf{Q}_k$ are all nonsingular matrices with integer elements, the equivalent decimation ratio for the kth subband signal is $\mathbf{P}_k^{-1}\mathbf{Q}_k$, which is a matrix with rational elements. Therefore, this filter bank is said to be an MD nonuniform *rational* filter bank. We will assume that $\mathbf{P}_k$ and $\mathbf{Q}_k$ are *left coprime* [MacDuffee, 1946], [Kailath, 1980], [Vidyasagar, 1985] for all k. This is not a significant constraint, because any common left factor of $\mathbf{P}_k$ and $\mathbf{Q}_k$ can be canceled without affecting the decimation ratio in that channel. This filter bank is said to be maximally decimated if $\sum_k |\det \mathbf{P}_k|/|\det \mathbf{Q}_k| = 1$. In this case, the sum of sampling rates of subband signals $x_k(\mathbf{n})$ is equal to the rate of the input signal $x(\mathbf{n})$.

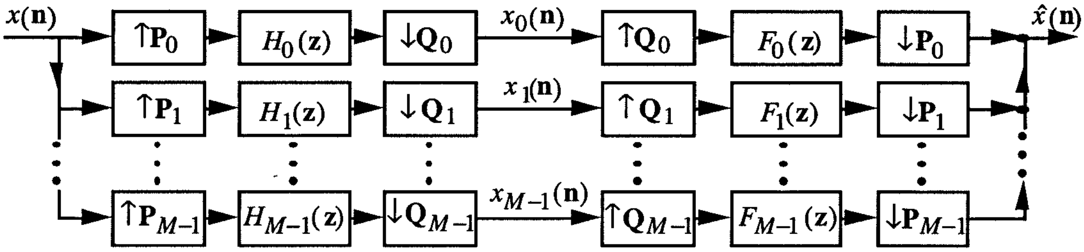

Figure 5.1-2 MD nonuniform rational filter bank.

A number of results in filter bank theory can be viewed using vector space notations. In this chapter, we will introduce a vector space framework which incorporates all kinds of filter banks as special cases. Such a framework simplifies the proofs of many important results. The usefulness of the vector space framework is not surprising in view of the fact that similar interpretations of filter banks have been made by a number of authors. Among others, these include the matrix (possibly infinite-dimensional) formulation in [Vetterli and Le Gall, 1989], the time domain analysis in [Nayebi, Barnwell, and Smith, 1991], and the linear transform formulation in [Nuri and Bamberger, 1992].

Chapter Outline

In Section 5.2, we will provide the vector space framework and derive several theorems in this setting. In the following sections, we will apply this framework, with some manipulations of integer matrices, to derive several theoretical results for MD nonuniform rational filter banks which represent the most general case of filter banks. Some of these results are summarized as follows:

1. Consider the following three properties in a maximally decimated filter bank: (a) the Hermitian image property between analysis filters and synthesis filters, i.e., $h_k(\mathbf{n}) = f_k^*(-\mathbf{n})$, (b) the orthonormality of the synthesis filters, and (c) the perfect reconstruction (PR) property. For the simplest case of 1D uniform filter banks, it has been shown that if a filter bank possesses any two of these properties, then it also satisfies the other one [Vaidyanathan, 1987b]. It turns out that the same result can be verified in the vector space framework, which covers even the most general MD nonuniform rational filter banks. (Section 5.3)
2. The analysis filters and synthesis filters are *biorthonormal* [Riesz and Sz.-Nagy, 1955], [Chui, 1992], [Vetterli and Herley, 1992], if and only if the filter bank achieves PR. This result has been informally known but never explicitly shown for the general case of MD nonuniform rational filter banks. In this chapter, we will prove it using vector space notations. (Section 5.3)

3. The analysis filters and the synthesis filters of a filter bank can be interchanged without changing its PR property. (Section 5.3)

4. A synthesis/analysis transmultiplexer [IEEE, 1982], [Vetterli, 1986b], [Koilpillai, Nguyen, and Vaidyanathan, 1991] that achieves PR can be obtained by interchanging the analysis part and the synthesis part of a PR maximally decimated analysis/synthesis filter bank. This has been a known result for the 1D uniform case [Koilpillai, Nguyen, and Vaidyanathan, 1991]. Using the vector space framework, we can extend it to the general case. (Section 5.4)

5. *MD subband convolution theorem:* We shall use the generalized Parseval's relation of vector space to derive the MD subband convolution scheme, for both the orthonormal case (Eqn. (5.6.11)) and the biorthonormal case (Eqn. (5.6.12)). This turns out to be the generalization of the results in [Vaidyanathan, 1993b]. We will also derive the coding gain formula which shows the main advantage of subband convolution. (Section 5.6)

6. *Wavelet transform and wavelet convolution theorem:* To show further the usefulness of the proposed vector space framework, we will apply it to the discrete wavelet transform [Daubechies, 1992], [Akansu and Haddad, 1992], [Chui, 1992], [Vaidyanathan, 1993a, Chapter 11] to obtain a number of important results. For example, we will show the relation among Hermitian image property, orthonormality, and the PR property, the well-known equivalence of biorthonormality and the PR property, and a new result called the wavelet convolution theorem (Eqn. (5.7.9)). (Section 5.7)

In Section 5.5, we will justify the linear independence of synthesis filters and their shifts in any PR maximally decimated filter bank, which is required to complete the proofs of results in this chapter. We will present a technique of converting an MD nonuniform rational filter bank into a uniform filter bank with larger number of channels, which will simplify the justification of such linear independence.

5.2. ANALYSIS/SYNTHESIS SCHEME IN THE VECTOR SPACE FRAMEWORK

Instead of dealing with the filter banks directly, we will consider a more general setting, viz., vector space (or, inner product space). Consider a vector space $\mathcal{V}$ defined over a field $\mathcal{F}$. For any two vectors $\mathbf{x}$ and $\mathbf{y}$ in $\mathcal{V}$, we can define the inner product, denoted as $(\mathbf{x}, \mathbf{y})$, which gives a scalar in $\mathcal{F}$. Note that the inner product is defined properly so that it satisfies several properties [Luenberger, 1969]: for all $\mathbf{x}$, $\mathbf{y}$, and $\mathbf{z}$ in $\mathcal{V}$ and all c in $\mathcal{F}$

a) $(\mathbf{x}+\mathbf{z}, \mathbf{y}) = (\mathbf{x}, \mathbf{y}) + (\mathbf{z}, \mathbf{y})$,

b) $(c\mathbf{x}, \mathbf{y}) = c(\mathbf{x}, \mathbf{y})$,

c) $(\mathbf{x}, \mathbf{y}) = (\mathbf{y}, \mathbf{x})^*$, where the asterisk denotes complex conjugation,

d) $(\mathbf{x}, \mathbf{x}) \geq 0$, and the equality holds if and only if $\mathbf{x} = \mathbf{0}$.

Consider the following analysis/synthesis scheme in a vector space. Given any vector $\mathbf{x}$ in $\mathcal{V}$, we want to *analyze* it by computing its inner product with a set of (possibly infinitely many) *analysis vectors* $\boldsymbol{\varphi}_i$ (i is an integer index)

$$x_i = (\mathbf{x}, \boldsymbol{\varphi}_i) \qquad \forall\, i. \tag{5.2.1}$$

Then, we want to *synthesize* the vector $\mathbf{x}$ by using x_i to form a linear combination of *synthesis vectors* $\boldsymbol{\eta}_i$

$$\widehat{\mathbf{x}} = \sum_i x_i \boldsymbol{\eta}_i. \tag{5.2.2}$$

Note that in general $\widehat{\mathbf{x}}$ and $\mathbf{x}$ are not identical. Combining the above two equations, we have

$$\widehat{\mathbf{x}} = \sum_i (\mathbf{x}, \boldsymbol{\varphi}_i)\boldsymbol{\eta}_i. \tag{5.2.3}$$

Usually, we want to choose $\boldsymbol{\varphi}_i$ and $\boldsymbol{\eta}_i$ such that the analysis/synthesis scheme satisfies the perfect reconstruction (PR) condition, i.e., $\widehat{\mathbf{x}} = \mathbf{x}$ for all $\mathbf{x}$ in $\mathcal{V}$.

Assumptions on $\boldsymbol{\eta}_i$: For PR to be possible, the span of the set $\{\boldsymbol{\eta}_i\}$ should cover the whole space $\mathcal{V}$, i.e., $\{\boldsymbol{\eta}_i\}$ should be *complete*. Furthermore, we shall assume that $\boldsymbol{\eta}_i$ are *linearly independent*. Therefore, any vector $\mathbf{x}$ in $\mathcal{V}$ can be expressed as

$$\mathbf{x} = \sum_i a_i \boldsymbol{\eta}_i, \tag{5.2.4}$$

for a *unique* set of a_i in $\mathcal{F}$. These assumptions about completeness and linearly independence will be justified in Section 5.5 for the case of filter banks.

In the rest of this section, we shall propose a number of theorems in this vector space framework. These theorems, being easy to prove in vector space notations, will be used to derive many filter bank results in the following sections. The generality of this vector space framework will enable us to derive these results for the 1D case as well as the MD case, for uniform filter banks as well as nonuniform ones, for the case of rational decimation as well as integer decimation.

Theorem 5.1. In the above-mentioned analysis/synthesis scheme, any two of the following three conditions imply the other:

a) $\boldsymbol{\varphi}_i = \boldsymbol{\eta}_i$ for all i.

b) $(\eta_i, \eta_j) = \delta(i-j)$ for all i and j, where $\delta(\cdot)$ is the Kronecker delta, i.e., $\delta(k)$ equals unity for $k=0$ and equals zero otherwise. This is called the orthonormality of the synthesis vectors and the set $\{\eta_i\}$ is said to be an orthonormal set.

c) $\hat{\mathbf{x}} = \mathbf{x}$ for all $\mathbf{x} \in \mathcal{V}$ (perfect reconstruction). ◇

Proofs:

1) We first prove that (a) and (b) imply (c). Because we assume that $\{\eta_i\}$ spans $\mathcal{V}$, any $\mathbf{x}$ in $\mathcal{V}$ can be expressed as $\mathbf{x} = \sum_j a_j \eta_j$. From (5.2.3), we get

$$\begin{aligned}\hat{\mathbf{x}} &= \sum_i (\mathbf{x}, \varphi_i)\eta_i \\ &= \sum_i (\mathbf{x}, \eta_i)\eta_i \qquad \text{(due to (a))} \\ &= \sum_i (\sum_j a_j \eta_j, \eta_i)\eta_i = \sum_i \sum_j a_j (\eta_j, \eta_i)\eta_i \\ &= \sum_i \sum_j a_j \delta(j-i)\eta_i \qquad \text{(due to (b))} \\ &= \sum_j a_j \eta_j = \mathbf{x}.\end{aligned} \tag{5.2.5}$$

Note that because of the continuity of inner product [Luenberger, 1969], the *infinite* summation and the inner product can be interchanged as above.

2) Next, suppose (a) and (c) are true. Equation (5.2.3) becomes

$$\mathbf{x} = \sum_i (\mathbf{x}, \eta_i)\eta_i, \qquad \forall \mathbf{x} \in \mathcal{V}. \tag{5.2.6}$$

We want to show that (b) is true, namely, $\{\eta_i\}$ is orthonormal. Letting $\mathbf{x} = \eta_j$ in (5.2.6), we get

$$\eta_j = \sum_i (\eta_j, \eta_i)\eta_i. \tag{5.2.7}$$

On the other hand, it is clear that $\eta_j = \sum_i \delta(j-i)\eta_i$. Since we have assumed that the expression of a vector as a linear combination of η_i's are unique, we conclude that $(\eta_j, \eta_i) = \delta(j-i)$.

3) Finally, suppose (b) and (c) are true. We need to prove that φ_i and η_i are identical for all i. When (c) is true, from (5.2.3),

$$\mathbf{x} = \sum_i (\mathbf{x}, \varphi_i)\eta_i. \tag{5.2.8}$$

Consider the inner product of $\mathbf{x}$ and η_j

$$\begin{aligned}(\mathbf{x}, \eta_j) = (\sum_i (\mathbf{x}, \varphi_i)\eta_i, \eta_j) &= \sum_i (\mathbf{x}, \varphi_i)(\eta_i, \eta_j) \\ &= \sum_i (\mathbf{x}, \varphi_i)\delta(i-j) \qquad \text{(due to (b))} \\ &= (\mathbf{x}, \varphi_j),\end{aligned} \tag{5.2.9}$$

so that $(\mathbf{x}, \boldsymbol{\eta}_j - \boldsymbol{\varphi}_j) = 0$. Letting $\mathbf{x} = \boldsymbol{\eta}_j - \boldsymbol{\varphi}_j$, the above implies that

$$(\boldsymbol{\eta}_j - \boldsymbol{\varphi}_j, \boldsymbol{\eta}_j - \boldsymbol{\varphi}_j) = 0. \tag{5.2.10}$$

From the fundamental properties of inner product, we know $\boldsymbol{\eta}_j - \boldsymbol{\varphi}_j = \mathbf{0}$, or $\boldsymbol{\eta}_j = \boldsymbol{\varphi}_j$, and hence complete the proof. Note that $\{\boldsymbol{\varphi}_i\}$ is also orthonormal in this case. △△△

Remark: If we do not make the assumption that the set $\{\boldsymbol{\eta}_i\}$ spans $\mathcal{V}$ and $\boldsymbol{\eta}_i$ are linearly independent, this theorem should be restated in three parts as:

1. If $\{\boldsymbol{\eta}_i\}$ spans $\mathcal{V}$, (a) and (b) imply (c).
2. If $\boldsymbol{\eta}_i$ are linearly independent, (a) and (c) imply (b).
3. (b) and (c) imply (a).

For the same vector space setting, we can relax the orthonormality condition and obtain the following theorem which deals with *biorthonormality*:

Theorem 5.2. The analysis/synthesis scheme achieves perfect reconstruction (PR) if and only if $\boldsymbol{\varphi}_i$ and $\boldsymbol{\eta}_i$ satisfy the biorthonormality condition

$$(\boldsymbol{\varphi}_i, \boldsymbol{\eta}_j) = \delta(i - j) \quad \forall i, j. \tag{5.2.11}$$

◇

Proof:

1) If PR is satisfied, we have

$$\mathbf{x} = \sum_i (\mathbf{x}, \boldsymbol{\varphi}_i)\boldsymbol{\eta}_i. \tag{5.2.12}$$

Letting $\mathbf{x} = \boldsymbol{\eta}_j$ in the above equation, we get

$$\boldsymbol{\eta}_j = \sum_i (\boldsymbol{\eta}_j, \boldsymbol{\varphi}_i)\boldsymbol{\eta}_i. \tag{5.2.13}$$

On the other hand, we know $\boldsymbol{\eta}_j = \sum_i \delta(j - i)\boldsymbol{\eta}_i$. Because $\boldsymbol{\eta}_i$ are assumed to be linearly independent, the expression of any vector in terms of $\boldsymbol{\eta}_i$ is unique. We conclude that $(\boldsymbol{\eta}_j, \boldsymbol{\varphi}_i) = \delta(j - i)$.

2) Conversely, suppose (5.2.11) is true. According to the assumption that all $\mathbf{x}$ in $\mathcal{V}$ can be

expressed as $\mathbf{x} = \sum_j a_j \boldsymbol{\eta}_j$, we have

$$\begin{aligned}
\widehat{\mathbf{x}} &= \sum_i (\mathbf{x}, \boldsymbol{\varphi}_i)\boldsymbol{\eta}_i \\
&= \sum_i (\sum_j a_j \boldsymbol{\eta}_j, \boldsymbol{\varphi}_i)\boldsymbol{\eta}_i = \sum_i \sum_j a_j (\boldsymbol{\eta}_j, \boldsymbol{\varphi}_i)\boldsymbol{\eta}_i \\
&= \sum_i \sum_j a_j \delta(j-i)\boldsymbol{\eta}_i \quad \text{(due to biorthonormality)} \\
&= \sum_j a_j \boldsymbol{\eta}_j = \mathbf{x}.
\end{aligned} \tag{5.2.14}$$

Therefore, the PR condition is satisfied. △△△

Remark: This theorem should be restated in two parts as follows, if we do not make the assumptions of completeness and linearly independence:

1. If $\boldsymbol{\eta}_i$ are linearly independent, then PR implies biorthonormality.
2. If $\{\boldsymbol{\eta}_i\}$ spans $\mathcal{V}$, then the biorthonormality implies PR.

Using Theorem 5.2, we can verify the following corollary easily:

Corollary 5.2.1. The vectors $\boldsymbol{\varphi}_i$ and $\boldsymbol{\eta}_i$ can be interchanged without affecting the PR property of the analysis/synthesis scheme. ◇

In some applications, e.g., transmultiplexers, the role of the analysis part and the synthesis part is reversed. More specifically, given a set of scalars x_i in $\mathcal{F}$, we first synthesize a vector $\mathbf{x}$ using synthesis vectors $\boldsymbol{\eta}_i$,

$$\mathbf{x} = \sum_i x_i \boldsymbol{\eta}_i. \tag{5.2.15}$$

Then, we want to recover x_i by analyzing $\mathbf{x}$ using analysis vectors $\boldsymbol{\varphi}_i$,

$$\widehat{x}_i = (\mathbf{x}, \boldsymbol{\varphi}_i) \qquad \forall i. \tag{5.2.16}$$

Combining the above two equations, we obtain the following expression for such a synthesis/analysis transmultiplexer scheme

$$\widehat{x}_i = (\sum_j x_j \boldsymbol{\eta}_j, \boldsymbol{\varphi}_i) \qquad \forall i. \tag{5.2.17}$$

If $\widehat{x}_i = x_i$ for all i and all $x_i \in \mathcal{F}$, we say this synthesis/analysis scheme achieves PR. This synthesis/analysis scheme is closely related with the previously mentioned analysis/synthesis scheme, as in the following theorem:

Theorem 5.3. The analysis/synthesis scheme achieves PR if and only if the corresponding synthesis/analysis scheme achieves PR. ◇

Proof:

1) Suppose the analysis/synthesis scheme achieves PR, i.e. $\mathbf{x} = \sum_i (\mathbf{x}, \boldsymbol{\varphi}_i)\boldsymbol{\eta}_i \; \forall \mathbf{x} \in \mathcal{V}$. Replacing $\mathbf{x}$ with $\sum_i x_i \boldsymbol{\eta}_i$, we get $\sum_i x_i \boldsymbol{\eta}_i = \sum_i (\sum_j x_j \boldsymbol{\eta}_j, \boldsymbol{\varphi}_i)\boldsymbol{\eta}_i$. Because $\boldsymbol{\eta}_i$ are linearly independent, we conclude that $x_i = (\sum_j x_j \boldsymbol{\eta}_j, \boldsymbol{\varphi}_i)$ and therefore the corresponding synthesis/analysis scheme is PR.

2) Conversely, suppose the synthesis/analysis scheme achieves PR, i.e. $x_i = (\sum_j x_j \boldsymbol{\eta}_j, \boldsymbol{\varphi}_i) \; \forall x_i \in \mathcal{F}$. Consider the corresponding analysis/synthesis scheme where $\hat{\mathbf{x}} = \sum_i (\mathbf{x}, \boldsymbol{\varphi}_i)\boldsymbol{\eta}_i$. Because $\{\boldsymbol{\eta}_i\}$ spans $\mathcal{V}$, we can let $\mathbf{x} = \sum_j x_j \boldsymbol{\eta}_j$. So, $\hat{\mathbf{x}} = \sum_i (\sum_j x_j \boldsymbol{\eta}_j, \boldsymbol{\varphi}_i)\boldsymbol{\eta}_i = \sum_i x_i \boldsymbol{\eta}_i = \mathbf{x}$. That is, the corresponding analysis/synthesis scheme also achieves PR. △△△

Remark: Without the linear independence and completeness assumptions on the synthesis vectors, this theorem must be restated as follows:

1. If the synthesis vectors $\boldsymbol{\eta}_i$ are linearly independent, then a PR analysis/synthesis scheme implies that the corresponding synthesis/analysis scheme achieves PR.
2. If $\{\boldsymbol{\eta}_i\}$ spans $\mathcal{V}$, then a PR synthesis/analysis scheme implies that the corresponding analysis/synthesis scheme is also PR.

The following theorem deals with the inner product in the vector space framework:

Theorem 5.4. Generalized Parseval's relation (biorthonormal case): Suppose $\boldsymbol{\varphi}_i$ and $\boldsymbol{\eta}_i$ satisfy the biorthonormality condition in (5.2.11). For any $\mathbf{x} = \sum_i x_i \boldsymbol{\eta}_i$ and any $\mathbf{y} = \sum_i y_i \boldsymbol{\varphi}_i$, the inner product of $\mathbf{x}$ and $\mathbf{y}$ can be obtained as follows:

$$(\mathbf{x}, \mathbf{y}) = \sum_i x_i y_i^*. \tag{5.2.18}$$

◇

Proof: Because $(\boldsymbol{\eta}_i, \boldsymbol{\varphi}_j) = \delta(i-j)$, we can obtain

$$\begin{aligned}(\mathbf{x}, \mathbf{y}) &= (\sum_i x_i \boldsymbol{\eta}_i, \sum_j y_j \boldsymbol{\varphi}_j) \\ &= \sum_i \sum_j x_i y_j^* (\boldsymbol{\eta}_i, \boldsymbol{\varphi}_j) \\ &= \sum_i x_i y_i^*.\end{aligned} \tag{5.2.19}$$

△△△

The following corollary, which applies to the orthonormal case, turns out to be a special case of Theorem 5.4:

Corollary 5.4.1. Parseval's relation (orthonormal case): Suppose the set $\{\boldsymbol{\eta}_i\}$ is orthonormal.

For any $\mathbf{x} = \sum_i x_i \boldsymbol{\eta}_i$ and any $\mathbf{g} = \sum_i g_i \boldsymbol{\eta}_i$, the inner product of $\mathbf{x}$ and $\mathbf{g}$ can be obtained as follows:

$$(\mathbf{x}, \mathbf{g}) = \sum_i x_i g_i^*. \tag{5.2.20}$$

◇

If we let $\mathbf{g} = \mathbf{x}$ in Corollary 5.4.1, (5.2.20) reduces to the energy conservation equation

$$(\mathbf{x}, \mathbf{x}) = \sum_i |x_i|^2. \tag{5.2.21}$$

Furthermore, we can show the following corollary which relates the energy conservation and the orthonormality:

Corollary 5.4.2. For all $\mathbf{x}$ which can be expressed as $\mathbf{x} = \sum_i x_i \boldsymbol{\eta}_i$, the energy is preserved by $\boldsymbol{\eta}_i$, i.e.,

$$(\mathbf{x}, \mathbf{x}) = \sum_i |x_i|^2, \tag{5.2.22}$$

if and *only if* the set $\{\boldsymbol{\eta}_i\}$ is orthonormal. ◇

Proof: Because the 'if' part is a special case of Corollary 5.4.1, we only have to prove the 'only if' part. Suppose (5.2.22) holds for all $\mathbf{x} = \sum_i x_i \boldsymbol{\eta}_i$. Letting $\mathbf{x} = \boldsymbol{\eta}_i$, we get $(\boldsymbol{\eta}_i, \boldsymbol{\eta}_i) = 1$. If we let $\mathbf{x} = a_i \boldsymbol{\eta}_i + a_j \boldsymbol{\eta}_j$, where $i \neq j$, we obtain

$$|a_i|^2 \underbrace{(\boldsymbol{\eta}_i, \boldsymbol{\eta}_i)}_{=1} + |a_j|^2 \underbrace{(\boldsymbol{\eta}_j, \boldsymbol{\eta}_j)}_{=1} + 2\mathrm{Re}[a_i a_j^* (\boldsymbol{\eta}_i, \boldsymbol{\eta}_j)] = |a_i|^2 + |a_j|^2, \tag{5.2.23}$$

where Re[·] denotes the real part of the argument. So, $\mathrm{Re}[a_i a_j^* (\boldsymbol{\eta}_i, \boldsymbol{\eta}_j)] = 0$, for any choice of a_i and a_j. This implies $(\boldsymbol{\eta}_i, \boldsymbol{\eta}_j) = 0$. Summarizing, we have shown $(\boldsymbol{\eta}_i, \boldsymbol{\eta}_j) = \delta(i - j)$, so the set $\{\boldsymbol{\eta}_i\}$ is orthonormal. △△△

5.3. APPLICATIONS TO FILTER BANKS

In this section, we will apply the vector space framework to the problem of filter banks. We will first consider the simple case of 1D uniform filter banks (Fig. 5.1-1). We then extend our discussion to the most general analysis/synthesis filter banks, namely, MD nonuniform filter banks with rational decimation matrices (Fig. 5.1-2).

1D Uniform Filter Banks (the simplest case)

Let us start with the 1D uniform filter bank shown in Fig. 5.1-1. Note that the decimation ratio M is equal to the number of channels, so that the sum of sampling rates of subband signals $x_k(n)$ is equal to the rate of the input signal $x(n)$. We say that such a filter bank is maximally decimated. We can express the subband signals as follows

$$x_k(m) = \sum_{n=-\infty}^{\infty} x(n)h_k(Mm-n), \qquad k = 0,\ldots,M-1. \tag{5.3.1}$$

Note that we have changed the time domain index of the subband signals from n to m for convenience in later discussion. Defining $\phi_{k,m}(n) \triangleq h_k^*(Mm-n)$, we can rewrite (5.3.1) as

$$x_k(m) = \sum_{n=-\infty}^{\infty} x(n)\phi_{k,m}^*(n), \qquad k = 0,\ldots,M-1. \tag{5.3.2}$$

Similarly, we can express the reconstructed signal $\widehat{x}(n)$ as

$$\widehat{x}(n) = \sum_{k=0}^{M-1}\sum_{m=-\infty}^{\infty} x_k(m)f_k(n-Mm). \tag{5.3.3}$$

Define $\eta_{k,m}(n) \triangleq f_k(n-Mm)$. The above equation can be rewritten as

$$\widehat{x}(n) = \sum_{k=0}^{M-1}\sum_{m=-\infty}^{\infty} x_k(m)\eta_{k,m}(n). \tag{5.3.4}$$

We say this system achieves perfect reconstruction (PR) if $\widehat{x}(n) = x(n)$ for all $x(n)$.

Such an analysis/synthesis filter bank is essentially a special case of the vector space analysis/synthesis framework mentioned in Section 2. To see this, consider the vector space $\mathcal{V}$ which is the set of all sequences with finite energy, i.e., all $x(n)$ such that $\sum_{n=-\infty}^{\infty}|x(n)|^2$ is finite (i.e., the ℓ_2 space [Luenberger, 1969]). With $\mathcal{F}$ being the field of complex numbers, we define the inner product of two signals in ℓ_2 as

$$(x(n), y(n)) \triangleq \sum_{n=-\infty}^{\infty} x(n)y^*(n). \tag{5.3.5}$$

It can be verified that this definition satisfies all the fundamental properties of inner product. Note that we use the ℓ_2 space here so that the inner product defined above always exists. Consider the following correspondences between sequences and vectors in the vector space framework

$$\begin{aligned} x(n) &\longleftrightarrow \mathbf{x} \\ \phi_{k,m}(n) &\longleftrightarrow \boldsymbol{\varphi}_i \\ x_k(m) &\longleftrightarrow x_i. \end{aligned} \tag{5.3.6}$$

Note that the time index n has been absorbed in the vector notations, and the indices k and m are combined and rearranged to become the single index i. That is, for any pair of k and m, there exists a unique i. Using (5.3.5) and (5.3.6), we can rewrite (5.3.2) in vector space notations and obtain

$x_i = (\mathbf{x}, \boldsymbol{\varphi}_i)$ which is exactly (5.2.1), the analysis part in the vector space framework. Similarly, using

$$\eta_{k,m}(n) \longleftrightarrow \boldsymbol{\eta}_i$$
$$\widehat{x}(n) \longleftrightarrow \widehat{\mathbf{x}}, \tag{5.3.7}$$

we can rewrite (5.3.4) as $\widehat{\mathbf{x}} = \sum_i x_i \boldsymbol{\eta}_i$ which is exactly (5.2.2), the synthesis part in the vector space framework. Therefore, we have shown that the 1D uniform filter bank is indeed a special case of the vector space framework mentioned in Section 5.2.

MD Nonuniform Rational Filter Banks (the most general case)

We now proceed to Fig. 5.1-2 which shows the most general analysis/synthesis filter bank, namely, an MD nonuniform filter bank with rational decimation matrices. As we will show, this is also covered as a special case by the proposed framework. Note that M denotes the number of channels. In the kth channel, the equivalent decimation ratio (in this case, a matrix) is $\mathbf{P}_k^{-1}\mathbf{Q}_k$. The matrices $\mathbf{P}_k$ and $\mathbf{Q}_k$ are assumed to be *left coprime* [MacDuffee, 1946], [Kailath, 1980], [Vidyasagar, 1985] for all k, because any common left factor can be canceled in $\mathbf{P}_k^{-1}\mathbf{Q}_k$. Also note that $\sum_k J(\mathbf{P}_k)/J(\mathbf{Q}_k) = 1$, so that the sum of sampling rates of subband signals $x_k(\mathbf{n})$ is equal to the rate of the input signal $x(\mathbf{n})$. Such a filter bank is said to be a maximally decimated filter bank.

Using the definitions of decimation and expansion, we can express the subband signal $x_k(\mathbf{n})$ as follows

$$x_k(\mathbf{m}) = \sum_{\mathbf{n}\in\mathcal{N}} x(\mathbf{n}) h_k(\mathbf{Q}_k\mathbf{m} - \mathbf{P}_k\mathbf{n}), \qquad k = 0, \ldots, M-1. \tag{5.3.8}$$

Again, we have changed the space domain index $\mathbf{n}$ of the subband signals to $\mathbf{m}$. Defining $\phi_{k\mathbf{m}}(\mathbf{n}) \triangleq h_k^*(\mathbf{Q}_k\mathbf{m} - \mathbf{P}_k\mathbf{n})$, we rewrite the above as

$$x_k(\mathbf{m}) = \sum_{\mathbf{n}\in\mathcal{N}} x(\mathbf{n}) \phi_{k\mathbf{m}}^*(\mathbf{n}), \qquad k = 0, \ldots, M-1. \tag{5.3.9}$$

Similarly, we express the reconstructed signal $\widehat{x}(\mathbf{n})$ as

$$\widehat{x}(\mathbf{n}) = \sum_{k=0}^{M-1} \sum_{\mathbf{m}\in\mathcal{N}} x_k(\mathbf{m}) f_k(\mathbf{P}_k\mathbf{n} - \mathbf{Q}_k\mathbf{m}). \tag{5.3.10}$$

Define $\eta_{k\mathbf{m}}(\mathbf{n}) \triangleq f_k(\mathbf{P}_k\mathbf{n} - \mathbf{Q}_k\mathbf{m})$. The above equation is then rewritten as

$$\widehat{x}(\mathbf{n}) = \sum_{k=0}^{M-1} \sum_{\mathbf{m}\in\mathcal{N}} x_k(\mathbf{m}) \eta_{k\mathbf{m}}(\mathbf{n}). \tag{5.3.11}$$

If $\widehat{x}(\mathbf{n}) = x(\mathbf{n})$ for all $x(\mathbf{n})$, we say this system achieves PR. With ideal filters, PR is always possible. However, PR is not always possible for practical filters, i.e., filters having rational transfer functions. Even for the 1D case where $P_k = 1$ (nonuniform filter bank with integer decimation ratios), it has been shown that some choices of Q_k will make PR impossible for practical filters [Hoang and Vaidyanathan, 1989]. Interested readers can read [Hoang and Vaidyanathan, 1989] for the idea of *compatible sets* of $\mathbf{Q}_k$. Even for the 1D case, finding a set of necessary and sufficient conditions on $\mathbf{Q}_k$ such that PR is possible still remains an open problem. In this chapter, we will assume that for our discussion, all $\mathbf{Q}_k$ are chosen properly such that PR is indeed possible.

To see that this filter bank is indeed a special case of the vector space analysis/synthesis scheme, consider the ℓ_2 space which is the set of all MD signals with finite energy, i.e., all $x(\mathbf{n})$ such that $\sum_{\mathbf{n}\in\mathcal{N}} |x(\mathbf{n})|^2$ is finite. Similar to the 1D case, we define the inner product of two MD signals as

$$(x(\mathbf{n}), y(\mathbf{n})) \triangleq \sum_{\mathbf{n}\in\mathcal{N}} x(\mathbf{n})y^*(\mathbf{n}). \tag{5.3.12}$$

Rearranging the indices $k = 0, \ldots, M-1$ and $\mathbf{m} \in \mathcal{N}$ as a single index i in the vector space framework, we obtain the following correspondences between MD signals and vectors

$$\begin{aligned} x(\mathbf{n}) &\longleftrightarrow \mathbf{x} \\ \phi_{k\mathbf{m}}(\mathbf{n}) &\longleftrightarrow \boldsymbol{\varphi}_i \\ x_k(\mathbf{m}) &\longleftrightarrow x_i \\ \eta_{k\mathbf{m}}(\mathbf{n}) &\longleftrightarrow \boldsymbol{\eta}_i \\ \widehat{x}(\mathbf{n}) &\longleftrightarrow \widehat{\mathbf{x}}. \end{aligned} \tag{5.3.13}$$

From (5.3.12) and (5.3.13), we see that (5.3.9) is essentially $x_i = (\mathbf{x}, \boldsymbol{\varphi}_i)$ and (5.3.11) is $\widehat{\mathbf{x}} = \sum_i x_i \boldsymbol{\eta}_i$. Hence we conclude that an MD nonuniform rational filter bank is indeed a special case of the proposed vector space framework.

Assumptions: The only detail missing here is the assumptions that $\eta_{k\mathbf{m}}(\mathbf{n})$ (i.e., $f_k(\mathbf{P}_k\mathbf{n} - \mathbf{Q}_k\mathbf{m})$, the $\mathbf{P}_k$-fold decimated versions of synthesis filters and their $\mathbf{Q}_k$-shifts) are linearly independent and the set $\{\eta_{k\mathbf{m}}(\mathbf{n})\}$ spans the ℓ_2 space. The following theorems hold only under these assumptions, which will be justified in Section 5.5. The readers may notice that the condition of maximal decimation ($\sum_k J(\mathbf{P}_k)/J(\mathbf{Q}_k) = 1$) has not been explicitly used so far. It turns out (Section 5.5) that maximal decimation is indeed what makes $\eta_{k\mathbf{m}}(\mathbf{n})$ linearly independent, as one would expect.

Now, we can prove the following theorem:

Theorem 5.5. For an MD nonuniform maximally decimated filter bank as shown in Fig. 5.1-2, any two of the following conditions imply the other:

a) The Hermitian image property

$$h_k(\mathbf{n}) = f_k^*(-\mathbf{n}) \qquad \text{for } k = 0, \ldots, M-1. \tag{5.3.14}$$

b) The orthonormality of the synthesis filters

$$\sum_{\mathbf{n}\in\mathcal{N}} \underbrace{f_k(\mathbf{P}_k\mathbf{n} - \mathbf{Q}_k\mathbf{m})}_{\eta_{k\mathbf{m}}(\mathbf{n})} \underbrace{f_{k'}^*(\mathbf{P}_{k'}\mathbf{n} - \mathbf{Q}_{k'}\mathbf{m}')}_{\eta^*_{k'\mathbf{m}'}(\mathbf{n})} = \delta(k-k')\delta(\mathbf{m}-\mathbf{m}') \tag{5.3.15}$$

for all $k, k' = 0, \ldots, M-1$, and for all $\mathbf{m}, \mathbf{m}' \in \mathcal{N}$. Here the Kronecker delta function $\delta(\mathbf{k})$ is extended to have a vector argument, and equals unity for $\mathbf{k} = \mathbf{0}$ and equals zero otherwise.

c) The perfect reconstruction (PR) property

$$\widehat{x}(\mathbf{n}) = x(\mathbf{n}), \qquad \text{for all } x(\mathbf{n}) \text{ with finite energy.} \tag{5.3.16}$$

◇

Proof: It turns out that these three conditions all correspond nicely to the three conditions in Theorem 5.1. For (b) and (c) this fact can be easily seen, because (5.3.15) can be written as $(\boldsymbol{\eta}_i, \boldsymbol{\eta}_{i'}) = \delta(i-i')$ and (5.3.16) as $\widehat{\mathbf{x}} = \mathbf{x}$ in vector space notations. Also, the equivalence of Condition (a) in Theorem 5.1 to Condition (a) in Theorem 5.5 can be proved as follows

$$\begin{aligned}
&\boldsymbol{\varphi}_i = \boldsymbol{\eta}_i \qquad \forall i \\
\Longleftrightarrow\ &\phi_{k\mathbf{m}}(\mathbf{n}) = \eta_{k\mathbf{m}}(\mathbf{n}) && k = 0, \ldots, M-1,\ \mathbf{m} \in \mathcal{N} \\
\Longleftrightarrow\ &h_k^*(\mathbf{Q}_k\mathbf{m} - \mathbf{P}_k\mathbf{n}) = f_k(\mathbf{P}_k\mathbf{n} - \mathbf{Q}_k\mathbf{m}) && k = 0, \ldots, M-1,\ \mathbf{m} \in \mathcal{N} \\
\Longleftrightarrow\ &h_k^*(\mathbf{n}) = f_k(-\mathbf{n}) && k = 0, \ldots, M-1.
\end{aligned} \tag{5.3.17}$$

The last equivalence is due to the fact that $\mathbf{P}_k$ and $\mathbf{Q}_k$ are left coprime (see Appendix A for details). Hence Theorem 5.5 is indeed a special case of Theorem 5.1, and the same relation holds. △△△

We also have the following theorem for the biorthonormal case, which is a direct result of Theorem 5.2:

Theorem 5.6. The MD nonuniform maximally decimated filter bank in Fig. 5.1-2 satisfies the PR condition if and only if the filters satisfy the biorthonormal property

$$\sum_{\mathbf{n}\in\mathcal{N}} h_k(\mathbf{Q}_k\mathbf{m} - \mathbf{P}_k\mathbf{n}) f_{k'}(\mathbf{P}_{k'}\mathbf{n} - \mathbf{Q}_{k'}\mathbf{m}') = \delta(k-k')\delta(\mathbf{m}-\mathbf{m}'), \tag{5.3.18}$$

for all $k, k' = 0, \ldots, M-1$, and for all $\mathbf{m}, \mathbf{m}' \in \mathcal{N}$. ◇

In (5.3.18), we can replace $\mathbf{n}$ with $-\mathbf{n}$, $\mathbf{m}$ with $-\mathbf{m}$, and $\mathbf{m}'$ with $-\mathbf{m}'$, to obtain

$$\sum_{\mathbf{n}\in\mathcal{N}} f_{k'}(\mathbf{Q}_{k'}\mathbf{m}' - \mathbf{P}_{k'}\mathbf{n}) h_k(\mathbf{P}_k\mathbf{n} - \mathbf{Q}_k\mathbf{m}) = \delta(k-k')\delta(\mathbf{m}-\mathbf{m}'). \tag{5.3.19}$$

This gives us the following corollary (which is also a direct result of Corollary 5.2.1):

Corollary 5.6.1. We can interchange the analysis filters and synthesis filters in any PR maximally decimated filter bank to obtain another PR maximally decimated filter bank. ◇

5.4. FILTER BANKS AND TRANSMULTIPLEXERS

A system which is closely related to filter banks is the so-called transmultiplexer [IEEE, 1982], [Vetterli, 1986b], [Koilpillai, Nguyen, and Vaidyanathan, 1991]. A transmultiplexer, as shown in Fig. 5.4-1, is obtained by interchanging the analysis part and the synthesis part of an analysis/synthesis filter bank. In this system, input signals $x_k(\mathbf{n})$ are interpolated by $\mathbf{Q}_k$-fold expanders, filters $F_k(\mathbf{z})$, and $\mathbf{P}_k$-fold decimators, and then summed up to form the signal $x(\mathbf{n})$. Effectively, the information in each $x_k(\mathbf{n})$ is now carried in a certain frequency band of $x(\mathbf{n})$. Therefore, this is also called the frequency division multiplexing (FDM) technique. Note that $x(\mathbf{n})$ has a higher sampling rate than any of the input signals $x_k(\mathbf{n})$. Usually, we choose $\sum_k J(\mathbf{P}_k)/J(\mathbf{Q}_k) = 1$ such that the sampling rate of $x(\mathbf{n})$ is equal to the sum of the sample rates of $x_k(\mathbf{n})$. At the other end, $x(\mathbf{n})$ is separated into M output signals $\widehat{x}_k(\mathbf{n})$ by $\mathbf{P}_k^{-1}\mathbf{Q}_k$-fold decimation with filters $H_k(\mathbf{z})$. A common requirement for this synthesis/analysis transmultiplexing scheme is that $\widehat{x}_k(\mathbf{n}) = x_k(\mathbf{n})$ for all k. When this is true, we say this transmultiplexer satisfies the perfect reconstruction (PR) condition.

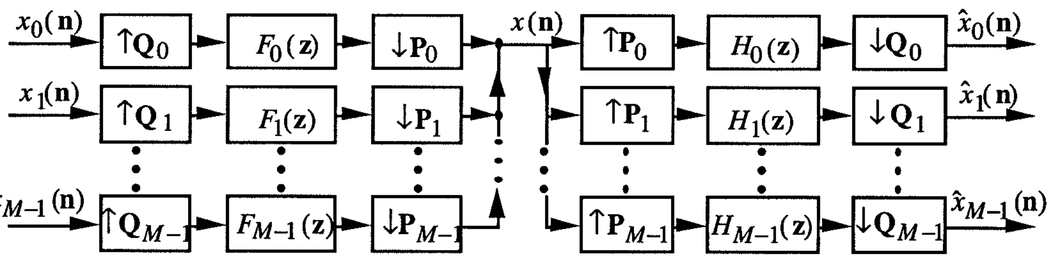

Figure 5.4-1 MD transmultiplexer.

Starting from Theorem 5.3 derived in the vector space framework, we can obtain the following theorem which states the close relation between analysis/synthesis filter banks and transmultiplexers:

Theorem 5.7. The MD nonuniform maximally decimated filter bank satisfies the PR condition if and only if the corresponding MD nonuniform transmultiplexer is PR. ◇

This theorem is very useful because it unifies the theory and design of PR maximally decimated filter banks and those of PR transmultiplexers. A similar result for the case of 1D uniform filter banks has been presented in [Koilpillai, Nguyen, and Vaidyanathan, 1991]. Here, we have generalized the result therein to the most general case, i.e., the case of MD nonuniform rational filter banks.

5.5. LINEAR INDEPENDENCE OF SYNTHESIS VECTORS

When we apply results in the vector space framework to derive Theorems 5.5, 5.6, and 5.7 for the case of filter banks, we assume that $\eta_{k\mathbf{m}}(\mathbf{n})$, or $f_k(\mathbf{P}_k\mathbf{n} - \mathbf{Q}_k\mathbf{m})$ (the $\mathbf{P}_k$-fold decimated versions of synthesis filters and their $\mathbf{Q}_k$-shifts), are linearly independent and $\{\eta_{k\mathbf{m}}(\mathbf{n})\}$ spans the whole space ℓ_2 (completeness). We will now justify these assumptions.

The second assumption about completeness is necessary. If it is not true, there exists an MD signal in ℓ_2 which cannot be represented using $\eta_{k\mathbf{m}}(\mathbf{n})$, hence cannot be perfectly reconstructed. In this case, PR is out of question, and none of the above theorems is meaningful. It only remains to show that $\eta_{k\mathbf{m}}(\mathbf{n})$ are linear independent whenever PR is possible for all $x(\mathbf{n})$. In other words, whenever there exist analysis filters and synthesis filters to achieve PR, the corresponding $\eta_{k\mathbf{m}}(\mathbf{n})$ should be linearly independent. The rest of this section is devoted to show this. The maximal decimation condition, which has not been *explicitly* used so far, is indeed what makes $\eta_{k\mathbf{m}}(\mathbf{n})$ linearly independent. We will prove this in two steps. First, we will show that $\eta_{k\mathbf{m}}(\mathbf{n})$ are linear independent for any maximally decimated *uniform* filter bank that has the PR property. We will then show that any MD maximally decimated nonuniform rational filter bank can be converted into a uniform one having the same set $\{\eta_{k\mathbf{m}}(\mathbf{n})\}$. Therefore, the corresponding $\eta_{k\mathbf{m}}(\mathbf{n})$ of the nonuniform system are also linear independent.

Linear Independence of $\eta_{k\mathbf{m}}(\mathbf{n})$ for the Uniform Case

Consider an MD maximally decimated uniform filter bank as shown in Fig. 5.5-1(a). We need to show that for this maximally decimated system to achieve PR, the corresponding $\eta_{k\mathbf{m}}(\mathbf{n}) = f_k(\mathbf{n} - \mathbf{L}\mathbf{m})$ are linearly independent. That is, the synthesis filters and their $\mathbf{L}$-shifts are linearly independent.

Using the polyphase decomposition (Section 2.3), we can represent the analysis filters and synthesis filters in the form

$$H_j(\mathbf{z}) = \sum_{k=0}^{J(\mathbf{L})-1} \mathbf{z}^{-\boldsymbol{\ell}_k} E_{j,k}(\mathbf{z}^{\mathbf{L}}) \qquad j = 0, \ldots, J(\mathbf{L}) - 1 \tag{5.5.1}$$

and

$$F_j(\mathbf{z}) = \sum_{k=0}^{J(\mathbf{L})-1} \mathbf{z}^{\boldsymbol{\ell}_k} R_{k,j}(\mathbf{z}^{\mathbf{L}}) \qquad j = 0, \ldots, J(\mathbf{L}) - 1. \tag{5.5.2}$$

Note that the vectors in $\mathcal{N}(\mathbf{L})$ are ordered as $\boldsymbol{\ell}_0, \boldsymbol{\ell}_1, \ldots, \boldsymbol{\ell}_{J(\mathbf{L})-1}$ and $\boldsymbol{\ell}_0$ is usually chosen to be the zero vector $\mathbf{0}$. Then, we can redraw this system as in Fig. 5.5-1(b). The $J(\mathbf{L}) \times J(\mathbf{L})$ matrices $\mathbf{E}(\mathbf{z})$ and $\mathbf{R}(\mathbf{z})$ which have elements $E_{j,k}(\mathbf{z})$ and $R_{k,j}(\mathbf{z})$ are called the polyphase matrices of the analysis

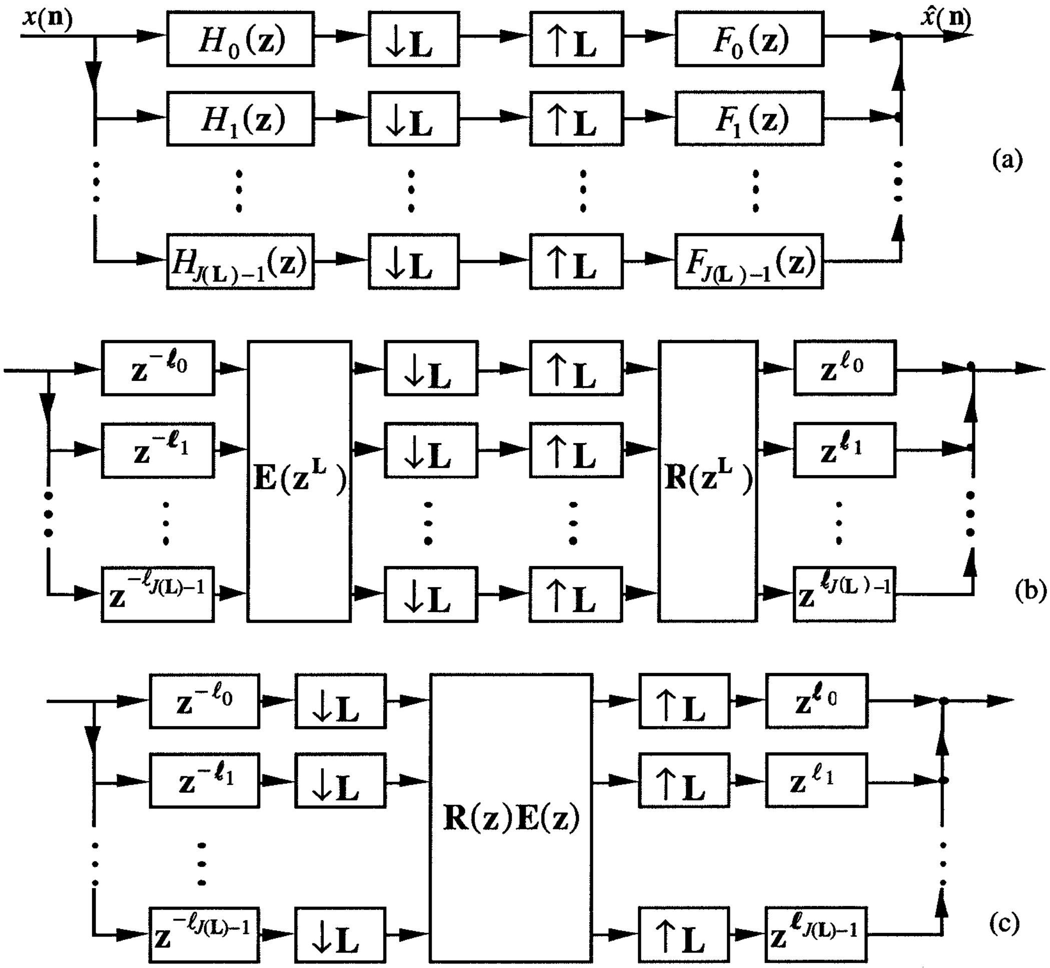

Figure 5.5-1 MD uniform maximally decimated filter bank.

bank and the synthesis bank, respectively. MD Noble identities allow us to move the decimators and expanders across $\mathbf{E}(\mathbf{z}^{\mathbf{L}})$ and $\mathbf{R}(\mathbf{z}^{\mathbf{L}})$, respectively, and obtain Fig. 5.5-1(c). For this system to achieve PR, we must have $\mathbf{R}(\mathbf{z})\mathbf{E}(\mathbf{z}) = \mathbf{I}$. This implies that $\mathbf{R}(\mathbf{z})$ is invertible. For the case where all transfer functions are rational function in $\mathbf{z}$ with finite degree, $\mathbf{R}(\mathbf{z})$ being invertible implies that $\det \mathbf{R}(\mathbf{z})$ is not identically zero (but can be zero only for some finite number of $\mathbf{z}_i$).

Now, suppose that $f_k(\mathbf{n} - \mathbf{Lm})$ are not linearly independent. That is, there exist $a_k(\mathbf{m})$ which are not all zero such that

$$\sum_{k=0}^{J(\mathbf{L})-1} \sum_{\mathbf{m}\in\mathcal{N}} a_k(\mathbf{m}) f_k(\mathbf{n} - \mathbf{Lm}) = 0. \tag{5.5.3}$$

Let $a_k(\mathbf{m})$ be the inputs to the synthesis filter bank as shown in Fig. 5.5-2(a). Equation (5.5.3) implies that the output is identically zero. With Fig. 5.5-2(a) redrawn as in Fig. 5.5-2(b), it can be verified that the outputs of $\mathbf{R}(\mathbf{z})$ are also zero. Letting $A_k(\mathbf{z})$ denote the $\mathbf{z}$-transform of $a_k(\mathbf{m})$

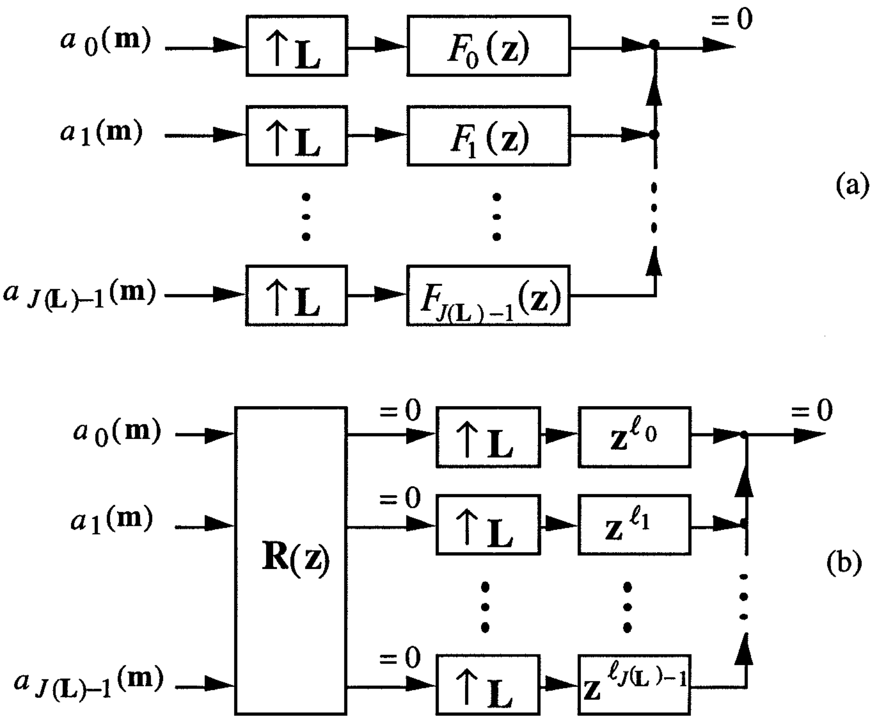

Figure 5.5-2 MD uniform synthesis filter bank.

and $\mathbf{a}(\mathbf{z}) = [A_0(\mathbf{z}) \ \cdots \ A_{J(\mathbf{L})-1}(\mathbf{z})]^T$, we have $\mathbf{R}(\mathbf{z})\mathbf{a}(\mathbf{z}) = \mathbf{0}$. Because $\det \mathbf{R}(\mathbf{z})$ is not identically zero, $\mathbf{a}(\mathbf{z})$ is zero almost everywhere except for some finite number of $\mathbf{z}_i$. For these $\mathbf{z}_i$, $\mathbf{a}(\mathbf{z}_i)$ can be nonzero but finite. This implies $a_k(\mathbf{m})$ are all zero. We hence conclude that $f_k(\mathbf{n}-\mathbf{L}\mathbf{m})$ are linearly independent.

Conversion to Uniform Filter Banks

Next, we will show how to convert an MD nonuniform rational filter bank into a uniform filter bank with a larger number of channels while preserving the same set of $\eta_{k\mathbf{m}}(\mathbf{n})$. For the 1D case, the problem of transforming a non-uniform filter bank into a uniform one has been addressed in [Hoang and Vaidyanathan, 1989] and [Kovačević and Vetterli, 1991a]. This idea has been extended to the MD case and a graphical derivation has been given in [Gopinath and Burrus, 1992]. The approach we present here will give the resulting uniform filter bank and the corresponding subband signals as well. Furthermore, we will show that the sets $\{\eta_{k\mathbf{m}}(\mathbf{n})\}$ and $\{\phi_{k\mathbf{m}}(\mathbf{n})\}$ of the converted uniform system are the same as those of the original nonuniform system.

Let us consider the set of functions $\eta_{k\mathbf{m}}(\mathbf{n}) = f_k(\mathbf{P}_k\mathbf{n} - \mathbf{Q}_k\mathbf{m})$ of the MD nonuniform rational filter bank in Fig. 5.1-2. The division theorem [Dudgeon and Mersereau, 1984, Sec. 2.4.2] says that, with respect to a nonsingular integer matrix $\mathbf{M}$, every integer vector $\mathbf{n}$ can be uniquely expressed as $\mathbf{n} = \mathbf{M}\mathbf{n}_0 + \mathbf{k}$, for some $\mathbf{k} \in \mathcal{N}(\mathbf{M})$, and $\mathbf{n}_0 \in \mathcal{N}$. Therefore, $\mathbf{Q}_k\mathbf{m}$ can be written as

$$\mathbf{Q}_k\mathbf{m} = \mathbf{P}_k\mathbf{r} + \mathbf{p}, \quad \text{for } \mathbf{r} \in \mathcal{N} \text{ and } \mathbf{p} \in \mathcal{N}(\mathbf{P}_k), \tag{5.5.4}$$

where $\mathbf{r}$ and $\mathbf{p}$ are unique for a given $\mathbf{m}$. Let $f_{k,\mathbf{p}}(\mathbf{n})$ denote the $\mathbf{P}_k$-fold Type 2 polyphase components of $f_k(\mathbf{n})$, i.e.,

$$f_{k,\mathbf{p}}(\mathbf{n}) \triangleq f_k(\mathbf{P}_k\mathbf{n} - \mathbf{p}), \qquad \mathbf{p} \in \mathcal{N}(\mathbf{P}_k). \tag{5.5.5}$$

We then have

$$\begin{aligned} f_k(\mathbf{P}_k\mathbf{n} - \mathbf{Q}_k\mathbf{m}) &= f_k(\mathbf{P}_k\mathbf{n} - \mathbf{P}_k\mathbf{r} - \mathbf{p}) \\ &= f_{k,\mathbf{p}}(\mathbf{n} - \mathbf{r}). \end{aligned} \tag{5.5.6}$$

In other words, $f_k(\mathbf{P}_k\mathbf{n} - \mathbf{Q}_k\mathbf{m})$ is the $\mathbf{p}$th polyphase component of $f_k(\mathbf{n})$, delayed by $\mathbf{r}$.

Because $\mathbf{P}_k$ and $\mathbf{Q}_k$ are left coprime, there exist integer matrices $\mathbf{A}_k$ and $\mathbf{B}_k$ which are right coprime such that $\mathbf{P}_k\mathbf{A}_k + \mathbf{Q}_k\mathbf{B}_k = \mathbf{I}$ (generalized Bezout theorem [MacDuffee, 1946], [Kailath, 1980], [Vidyasagar, 1985]). Furthermore, there exist right coprime matrices $\mathbf{S}_k$ and $\mathbf{R}_k$ such that $\mathbf{P}_k\mathbf{S}_k = \mathbf{Q}_k\mathbf{R}_k$ and $J(\mathbf{S}_k) = J(\mathbf{Q}_k)$ [Chen and Vaidyanathan, 1993a]. For these $\mathbf{A}_k$ and $\mathbf{S}_k$, it is shown in Appendix B that any pair of $\mathbf{r}$ and $\mathbf{p}$ obtained in (5.5.4) satisfies

$$\mathbf{r} = \mathbf{S}_k\mathbf{j} - \mathbf{A}_k\mathbf{p} \quad \text{for some } \mathbf{j} \in \mathcal{N}. \tag{5.5.7}$$

Now, (5.5.6) can be written as

$$f_k(\mathbf{P}_k\mathbf{n} - \mathbf{Q}_k\mathbf{m}) = f_{k,\mathbf{p}}(\mathbf{n} + \mathbf{A}_k\mathbf{p} - \mathbf{S}_k\mathbf{j}). \tag{5.5.8}$$

Let $\mathbf{L}$ be a *common right multiple* (crm) [MacDuffee, 1946] of $\mathbf{S}_0$, $\mathbf{S}_1$, ... $\mathbf{S}_{M-1}$, and denote it as $\text{crm}(\mathbf{S}_0, \ldots, \mathbf{S}_{M-1})$. That is, $\mathbf{L} = \mathbf{S}_k\mathbf{T}_k$ for all k, where $\mathbf{T}_k$ are integer matrices. In particular, we can choose a *least* common right multiple (lcrm) [MacDuffee, 1946]. Next, we use the division theorem again to write $\mathbf{j}$ as

$$\mathbf{j} = \mathbf{T}_k\mathbf{i} + \mathbf{t} \quad \text{for } \mathbf{i} \in \mathcal{N} \text{ and } \mathbf{t} \in \mathcal{N}(\mathbf{T}_k). \tag{5.5.9}$$

Note that $\mathbf{i}$ and $\mathbf{t}$ are unique for a given $\mathbf{j}$. Then, (5.5.8) can be written as

$$\begin{aligned} f_k(\mathbf{P}_k\mathbf{n} - \mathbf{Q}_k\mathbf{m}) &= f_{k,\mathbf{p}}(\mathbf{n} + \mathbf{A}_k\mathbf{p} - \mathbf{S}_k\mathbf{t} - \mathbf{S}_k\mathbf{T}_k\mathbf{i}) \\ &= f_{k,\mathbf{p}}(\mathbf{n} + \mathbf{A}_k\mathbf{p} - \mathbf{S}_k\mathbf{t} - \mathbf{L}\mathbf{i}) \\ &= f'_{k\mathbf{pt}}(\mathbf{n} - \mathbf{L}\mathbf{i}), \end{aligned} \tag{5.5.10}$$

where $f'_{k\mathbf{pt}}(\mathbf{n})$ is defined as $f'_{k\mathbf{pt}}(\mathbf{n}) \triangleq f_{k,\mathbf{p}}(\mathbf{n} + \mathbf{A}_k\mathbf{p} - \mathbf{S}_k\mathbf{t})$.

Combining (5.5.4), (5.5.7) and (5.5.9), we can get the following expression for $\mathbf{m}$

$$\mathbf{m} = \mathbf{R}_k\mathbf{T}_k\mathbf{i} + \mathbf{R}_k\mathbf{t} + \mathbf{B}_k\mathbf{p}. \tag{5.5.11}$$

It is shown in Appendix C that (5.5.4), (5.5.7) and (5.5.9) altogether define a one-to-one and onto mapping from a single index $\mathbf{m} \in \mathcal{N}$ to a triple index $(\mathbf{p}, \mathbf{t}, \mathbf{i})$ where $\mathbf{p} \in \mathcal{N}(\mathbf{P}_k)$, $\mathbf{t} \in \mathcal{N}(\mathbf{T}_k)$ and $\mathbf{i} \in \mathcal{N}$. Using the same mapping to map subband signals $x_k(\mathbf{m})$ to $x_{k\mathbf{pt}}(\mathbf{i})$, we can rewrite (5.3.10) as

$$\begin{aligned}\widehat{x}(\mathbf{n}) &= \sum_{k=0}^{M-1} \sum_{\mathbf{m}\in\mathcal{N}} x_k(\mathbf{m}) f_k(\mathbf{P}_k\mathbf{n} - \mathbf{Q}_k\mathbf{m}) \\ &= \sum_{k=0}^{M-1} \sum_{\mathbf{p}\in\mathcal{N}(\mathbf{P}_k)} \sum_{\mathbf{t}\in\mathcal{N}(\mathbf{T}_k)} \sum_{\mathbf{i}\in\mathcal{N}} x_{k\mathbf{pt}}(\mathbf{i}) f'_{k\mathbf{pt}}(\mathbf{n} - \mathbf{L}\mathbf{i}).\end{aligned} \tag{5.5.12}$$

Note that the summation over $\mathbf{m}$ is replaced by a triple summation over $\mathbf{p}$, $\mathbf{t}$, and $\mathbf{i}$.

We can preform similar operations on the analysis filter bank also. We use $h_{k,\mathbf{p}}(\mathbf{n})$ to denote the $\mathbf{P}_k$-fold Type 1 polyphase components of $h_k(\mathbf{n})$, i.e., $h_{k,\mathbf{p}}(\mathbf{n}) \stackrel{\triangle}{=} h_k(\mathbf{P}_k\mathbf{n} + \mathbf{p})$, and rewrite $h_k(\mathbf{Q}_k\mathbf{m} - \mathbf{P}_k\mathbf{n})$ as

$$\begin{aligned}h_k(\mathbf{Q}_k\mathbf{m} - \mathbf{P}_k\mathbf{n}) &= h_k(\mathbf{P}_k\mathbf{r} + \mathbf{p} - \mathbf{P}_k\mathbf{n}) \\ &= h_{k,\mathbf{p}}(\mathbf{r} - \mathbf{n}) \\ &= h_{k,\mathbf{p}}(\mathbf{S}_k\mathbf{j} - \mathbf{A}_k\mathbf{p} - \mathbf{n}) \\ &= h_{k,\mathbf{p}}(\mathbf{L}\mathbf{i} + \mathbf{S}_k\mathbf{t} - \mathbf{A}_k\mathbf{p} - \mathbf{n}) \\ &= h'_{k\mathbf{pt}}(\mathbf{L}\mathbf{i} - \mathbf{n}),\end{aligned} \tag{5.5.13}$$

where $h'_{k\mathbf{pt}}(\mathbf{n})$ is defined as $h'_{k\mathbf{pt}}(\mathbf{n}) \stackrel{\triangle}{=} h_{k,\mathbf{p}}(\mathbf{n} - \mathbf{A}_k\mathbf{p} + \mathbf{S}_k\mathbf{t})$. So, (5.3.8) becomes

$$x_{k\mathbf{pt}}(\mathbf{i}) = \sum_{\mathbf{n}\in\mathcal{N}} x(\mathbf{n}) h'_{k\mathbf{pt}}(\mathbf{L}\mathbf{i} - \mathbf{n}), \qquad k = 0, \ldots, M-1,\ \mathbf{p} \in \mathcal{N}(\mathbf{P}_k),\ \mathbf{t} \in \mathcal{N}(\mathbf{T}_k). \tag{5.5.14}$$

Looking at (5.5.12) and (5.5.14), we realize that the original nonuniformly decimated analysis/synthesis filter bank has been converted into a uniformly decimated filter bank with decimation ratio $\mathbf{L}$. The channels are now labeled by three indices k, $\mathbf{p}$ and $\mathbf{t}$. One channel (the '$(k\mathbf{pt})$th' channel) of this uniform filter bank is shown in Fig. 5.5-3. The new subband signals are $x_{k\mathbf{pt}}(\mathbf{i})$, where $\mathbf{i}$ is the space domain index. Because $x_{k\mathbf{pt}}(\mathbf{i}) = x_k(\mathbf{m})$ where $\mathbf{m}$ is obtainable as in (5.5.11), each $x_{k\mathbf{pt}}(\mathbf{i})$ is a $\mathbf{R}_k\mathbf{T}_k$-fold polyphase component (with proper shifts) of the original subband signal $x_k(\mathbf{m})$. Similarly, the new analysis filters $H'_{k\mathbf{pt}}(\mathbf{z})$ and the synthesis filters $F'_{k\mathbf{pt}}(\mathbf{z})$ are the $\mathbf{P}_k$-fold polyphase components (with proper shifts) of $H_k(\mathbf{z})$ and $F_k(\mathbf{z})$, respectively. The corresponding new $\phi'_{k\mathbf{pti}}(\mathbf{n})$ and $\eta'_{k\mathbf{pti}}(\mathbf{n})$ are $h'_{k\mathbf{pt}}(\mathbf{L}\mathbf{i} - \mathbf{n})$ and $f'_{k\mathbf{pt}}(\mathbf{n} - \mathbf{L}\mathbf{i})$, respectively. From (5.5.10) and (5.5.13), we see that these are indeed the $\phi_{k\mathbf{m}}(\mathbf{n})$ and $\eta_{k\mathbf{m}}(\mathbf{n})$ of the original rational filter bank. In other words, $\{\phi_{k\mathbf{m}}(\mathbf{n})\} = \{\phi'_{k\mathbf{pti}}(\mathbf{n})\}$ and $\{\eta_{k\mathbf{m}}(\mathbf{n})\} = \{\eta'_{k\mathbf{pti}}(\mathbf{n})\}$. Counting the number of channels in this extended uniform filter bank, we get

$$\sum_{k=0}^{M-1} J(\mathbf{P}_k)J(\mathbf{T}_k) = \sum_{k=0}^{M-1} J(\mathbf{P}_k)\frac{J(\mathbf{L})}{J(\mathbf{S}_k)} = \sum_{k=0}^{M-1} J(\mathbf{P}_k)\frac{J(\mathbf{L})}{J(\mathbf{Q}_k)} = J(\mathbf{L}), \tag{5.5.15}$$

so the resulting uniform filter bank is also maximally decimated. It is also clear that the resulting uniform system achieves PR if and only if the original nonuniform system achieves PR.

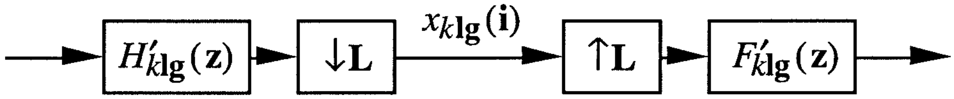

Figure 5.5-3 One branch of an MD uniformly decimated filter bank converted from a nonuniform filter bank.

Remark: This approach of converting nonuniform filter banks places in evidence the resulting uniform filter bank, the corresponding new $\phi'_{k\mathbf{pti}}(\mathbf{n})$ and $\eta'_{k\mathbf{pti}}(\mathbf{n})$, and the expressions for the corresponding subband signals as well.

For the uniform case, we have already shown that $\eta'_{k\mathbf{pti}}(\mathbf{n})$ are linearly independent if PR is possible. Because $\{\eta_{k\mathbf{m}}(\mathbf{n})\}$ and $\{\eta'_{k\mathbf{pti}}(\mathbf{n})\}$ are identical sets, $\eta_{k\mathbf{m}}(\mathbf{n})$ of the nonuniform rational filter bank are also linearly independent.

5.6. MULTIDIMENSIONAL SUBBAND CONVOLUTION THEOREM

For the 1D case, it has been shown that, under some conditions, the convolution of two signals can be obtained by convolving corresponding subband signals and adding these up [Vaidyanathan, 1993b]. This result, which is called the subband convolution theorem, holds for both orthonormal filter banks and biorthonormal filter banks. When signals are to be quantized, subband convolution provides better performance (less quantization error) than direct convolution. We will show that the same result can be obtained by starting from the generalized Parseval's relation in vector space notations. We can therefore extend the subband convolution theorem to the most general filter banks, namely, MD nonuniform filter banks with rational decimation matrices.

Suppose we want to compute the convolution of two MD signals $x(\mathbf{n})$ and $g^*(-\mathbf{n})$,

$$w(\mathbf{k}) = x(\mathbf{k}) * g^*(-\mathbf{k}) \triangleq \sum_{\mathbf{n}\in\mathcal{N}} x(\mathbf{n})g^*(\mathbf{n}-\mathbf{k}). \tag{5.6.1}$$

This is also called the deterministic cross correlation between $x(\mathbf{n})$ and $g(\mathbf{n})$. Instead of directly computing the convolution, we shall feed $x(\mathbf{n})$ and $g(\mathbf{n})$ into a PR filter bank where the synthesis

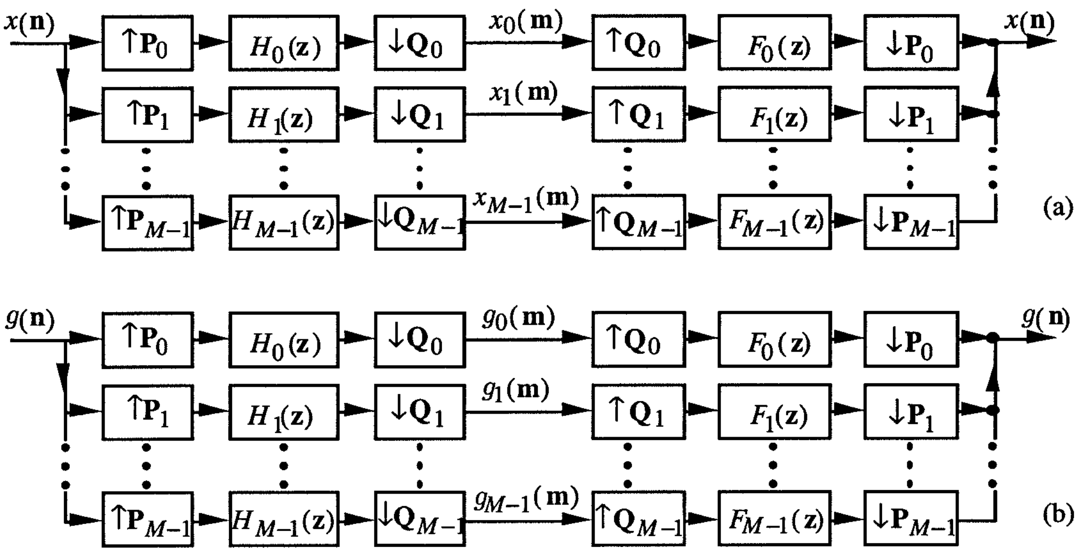

Figure 5.6-1 MD PR rational filter bank, (a) with input $x(\mathbf{n})$, and (b) with input $g(\mathbf{n})$.

filters are orthonormal, i.e., (5.3.15) is satisfied. This is shown in Fig. 5.6-1(a) and Fig. 5.6-1(b), where $x_k(\mathbf{m})$ and $g_k(\mathbf{m})$ denote the corresponding subband signals. Using the same correspondence between vector space and filter banks as mentioned in Section 5.3, we can apply Corollary 5.4.1 to obtain

$$w(\mathbf{0}) = \sum_{\mathbf{n}\in\mathcal{N}} x(\mathbf{n})g^*(\mathbf{n}) = \sum_{k=0}^{M-1} \sum_{\mathbf{m}\in\mathcal{N}} x_k(\mathbf{m})g_k^*(\mathbf{m}). \tag{5.6.2}$$

In other words, the inner product of $x(\mathbf{n})$ and $g(\mathbf{n})$ can be obtained by computing the inner product of each pair of $x_k(\mathbf{m})$ and $g(\mathbf{m})$, and adding the results.

Energy conservation and orthonormality: If we let $g(\mathbf{n}) = x(\mathbf{n})$ in (5.6.2), we get the energy conservation equation

$$\sum_{\mathbf{n}\in\mathcal{N}} |x(\mathbf{n})|^2 = \sum_{k=0}^{M-1} \sum_{\mathbf{m}\in\mathcal{N}} |x_k(\mathbf{m})|^2. \tag{5.6.3}$$

Furthermore, using Corollary 5.4.2, we can show that a PR filter bank is indeed an orthonormal filter bank if and only if the energy of any input signal is preserved in the subband signals.

We proceed to relate the inner product in (5.6.2) to convolution. Equation (5.6.2) gives only one sample of the convolution, i.e., $w(\mathbf{0})$. We can obtain $w(\mathbf{k})$ for another value of $\mathbf{k}$ by shifting the input in Fig. 5.6-1(b) by $\mathbf{k}$. Let us consider the case of uniform filter banks first. For this case, all $\mathbf{P}_k$ are identity matrices and all $\mathbf{Q}_k$ are equal to $\mathbf{L}$, as shown in Fig. 5.6-2(a) and Fig. 5.6-2(b). Due to maximal decimation, the decimation ratio $J(\mathbf{L})$ is equal to the number of channels. Let us

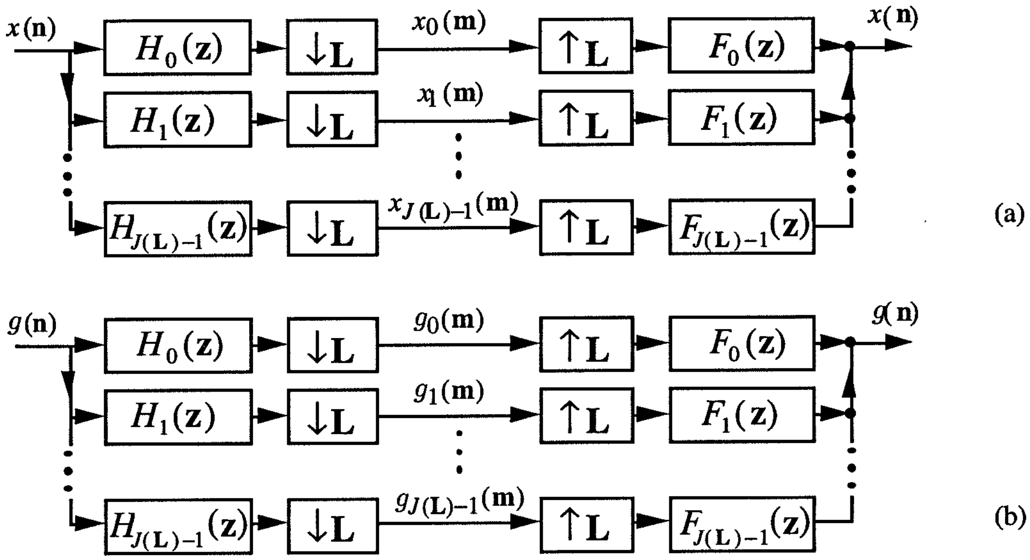

Figure 5.6-2 MD PR uniform filter bank, (a) with input $x(\mathbf{n})$, and (b) with input $g(\mathbf{n})$.

conceptually shift $g(\mathbf{n})$ in Fig. 5.6-2(b) by $\mathbf{Lk}$. That is, we let $g'(\mathbf{n}) = g(\mathbf{n} - \mathbf{Lk})$ and let $g'_k(\mathbf{m})$ denote the corresponding subband signals. It can be verified that $g'_k(\mathbf{m}) = g_k(\mathbf{m} - \mathbf{k})$. So,

$$\begin{aligned} w(\mathbf{Lk}) &= \sum_{\mathbf{n}\in\mathcal{N}} x(\mathbf{n})g^*(\mathbf{n} - \mathbf{Lk}) \\ &= \sum_{\mathbf{n}\in\mathcal{N}} x(\mathbf{n})g'^*(\mathbf{n}) \\ &= \sum_{k=0}^{J(\mathbf{L})-1} \sum_{\mathbf{m}\in\mathcal{N}} x_k(\mathbf{m})g'^*_k(\mathbf{m}) \\ &= \sum_{k=0}^{J(\mathbf{L})-1} \sum_{\mathbf{m}\in\mathcal{N}} x_k(\mathbf{m})g^*_k(\mathbf{m} - \mathbf{k}). \end{aligned} \tag{5.6.4}$$

This can be written as

$$\underbrace{[x(\mathbf{k}) * g^*(-\mathbf{k})]}_{w(\mathbf{k})}{}_{\downarrow\mathbf{L}} = \sum_{k=0}^{J(\mathbf{L})-1} [x_k(\mathbf{k}) * g^*_k(-\mathbf{k})] \tag{5.6.5}$$

where $[\cdot]_{\downarrow\mathbf{L}}$ denotes the result of $\mathbf{L}$-fold decimation. In other words, the $\mathbf{L}$-fold decimated version of $w(\mathbf{k})$ is obtainable by adding up the convolution of corresponding subband signals. This is the MD subband convolution theorem for the case of uniform filter banks.

Note that (5.6.5) only gives the $\mathbf{L}$-fold decimated version of $w(\mathbf{k})$, i.e., the $\mathbf{0}$th polyphase components of $w(\mathbf{k})$. To obtain other polyphase components of $w(\mathbf{k})$, we can shift the input in Fig. 5.6-2(b) by $\mathbf{j}$, where $\mathbf{j} \in \mathcal{N}(\mathbf{L})$, and repeat the computation in (5.6.5) again. More specifically, letting $g^{(\mathbf{j})}(\mathbf{n}) = g(\mathbf{n} - \mathbf{j})$ and $g^{(\mathbf{j})}_k(\mathbf{m})$ denote the corresponding subband signals, we can obtain the jth polyphase components of $w(\mathbf{k})$ by

$$\begin{aligned} w(\mathbf{Lk}+\mathbf{j}) &= \sum_{\mathbf{n}\in\mathcal{N}} x(\mathbf{n})g^*(\mathbf{n}-\mathbf{Lk}-\mathbf{j}) \\ &= \sum_{\mathbf{n}\in\mathcal{N}} x(\mathbf{n})[g^{(\mathbf{j})}(\mathbf{n}-\mathbf{Lk})]^* \\ &= \sum_{k=0}^{J(\mathbf{L})-1} \sum_{\mathbf{m}\in\mathcal{N}} x_k(\mathbf{m})[g^{(\mathbf{j})}(\mathbf{m}-\mathbf{k})]^*, \end{aligned} \tag{5.6.6}$$

or

$$w(\mathbf{Lk}+\mathbf{j}) = [x(\mathbf{k}) * g^{(\mathbf{j})*}(-\mathbf{k})]_{\downarrow\mathbf{L}} = \sum_{k=0}^{M-1} x_k(\mathbf{k}) * [g_k^{(\mathbf{j})}(-\mathbf{k})]^*. \tag{5.6.7}$$

Therefore, the complete convolution $w(\mathbf{k})$ is obtainable by recombining these $w(\mathbf{Lk}+\mathbf{j})$, where $\mathbf{j} \in \mathcal{N}(\mathbf{L})$.

We can now extend the MD subband convolution theorem to the nonuniform case. Reconsider the MD nonuniform filter bank in Fig. 5.6-1. It has been shown in Section 5.5 that this nonuniform filter bank can be converted to an equivalent uniform filter bank. Using the notations in Section 5.5, we modify (5.6.4) to get the following equation for resulting uniform filter bank:

$$w(\mathbf{Lk}) = \sum_{k=0}^{M-1} \sum_{\mathbf{p}\in\mathcal{N}(\mathbf{P}_k)} \sum_{\mathbf{t}\in\mathcal{N}(\mathbf{T}_k)} \sum_{\mathbf{i}\in\mathcal{N}} x_{k\mathbf{pt}}(\mathbf{i})g_{k\mathbf{pt}}^*(\mathbf{i}-\mathbf{k}). \tag{5.6.8}$$

Rewriting the triple summation over $\mathbf{p}$, $\mathbf{t}$, and $\mathbf{i}$ into one single summation over $\mathbf{m}$ using (5.5.11), we get

$$w(\mathbf{Lk}) = \sum_{k=0}^{M-1} \sum_{\mathbf{m}\in\mathcal{N}} x_k(\mathbf{m})g_k^*(\mathbf{m}-\mathbf{R}_k\mathbf{T}_k\mathbf{k}), \tag{5.6.9}$$

which is the same as

$$[x(\mathbf{k}) * g^*(-\mathbf{k})]_{\downarrow\mathbf{L}} = \sum_{k=0}^{M-1} [x_k(\mathbf{k}) * g_k^*(-\mathbf{k})]_{\downarrow\mathbf{R}_k\mathbf{T}_k}. \tag{5.6.10}$$

Again, to obtain the complete $w(\mathbf{k})$, we can shift $g(\mathbf{n})$ by $\mathbf{j}$, where $\mathbf{j} \in \mathcal{N}(\mathbf{L})$, to compute the $\mathbf{j}$th polyphase component and then recombine these results.

Summarizing, we have derived the following theorem using vector space notations:

Theorem 5.8. Subband convolution theorem (orthonormal case): Suppose we have an MD nonuniform rational filter bank which achieves PR and the synthesis filters are orthonormal. The $\mathbf{L}$-fold decimated version of the convolution of $x(\mathbf{k})$ and $g^*(-\mathbf{k})$ can be obtained by convolving corresponding subband signals, decimating each convolution by $\mathbf{R}_k\mathbf{T}_k$, and adding up the results. In other words,

$$[x(\mathbf{k}) * g^*(-\mathbf{k})]_{\downarrow\mathbf{L}} = \sum_{k=0}^{M-1} [x_k(\mathbf{k}) * g_k^*(-\mathbf{k})]_{\downarrow\mathbf{R}_k\mathbf{T}_k}. \tag{5.6.11}$$

◇

Generalization to the Biorthonormal Case

The MD subband convolution theorem can also be extended to the case of biorthonormal filter banks. Starting from Theorem 5.4, the generalized Parseval's relation for the biorthonormal case, we can derive the following:

Theorem 5.9. Subband convolution theorem (biorthonormal case): Suppose we have an MD nonuniform rational filter bank which achieves PR. In other words, the analysis and synthesis filters are biorthonormal. We feed $x(\mathbf{n})$ into to this filter bank and let $x_k(\mathbf{m})$ denote the resulting subband signals. Interchanging the analysis and the synthesis filters, we get another PR filter bank (Corollary 5.6.1). We feed $y(\mathbf{n})$ into to this new filter bank and let $y_k(\mathbf{m})$ denote the resulting subband signals, as shown in Fig. 5.6-3. Let $w(\mathbf{k})$ denote the convolution of $x(\mathbf{k})$ and $y(\mathbf{k})$. The $\mathbf{L}$-fold decimated version of $w(\mathbf{k})$ can be obtained by convolving corresponding subband signals, decimating each convolution by $\mathbf{R}_k\mathbf{T}_k$, and adding up the results. In other words,

$$\underbrace{[x(\mathbf{k}) * y(\mathbf{k})]}_{w(\mathbf{k})}{}_{\downarrow\mathbf{L}} = \sum_{k=0}^{M-1} [x_k(\mathbf{k}) * y_k(\mathbf{k})]_{\downarrow\mathbf{R}_k\mathbf{T}_k}. \tag{5.6.12}$$

◇

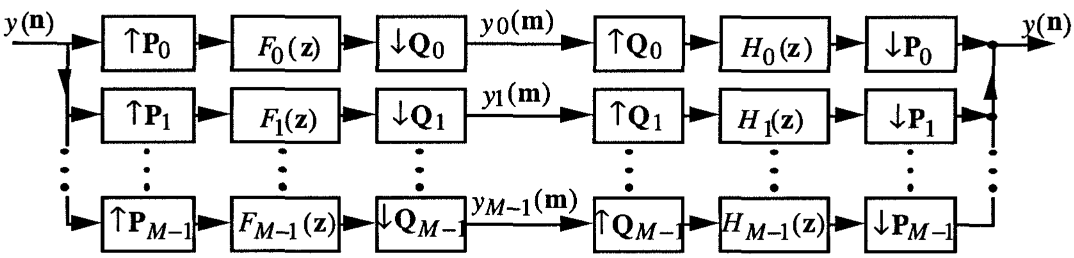

Figure 5.6-3 MD PR rational filter bank, with interchanged analysis and synthesis filters, and with input $y(\mathbf{n})$.

Remarks:

1. The other polyphase components of $w(\mathbf{k})$ can be obtained by advancing $y(\mathbf{n})$ by $\mathbf{j}$, say $y^{(\mathbf{j})}(\mathbf{n}) = y(\mathbf{n}+\mathbf{j})$, and repeating (5.6.12) for the corresponding subband signals $y_k^{(\mathbf{j})}(\mathbf{m})$.

2. Note that the convolution, rather than the deterministic cross correlation, of $x(\mathbf{n})$ and $y(\mathbf{n})$ is obtained in this theorem.

3. For the case that the synthesis filters are indeed orthonormal, we know $f_k(\mathbf{n}) = h_k^*(-\mathbf{n})$ (Theorem 5.5). Therefore, according to the above theorem, $y(\mathbf{n})$ should be analyzed using

$h_k^*(-\mathbf{n})$. Letting $g(\mathbf{n}) = y^*(-\mathbf{n})$, we see this is same as analyzing $g(\mathbf{n})$ using $h_k(\mathbf{n})$. Now, $x(\mathbf{k}) * g^*(-\mathbf{k}) = x(\mathbf{k}) * y(\mathbf{k})$, and Theorem 5.8 is hence obtained as a special case of Theorem 5.9.

The proof of Theorem 5.9 is similar to the orthonormal case, so it is omitted here. Instead, we will give a graphical proof as follows. This will also give an implementation of the subband convolution. First, let us treat $y(\mathbf{n})$ as an MD filter. As shown in Fig. 5.6-4(a), the convolution of $x(\mathbf{n})$ and $y(\mathbf{n})$ can be obtained by passing $x(\mathbf{n})$ through a PR filter bank and an MD filter $Y(\mathbf{z})$, where $Y(\mathbf{z})$ is the $\mathbf{z}$-transform of $y(\mathbf{n})$. For simplicity, only one channel in each filter bank is shown in this and the following figures. Using Noble identity, we can move $Y(\mathbf{z})$ to the left of $\mathbf{P}_k$-fold decimators to obtain Fig. 5.6-4(b). With $y(\mathbf{n})$ treated as an MD signal again, Fig. 5.6-4(b) can be redrawn as Fig. 5.6-4(c), which gives an implementation of MD subband convolution.

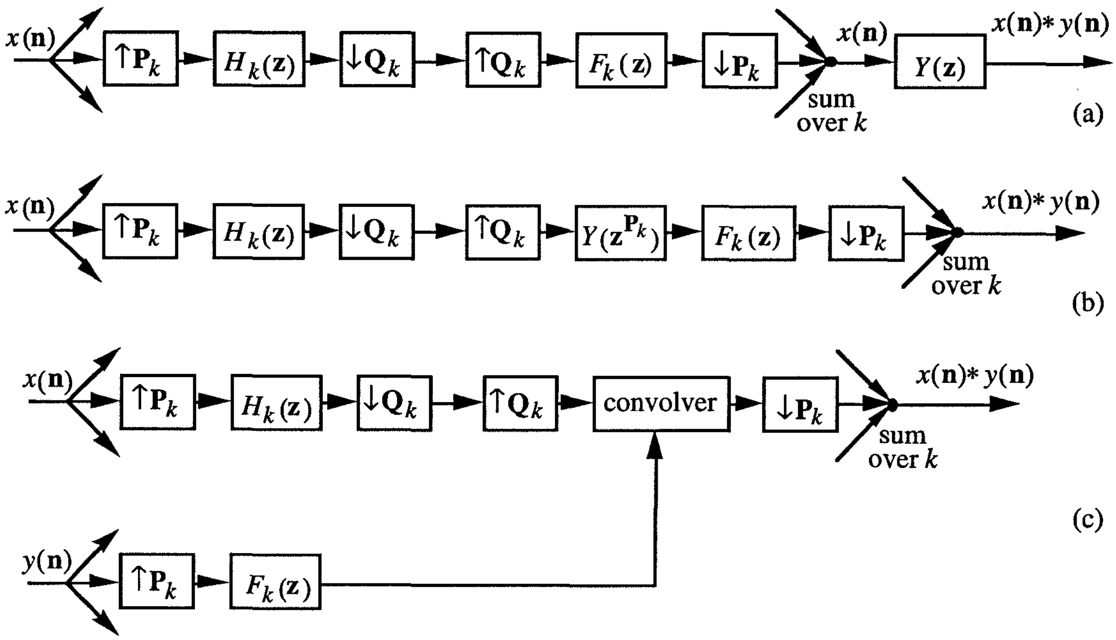

Figure 5.6-4 MD subband convolution of $x(\mathbf{n})$ and $y(\mathbf{n})$.

To prove the subband convolution theorem, we cascade the system in Fig. 5.6-4 by an $\mathbf{L}$-fold decimator to obtain $[x(\mathbf{n}) * y(\mathbf{n})]_{\downarrow\mathbf{L}}$. Inserting a so-called delay-chain system [Chen and Vaidyanathan, 1993a] after each filter $F_k(\mathbf{z})$, we obtain Fig. 5.6-5(a), where the notation $\circledast$ stands for a convolver. The delay-chain system has $J(\mathbf{Q}_k)$ branches and $\mathbf{q}_i$ are the elements in $\mathcal{N}(\mathbf{Q}_k)$. It can be verified that a delay-chain system is a perfect reconstruction system so that Fig. 5.6-5(a) is indeed equivalent to Fig. 5.6-4(c) followed by an $\mathbf{L}$-fold decimator. Moving convolvers to the left, we can redraw Fig. 5.6-5(a) to get Fig. 5.6-5(b). Moving the $\mathbf{L}$-fold decimator to the left and combining it with the

$\mathbf{P}_k$-fold decimator, we obtain Fig. 5.6-5(c), because $\mathbf{P}_k\mathbf{L} = \mathbf{P}_k\mathbf{S}_k\mathbf{T}_k = \mathbf{Q}_k\mathbf{R}_k\mathbf{T}_k$. It can be shown that a filter $h(\mathbf{n})$ preceded by a $\mathbf{Q}_k$-fold expander and followed by a $\mathbf{Q}_k$-fold decimator is equivalent to a filter with impulse response $h(\mathbf{Q}_k\mathbf{n})$. Therefore, each $\mathbf{z}^{\mathbf{q}_i}$ preceded by a $\mathbf{Q}_k$-fold expander and followed by a $\mathbf{Q}_k$-fold decimator has transfer function zero unless $\mathbf{q}_i = \mathbf{0}$. Hence, we can remove $J(\mathbf{Q}_k) - 1$ branches in each channel and obtain Fig. 5.6-5(d). This indeed gives the result stated in Theorem 5.9.

Coding Gain of Subband Convolution (Biorthonormal Case)

The main advantage of subband convolution is that we can quantize the subband signals according to the signal variance in each subband and other perceptual considerations, as in the traditional subband coding [Jayant and Noll, 1984]. For a fixed bit rate, the result of subband convolution is more accurate than that of direct convolution, and we hence obtain a *coding gain* over direct convolution. To analyze the coding gain for MD subband convolution, we shall make the following assumptions:

1. We assume $x(\mathbf{n})$ is an MD zero-mean wide-sense-stationary (WSS) random process and $y(\mathbf{n})$ is an MD deterministic signal.
2. Given that $x(\mathbf{n})$ is WSS, $x_k(\mathbf{m})$ is in general not WSS, but *cyclo-wide-sense-stationary* with period $\mathbf{Q}_k^{-1}\text{lcrm}(\mathbf{P}_k, \mathbf{Q}_k)$ [Chen and Vaidyanathan, 1993a]. However, we shall assume that $x_k(\mathbf{m})$ are all zero-mean WSS with variance $\sigma_{x_k}^2$. It can be shown that this assumption is true if $\mathbf{P}_k$ are unimodular (i.e., with determinant ± 1) or all the analysis filters $H_k(\mathbf{z})$ are ideal filters. The reason is similar to that of the 1D case [Sathe and Vaidyanathan, 1993]. For the case that filters are not ideal but having large stopband attenuation, $x_k(\mathbf{m})$ are *approximately* WSS.
3. Let $q_k(\mathbf{m})$ denote the quantization error for $x_k(\mathbf{m})$. That is, $x_k(\mathbf{m})$ is quantized to $x_k(\mathbf{m}) + q_k(\mathbf{m})$. Assume $q_k(\mathbf{m})$ are zero-mean WSS with variance $\sigma_{q_k}^2$. Assume that all $q_k(\mathbf{m})$ are white and uncorrelated, and that all $q_k(\mathbf{m})$ are uncorrelated to $x_k(\mathbf{m})$. With b_k denoting the number of bits assigned to the quantizer for $x_k(\mathbf{m})$, $\sigma_{q_k}^2$ is related to $\sigma_{x_k}^2$ as

$$\sigma_{q_k}^2 = c\sigma_{x_k}^2 2^{-2b_k}, \tag{5.6.13}$$

for some constant c [Jayant and Noll, 1984], [Vaidyanathan, 1993a, Appendix C].

Under these assumptions, we can compute the error in $w(\mathbf{Lk})$ due to quantization

$$q(\mathbf{k}) = \sum_{k=0}^{M-1} [q_k(\mathbf{k}) * y_k(\mathbf{k})]_{\downarrow \mathbf{R}_k\mathbf{T}_k}. \tag{5.6.14}$$

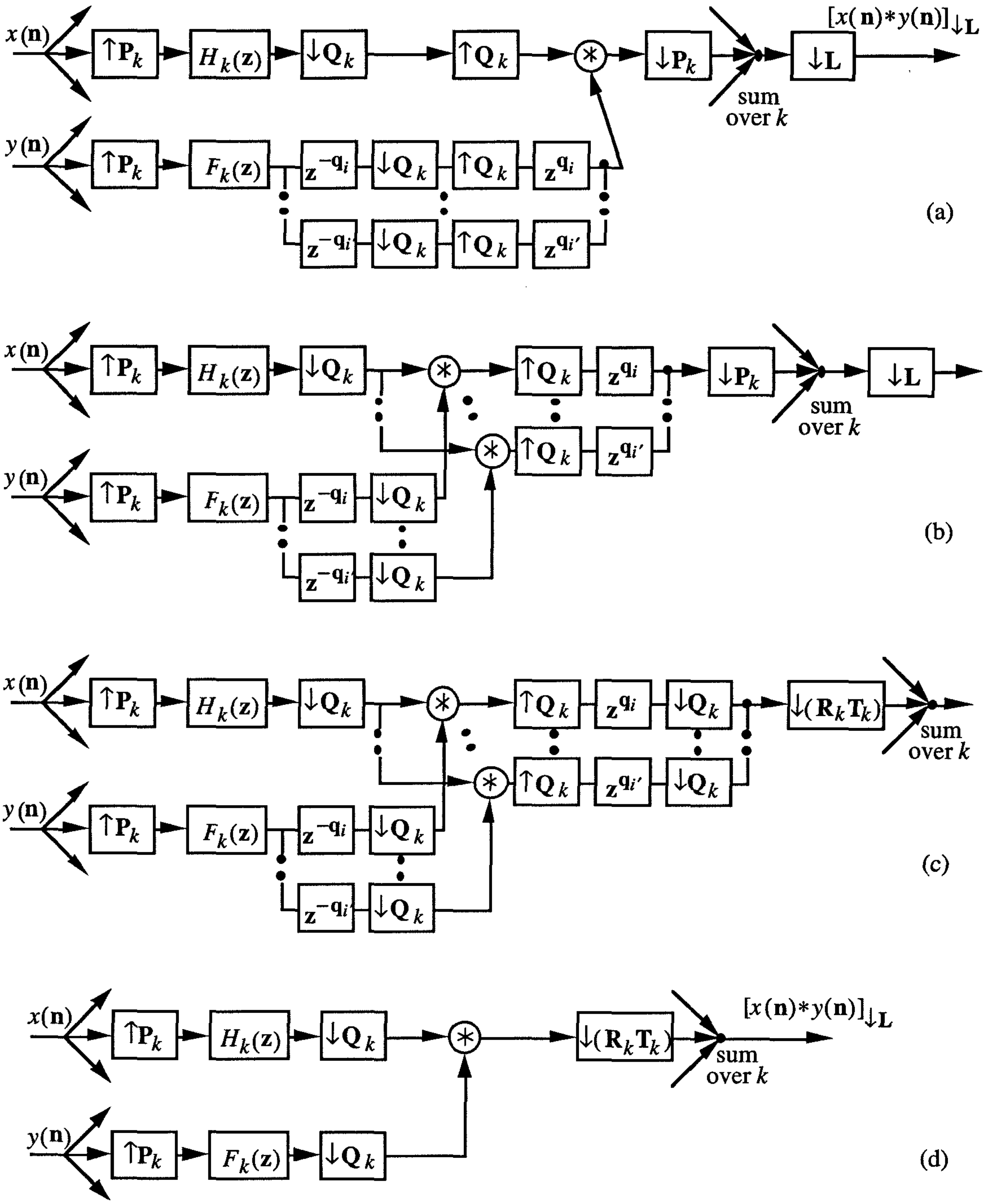

Figure 5.6-5 Obtaining the **L**-fold decimated version of $x(\mathbf{n}) * y(\mathbf{n})$.

We obtain that the variance of $q_k(\mathbf{k}) * y_k(\mathbf{k})$ is $\sigma_{q_k}^2 \sum_{\mathbf{i}\in\mathcal{N}} |y_k(\mathbf{i})|^2$ and the variance of $q(\mathbf{k})$ is

$$\sigma_{q(\mathbf{k})}^2 = \sum_{k=0}^{M-1} \sigma_{q_k}^2 \sum_{\mathbf{i}\in\mathcal{N}} |y_k(\mathbf{i})|^2 = c \sum_{k=0}^{M-1} 2^{-2b_k} \sigma_{x_k}^2 \sum_{\mathbf{i}\in\mathcal{N}} |y_k(\mathbf{i})|^2. \qquad (5.6.15)$$

Note that the $\mathbf{R}_k\mathbf{T}_k$-fold decimation does not change the variance. To compute the whole $w(\mathbf{k})$, we need to advance $y(\mathbf{n})$ by $\mathbf{j}$ and repeat (5.6.12) for $J(\mathbf{L})$ times. So, we need to average (5.6.15) over all $\mathbf{j} \in \mathcal{N}(\mathbf{L})$ to obtain the variance of overall quantization error

$$\sigma_q^2 = \frac{c}{J(\mathbf{L})} \sum_{k=0}^{M-1} 2^{-2b_k} \sigma_{x_k}^2 \sum_{\mathbf{j}\in\mathcal{N}(\mathbf{L})} \sum_{\mathbf{i}\in\mathcal{N}} |y_k^{(\mathbf{j})}(\mathbf{i})|^2. \tag{5.6.16}$$

Define

$$\alpha_k^2 \triangleq \frac{M}{J(\mathbf{L})} \sum_{\mathbf{j}\in\mathcal{N}(\mathbf{L})} \sum_{\mathbf{i}\in\mathcal{N}} |y_k^{(\mathbf{j})}(\mathbf{i})|^2, \tag{5.6.17}$$

which can be shown to be proportional to the energy of $y_k(\mathbf{m})$. We can rewrite (5.6.16) as

$$\sigma_q^2 = \frac{c}{M} \sum_{k=0}^{M-1} 2^{-2b_k} \sigma_{x_k}^2 \alpha_k^2. \tag{5.6.18}$$

Let b denote the overall bit rate, so

$$b = \sum_{k=0}^{M-1} \frac{J(\mathbf{P}_k)}{J(\mathbf{Q}_k)} b_k. \tag{5.6.19}$$

Under the constraint of fixed b, it can be shown that σ_q^2 is minimized when

$$b_k = b + 0.5 \log_2 \left(\frac{J(\mathbf{Q}_k)}{J(\mathbf{P}_k)} \sigma_{x_k}^2 \alpha_k^2 \right) - 0.5 \sum_{i=0}^{M-1} \frac{\log_2 \left(\frac{J(\mathbf{Q}_i)}{J(\mathbf{P}_i)} \sigma_{x_i}^2 \alpha_i^2 \right)}{J(\mathbf{Q}_i)/J(\mathbf{P}_i)}. \tag{5.6.20}$$

The proof of this uses the Lagrange multiplier method and is similar to that in [Vaidyanathan, 1993b]. Substituting (5.6.20) into (5.6.13), we can see that σ_q^2 is minimized when $\sigma_{q_k}^2$ is proportional to $J(\mathbf{P}_k)/\alpha_k^2 J(\mathbf{Q}_k)$. The minimized error variance under the above *optimal bit allocation* is

$$\sigma_{q,\text{opt}}^2 = \frac{c2^{-2b}}{M} \prod_{k=0}^{M-1} \left(\frac{J(\mathbf{Q}_k)}{J(\mathbf{P}_k)} \sigma_{x_k}^2 \alpha_k^2 \right)^{J(\mathbf{P}_k)/J(\mathbf{Q}_k)}. \tag{5.6.21}$$

Comparing this with direct convolution, where the error variance is

$$\sigma_{q,\text{direct}}^2 = c2^{-2b} \sigma_x^2 \sum_{\mathbf{i}\in\mathcal{N}} |y(\mathbf{i})|^2, \tag{5.6.22}$$

we see that the coding gain of subband convolution over direct convolution is

$$G_{\text{opt}} = \frac{\sigma_{q,\text{direct}}^2}{\sigma_{q,\text{opt}}^2} = \frac{\sigma_x^2 \sum_{\mathbf{i}\in\mathcal{N}} |y(\mathbf{i})|^2}{\frac{1}{M} \prod_{k=0}^{M-1} \left(\frac{J(\mathbf{Q}_k)}{J(\mathbf{P}_k)} \sigma_{x_k}^2 \alpha_k^2 \right)^{J(\mathbf{P}_k)/J(\mathbf{Q}_k)}}. \tag{5.6.23}$$

Remarks:

1. For the orthonormal case, it can be shown that the coding obtained above is always greater or equal to unity. It is unity if and only if $\sigma_{x_k}^2$ and $\alpha_k^2 J(\mathbf{Q}_k)/J(\mathbf{P}_k)$ are both independent of k.
2. For the orthonormal case, if we let $y(\mathbf{n}) = \delta(\mathbf{n})$, the above analysis can be used to get the optimal coding gain for MD subband coding, i.e., the coding gain of quantizing subband signals

$x_k(\mathbf{m})$ over directly quantizing $x(\mathbf{n})$ [Soman and Vaidyanathan, 1993]. When $y(\mathbf{n}) = \delta(\mathbf{n})$, it can be shown that $\alpha_k^2 = MJ(\mathbf{P}_k)/J(\mathbf{Q}_k)$. Therefore, the optimal bit allocation is given by

$$b_k = b + 0.5\log_2\left(\sigma_{x_k}^2\right) - 0.5\sum_{i=0}^{M-1}\frac{\log_2\sigma_{x_i}^2}{J(\mathbf{Q}_i)/J(\mathbf{P}_i)}. \tag{5.6.24}$$

Substituting (5.6.24) into (5.6.13), we see that all $\sigma_{q_k}^2$ are equal. For the case of fixed-point quantization, this implies that the right most bit (least significant bit) of all channels should be aligned [Vaidyanathan, 1993a, Appendix C], [Soman and Vaidyanathan, 1993]. The minimized error variance is

$$\sigma_{q,\mathrm{opt}}^2 = c2^{-2b}\prod_{k=0}^{M-1}\left(\sigma_{x_k}^2\right)^{J(\mathbf{P}_k)/J(\mathbf{Q}_k)}. \tag{5.6.25}$$

The coding gain over direct quantization is

$$G_{\mathrm{opt}} = \frac{\sigma_x^2}{\prod_{k=0}^{M-1}\left(\sigma_{x_k}^2\right)^{J(\mathbf{P}_k)/J(\mathbf{Q}_k)}}. \tag{5.6.26}$$

It can be shown that $G_{\mathrm{opt}} \geq 1$ and the equality holds if and only if $\sigma_{x_k}^2$ is independent of k.

Computation Complexity

Assume for simplicity that both $x(\mathbf{n})$ and $y(\mathbf{n})$ have finite impulse response (FIR) and have N samples each. Direct convolution of $x(\mathbf{n})$ and $y(\mathbf{n})$ requires N^2 multiplications. Assume that N is much larger than the number of multipliers required to implement the filter bank, so that the computation complexity of analysis filter banks in Fig. 5.6-1 and Fig. 5.6-3 can be neglected. Since each subband signal $x_k(\mathbf{m})$ (or $y_k(\mathbf{m})$) has approximately $NJ(\mathbf{P}_k)/J(\mathbf{Q}_k)$ samples, each subband convolution seems to require nearly $[NJ(\mathbf{P}_k)/J(\mathbf{Q}_k)]^2$ multiplications. However, note that only the $\mathbf{R}_k\mathbf{T}_k$-fold decimated version of each subband convolution is computed, so only $[NJ(\mathbf{P}_k)/J(\mathbf{Q}_k)]^2/J(\mathbf{R}_k\mathbf{T}_k)$ multiplications are required. This is repeated for $J(\mathbf{L})$ times to obtain the whole convolution. Therefore, the total number of required multiplications is

$$J(\mathbf{L})\sum_{k=0}^{M-1}\frac{[NJ(\mathbf{P}_k)/J(\mathbf{Q}_k)]^2}{J(\mathbf{R}_k\mathbf{T}_k)} = N^2\sum_{k=0}^{M-1}\frac{J(\mathbf{P}_k)^2J(\mathbf{L})}{J(\mathbf{Q}_k)^2J(\mathbf{R}_k\mathbf{T}_k)} = N^2, \tag{5.6.27}$$

since $\mathbf{L} = \mathbf{S}_k\mathbf{T}_k$ and $\mathbf{P}_k\mathbf{S}_k = \mathbf{Q}_k\mathbf{R}_k$. In summary, when the computation in analysis bank implementation is negligible, the subband convolution has the same complexity as direct convolution.

5.7. THE WAVELET TRANSFORM

The vector space framework is so general that it also covers the so-called discrete wavelet transform [Daubechies, 1992], [Akansu and Haddad, 1992], [Chui, 1992], [Vaidyanathan, 1993a, Chapter 11]. In this section, we will illustrate this only for the 1D case, since the MD case can be obtained similarly. For a continuous-time signal $x(t)$, its discrete wavelet transform (DWT) is defined as

$$x_{\mathrm{DWT}}(k,n) = \int_{-\infty}^{\infty} x(t) \underbrace{a^{-k/2} h(nT - a^{-k}t)}_{\phi^*_{k,n}(t)} \, dt. \tag{5.7.1}$$

In the above expression, k and n are integer indices, and a and T are some real constant. The case $a = 2$ is often used. The DWT is therefore a mapping of a continuous-time signal $x(t)$ into a two-dimensional sequence $x_{\mathrm{DWT}}(k,n)$. The quantities $x_{\mathrm{DWT}}(k,n)$ are also called the wavelet coefficients. Also note that $\phi^*_{k,n}(t)$ are all dilated and shifted versions of $h^*(-t)$.

Suppose we want to reconstruct the signal $x(t)$ from its wavelet coefficients. We can use the following expression

$$\widehat{x}(t) = \sum_k \sum_n x_{\mathrm{DWT}}(k,n) \underbrace{a^{-k/2} f(a^{-k}t - nT)}_{\eta_{k,n}(t)}. \tag{5.7.2}$$

If $\widehat{x}(t) = x(t)$ for all $x(t)$, we get perfect reconstruction (PR) and the above expression is called the inverse discrete wavelet transform (IDWT). Note that $\eta_{k,n}(t)$ are all dilated and shifted versions of $f(t) = \eta_{0,0}(t)$, which is called the wavelet function, or mother wavelet.

Define the inner product of two continuous-time signals as

$$(x(t), y(t)) \triangleq \int_{-\infty}^{\infty} x(t) y^*(t) dt. \tag{5.7.3}$$

We shall consider only signals with finite energy, i.e., signals in the L^2 space [Luenberger, 1969], so that the above inner product always exists. By using (5.7.3), Equation (5.7.1) can be written in vector space notations as (5.2.1) and Equation (5.7.2) can be written as (5.2.2). In other words, the above DWT analysis/synthesis scheme is in fact a special case of the vector space framework. Assuming that the set $\{\eta_{k,n}(t)\}$ spans the L^2 space and that $\eta_{k,n}(t)$ are linearly independent, the following results can be obtained directly from the discussion of Section 5.2:

1. Any two of the following properties imply the other:

   a) the Hermitian image property $h^*(-t) = f(t)$ (so that $\phi_{k,n}(t) = \eta_{k,n}(t)$ for all k and n),

   b) the orthonormality of $\eta_{k,n}(t)$

$$\int_{-\infty}^{\infty} \eta_{k,n}(t) \eta^*_{k',n'}(t) dt = \delta(k-k')\delta(n-n'), \tag{5.7.4}$$

c) the PR property $\widehat{x}(t) = x(t)$.

2. The PR property is satisfied if and only if

$$\int_{-\infty}^{\infty} \phi_{k,n}(t)\eta^*_{k',n'}(t)dt = \delta(k-k')\delta(n-n'), \tag{5.7.5}$$

which is the biorthonormality property.

3. Suppose there exists a pair of DWT and IDWT, i.e., the PR condition is satisfied. We can interchange $h(t)$ and $f(t)$ in (5.7.1) and (5.7.2) without affecting the PR property.

4. Suppose there exists a pair of DWT and IDWT so that the PR condition is satisfied. We can switch the roles of (5.7.1) and (5.7.2) and obtain a synthesis/analysis transmultiplexing systems. More specifically, given a set of wavelet coefficients $x_{\mathrm{DWT}}(k,n)$, we can synthesize a signal $x(t)$ using (5.7.2). If we analyze such $x(t)$ using (5.7.1), we can recover the original coefficients $x_{\mathrm{DWT}}(k,n)$.

5. When the functions $\eta_{k,n}(t)$ satisfy the orthonormality in (5.7.4), we can compute the inner product of two signals by their wavelet coefficients, i.e.,

$$\int_{-\infty}^{\infty} x(t)g^*(t)dt = \sum_k \sum_n x_{\mathrm{DWT}}(k,n)g^*_{\mathrm{DWT}}(k,n), \tag{5.7.6}$$

which is exactly the Parseval Identity in [Chui, 1992]. The biorthonormal case can be obtained similarly.

6. Letting $x(t) = g(t)$ in (5.7.6), we get the energy conservation equation. Furthermore, the energy is preserved for all $x(t)$ if and only if the orthonormality condition is satisfied.

Wavelet Convolution Theorem

We can also derive the 'wavelet convolution theorem' for the biorthonormal case (with the orthonormal case covered as a special case). Unlike the filter bank case, it is not easy to derive this starting from the Parseval's relation, because we would need to shift $g(t)$ in (5.7.6) *continuously* to obtain the whole convolution. Instead, we will use the graphical derivation as we did in Fig. 5.6-4. First, we let $h_k(t) \triangleq a^{-k/2}h(a^{-k}t)$ and $f_k(t) \triangleq a^{-k/2}f(a^{-k}t)$. We can then rewrite (5.7.1) as

$$x_{\mathrm{DWT}}(k,n) = \int_{-\infty}^{\infty} x(t)h_k(na^kT - t)dt, \tag{5.7.7}$$

and (5.7.2) as

$$x(t) = \sum_k \sum_n x_{\mathrm{DWT}}(k,n)f_k(t - na^kT), \tag{5.7.8}$$

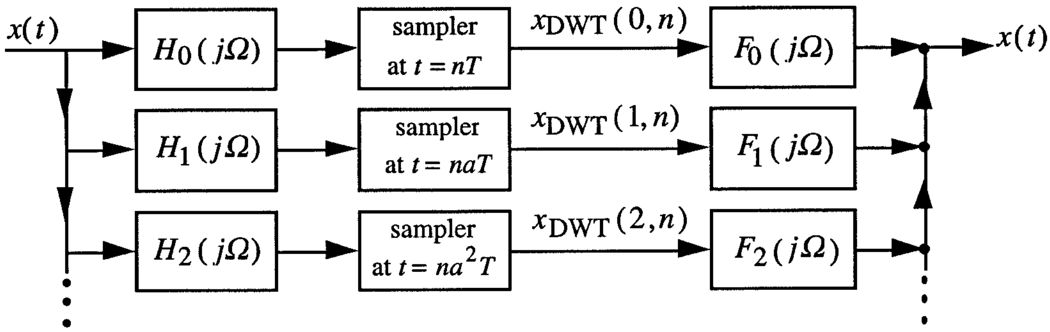

Figure 5.7-1 Filter bank implementation of a DWT/IDWT system with input $x(t)$. The signal $x_{\mathrm{DWT}}(k,n)$ in this figure indicates a continuous-time impulse train.

since $\widehat{x}(t) = x(t)$ for the biorthonormal case. These two equations give the filter bank implementation of a DWT/IDWT system shown in Fig. 5.7-1. In this figure, $H_k(j\Omega)$ and $F_k(j\Omega)$ denote the Fourier transform of $h_k(t)$ and $f_k(t)$, respectively. The sampler in the kth channel samples the input signal at $t = na^kT$ and produces an impulse train at the output. It can be verified that the output is $\sum_n x_{\mathrm{DWT}}(k,n)\delta(t - na^kT)$, where $\delta(t)$ denotes the continuous-time impulse function.

If we want to compute the convolution of two continuous-time signals $x(t)$ and $y(t)$, we can use the system in Fig. 5.7-2(a), where $Y(j\Omega)$ is the Fourier transform of $y(t)$. Note that only one channel in the filter bank of Fig. 5.7-1 is shown. With $Y(j\Omega)$ moved to the left, Fig. 5.7-2(a) can be redrawn as Fig. 5.7-2(b). It can be verified that Fig. 5.7-2(b) is equivalent to Fig. 5.7-2(c), which gives the following theorem:

Theorem 5.10. Wavelet convolution theorem (biorthonormal case): Suppose there exists a pair of DWT and IDWT so that the PR condition (biorthonormality) is satisfied. The convolution of two signals $x(t)$ and $y(t)$ can be computed as

$$x(t) * y(t) \triangleq \int_{-\infty}^{\infty} x(\tau)y(t-\tau)d\tau = \sum_k x_{\mathrm{DWT}}(k,n)y_k(t - na^kT), \tag{5.7.9}$$

where $x_{\mathrm{DWT}}(k,n)$ are the wavelet coefficients of $x(t)$, and $y_k(t)$ is the output of the filter $f_k(t)$ for the input $y(t)$. ◊

5.8. REMARKS AND CONCLUSIONS

Here, we add a remark on the orthonormality defined in (5.3.15) and the biorthonormality in (5.3.18). For the 1D case with all $P_k = 1$, (5.3.15) becomes

$$\sum_{n=-\infty}^{\infty} f_k(n - Q_k m) f_{k'}^*(n - Q_{k'}m') = \delta(k-k')\delta(m-m') \tag{5.8.1}$$

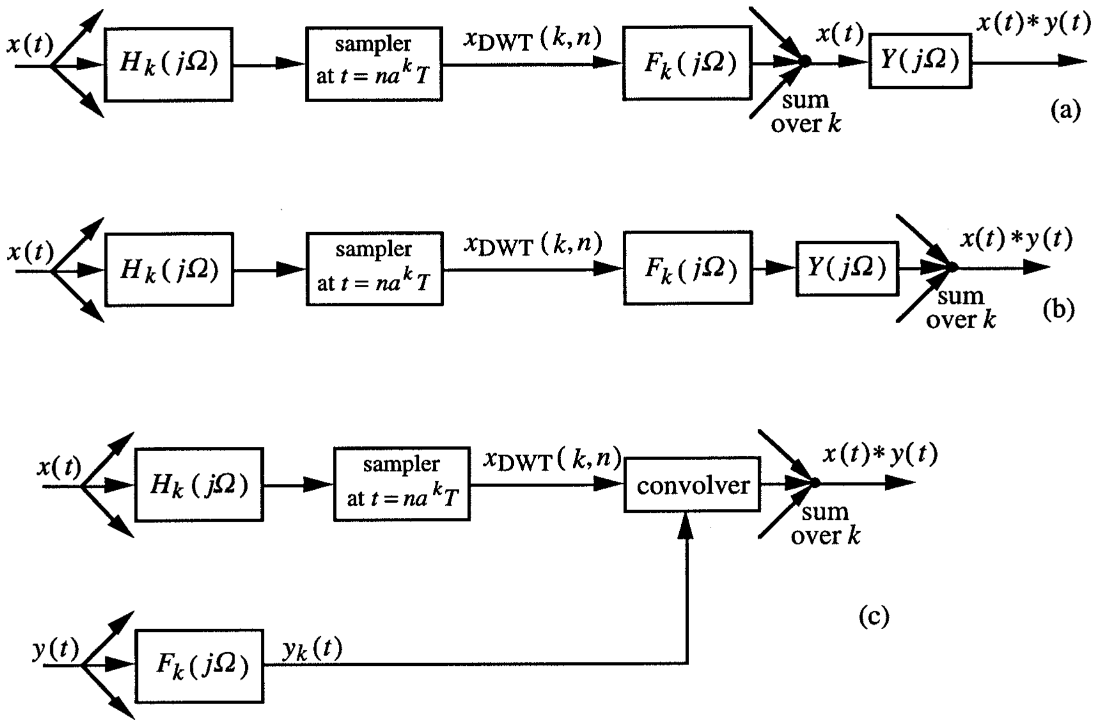

Figure 5.7-2 DWT subband convolution of $x(t)$ and $y(t)$.

for all $k, k' = 0, \ldots, M-1$ and all m and m'. In [Soman and Vaidyanathan, 1992], it has been shown that this condition can be simplified to

$$\sum_{n=-\infty}^{\infty} f_k(n) f_{k'}^*\big(n - \gcd(Q_k, Q_{k'}) i\big) = \delta(k-k')\delta(i) \tag{5.8.2}$$

for all $k, k' = 0, \ldots, M-1$ and all i, where $\gcd(Q_k, Q_{k'})$ denotes the greatest common divisor of Q_k and $Q_{k'}$. Similarly, here it can be shown that for the MD case, the orthonormality condition in (5.3.15) can be rewritten in terms of $f_{k,\mathbf{p}}(\mathbf{n})$, the $\mathbf{P}_k$-fold polyphase components of $f_k(\mathbf{n})$, as follows

$$\sum_{\mathbf{n}\in\mathcal{N}} f_{k,\mathbf{p}}(\mathbf{n} + \mathbf{A}_k\mathbf{p}) f_{k',\mathbf{p}'}^*\big(\mathbf{n} + \mathbf{A}_{k'}\mathbf{p}' - \mathrm{gcld}(\mathbf{S}_k, \mathbf{S}_{k'})\mathbf{i}\big) = \delta(k-k')\delta(\mathbf{p}-\mathbf{p}')\delta(\mathbf{i}) \tag{5.8.3}$$

for all $k, k' = 0, \ldots, M-1$, $\mathbf{p} \in \mathcal{N}(\mathbf{P}_k)$, $\mathbf{p}' \in \mathcal{N}(\mathbf{P}_{k'})$, and all $\mathbf{i} \in \mathcal{N}$, where $\mathrm{gcld}(\mathbf{Q}_k, \mathbf{Q}_{k'})$ denotes the greatest common *left* divisor [MacDuffee, 1946] of $\mathbf{Q}_k$ and $\mathbf{Q}_{k'}$. For the case where all $\mathbf{P}_k = \mathbf{I}$, this can be simplified further as

$$\sum_{\mathbf{n}\in\mathcal{N}} f_k(\mathbf{n}) f_{k'}^*\big(\mathbf{n} - \mathrm{gcld}(\mathbf{Q}_k, \mathbf{Q}_{k'})\mathbf{i}\big) = \delta(k-k')\delta(\mathbf{i}). \tag{5.8.4}$$

Similarly, the biorthonormality in (5.3.18) can also be simplified. Note that although the above simplifies the expression of orthonormality, it does not necessarily simplify derivations of results in this chapter.

In this chapter, we proposed the vector space notations which provide a framework for deriving a number of theoretical results in maximally decimated filter banks. Because of the generality of vector space, these theoretical results can be applied to the most general filter banks, namely, MD nonuniform rational filter banks. Among these results, we have shown the relation among the Hermitian image property, orthonormality, and the perfect reconstruction property in a maximally decimated filter bank. With vector space notations, it can also been shown that perfect reconstruction is achieved if and only if the biorthonormality condition is satisfied. We proved that we can obtain a PR synthesis/analysis transmultiplexer from a PR maximally decimated analysis/synthesis filter bank, and vice versa. We also derived the MD subband convolution scheme starting from the generalized Parseval's relation in vector space. Put in vector space notations, many of these results become very explicit and easy to prove. Therefore, the vector space interpretation provides a very powerful tool in deriving these filter bank results. To illustrate the generality of this framework, we have also applied it to another analysis/synthesis scheme, namely, the wavelet transform, and obtained a number of useful results. In particular, we have derived the so-called wavelet convolution theorem.

5.9. APPENDICES

Appendix A

We need to prove

$$h_k^*(\mathbf{Q}_k\mathbf{m} - \mathbf{P}_k\mathbf{n}) = f_k(\mathbf{P}_k\mathbf{n} - \mathbf{Q}_k\mathbf{m}) \text{ for } \mathbf{m} \in \mathcal{N} \iff h_k^*(\mathbf{n}) = f_k(-\mathbf{n}), \tag{5.A.1}$$

where $\mathbf{n} \in \mathcal{N}$ is the space domain index. It is clear the second half implies the first half of this statement. Conversely, suppose $h_k^*(\mathbf{Q}_k\mathbf{m} - \mathbf{P}_k\mathbf{n}) = f_k(\mathbf{P}_k\mathbf{n} - \mathbf{Q}_k\mathbf{m})$, we want to show $h_k^*(\mathbf{n}) = f_k(-\mathbf{n})$ for all $\mathbf{n}$. Because $\mathbf{P}_k$ and $\mathbf{Q}_k$ are left coprime, there exist integer matrices $\mathbf{A}$ and $\mathbf{B}$ such that $\mathbf{Q}_k\mathbf{B} + \mathbf{P}_k\mathbf{A} = \mathbf{I}$ (generalized Bezout theorem [MacDuffee, 1946], [Kailath, 1980], [Vidyasagar, 1985]). So, any $\mathbf{p} \in \mathcal{N}$ can be expressed as

$$\mathbf{p} = \mathbf{Q}_k \underbrace{\mathbf{A}\mathbf{p}}_{\mathbf{m}} + \mathbf{P}_k \underbrace{\mathbf{B}\mathbf{p}}_{-\mathbf{n}}. \tag{5.A.2}$$

Therefore, $h_k^*(\mathbf{p}) = h_k^*(\mathbf{Q}_k\mathbf{m} - \mathbf{P}_k\mathbf{n}) = f_k(\mathbf{P}_k\mathbf{n} - \mathbf{Q}_k\mathbf{m}) = f_k(-\mathbf{p})$ for all $\mathbf{p} \in \mathcal{N}$.

Appendix B

Any nonsingular rational matrix $\mathbf{H}$ can be written as $\mathbf{H} = \mathbf{Q}^{-1}\mathbf{P}$, where $\mathbf{P}$ and $\mathbf{Q}$ are left coprime integer matrices. This is called an irreducible left 'matrix fraction description' (MFD) of

H [Kailath, 1980], [Vidyasagar, 1985]. Similarly, H can be written as $\mathbf{H} = \mathbf{R}\mathbf{S}^{-1}$ with R and S being right coprime integer matrices. This is called an irreducible right MFD of H. We then have $\mathbf{PS} = \mathbf{QR}$. It has been shown that the denominator matrices of all irreducible right or left MFD's have the same absolute determinant, i.e., $J(\mathbf{Q}) = J(\mathbf{S})$ [Chen and Vaidyanathan, 1993a]. With these properties, we can prove the following lemma:

Lemma 5.1. Given P and Q (both nonsingular), we first find R and S which are right coprime such that $\mathbf{PS} = \mathbf{QR}$. In other words, we find $\mathbf{RS}^{-1}$ which is a irreducible right MFD of $\mathbf{Q}^{-1}\mathbf{P}$. Then,

$$\mathbf{Pr} = \mathbf{Qm} \qquad \text{if and only if} \qquad \begin{cases} \mathbf{r} = \mathbf{Sj} \in LAT(\mathbf{S}), \text{ and} \\ \mathbf{m} = \mathbf{Rj} \in LAT(\mathbf{R}). \end{cases} \tag{5.B.1}$$

◇

Proof: Suppose $\mathbf{k} = \mathbf{Pr} = \mathbf{Qm}$, so $\mathbf{k} \in LAT(\mathbf{P}) \cap LAT(\mathbf{Q})$. It can be proved that the intersection of two lattices is a lattice generated by the lcrm of the two generating matrices [MacDuffee, 1946], [Chen and Vaidyanathan, 1993a], i.e., $LAT(\mathbf{P}) \cap LAT(\mathbf{Q}) = LAT(\text{lcrm}(\mathbf{P},\mathbf{Q}))$. Hence we have $\mathbf{k} \in LAT(\mathbf{P}) \cap LAT(\mathbf{Q}) = LAT(\text{lcrm}(\mathbf{P},\mathbf{Q}))$, so $\mathbf{k} = \text{lcrm}(\mathbf{P},\mathbf{Q})\mathbf{j}$. It has been shown that if R and S are right coprime, then $\mathbf{PS} = \mathbf{QR}$ is indeed an $\text{lcrm}(\mathbf{P},\mathbf{Q})$ [Chen and Vaidyanathan, 1993a]. Therefore, $\mathbf{k} = \mathbf{PSj} = \mathbf{QRj}$ and hence $\mathbf{r} = \mathbf{Sj}$ and $\mathbf{m} = \mathbf{Rj}$. The proof of the converse is straightforward. △△△

We can generalize Lemma 5.1 to the following lemma:

Lemma 5.2. Given nonsingular left coprime matrices P and Q, we first find the corresponding R and S as in Lemma 5.1. Furthermore, since P and Q are left coprime, we can find A and B such that $\mathbf{PA} + \mathbf{QB} = \mathbf{I}$. Then,

$$\mathbf{Pr} + \mathbf{p} = \mathbf{Qm} \qquad \text{if and only if} \qquad \mathbf{r} + \mathbf{Ap} = \mathbf{Sj}, \text{ i.e., } \mathbf{r} + \mathbf{Ap} \in LAT(\mathbf{S}). \tag{5.B.2}$$

◇

Proof: Suppose $\mathbf{Pr} + \mathbf{p} = \mathbf{Qm}$. Using $\mathbf{PA} + \mathbf{QB} = \mathbf{I}$, we have $\mathbf{PAp} + \mathbf{QBp} = \mathbf{p}$ so that $\mathbf{Pr} + \mathbf{PAp} + \mathbf{QBp} = \mathbf{Qm}$. Rearrange terms to get $\mathbf{P}(\mathbf{r} + \mathbf{Ap}) = \mathbf{Q}(\mathbf{m} - \mathbf{Bp})$. Using Lemma 5.1, we conclude $\mathbf{r} + \mathbf{Ap} = \mathbf{Sj} \in LAT(\mathbf{S})$. Conversely, suppose $\mathbf{r} + \mathbf{Ap} = \mathbf{Sj}$, or $\mathbf{r} = \mathbf{Sj} - \mathbf{Ap}$. Compute $\mathbf{Pr}$ as follows: $\mathbf{Pr} = \mathbf{PSj} - \mathbf{PAp} = \mathbf{PSj} - \mathbf{p} + \mathbf{QBp} = \mathbf{Q}\underbrace{(\mathbf{Rj} + \mathbf{Bp})}_{\mathbf{m}} - \mathbf{p}$. So, $\mathbf{Pr} + \mathbf{p} = \mathbf{Qm}$. △△△

Appendix C

Equations (5.5.4), (5.5.7) and (5.5.9) define a mapping from one index $\mathbf{m} \in \mathcal{N}$ to a triple index

$(\mathbf{p}, \mathbf{t}, \mathbf{i})$ where $\mathbf{p} \in \mathcal{N}(\mathbf{P}_k)$, $\mathbf{t} \in \mathcal{N}(\mathbf{T}_k)$ and $\mathbf{i} \in \mathcal{N}$. These are restated here for convenience:

$$\mathbf{Q}_k\mathbf{m} = \mathbf{P}_k\mathbf{r} + \mathbf{p}, \quad \text{for } \mathbf{r} \in \mathcal{N} \text{ and } \mathbf{p} \in \mathcal{N}(\mathbf{P}_k), \tag{5.C.1}$$

$$\mathbf{r} = \mathbf{S}_k\mathbf{j} - \mathbf{A}_k\mathbf{p}, \quad \text{for } \mathbf{j} \in \mathcal{N}, \tag{5.C.2}$$

$$\mathbf{j} = \mathbf{T}_k\mathbf{i} + \mathbf{t}, \quad \text{for } \mathbf{i} \in \mathcal{N} \text{ and } \mathbf{t} \in \mathcal{N}(\mathbf{T}_k). \tag{5.C.3}$$

We need to show that this mapping is one-to-one and onto.

We first show that such mapping is one-to-one. In other words, starting from different $\mathbf{m}$ and $\mathbf{m}'$ and using this mapping to obtain $(\mathbf{p}, \mathbf{t}, \mathbf{i})$ and $(\mathbf{p}', \mathbf{t}', \mathbf{i}')$, respectively, we should get $(\mathbf{p}, \mathbf{t}, \mathbf{i}) \neq (\mathbf{p}', \mathbf{t}', \mathbf{i}')$ ($\mathbf{p} \neq \mathbf{p}'$ *or* $\mathbf{t} \neq \mathbf{t}'$ *or* $\mathbf{i} \neq \mathbf{i}'$). According to (5.C.1), if $\mathbf{m} \neq \mathbf{m}'$ then $\mathbf{r} \neq \mathbf{r}'$ or $\mathbf{p} \neq \mathbf{p}'$. If $\mathbf{p} \neq \mathbf{p}'$, the proof is completed. If $\mathbf{p} = \mathbf{p}'$, we know $\mathbf{r} \neq \mathbf{r}'$. From (5.C.2), we know $\mathbf{j} \neq \mathbf{j}'$. Then, using (5.C.3), we can conclude that $\mathbf{t} \neq \mathbf{t}'$ or $\mathbf{i} \neq \mathbf{i}'$.

Secondly, we show that this mapping is onto. That is, for any $(\mathbf{p}, \mathbf{t}, \mathbf{i})$ such that $\mathbf{p} \in \mathcal{N}(\mathbf{P}_k)$, $\mathbf{t} \in \mathcal{N}(\mathbf{T}_k)$ and $\mathbf{i} \in \mathcal{N}$, there exist a vector $\mathbf{m} \in \mathcal{N}$ from which $(\mathbf{p}, \mathbf{t}, \mathbf{i})$ will be obtained by using this mapping. Recall that (5.C.1), (5.C.2) and (5.C.3) can be combined to get 13), which is restated here

$$\mathbf{m} = \mathbf{R}_k\mathbf{T}_k\mathbf{i} + \mathbf{R}_k\mathbf{t} + \mathbf{B}_k\mathbf{p}. \tag{5.C.4}$$

Given any $(\mathbf{p}, \mathbf{t}, \mathbf{i})$, we can use (5.C.4) to compute the vector $\mathbf{m}$. It can be verified that this $\mathbf{m}$ will generate the given $(\mathbf{p}, \mathbf{t}, \mathbf{i})$ as required. Hence, we proved that this mapping is indeed onto.

Bibliography

This bibliography contains two parts. The first part is a list of all the books and articles cited in the text. This list is ordered alphabetically by authors' names. The second part, *Selected References by Topic*, contains some entries in the first list for special topics.

ALPHABETICAL LISTING BY AUTHORS

Akansu, A. N., and Haddad, R. A., *Multiresolution Signal Decomposition: Transforms, Subbands, and Wavelets*, Academic Press, Inc., 1992.

Ansari, R., and Lau, C.-L., "Two-dimensional IIR filters for exact reconstruction in tree structured sub-band decomposition," *Electronic Letters*, vol. 23, pp. 633–634, June 1987.

Ansari, R., "Efficient IIR and FIR fan filters," *IEEE Trans. on Circuits and Systems*, vol. CAS-34, no. 8, pp. 941–945, August 1987.

Ansari, R., and Lee, S. H., "Two-dimensional non-rectangular interpolation, decimation and filter banks," *Proc. IEEE Int. Conf. on ASSP*, New York, April 1988.

Ansari, R., and Guillemot, C., "Exact reconstruction filter banks using diamond FIR filters," *Communication, Control, and Signal Processing*, vol. 2, pp. 1412–1424, Elsevier Science Publishers, July 1990.

Bamberger, R. H., *The directional filter bank: A multirate filter bank for the directional decomposition of images*, Doctoral dissertation, Georgia Institute of Technology, November 1990.

Bamberger, R. H., and Smith, M. J. T., "A filter bank for the directional decomposition of images: Theory and design," *IEEE Trans. on Signal Processing*, vol. 40, no. 4, pp. 882–893, April 1992.

Blahut, R. E., *Theory and Practice of Error Control Codes*. Massachusetts: Addison-Wesley, 1983.

Cassels, J. W. S., *An Introduction to the Geometry of Numbers*. Berlin: Springer-Verlag, 1959.

Chen, T., and Vaidyanathan, P. P., "Multidimensional multirate filters derived from one dimensional filters," *Electronics Letters*, vol. 27, no. 3, pp. 225–228, January 1991.

Chen, T., and Vaidyanathan, P. P., "Commutativity of D-dimensional decimation and expansion matrices, and application to rational decimation systems," *Proc. IEEE Int. Conf. on ASSP*, vol. 4, pp. 637–640, San Francisco, March 1992a.

Chen, T., and Vaidyanathan, P. P., "Least common right/left multiples of integer matrices and applications to multidimensional multirate systems," *Proc. IEEE Int. Symp. on Circuits and Systems*, pp. 935–938, San Diego, May 1992b.

Chen, T., and Vaidyanathan, P. P., "Results on multidimensional nonuniform rational maximally-decimated filter banks with orthonormal filters," *Conf. Record of 26th Annual Asilomar Conference on Signals, Systems, and Computers*, vol. 1, pp. 145–149, Pacific Grove, CA, October 1992c.

Chen, T., Djoković, I., and Vaidyanathan, P. P., "General theory of time-reversed inversion for perfect reconstruction filter banks," *Conf. Record of 26th Annual Asilomar Conference on Signals, Systems, and Computers*, vol. 2, pp. 821–825, Pacific Grove, CA, October 1992d.

Chen, T., and Vaidyanathan, P. P., "Vector space framework for unification of one- and multidimensional filter bank theory," submitted to *IEEE Trans. on Signal Processing*, October 1992e.

Chen, T., and Vaidyanathan, P. P., "The role of integer matrices in multidimensional multirate systems," *IEEE Trans. on Signal Processing*, vol. 41, no. 3, pp. 1035–1047, March 1993a.

Chen, T., and Vaidyanathan, P. P., "Recent developments in multidimensional multirate systems," *IEEE Trans. on Circuits and Systems for Video Technology*, vol. 3, no. 2, pp. 116–137, April 1993b.

Chen, T., and Vaidyanathan, P. P., "On the choice of rational decimation systems for multidimensional signals," *Proc. IEEE Int. Conf. on ASSP*, vol. 5, pp. 527–530, Minneapolis, April 1993c.

Chen, T., and Vaidyanathan, P. P., "Multidimensional multirate filters and filter banks derived from one-dimensional filters," *IEEE Trans. on Signal Processing*, vol. 41, no. 5, pp. 1749–1765, May 1993d.

Chen, T., and Vaidyanathan, P. P., "Considerations in multidimensional filter bank design," *Proc. IEEE Int. Symp. on Circuits and Systems*, pp. 643–646, Chicago, May 1993e.

Chen, T., and Vaidyanathan, P. P., "Nonuniform decimation and reconstruction of generalized-bandlimited MD signals," *Proc. IEEE Int. Symp. on Circuits and Systems*, pp. 120–123, Chicago, May 1993f.

Chen, T., "Unified eigenfilter approach: with applications to spectral/spatial filtering," *Proc. IEEE Int. Symp. on Circuits and Systems*, pp. 331–334, Chicago, May 1993g.

Chui, C. K., *An Introduction to Wavelets*, Academic Press, Inc., 1992.

Crochiere, R. E., Webber, S. A., and Flanagan, J. L., "Digital coding of speech in subbands," *Bell System Tech. J.*, vol. 55, pp. 1069–1085, October 1976.

Crochiere, R. E., and Rabiner, L. R., *Multirate Digital Signal Processing.* Englewood Cliffs, New Jersey: Prentice-Hall, 1983.

Daubechies, I., *Ten Lectures on Wavelets*, SIAM, CBMS series, April 1992.

Dubois, E., "The sampling and reconstruction of time-varying imagery with application in video systems," *Proc. IEEE*, vol. 73, pp. 502–522, April 1985.

Dudgeon, D. E., and Mersereau, R. M., *Multidimensional Digital Signal Processing.* Englewood Cliffs, New Jersey: Prentice-Hall, 1984.

Evans, B. L., McClellan, J. H., and Bamberger, R. H., "A symbolic algebra for linear multidimensional multirate systems," 1992 Conference on Information Sciences and Systems, Princeton, NJ, March 1992.

Evans, B. L., Bamberger, R. H., and McClellan, J. H., "Rules for multidimensional multirate structures," to be published in *IEEE Trans. on Signal Processing.*

Forney, G. D., Jr., "Convolutional codes I: Algebraic structure," *IEEE Trans. on Information Theory*, vol. IT-16, no. 6, pp. 720–738, Nov. 1970.

Gantmacher, F. R., *The Theory of Matrices*, vol. 1. New York, N. Y.: Chelsea Publishing Company, 1977.

Gharavi, H., and Tabatabai, A., "Subband coding of monochrome and color images," *IEEE Trans. on Circuits and Systems*, vol. 35, pp. 207–214, February 1988.

Gopinath, R. A., and Burrus, C. S., "On upsampling, downsampling and rational sampling rate filter banks," submitted for publication, *IEEE Trans. on Signal Processing*, 1992.

Guessoum, A., and Mersereau, R. M., "Fast algorithms for the multidimensional discrete Fourier transform," *IEEE Trans. on Acoustics, Speech, and Signal Processing*, vol. 34, no. 4, pp. 937–943, August 1986.

Hoang, P.-Q., and Vaidyanathan, P. P., "Non-uniform multirate filter banks: theory and design," *Proc. IEEE Int. Symp. Circuits and Systems*, pp. 371–374, Portland, 1989.

Hsiao, C.-C., "Polyphase filter matrix for rational sampling rate conversions," in *Proc. IEEE Int. Conf. on ASSP*, pp. 2173–2176, Dallas, April 1987.

IEEE Trans. on Communications, Special Issue on Transmultiplexers, vol. 30, no. 7, July 1982.

Jayant, N. S., and Noll, P., *Digital Coding of Waveforms*, Prentice Hall, Inc., Englewood Cliffs, 1984.

Johnston, J. D., "A filter family designed for use in quadrature mirror filter banks," *Proc. of the IEEE Int. Conf. on Acoustics, Speech, and Signal Processing*, pp. 291–294, April 1980.

Kailath, T., *Linear Systems.* Englewood Cliffs, New Jersey: Prentice-Hall, 1980.

Kalker, A. A. C. M., "Commutativity of up/down sampling," *Electronics Letters*, vol. 28, no. 6, pp. 567–569, March 1992.

Karlsson, G., and Vetterli, M., "Theory of two-dimensional multirate filter banks," *IEEE Trans. on Acoustics, Speech, and Signal Processing*, vol. 38, no. 6, pp. 925–937, June 1990.

Koilpillai, R. D., Nguyen, T. Q., and Vaidyanathan, P. P., "Some results in the theory of crosstalk-free transmultiplexers," *IEEE Trans. on Signal Processing*, vol. 39, no. 10, pp. 2174–2183, October 1991.

Kovačević, J., and Vetterli, M., "Perfect reconstruction filter banks with rational sampling rate changes," *Proc. IEEE Int. Conf. on Acoustics, Speech, and Signal Processing*, pp. 1785–1788, Toronto Canada, May 1991a.

Kovačević, J., and Vetterli, M., "The commutativity of up/downsampling in two dimensions," *IEEE Trans. on Information Theory*, vol. 37, no. 3, pp. 695–698, May 1991b.

Kovačević, J., and Vetterli, M., "Nonseparable multidimensional perfect reconstruction filter banks and wavelet bases for $\mathcal{R}^n$," *IEEE Trans. on Information Theory*, vol. 38, no. 2, pp. 533–555, March 1992.

Kunt, M., "Recent HDTV systems," *Signal Processing VI: Theories and Applications*, pp. 83–89, Elsevier Science Publisher, 1992.

Lau, C.-L., and Ansari, R., "Two dimensional digital filter design and implementation based on generalized decimation," *Proc. of the 20th Conference on Information Sciences and Systems*, Princeton, NJ, pp. 626–631, March 1986.

Liu, V. C., and Vaidyanathan, P. P., "Alias cancellation and distortion elimination in multidimensional QMF banks," *Proc. IEEE Int. Symp. on Circuits and Systems*, pp. 1281–1284, Espoo, Finland, June 1988.

Luenberger, D. G., *Optimization by vector space methods*, John Wiley, 1969.

MacDuffee, C. C., *The Theory of Matrices.* New York, New York: Chelsea Publishing Company, 1946.

Mallat, S., "A theory for multiresolution signal decomposition: the wavelet representation," *IEEE Trans. on Pattern Analysis and Machine Intelligence*, vol. 11, pp. 674–693, July 1989.

Malvar, H. S., *Signal Processing with Lapped Transforms*, Artech House, Norwood, MA, 1992.

Manduchi, R., Cortelazzo, G. M., and Mian, G. A., "Multistage sampling structure conversion of video signals," preprint.

Mersereau, R. M., and Speake, T. C., "The processing of periodically sampled multidimensional signals," *IEEE Trans. on Acoustics, Speech, and Signal Processing*, vol. 31, no. 1, pp. 188–194, February 1983.

Mitra, S. K., Creusere, C. D., and Babic, H., "A novel implementation of perfect reconstruction QMF banks using IIR filters for infinite length signals," *Proc. of the IEEE Int. Symp. on Circuits and Systems*, pp. 2312–2315, San Diego, May 1992.

Nayebi, K., Barnwell, T. P., III, and Smith, M. J. T., "The design of perfect reconstruction nonuniform band filter banks," *Proc. IEEE Int. Conf. on Acoustics, Speech, and Signal Processing*, pp. 1781–1784, Canada, 1991.

Neuvo, Y., Dong, C. Y., and Mitra, S. K., "Interpolated finite impulse response filters", *IEEE Trans. on Acoustics, Speech, and Signal Processing*, vol. ASSP-32, no. 3, pp. 563–570, June 1984.

Newman, M., *Integral Matrices.* New York: Academic Press, 1972.

Nguyen, T. Q., and Vaidyanathan, P. P., "Maximally decimated perfect reconstruction FIR filter banks with pairwise mirror-image analysis (and synthesis) frequency responses," *IEEE Trans. on Acoustics, Speech, and Signal Processing*, vol. 36, no. 5, pp. 693–705, May 1988.

Nuri, V., and Bamberger, R. H., "A theoretical framework for the analysis and design of size-limited multirate filter banks," *IEEE-SP Int. Symp. on Time-Frequency and Time-Scale Analysis*, 1992.

Petersen, D. P., and Middleton, D., "Sampling and reconstruction of wave-number-limited functions in N-dimensional Euclidean spaces," *Information and Control*, vol. 5, pp. 279–323, 1962.

Rabiner, L. R., and Gold, B., *Theory and Application of Digital Signal Processing.* Englewood Cliffs, New Jersey: Prentice-Hall, 1975.

Ramstad, T. A., "IIR filter bank for subband coding of images," *Proc. of the IEEE Int. Symp. on Circuits and Systems*, pp. 827–830, Espoo, Finland, June 1988.

Rao, K. R., and Yip, P., *Discrete Cosine Transform: Algorithms, Advantages, Applications*, Academic Press, Inc., 1990.

Renfors, M., and Saramäki, T., "Recursive Nth-band digital filters—Part I: Design and properties," *IEEE Trans. on Circuits and Systems*, vol. CAS-34, no. 1, pp. 24–39, January 1987.

Renfors, M., "Multi-dimensional sampling structure conversion with one-dimensional Nth-band filters," *Proc. IEEE Int. Symp. on Circuits and Systems*, pp. 1502–1507, Portland, May 1989.

Riesz, F., and Sz.-Nagy, B.,*Functional Analysis*, Frederick Ungar Publishing Company, New York, 1955.

Sathe, V., and Vaidyanathan, P. P., "Effects of multirate systems on the statistical properties of random inputs," *IEEE Trans. on Signal Processing*, vol. 41, no. 1, pp. 131–146, January 1993.

Shah, I. A., and Kalker, A. A. C. M., "Generalized theory of multidimensional M-band filter bank design," *Proc. of the Sixth EUSIPCO*, pp. 969–972, August 1992.

Simoncelli, E. P., and Adelson, E. H., "Nonseparable extensions of quadrature mirror filters to multiple dimensions," *Proc. IEEE*, vol. 78, pp. 652–664, April 1990.

Sjogren, J. A., AFOSR, personal e-mail correspondences.

Smith, H. J. S., "On systems of linear indeterminate equations and congruences", *Philos. Trans. Royal Society*, London, vol. 151, pp. 293–326, 1861.

Smith, M. J. T., and Barnwell, T. P., III, "A new filter-bank theory for time-frequency representation," *IEEE Trans. on Acoustics, Speech, and Signal Processing*, vol. 35, pp. 314–327, March 1987.

Smith M. J. T., and Eddins, S. L., "Analysis/Synthesis techniques for subband image coding," *IEEE Trans. on Acoustics, Speech, and Signal Processing*, vol. 38, no. 8, pp. 1446–1456, August 1990.

Soman, A. K., and Vaidyanathan, P. P., "Paraunitary filter banks and wavelet packets," *Proc. IEEE Int. Conf. on Acoustics, Speech, and Signal Processing*, vol. 4, pp. 397–400, San Francisco, March 1992.

Soman, A. K., and Vaidyanathan, P. P., "Coding gain in paraunitary analysis/synthesis systems," *IEEE Trans. on Signal Processing*, 1993.

Swaminathan, K., and Vaidyanathan, P. P., "Theory and design of uniform DFT, parallel, quadrature mirror filter banks," *IEEE Trans. on Circuits and Systems*, vol. CAS-33, no. 2, pp. 1170–1191, December 1986.

Vaidyanathan, P. P., "Design of doubly-complementary IIR digital filters using a single complex allpass filter, with multirate application," *IEEE Trans. on Circuits and Systems*, vol. CAS-34, no. 4, pp. 378–389, April 1987a.

Vaidyanathan, P. P., "Theory and design of M-channel maximally decimated quadrature mirror filters with arbitrary M, having the perfect-reconstruction property," *IEEE Trans. on Acoustics, Speech, and Signal Processing*, vol. ASSP-35, no. 4, pp. 476–492, April 1987b.

Vaidyanathan, P. P., "Quadrature mirror filter banks, M-Band extensions and perfect-reconstruction techniques," *IEEE ASSP Magazine*, pp. 4–20, July 1987c.

Vaidyanathan, P. P., and Mitra, S. K., "Polyphase networks, block digital filtering, LPTV systems, and alias-free QMF banks: A unified approach based on pseudocirculants," *IEEE Trans. on Acoustics, Speech, and Signal Processing*, vol. 36, no. 3, pp. 381–391, March 1988.

Vaidyanathan, P. P., "Multirate digital filters, filter banks, polyphase networks, and applications: A tutorial," *Proc. IEEE*, pp. 56–93, January 1990a.

Vaidyanathan, P. P., "Fundamentals of multidimensional multirate digital signal processing," *Sadhana*, vol. 15, pp. 157–176, November 1990b.

Vaidyanathan, P. P., "The role of Smith-form decomposition of integer-matrices, in multidimensional multirate systems," *Proc. IEEE Int. Conf. on ASSP*, pp. 1777-1780, Toronto, Canada, May 1991a.

Vaidyanathan, P. P., "New results in multidimensional multirate systems," *Proc. IEEE Int. Symp. on Circuits and Systems*, pp. 468–471, Singapore, June 1991b.

Vaidyanathan, P. P., *Multirate Systems and Filter Banks.* Englewood Cliffs, New Jersey: Prentice-Hall, 1993a.

Vaidyanathan, P. P., "Orthonormal and biorthonormal filter-banks as convolvers, and convolutional coding gain," *IEEE Trans. on Signal Processing*, June 1993b.

Veldhuis, R. N. J., Breeuwer, M., and van der Waal, R.G., "Subband coding of digital audio signals," *Philips Journal of Research*, vol. 44, pp. 329–343, 1989.

Vetterli, M., "Multidimensional subband coding: some theory and algorithms," *Signal Processing*, vol. 6, no. 2, pp. 97–112, February 1984.

Vetterli, M., "Filter banks allowing for perfect reconstruction," *Signal Processing*, vol. 10, pp. 219–244, April 1986a.

Vetterli, M., "Perfect transmultiplexers," *Proc. IEEE Int. Conf. on Acoustics, Speech, and Signal Processing*, pp. 2567–2570, Tokyo, Japan, April 1986b.

Vetterli, M., "A theory of multirate filter banks," *IEEE Trans. on Acoustics, Speech, and Signal Processing*, vol. 35, pp. 356–372, March 1987.

Vetterli, M., and Le Gall, D., "Perfect reconstruction FIR filter banks: some properties and factorization," *IEEE Trans. on Acoustics, Speech, and Signal Processing*, vol. 37, no. 7, pp. 1057–1071, July 1989.

Vetterli, M., Kovačević, J., and Le Gall, D., "Perfect reconstruction filter banks for HDTV representation and coding," *Signal Processing: Image Communication* 2, pp. 349–363, Elsevier Science Publisher, 1990.

Vetterli, M., and Herley, C., "Wavelets and filter banks: theory and design," *IEEE Trans. on Signal Processing*, vol. 40, no. 9, pp. 2209–2232, September 1992.

Vidyasagar, M., *Control System Synthesis: A Factorization Approach.* Cambridge, Massachusetts: The MIT Press, 1985.

Viscito, E., and Allebach, J. P., "Design of perfect reconstruction multi-dimensional filter banks using cascaded Smith form matrices," *Proc. IEEE Int. Symp. Circuits and Systems*, Espoo, Finland, pp. 831–834, June 1988.

Viscito, E., and Allebach, J. P., "The analysis and design of multidimensional FIR perfect reconstruction filter banks for arbitrary sampling lattices," *IEEE Trans. on Circuits and Systems*, vol. CAS-38, no. 1, pp. 29–41, January 1991.

Woods, J. W., and O'Neil, S. D.,"Subband coding of images," *IEEE Trans. on Acoustics, Speech, and Signal Processing*, vol. 34, no. 5, pp. 1278–1288, October 1986.

Woods, J. W., *Subband Image Coding*, Kluwer Academic Publishers, Inc., 1991.

SELECTED REFERENCES BY TOPIC

Lattices and Integer Matrices

Cassels, 1959.

MacDuffee, 1946.

Newman, 1972.

Smith, 1861.

Vidyasagar, 1985.

One-dimensional Multirate Systems

Chen and Vaidyanathan, 1992d.

Crochiere and L. R. Rabiner, 1983.

Hsiao, 1987.

Nguyen and Vaidyanathan, 1988.

Sathe and Vaidyanathan, 1993.

Soman and Vaidyanathan, 1992, 1993.

Vaidyanathan, 1990.

Vetterli, 1987.

Multidimensional Lattice Sampling

Dubois, 1985.

Dudgeon and Mersereau, 1984.

Mersereau and Speake, 1983.

Petersen and Middleton, 1962.

Multidimensional Multirate Theory

Chen and Vaidyanathan, 1992c, 1992e, 1993a, 1993b, 1993c, 1993f.

Evans, McClellan, and Bamberger, 1992.

Gopinath and Burrus, 1992.

Kalker, 1992.

Karlsson and Vetterli, 1990.

Kovačević and Vetterli, 1991b, 1992.

Liu and Vaidyanathan, 1988.

Mersereau and Speake, 1983.

Vetterli, 1984.

Viscito and Allebach, 1991.

Multidimensional Systems and Filter Design

Ansari, 1987.

Ansari and Guillemot, 1990.

Ansari and Lau, 1987.

Ansari and Lee, 1988.

Bamberger and Smith, 1992.

Chen, 1993g.

Chen and Vaidyanathan, 1991, 1993d, 1993e.

Guessoum and Mersereau, 1986.

Renfors, 1989.

Shah and Kalker, 1992.

Smith and Eddins, 1990.

Viscito and Allebach, 1988, 1991.

Image and Video Coding

Gharavi and Tabatabai, 1988.

Jayant and Noll, 1984.

Kunt, 1992.

Smith and Eddins, 1990.

Vetterli, 1984.

Woods, 1991.

Woods and O'Neil, 1986.

Books and Papers of Tutorial Value

Chen and Vaidyanathan, 1993b.

Crochiere and Rabiner, 1983.

Dubois, 1985.

Dudgeon and Mersereau, 1984.

Kunt, 1992.

Mersereau and Speake, 1983.

Vaidyanathan, 1990a, 1990b, 1993a.

Vetterli, 1987.

Viscito and Allebach, 1991.

Woods, 1991.